Structural and functional characterisation of Skp2-containing complexes

Bailey Catherine Massa

Thesis submitted for the degree of Doctor of Philosophy

Newcastle University

Faculty of Medical Sciences

Northern Institute for Cancer Research

March 2016

Abstract

The eukaryotic cell cycle is driven by a set of kinases called the cyclin-dependent kinases (CDKs). During G1, CDK2/cyclin E phosphorylates the CDK inhibitor, p27, leading to its ubiquitination by the SCF^{Skp2} complex and subsequent degradation. Skp2 is the substrate recognition component of the SCF^{Skp2} complex and has been found to be up-regulated in many cancers. High levels of Skp2 indicate poor prognosis. Its overexpression often correlates with low p27 levels. Skp2 was first identified in a complex with CDK2, cyclin A, Cks1 and Skp1. CDK2/cyclin A binds to SCF^{Skp2} and is required for the recruitment of p27 to the SCF^{Skp2} complex.

The aims of this project were to structurally characterize the CDK2/cyclin A/Skp1/Skp2 complex and to identify the functional significance of the Skp2/cyclin A interaction. In the absence of a crystal structure, site-directed mutagenesis was used to identify the regions on cyclin A and Skp2 which mediate this interaction. Mutation of residues 244-247 of cyclin A blocked its interaction with Skp2. Mutation of this region did not interfere with binding to CDK2, or p27, and CDK2/cyclin A kinase activity did not appear to be affected. CDK2 was found not to have a role in binding to Skp2.

Cyclin A binds to an extended region within the N-terminus of Skp2. Residues Leu32, Leu33, Ser39 and Leu41 of Skp2 have been reported to comprise the cyclin A binding region (Ji et al., 2006). This site was confirmed and a further two residues were identified as contributing to the interaction. The Skp2 N-terminal region is involved in binding many regulatory proteins and is heavily post-translationally modified. The binding of cyclin A to this sequence may therefore affect the structure and/or accessibility to modifying enzymes. The characterisation of these mutants has shown that they are potentially useful tool mutants for studying Skp2 function and regulation in human cell-based assays.

Acknowledgements

I would first like to thank my primary supervisor, Jane Endicott, for her help and support over the past four years. Jane has been a great mentor and a positive person to work with. I would also like to thank Martin Noble and Herbie Newell for their support and guidance. I would like to thank my supervisory team for giving me the opportunity to undertake my PhD at the NICR. A special thank you to Jane and Julie who read through this thesis and provided helpful feedback. Many thanks go to Cancer Research UK for their financial support, and Newcastle University for their academic support.

I would like to thank the members of the Endicott/Noble lab as well as former members for invaluable input, help and advice. There are now too many members to mention them all. I would like to thank the whole DDI lab, who have always been willing to help and offer advice. I would also like to thank the folks over in the structural biology lab, particularly Arnaud, for his help and guidance. I would also like to thank the members of the lab for their friendship. I have had endless laughs with them and they have always been the most supportive and friendly bunch who all know how to make a bad day in the lab better- with cake! They have made it a pleasure to spend the last four year at the NICR.

On a more personal note, I would like to thank my family who have been so encouraging in all of my endeavours. I am very fortunate to have a family who are so willing to help, and have even lent a hand through countless house moves. A huge thank you to my boyfriend, Kieran, who has been my pillar of strength throughout this process and to Mum and Casey as I couldn't have made it to the end without them.

Table of Contents

Table of Figures

Table of Tables

Table of Abbreviations

AMP	Adenosine mono-phosphate
APC/C	Anaphase-promoting complex/ cyclosome
ATP	Adenosine tri-phosphate
BCA	Bicinchoninic acid
BSA	Bovine serum albumin
CCP4	Collaborative Computational Project number 4
CD	Circular dichroism
Cdc34	Cell division cycle 34
CDK	Cyclin-dependent kinase
Cks1	Cdc kinase subunit 1
CRL	Cullin-RING ligase
C-terminal	Carboxy-terminal
DMSO	Dimethyl suphoxide
DNA	Deoxyribonucleic acid
dNTP	Deoxyribonucleotide triphosphate
DTT	Dithiothreitol
E. coli	*Escherichia coli*
EC_{50}	Half maximal effective concentration
ECL	Enhanced chemoluminescence
ER	Oestrogen receptor
FBL	F-box/leucine-rich repeat containing protein
FBW	F-box/WD40 domain containing protein
FCS	Foetal calf serum
FRET	Fluorescence resonance energy transfer
G1/G0	Gap phase 1/0
GAPDH	Glyceraldehyde 3-phosphate dehydrogenase
GI_{50}	Half maximal growth inhibitory concentration
GLUT1	Glucose transporter 1
GST	Glutathione-S-transferase
HBS	HEPES-buffered saline
HEK293T	Human embryonic kidney 293T
HEPES	N-[2-hydroxyethyl] piperazine-N-[2-ethanesulphonic acid]
His tag	Histidine tag

IP	Immunoprecipitation
IPTG	Isopropyl β-thiogalactoside
ITC	Isothermal titration calorimetry
kDa	kiloDalton
LB	Luria Bertani Broth
LRR	Leucine-rich repeat
M	Molar
mAU	Milli absorbance unit
MBP	Maltose-binding protein
MCS	Multiple cloning site
MEFs	Mouse embryonic fibroblasts
MWCO	Molecular weight cut-off
NF-κB	Nuclear factor kappa-light-chain-enhancer of activated B cells
NLS	Nuclear localisation signal
nm	Nanometre
N-terminal	Amino-terminal
OD_x	Optical density at x nm
PAGE	Polyacrylamide gel electrophoresis
PBS	Phosphate-buffered saline
PCa	Prostate cancer
PDB	Protein databank
PEG	Polyethylene glycol
PI3K	Phosphoinositide 3-kinase
PTEN	Phosphatase and tensin homolog
PVDF	Polyvinyl difluoride
Rb	Retinoblastoma protein
Rbx1	RING-box protein 1
RING	Really interesting new gene
Rmsd	Root mean square deviations
RNA	Ribonucleic acid
Rpm	Revolutions per minute
S. cerevisiae	*Saccharomyces cerevisiae*
S. pombe	*Schizosaccharomyces pombe*
SCF	Skp1/Cullin1/F-box ubiquitin ligase

Table of Abbreviations

SDS	Sodium dodecyl sulphate
SEC	Size-exclusion chromatography
SEC-MALLS	SEC-multi-angle laser light scattering
siRNA	Small interfering RNA
Skp	S-phase kinase-associated protein
S-phase	Synthesis phase
T_m	Melting temperature
Tris	2-amino-2-(hydroxymethyl)-1,3-propanediol
Ub	Ubiquitin
UPS	Ubiquitin-proteasome system
UTR	Untranslated region
UV	Ultraviolet
WCL	Whole cell lysate
WT	Wild type

Chapter 1: Introduction

1.1 The eukaryotic cell cycle

1.1.1 The eukaryotic cell division cycle

The normal cell division of somatic cells exists to renew tissues. For proliferating cells, cell division occurs about every 24 hours (Bernard and Herzel, 2006). The cell cycle is properly executed through a tightly regulated orchestration of events that allows a cell to grow, replicate its DNA, separate the sister chromatids and form two daughter cells. The division event is initiated by both intra- and extracellular signals. The external signalling molecules are known as mitogens. When these signals aberrantly trigger cell division or when the signalling pathways they initiate become constitutively activated this can lead to tumour development.

One of the hallmarks of cancer is the ability of cells to proliferate uncontrollably (Hanahan and Weinberg, 2011). The cell cycle occurs in four main stages comprising two growth phases (G1 and G2 phases) separated by DNA replication (S phase) and mitosis (M phase). During the cell cycle, a series of checkpoints are passed before mitotic cell division and distribution of genetic material to the daughter cells. For example, in response to genotoxic stress, the cell initiates the DNA damage response (DDR) and delays cell cycle progression, halting the cell at the so-called checkpoints until the damage is repaired (Jackson and Bartek, 2009, Bartek and Lukas, 2007). After a cell division cycle the cell can enter into the quiescent, G0 phase. The cell can then either re-enter the cell cycle in response to mitogenic signals or remain in this quiescent stage.

Progression through the cell cycle in higher eukaryotes is governed by a set of serine-threonine protein kinases called the cyclin-dependent kinases (CDKs), whose levels and activities are tightly regulated to ensure proper progression. As the name suggests, CDKs require a cyclin protein for full activity (Desai et al., 1992). The cyclins act as regulatory subunits with the levels of these proteins changing during the cell cycle, as a result of increased transcriptional activity, and decreasing due to ubiquitin-mediated proteasomal degradation (Pines, 2006, Pines, 1995, Pines, 1996, Reed, 2003). CDKs act as the catalytic subunits catalysing a phosphorylation reaction when

in their active cyclin-bound form. Protein phosphorylation is a post-translational modification which performs an essential role in the control of cell cycle events. The transient nature of this modification lends itself to the timely regulation that is required for the cell cycle. Kinases form a large superfamily of about 600 structurally similar proteins, of which the CDKs make up a sub-branch of *circa* 20 kinases (Cao et al., 2014). As CDKs are the master regulators of the cell cycle it is not surprising that dysregulation of their activity is strongly implicated in carcinogenesis.

1.1.2 Cyclin-dependent kinases (CDKs)

Protein phosphorylation is catalysed by kinases. The CDKs belong to the CMGC (cyclin-dependent kinase [CDK], mitogen-activated protein kinase [MAPK], glycogen synthase kinase [GSK3], CDC-like protein kinase [CLK]) family of protein kinases. The first identified CDK protein was CDK1 in *Saccharomyces cerevisiae* and *Schizosaccharomyces pombe*, at the time called Cdc28 or Cdc2 respectively. It was found that mutations to the *Cdc28* gene caused the cell cycle to stop (Pines, 1993). The next CDK protein to be identified was CDK2, which shares 65% sequence homology with CDK1 (Elledge and Spottswood, 1991). Subsequently additional family members were cloned and classified as CDKs (Matsushime et al., 1992, Bates et al., 1994, Meyerson et al., 1992). CDK1, CDK2, CDK4 and CDK6 have the most significant roles in control of the cell cycle (Figure 1.1) and CDK3, CDK7 and CDK11 are also required (Satyanarayana and Kaldis, 2009). CDK1 is the only essential CDK protein, with knockout of CDK1 leading to embryonic lethality at around embryonic day two (Malumbres and Barbacid, 2009, Satyanarayana and Kaldis, 2009). This result can be explained by the ability of CDK1 to bind all of the cell cycle cyclins (A, B, D and E). In the absence of other interphase CDKs such as CDK2, -4 and -6, CDK1 can take over their role (Santamaria et al., 2007). Surprisingly, it was found that $CDK2^{-/-}$ mice are viable, with the only significant defect being sterility in both male and female mice (Berthet et al., 2003, Ortega et al., 2003). Certain CDKs, such as CDK9 and CDK11, have been found to have a role in transcription and other processes, but for the purpose of this thesis I will focus on the cell cycle CDKs.

CDKs are subject to regulation by phosphorylation. Full activity of CDKs is achieved upon phosphorylation of a conserved threonine residue within the activation segment also known as the T-loop, for example Thr160 in CDK2 (Gu et al., 1992). By comparing the structures of the non-phosphorylated and phosphorylated CDK2/cyclin

A structures, it was determined that a conformational change occurs upon phosphorylation. The T-loop moves by as much as 7 Å after phosphorylation, so that the phosphate group is stabilised by three arginine residues (Russo et al., 1996b).

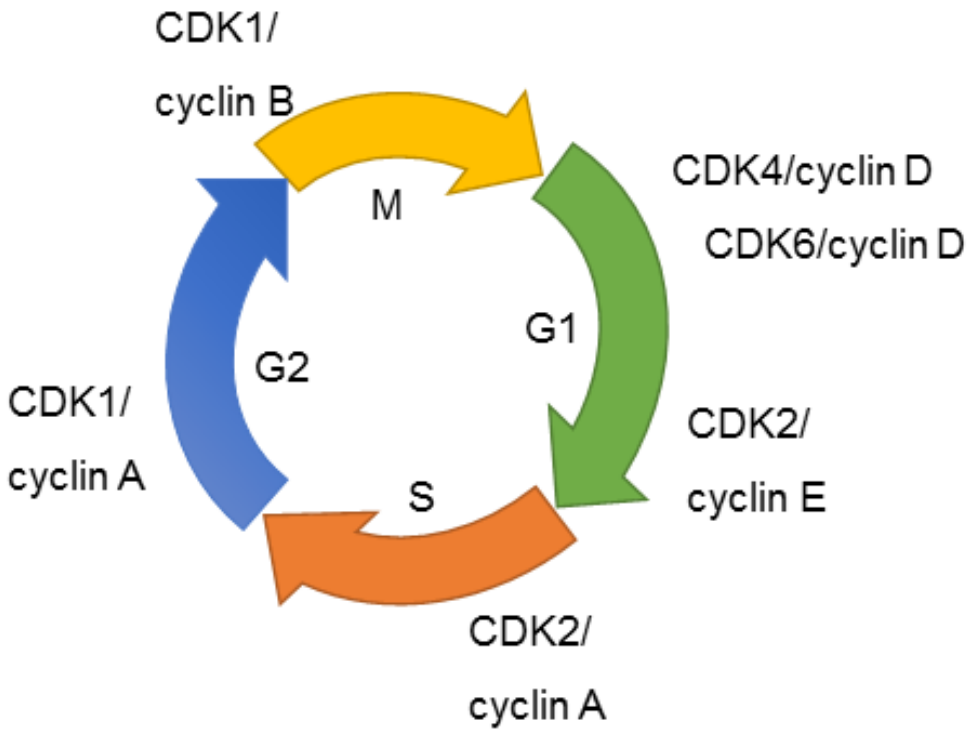

Figure 1.1: The cell cycle is driven forward by CDK/cyclin complexes. Four CDKs are responsible for driving the cell cycle, CDK1, CDK2, CDK4 and CDK6. The levels of CDKs are fairly constant throughout the cell cycle, but the levels of cyclins A, B and E rise and fall at various stages of the cell cycle (Figure 1.3) leading to particular CDK/cyclin complexes being active at particular phases of the cell cycle.

In addition to the activating phosphorylation, cell cycle CDKs are inhibited by phosphorylation. The importance of this event in regulating CDK1 activity at G2/M was recognised following the identification of Cdc25 and Wee1 as cell division cycle genes in *S. cerevisiae* and *S. pombe* (Aligue et al., 1997, Russell et al., 1989) Cdc25 phosphatase and Wee1 kinase antagonistically regulate the phosphorylation status of CDK1 Thr14 and Tyr15 within the CDK active site. Subsequently, other members of the CDK family were also shown to be subject to inhibitory phosphorylation events within the active site. For example, CDK2 can be inactivated by phosphorylation of Thr14 and Tyr15 by Wee1 and Myt1, respectively, to maintain genome integrity (Hughes et al., 2013).

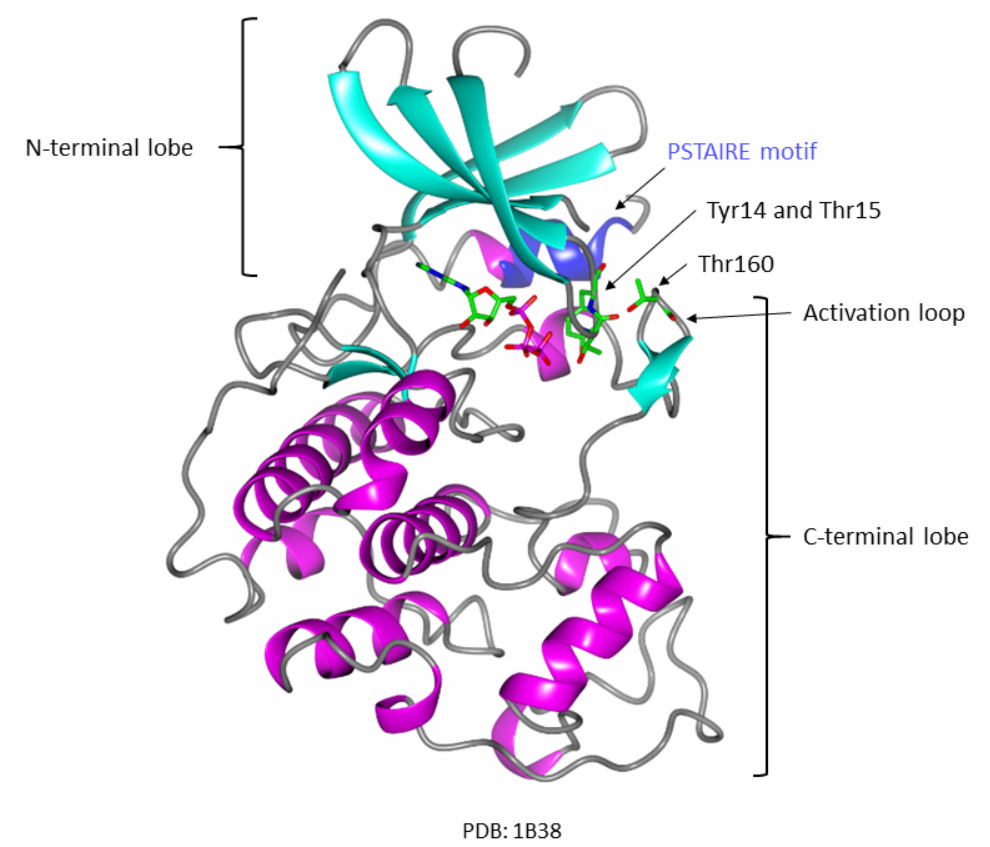

Figure 1.2: The structure of CDK2. The CDK2 structure is bi-lobate with an N-terminal lobe rich in β-sheets with a single helix, and a C-terminal lobe comprised predominantly of α-helices (De Bondt et al. 1993). The PSTAIRE helix of the N-terminal lobe (in blue) contains a catalytic glutamate residue. The ATP-binding site lies in a cleft between the two lobes (Brown et al., 1999).

CDK2 exhibits the classical kinase fold (Morgan, 1997), which consists of an N-terminal lobe which primarily comprises β-strands and a C-terminal lobe which is primarily α- helical (Figure 1.2, (De Bondt et al., 1993)). CDKs are catalytically inactive on their own requiring their cognate cyclins for activity. Cyclin A binding to CDK2 alters the conformation of the PSTAIRE helix of CDK2, T-loop conformation and the relative orientation of the N- and C-terminal lobes (Jeffrey et al., 1995). The T-loop moves out of the active site entrance and no longer blocks the substrate binding site. Extensive hydrogen bonding to cyclin A induces a conformational change to the loop immediately preceding the PSTAIRE helix. This moves the helix into the catalytic cleft towards the ATP. The PSTAIRE contains Glu51 which is important for positioning the ATP phosphates (Jeffrey et al., 1995).

1.1.3 Cyclins

The levels of cyclins involved in the cell cycle oscillate throughout the cell cycle (Figure 1.3). Their periodic accumulation and disappearance are carefully timed for accurate progression through the cell cycle. Four major classes of cell-cycle regulating cyclins exist classified into the A-, B-, D- and E- type cyclins. Each class consists of a small number of closely related sequences that are not functionally equivalent but do exhibit redundancy. For example, *CCNE1* or *CCNE2* knockout mice are viable, but double *CCNE1*/*CCNE2* knockout mice die at embryonic day 11.5 (Satyanarayana and Kaldis, 2009). Cyclin A2 and B1 appear, however, to be the least redundant of the cyclins and knockout of these genes encoding either cyclin is embryonic lethal (Satyanarayana and Kaldis, 2009, Brandeis et al., 1998, Murphy et al., 1997). However, like the cyclins, CDKs also exhibit high levels of redundancy in that in the absence of the appropriate cognate partner, CDKs can be activated by pairing with non-cognate partners (Sherr and Roberts, 2004).

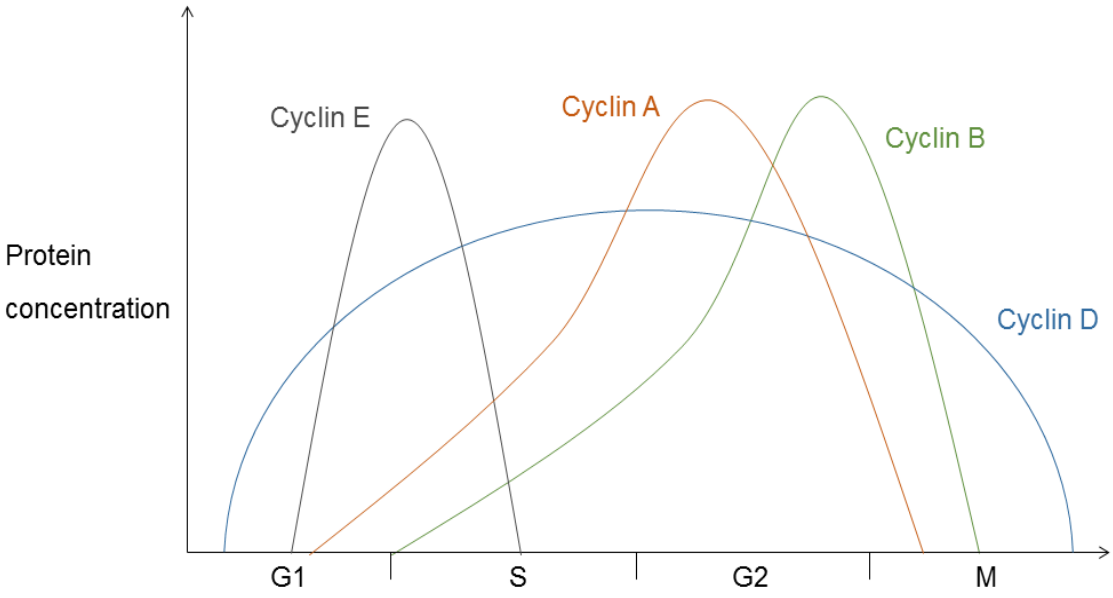

Figure 1.3: Protein levels of cyclins oscillate during the cell cycle. Cyclin D is present throughout the cell cycle, however the other cell cycle cyclins are expressed and degraded periodically.

The levels of cyclins A, B and E rise and fall due to changes in expression and degradation (Figure 1.3, (Vermeulen et al., 2003)). Cyclin D however is not expressed periodically, but rather is synthesised upon growth factor stimulation (Sherr, 1993). Cyclins exhibit diverse sequences, but all share homology in the cyclin box, which is

a region of about 100 amino acids comprising five α helices that bind to CDKs (Brown et al., 1995, Gibson et al., 1994). The cell cycle cyclins share the tandem cyclin box fold (CBF), but differ in the sequences which surround this core fold (Figure 1.4). Cyclins were originally named due to their concentration changes during the cell cycle (Evans et al., 1983), however they were later classified based on their CBF, and many other cyclins not involved in the cell cycle have been identified (Morgan, 2007). Although a large conformational change occurs in the CDK when it binds to its cyclin partner, the cyclin is unchanged between its free and bound states (De Bondt et al., 1993, Brown et al., 1995, Jeffrey et al., 1995).

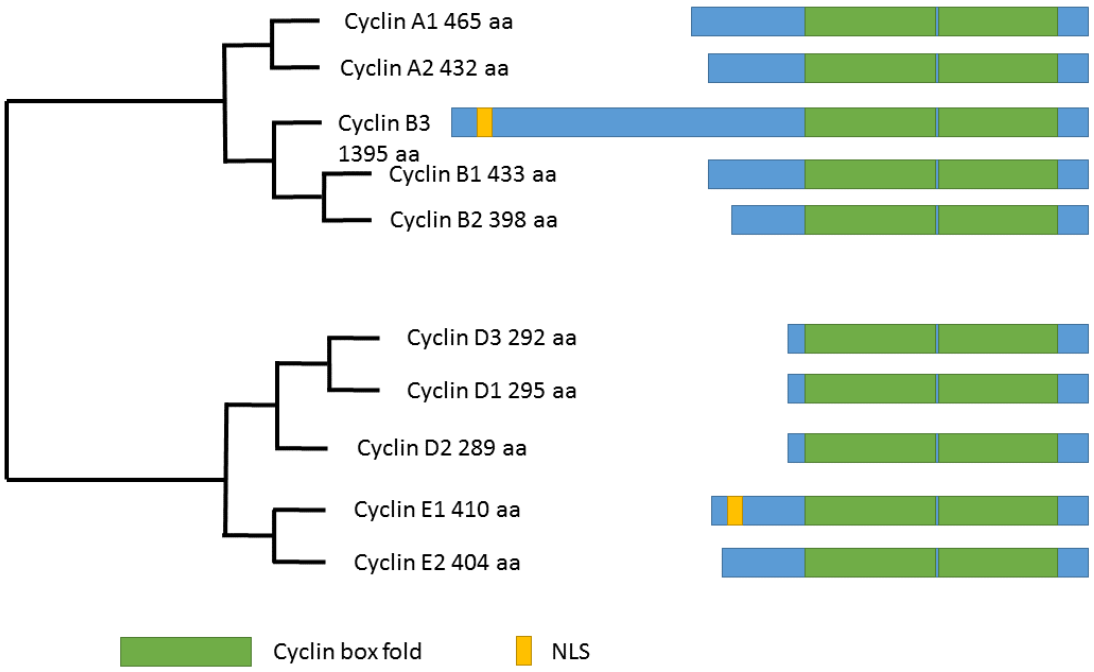

Figure 1.4: Phylogenetic tree of cell cycle cyclins. Principle structural domains are shown. Figure is adapted from Malumbres and Barbacid (2005).

1.1.3.1 Cyclin A

Cyclin A isoforms partner to both CDK1 and CDK2 during the mitotic and meiotic cell cycles. There are two forms of cyclin A, an embryonic and a somatic form, called cyclin A1 and A2 respectively. Cyclin A1 is expressed during spermatogenesis, whereas cyclin A2 is expressed in proliferating somatic cells (Yang et al., 1997, Liu et al., 1998). Targeted deletion of the cyclin A2 gene, *Ccna2*, in mice causes embryonic lethality (Murphy et al., 1997). In contrast, deletion of *Ccna1* (encoding cyclin A1) produces a sterile male mouse due to a block of spermatogenesis before the first

meiotic division, whereas female mice are phenotypically normal (Liu et al., 1998). For the purpose of this thesis cyclin A will be used to refer to cyclin A2.

Cyclin A levels are mainly controlled at the transcriptional level. Cyclin A mRNA accumulates during S-phase and declines at mitosis (Evans et al., 1983). The protein is required at two points in the cell cycle: for the initiation of DNA replication, and hence, the successful completion of S-phase (Girard et al., 1991) and for the completion of mitosis, respectively (Pagano et al., 1992, Walker and Maller, 1991). The role of E2F transcription factors are well characterised in the regulation of cyclin A transcription. Reporter gene assays have revealed that mutation of the cell-cycle-responsive element (CCRE) or cell-cycle-dependent element (CDE) of the cyclin A gene, located at chromosome 4p27, results in deregulation of the gene in G_0/G1 (Huet et al., 1996). This observation led to the hypothesis that the CCRE/CDE region is a repressor binding site (Huet et al., 1996, Schulze et al., 1995). It was subsequently found that this region contains an E2F-binding site (Schulze et al., 1995). E2F is a transcription factor family which are involved in transactivation of several genes whose products are involved in cell cycle regulation or DNA replication, of which some are transcriptional activators and some are transcriptional repressors. Binding of p107 to E2F at the cyclin A promoter represses transcription (Devoto et al., 1992). Cyclins synthesised during G1 can stimulate the expression of cyclin A. CDK2/cyclin E can directly bind to E2F/p107 complexes and activate transcription of cyclin A (Zerfass-Thome et al., 1997). Similarly, cyclin D can activate cyclin A transcription (Schulze et al., 1995). Cyclin A can interact with E2F and inhibit its own expression by CDK2/cyclin A-mediated phosphorylation of E2F (Krek et al., 1995, Xu et al., 1994) completing a negative feedback loop to limit cyclin A expression.

The structure of CDK2/cyclin A was solved in 1995 (Jeffrey et al., 1995), shortly followed by the bovine cyclin A structure (Brown et al., 1995). This CDK2/cyclin A structure does not include the N-terminal region of cyclin A, but does include residues 173-432 that encode the CBF. The N-terminal region is predicted to be unstructured but does contain sequence elements that regulate cyclin A activity that include sites of post-translational modification and destruction boxes (D-boxes) that are recognised by the anaphase-promoting complex/cyclosome (APC/C) and are required for cyclin destruction (Glotzer et al., 1991).

The CBF is common to members of the cyclin family, and includes the CDK2 binding site (Figure 1.5) (Jeffrey et al., 1995). The structure revealed two sequential subdomains of 90 amino acids with identical folds (residues 208-306 and 310-397). This fold comprises a compact five-helical domain termed the cyclin box. Although the two domains have very similar structure, their sequence homology is only 12% (Jeffrey et al., 1995). The CDK2/cyclin A interface consists of many interlocking CDK2 and cyclin A elements, including the conserved PSTAIRE motif of CDK2 (Noble et al., 1997).

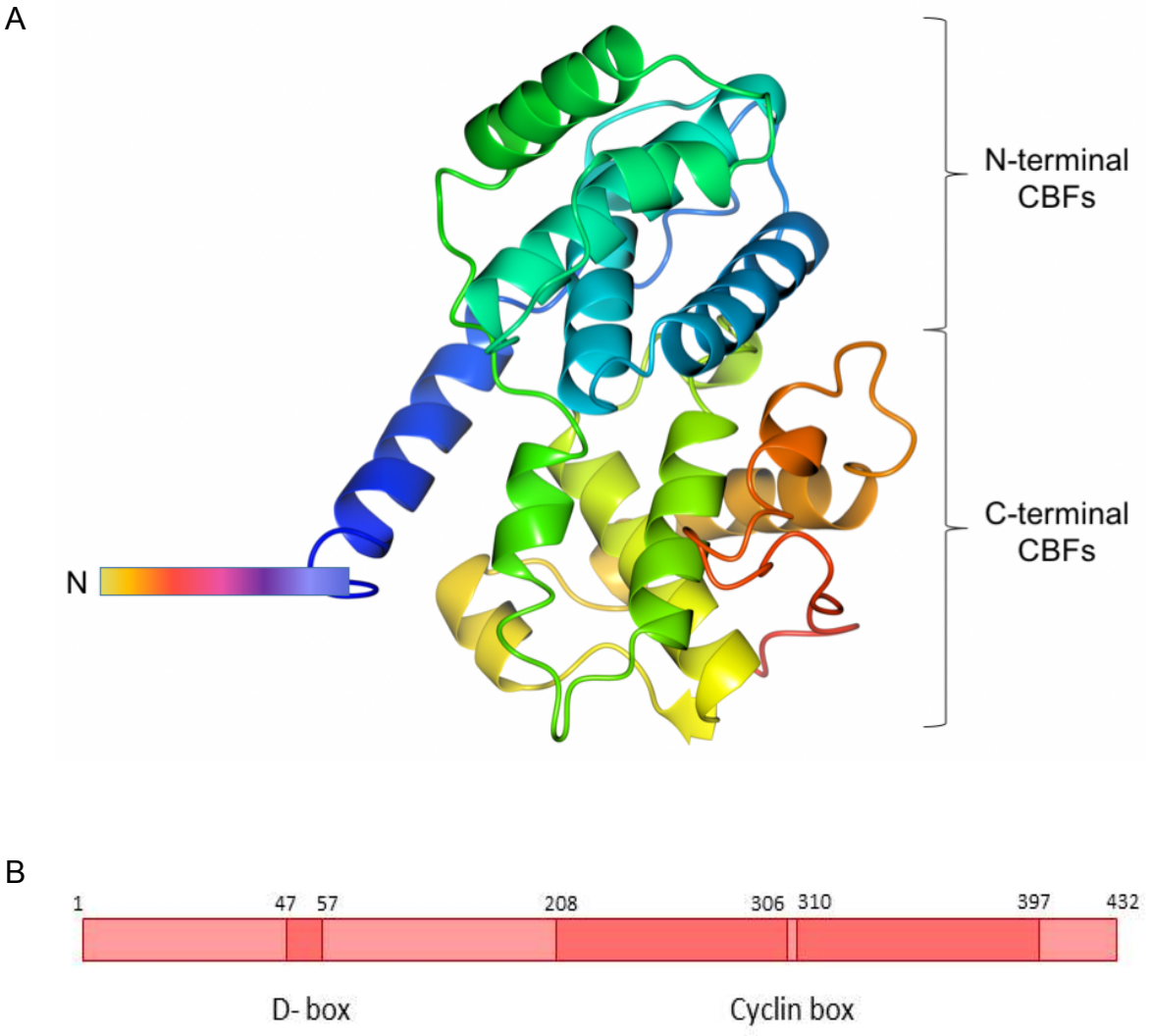

Figure 1.5: Human cyclin A2 structural domains. A) The structure of cyclin A (173-432) is shown. The N-terminal 172 amino acids have not been structurally characterised. B) Schematic of cyclin A. The positions of the D-box and CBFs are shown. The numbers represent amino acid positions. Adapted from (Yam et al., 2002).

The role of cyclin A within the CDK2/cyclin A complex is not simply activation of CDK2. Cyclin A also has a role in substrate recruitment through a hydrophobic patch which binds to substrates via their RXL (arginine, any amino acid, leucine) motif (Adams et al., 1996). Interestingly, the CDK2/cyclin A complex has a wide range of substrates, whereas the CDK2/cyclin E complex has fewer substrates. The two complexes share only a small subset of substrates such as Rb and p27 (Sarcevic et al., 1997). This shows that the cyclin plays a significant role in substrate selection.

It remains poorly understood how specificity for substrates is determined by the cyclin. It might be argued that cyclins are interchangeable and that their substrate specificity arises from their accumulation rather than binding capabilities (Murray, 2004). However, there are some differences in substrate specificity between the cyclins as there are differences in cell cycle events when one cyclin is substituted for another by expression at an adjusted time (Cross et al., 1999).

1.1.4 CDK activation by cyclin binding

CDK2 activation has been extensively studied at the structural level. Binding of cyclin A induces structural changes in the activation loop and the ATP-binding site causing partial activation of CDK2 (Jeffrey et al., 1995). Phosphorylation of Thr160 of CDK2 by CDK-activating kinase (CAK (composed of CDK7, cyclin H and Mat1 in most eukaryotes)) leads to its full activation (Russo et al., 1996b, Stevenson et al., 2002). These events were believed at the time to represent a general mechanism of activation for all CDKs. However, many examples of alternate mechanisms of CDK activation and regulation have emerged since the CDK2/cyclin A structure was published. The discovery of a CDK-binding protein which is not a cyclin, Speedy/Spy1, showed that Thr160 phosphorylation is not always required for full activation of CDK2 as Spy1 can fully activate CDK2 upon binding (Cheng et al., 2005).

Two CDK4/cyclin D structures were published in 2009 and revealed the differences between cyclin D binding to CDK4, and cyclin A binding to CDK2 (Figure 1.6) (Takaki et al., 2009, Day et al., 2009). Cyclin D binds in a more elevated position with a much smaller interface between CDK4 and cyclin D (Figure 1.6B) and binding is not sufficient to drive CDK4 into an active conformation. Even when phosphorylated and bound to cyclin D, the CDK4 active site remains in a conformation which appears to be unable to support catalysis. It is thought that activation occurs when

phosphorylated CDK4/cyclin D forms a Michaelis complex with ATP and protein substrates (Takaki et al., 2009). Determination of the CDK9/cyclin T1 (positive transcription elongation factor b (P-TEFb)) structure also revealed a buried interface that is smaller further than that of CDK4/cyclin D (Baumli et al., 2008). In contrast, the structure of CDK1/cyclin B (Figure 1.6C) is most reminiscent of that of CDK2/cyclin A but again has a slightly enlarged cleft between the CDK1 and cyclin B subunits that suggests it might be subject to additional regulation in this region (Brown et al., 2015). Taken together, the structures of various CDK/cyclin complexes suggest that though there are many common elements to CDK activation by cyclin binding, important differences exist.

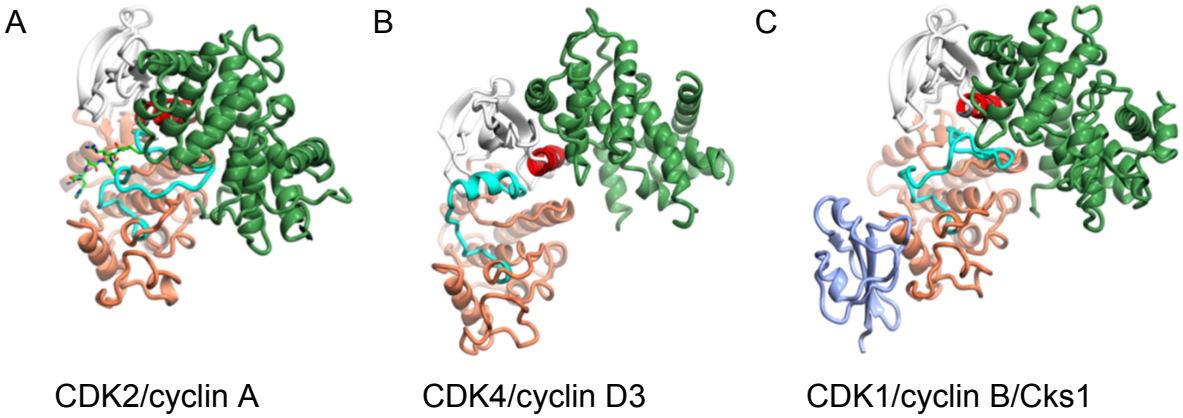

Figure 1.6: Comparison of CDK2/cyclin A structure with that of CDK4/cyclin D3 and CDK1/cyclin B/Cks1. CDK2/cyclin A (A), CDK4/cyclin D3 (B) and CDK1/cyclin B/Cks1 (C). The CDK is coloured in white (N-terminal lobe) and coral (C-terminal lobe) with the C-helix and activation segment coloured red and cyan, respectively. The cyclin is coloured lawn green and Cks1 in ice-blue.

Positive and negative regulators of P-TEFb such as human immunodeficiency virus (HIV1) transactivator of transcription (Tat) protein, hexamethylene bisacetamide-inducible protein 1 (HEXIM1) and BRD4 were found to bind to a site on the C-terminal CBF of cyclin T1 (Baumli et al., 2008, Bigalke et al., 2011, Tahirov et al., 2010, Barboric et al., 2007). Adjacent to this binding site is the binding site of AFF4, a key component of the super elongation complex (Gu et al., 2014). This suggests this cyclin T1 site is somewhat analogous to the N-terminal CBF recruitment site of cyclins A, B, D and E with exceptions being that a specific binding motif is not required and

the binding surface is extended with some interactions being mutually exclusive and others being cooperative.

CDK2/cyclin A regulators bind to the cyclin recruitment site which recognises RXL motifs. No other sites on cyclin A involved in binding regulators have been identified, and therefore the cyclin A and cyclin T1 regulatory/substrate binding site appear to be very different. With further investigation, however, the cyclin A recruitment site could be identified as being a larger area of the cyclin A surface than identified thus far with other substrates and regulators not requiring an RXL motif. For example, S-phase kinase-associated protein 2 (Skp2) has been identified as a cyclin A-binding protein, but does not have an RXL motif and therefore is expected to not bind to the cyclin recruitment site (Ji et al., 2006).

The cyclin can confer inhibitor specificity as well as substrate specificity. Interestingly, it was determined that p27 and p21 act as inhibitors of CDK1- and CDK2/cyclin complexes, but they act as activators for CDK4 and CDK6/cyclin D complexes (Sherr and Roberts, 1999, Soos et al., 1996, Blain et al., 1997, LaBaer et al., 1997). However, recently it was reported that p21 and p27 exert their major effects on CDK4/6 as inhibitors, rather than as activators (Cerqueira et al., 2014). It is believed that CDK/cyclin D complexes are able to sequester p21 and p27 thereby facilitating CDK2/cyclin E activation, and allowing the cell cycle to continue to move forward (Sherr, 2000).

1.1.5 Initiation and control of the G1/S transition

Two major events occur in G1 phase, the restriction point and the G1 checkpoint. The restriction point is the point at which the cell is committed to a new division cycle (Pardee, 1989). In a normal cell, growth factors are required to progress the cell into G1 phase. After the restriction point, no further growth factor stimulation is required (Zetterberg et al., 1995, Johnson and Skotheim, 2013). The G1 checkpoint is the point at which the cell ‘checks’ for DNA damage before beginning DNA synthesis (Bartek and Lukas, 2001).

A new round of the cell cycle occurs upon reception of an external mitogenic signal which starts a signalling cascade with propagation of the signal until it has reached the effector molecule. Effector molecules include transcription factors which are involved in inducing the expression of cyclin D (Shichiri et al., 1993, Sherr, 1995).

Cyclin D binds to and activates CDK4 and CDK6 and these complexes localise to the nucleus due to the nuclear localisation signal (NLS) on cyclin D. In the nucleus CDK4/- and CDK6/cyclin D then mono-phosphorylate retinoblastoma (Rb) (Narasimha et al., 2014). Before phosphorylation by CDKs, Rb binds strongly to E2F transcription factor family members and acts as an inhibitor preventing them from inducing the expression of their target genes (Helin et al., 1992, Dyson, 1998). Phosphorylation by CDK4- and CDK6/cyclin D causes a large change in the molecular shape and dimensions of Rb (Lamber et al., 2013) and leads to its dissociation from E2F, releasing it from repression and switching on transcription of target genes such as cyclin E (Figure 1.7). As the cell progresses through G1, Rb is hyper-phosphorylated by CDK2/cyclin E and this is required for full inactivation of Rb (Harbour et al., 1999, Zarkowska and Mittnacht, 1997). There are 16 potential CDK phosphorylation sites on Rb (Martinsson et al., 2005).The release of E2F from repression by Rb and the expression of cyclin E leads to a positive feedback loop resulting in fully active E2F target genes and expression of proteins required for synthesis and replication (Harbour et al., 1999).

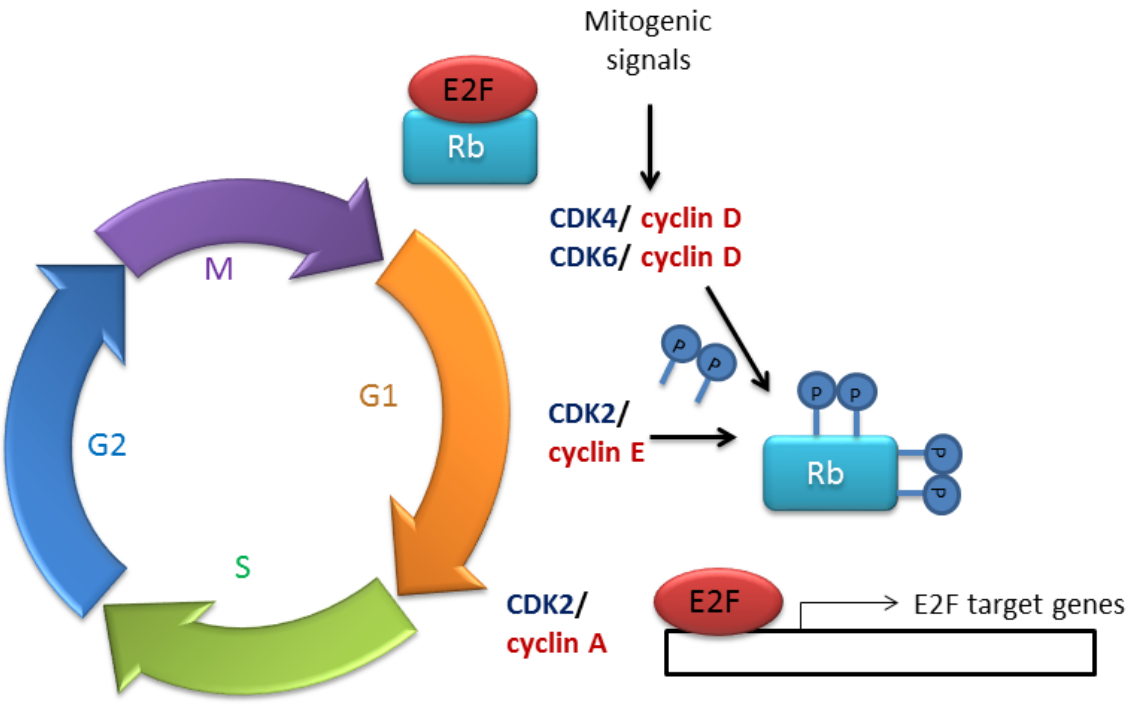

Figure 1.7: Schematic of G1 progression by Rb phosphorylation. Mitogenic signalling activate CDK4/- and CDK6/cyclin D complexes which then phosphorylate Rb. As the cell moves through G1 phase, CDK2/cyclin E complexes become active and also phosphorylate Rb. In a hyperphosphorylated state, Rb no longer binds to E2F which is then released from repression of its transcriptional activity.

Several proteins have been hypothesised to be responsible for transition to post restriction point, referred to at times as the 'R-factor' (Blagosklonny and Pardee, 2002, Foster et al., 2010). Phosphorylation of Rb was also thought to be the key event causing the restriction point to be overcome (Weinberg, 1995). Cyclin D is also postulated to be the R-factor since it acts as a readout of growth factor stimulation (Blagosklonny and Pardee, 2002). Therefore, perhaps it is the integrity of the whole signalling system that is required for passing through the restriction point rather than any one factor alone.

If there is DNA damage at the G1 checkpoint, the cell triggers the DNA damage response (DDR) in an attempt to repair the damage. When the damage is detected, there is a delay in cell cycle progression brought about by the activation of p53 (Kuerbitz et al., 1992, Kastan et al., 1991, Sakaguchi et al., 1998). If the damage is excessive, the cell undergoes apoptosis (Levine, 1997, Evan and Littlewood, 1998). DNA damage can occur due to errors in DNA replication and/or genotoxic damage caused by reactive metabolic toxins or by exogenous radiation such as ultraviolet light. Two protein kinases, ataxia-telangiectasia mutated (ATM) and ataxia-telangiectasia (ATR) are recruited to DNA upon damage. ATM is recruited to DNA double-strand breaks by the Mre11-Rad50-Nbs1 (MRN) complex (Lee and Paull, 2005). ATR is recruited to DNA single-strand breaks via replication protein A (RPA) (Zou and Elledge, 2003). ATM and ATR initiate a signal transduction pathway involving as many as hundreds of proteins involved in the DDR (Matsuoka et al., 2007). When these pathways are defective, cancers can develop. For example, the *BRCA1* and *BRCA2* genes which encode proteins involved in the repair of double strand breaks through homologous recombination, are the most prevalent mutations linked to hereditary breast and ovarian cancer (Fackenthal and Olopade, 2007, Moynahan and Jasin, 2010). Mutation of p53 is another common occurrence in many cancers as p53 is involved in determining whether or not the cell will undergo cell cycle arrest or apoptosis after DNA damage (Nigro et al., 1989, Riley et al., 2008).

1.1.6 Control of the cell cycle through ubiquitin-mediated proteasomal degradation

Cell cycle transitions are often actioned by ubiquitin-mediated degradation of cell cycle regulators. Proteolysis is particularly advantageous due to its irreversibility, thus allowing for directionality. The timing of cell cycle events is co-ordinated by the levels

of various cyclins. Certain cyclins and proteins that regulate CDK/cyclin complexes are subject to ubiquitin-mediated degradation (Teixeira and Reed, 2013, Sudakin et al., 1995). Ubiquitination is the process by which one or several ubiquitin molecules are covalently attached to lysine residues of a protein as a post-translational modification and this can act to target the protein to the 26S proteasome for degradation (Chau et al., 1989, Hochstrasser, 1995).

Ubiquitin chains can be linked through different lysine residues of ubiquitin, or methionine 1, and the nature of the linking determines the response to modification. The residues of ubiquitin that can be used to link to another ubiquitin molecule are Met1, Lys6, Lys11, Lys27, Lys29, Lys33, Lys48 and Lys63 (Komander and Rape, 2012). The linkage type defines the chain conformation, and these chain types can then be specifically recognised. For example, Lys48-linked ubiquitin chains adopt a compact conformation, whereas Lys63-linked ubiquitin chains form an open conformation resembling beads on a string (Tenno et al., 2004, Varadan et al., 2004). Lys48-linked chains lead to proteolysis of the ubiquitinated protein; the polyubiquitin chain is recognised by the ATPase subunit of the proteasome (Lam et al., 2002, Dikic et al., 2009). Other ubiquitin linkages lead to a range of molecular signals in the cell (Ikeda and Dikic, 2008). Similar to the process of phosphorylation, ubiquitination is reversible, and the removal of ubiquitin chains is carried out by specific de-ubiquitinating enzymes (DUBs; (Hochstrasser, 1995, Komander et al., 2009)).

The ubiquitin-proteasome pathway consists of two distinct stages. The first is the covalent attachment of ubiquitin to a protein, and the second is the degradation of the ubiquitinated protein by the 26S proteasome (Figure 1.8). The first stage is mediated by at least three enzymes. First, ubiquitin is transferred to an E1 ubiquitin-activating enzyme in an ATP-dependent manner. This activated ubiquitin is then transferred to an E2 ubiquitin-conjugating enzyme. Finally the ubiquitin is conjugated to the substrate protein by an E3 ubiquitin-ligase (Hershko, 1983, Hershko, 2005). The E3 ubiquitin ligase confers substrate specificity. Multiple ubiquitin molecules can be added, leading to the formation of a polyubiquitin chain, which in the case of Lys48-linked ubiquitin chains and possibly other linkages, is recognised by the 26S proteasome (Finley, 2009). The protein is then destroyed in an ATP-dependent manner.

In humans, there are two E1 proteins, 38 E2 proteins and over 600 E3 ubiquitin ligases (Ye and Rape, 2009). No evidence links the E1 enzymes to cancer, and there have been few reports of E2 dysregulation in cancer (Okamoto et al., 2003). E3 enzymes, on the other hand, are widely reported to be deregulated in cancer (Nakayama and Nakayama, 2006) as are the deubiquitinating enzymes (DUBs) that selectively remove ubiquitin moieties (Hussain et al., 2009).

E3 ubiquitin ligases are grouped into one of three classes based on their conserved structural domains and the mechanism by which the ubiquitin is transferred from the E2. The Really Interesting New Gene (RING) family catalyses the transfer of ubiquitin from the E2 onto a lysine residue of the substrate (Deshaies and Joazeiro, 2009). Whereas, the homology to E6AP C-terminus (HECT) and RING-between-RING (RBR) family of E3s play a more direct role in catalysis of ubiquitin transfer by forming a catalytic thioester intermediate between an active site cysteine and the C-terminus of the ubiquitin before the ubiquitin is transferred onto the substrate (Berndsen and Wolberger, 2014).

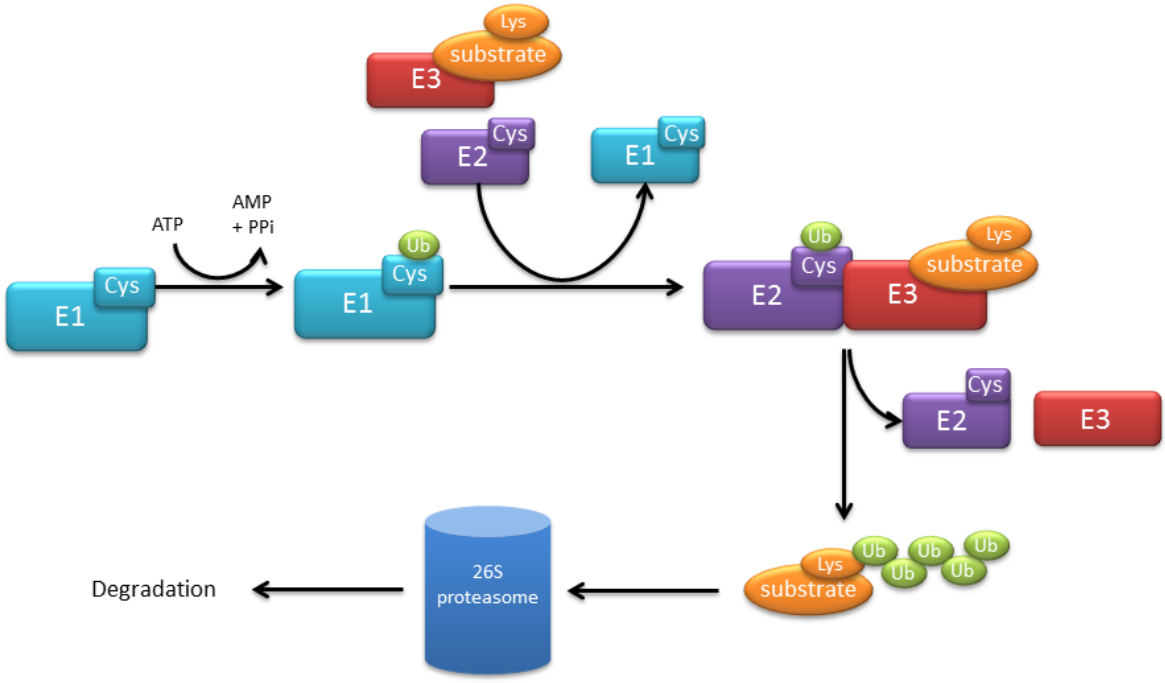

Figure 1.8: Schematic of the ubiquitin-proteasome cascade. Three enzymes are required for ubiquitination of protein substrates, an E1 ubiquitin-activating enzyme, an E2 ubiquitin-conjugating enzyme and an E3 ubiquitin ligase. Shown here is the mechanism of transfer used by the RING family of ubiquitin ligases. Lys48-linked ubiquitin chains are recognised by the 26S proteasome and the substrate is degraded.

The levels of cell cycle regulators are controlled through ubiquitination by two key E3 ubiquitin ligases, the Skp1/Cul1/F-box (SCF) and anaphase promoting complex/ cyclosome (APC/C) complexes. SCF complexes belong to the RING-type E3 ubiquitin ligase family (Joazeiro and Weissman, 2000). Each SCF complex includes an F-box protein, a cullin subunit, an adaptor protein which bridges the cullin and F-box protein and a zinc finger RING protein. F-box proteins share a conserved F-box region which is required for binding to the adaptor protein Skp1 (Schulman et al., 2000). In humans there are 69 known F-box proteins (Jin et al., 2004). These F- box proteins (FBPs) can be classified into three classes: those with WD40 repeats (FBXWs), those with leucine rich repeats (FBXLs) and those with diverse domains (FBXOs) (Frescas and Pagano, 2008). Many FBPs have been reported to require phosphorylation of a substrate before binding can occur (Ganoth et al., 2001, Orlicky et al., 2003). The extent of phosphorylation has been found to differ between substrates. Cyclin E is required to be phosphorylated at multiple sites for recognition by the Fbw7 complex (Hao et al., 2007). In contrast, p27 requires mono-phosphorylation for recognition by the SCF^{Skp2} complex (Hao et al., 2005, Ganoth et al., 2001). Dimerisation of the FBP has also been reported for Fbw7 for the ubiquitination of cyclin E (Welcker et al., 2013). The requirement of an accessory protein for ubiquitination of one and possibly more substrate(s) has been reported for the FBXL, Skp2 (Ganoth et al., 2001, Spruck et al., 2001) The difference in binding requirements might be due to the FBP needing to bind many biologically diverse proteins thus dimerisation, varying levels of phosphorylation and accessory proteins may facilitate the vast amount of substrates required to bind.

The SCF and APC/C complexes control the proteolysis of many key regulators of the cell cycle such as the cyclins and CDK inhibitors. It is believed that the SCF and APC/C complexes play a large role in cancer progression (Nakayama and Nakayama, 2006), however only the dysregulated activity of some of the substrate recognition subunits has been shown to result in tumourigenesis.

1.2 The SCF complex

1.2.1 The SCF^{Skp2} ubiquitin ligase

SCF complexes are involved in the degradation of hundreds of proteins. SCF substrate specificity is conferred by F-box proteins which are the variable units. These proteins share an F-box domain which mediates binding to Skp1 (Figure 1.9). The name F-box comes from the first protein identified as having this domain; cyclin F (Bai et al., 1996). There are 69 F-box proteins, of which only three (Skp2, β-TrCP and Fbxw7) have been extensively studied due to their roles in regulating the activities of tumour suppressor and activator proteins that regulate cancer progression (Skaar and Pagano, 2009, Jia and Sun, 2011).

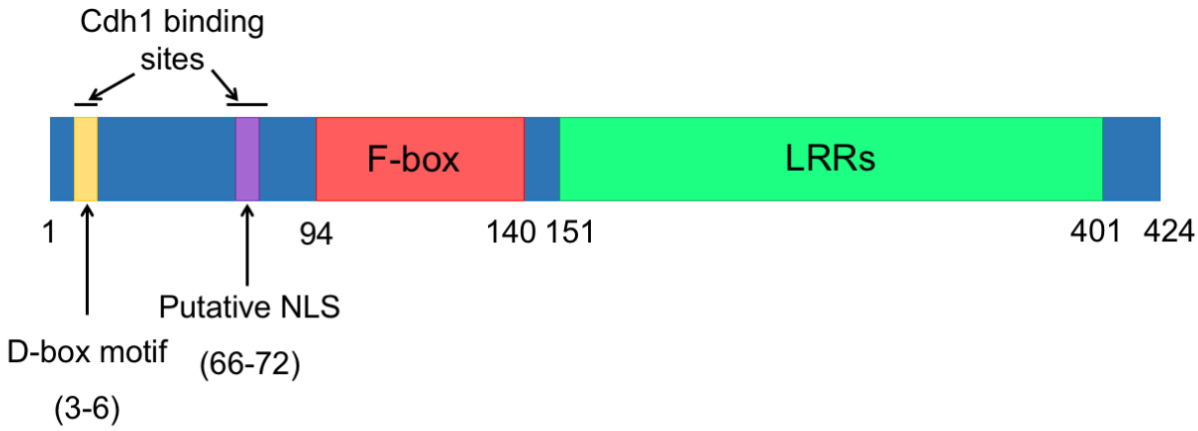

Figure 1.9: Functional domains of Skp2. The N-terminus of Skp2 is disordered and contains multiple binding sites including the Cdh1 binding site, as well as phosphorylation sites and an NLS.

Many Skp2 targets, such as E2F1, do not accumulate in Skp2 knockout mice suggesting that there is redundancy in the ubiquitination of these proteins (Nakayama and Nakayama, 2006). Levels of p27, however, do increase in Skp2 $^{-/-}$ mouse embryonic fibroblasts (MEFs) and the Skp2 knockout phenotype can be rescued by deletion of p27, showing that the Skp2/p27 axis is non-redundant and p27 is a key substrate of Skp2 *in vivo* (Nakayama et al., 2000, Nakayama et al., 2004). Skp2 knockout mice display reduced organ size and markedly larger, polyploid nuclei (Nakayama et al., 2004).

1.2.2 SCF^{Skp2} substrates

There are many targets of the SCF^{Skp2} complex including p21 (Bornstein et al., 2003), p27 (Tsvetkov et al., 1999), p57 (Kamura et al., 2003), p130 (Tedesco et al., 2002), cyclin E (Nakayama et al., 2004) and E2F1 (Marti et al., 1999). p21 was the first CDK inhibitor (CKI) to be discovered, and is a universal inhibitor of CDKs (Xiong et al., 1993a). p130 is a member of the retinoblastoma family of proteins, also known as pocket proteins (Mulligan and Jacks, 1998), which associate with and inhibit the E2F family of transcription factors. Like p27, p130 can also inhibit CDK2/cyclin E and CDK2/cyclin A complexes, and p130 is also down-regulated at the G1-S boundary (Bhattacharya et al., 2003). Cyclin E is ubiquitinated by SCF^{Skp2} during late G1 and S phases of the cell cycle. Binding to CDK2 was found to protect cyclin E from ubiquitination by SCF^{Skp2} (Clurman et al., 1996, Nakayama et al., 2000). The reason for this is unclear, however it could function to ensure prompt switching of CDK2/cyclin E complexes for CDK2/cyclin A complexes as cyclin A levels rise toward the end of G1-phase. Auto-phosphorylation of cyclin E by CDK2/cyclin E on Thr380 is required for recognition by the SCF^{Skp2} complex (Yeh et al., 2001).

1.2.3 The SCF^{Skp2} accessory factor, Cks1

Cks1 was originally identified in 1986 in fission yeast through a genetic screen to identify multicopy suppressors of a Cdc2 temperature-sensitive mutation (Hayles et al., 1986). It was subsequently shown to be an essential gene producing a mitotic arrest in *S. pombe* cells (Hadwiger et al., 1989). The human homologue was identified in 1987 in complex with CDK1 (Draetta et al., 1987, Lee and Nurse, 1987). Cks1 is a member of the Cdc kinase subunit (Cks)/ suppressor of Cdc 1 (Suc1) family of small proteins which interact with CDKs. The structure of Cks1 bound to CDK2 was published in 1996 where its location bound to the CDK2 C-terminal domain suggested that it might be in a position to increase CDK2 activity towards phosphorylated substrates through phospho-amino acid binding to its anion-binding pocket (Bourne et al., 1996). Cks1 was then identified as an essential phosphomotif-binding component of the SCF^{Skp2} complex for degradation of p27. Together with Skp2 it forms the substrate recognition site that binds to the phosphorylated Thr187 of p27 and mediates the majority of the interaction of the SCF^{Skp2} complex with p27 (Ganoth et al., 2001). p57 and p21 have been shown to be ubiquitinated *in vitro* by the SCF^{Skp2}-Cks1 complex (Bornstein et al., 2003, Kamura et al., 2003). This role of Cks1 in SCF-

mediated ubiquitination is believed to be specific to Skp2 as no other F-box proteins have been found to bind to Cks1 (Hao et al., 2005).

Mammalian cells contain two Cks paralogues, Cks1 and Cks2 sharing 80% sequence identity (Figure 1.10). Cks1 and Cks2 both contain a four-stranded β-sheet surface, which is involved in binding CDKs. They also both have an anion-binding site which can bind to phosphate, sulphate or acidic residues (Arvai et al., 1995, Parge et al., 1993). It was initially surprising when it was found that Cks2 cannot substitute for Cks1 in the ubiquitination of p27 (Ganoth et al., 2001, Spruck et al., 2001), an observation explained by the finding that Skp2 binds to Cks1 but not Cks2 (Ganoth et al., 2001, Spruck et al., 2001). However, both Cks1 and Cks2 bind to CDK2 (Bourne et al., 1996) and it was therefore proposed that the binding sites of Skp2 and CDK2 on Cks1 are mutually exclusive. When the structure of Cks1 bound to Skp2 was published (Hao et al., 2005), it was indeed shown that these sites do not in fact overlap and that the Cks1/CDK2 interaction could remain intact while Cks1 is bound to the SCF^{Skp2} complex (Hao et al., 2005). The Pagano and Hershko groups used site-directed mutagenesis to confirm where Skp2, CDK2 and p27 bind on the Cks1 surface and subsequently demonstrated using these mutant proteins that all three interactions are required for Cks1 to promote p27 ubiquitination (Sitry et al., 2002).

```
Cks1    MSHKQIYYSDKYDDEEFEYRHVMLPKDIAKLVPKTHLMSESEWRNLGVQQSQGWVHYMIH
Cks2    MAHKQIYYSDKYFDEHYEYRHVMLPRELSKQVPKTHLMSEEEWRRLGVQQSLGWVHYMIH
        *:********** **.:********::::* *********.***.****** ********

Cks1    EPEPHILLFRRPLPKKPKK
Cks2    EPEPHILLFRRPLPKDQQK
        ***************. :*
```

Figure 1.10: Sequence alignment of Cks1 and Cks2. Sequence homology is high, but despite this, only Cks1 binds to Skp2. Clustal W was used for sequence alignment (Larkin et al., 2007). An asterisk indicates positions that are fully conserved. A colon indicates conservation between groups of strongly similar properties, scoring >0.5 in the Gonnet PAM 250 matrix. A full stop indicates conservation between groups of weakly similar properties, scoring =<0.5 in the Gonnet PAM 250 matrix.

Until recently, the major roles of Cks1 were thought to be the control of cell cycle progression and facilitating the degradation of p27. However, emerging evidence suggest Cks1 also plays a role in growth signalling pathways, apoptosis and the DNA

damage response. A few studies have suggested a role for Cks1 in MAPK, JAK-STAT and NF-κB pathways. The role of Cks1 in these signalling pathways appears to be independent of Skp2 and p27 (Shi et al., 2010). The DNA repair pathway involves inactivation of CDK2 by degradation of its activating phosphatase, Cdc25A. Cks1 binding to CDK2 can override Tyr15 phosphorylation of CDK2 activating it (Liberal et al., 2012). Therefore Cks1 may contribute to oncogenesis following aberrant execution of DNA repair.

Similar to the Skp2 knockout mice, $Cks1^{-/-}$ mice are smaller than wild type (WT) littermates and have increased levels of p27 and cyclin E (Spruck et al., 2001). This accumulation of p27 occurs despite phosphorylation of Thr187, showing that Cks1 is required for p27 binding to the SCF^{Skp2} complex. Parallel experiments showed that Cks1 is required for the *in vitro* ubiquitination of p27 (Ganoth et al. 2001). Cells derived from $Cks1^{-/-}$ mice proliferate slowly probably due to the increase in p27 levels (Spruck et al., 2001). Similarly, $Cks2^{-/-}$ mice are viable with no major defects apart from sterility. However, Cks1 and Cks2 double knockout mice are not viable indicating that they have a redundant function (Spruck et al., 2003, Martinsson-Ahlzen et al., 2008). Silencing of Cks1 and Cks2 in MEFs leads to cell cycle arrest in G2, replication and polyploidy, signifying their essential role in recruiting substrates to CDK1/cyclin B during mitosis (Martinsson-Ahlzen et al., 2008).

1.3 The APC/C

The APC/C is a high molecular weight complex of 1.2 MDa composed of 13 subunits (Schreiber et al., 2011), which has specific degradative activity for cell cycle regulatory proteins (Chang et al., 2014). Substrate recognition by the APC/C is mediated by substrate binding to one of two co-activator proteins, Cdc20 or Cdh1 (also known as fizzy and fizzy-related 1, respectively). In contrast to the way in which FBPs commonly recognise phosphodegron motifs, APC/C ubiquitin ligases recognise specific degron sequences. Substrates that are targeted to the APC/C for ubiquitination encode a destruction box (D-box), the canonical sequence of which is RXXL (Glotzer et al., 1991, Pfleger and Kirschner, 2000). Most substrates also have a conserved KEN (lysine, glutamate, asparagine) box motif (Chan et al., 2013, Pfleger and Kirschner, 2000). Other motifs that are less well conserved motifs are the A box and the GEN box (Littlepage and Ruderman, 2002, Castro et al., 2003). These motifs are

degenerate and the presence of one or more motifs varies from substrate to substrate (Pines, 2011). APC/C substrates include mitotic cyclins (cyclin A and B), mitotic kinases and their regulators (Aurora A, survivin, Plk1); a protein involved in coordination of anaphase (securin); proteins involved in replication (such as geminin); and proteins involved in ubiquitin-mediated degradation (such as Skp2) (García-Higuera et al., 2008). Many of the substrates of the APC/C complex are overexpressed in cancer and are associated with poor prognosis. It is unsurprising therefore that $Cdh1^{+/-}$ mice develop a range of tumours in later life including tumours of the lungs, liver, kidneys, testes and sebaceous gland (García-Higuera et al., 2008).

There is a multitude of interplay between the APC/C and its substrates. For example, the APC/C^{Cdh1} degrades Cdc20 ensuring that only Cdh1 is active during this period. Additionally, the APC/C is activated by CDK1/cyclin B and cyclin B is degraded by the APC/C^{Cdh1} complex therefore ensuring that once cyclin B levels reach a certain point, cyclin B undergoes proteolysis (Harper et al., 2002). CDK2 is involved in the removal of Cdh1 from the APC/C complex through phosphorylation, and CDK2 is involved in protecting Skp2 from degradation through phosphorylation of Skp2 (Fukushima et al., 2013, Yam et al., 1999, Rodier et al., 2008). There is also much crosstalk between the APC/C and SCF complexes. The SCF scaffold with the F-box substrate receptor β-TrCP is responsible for ubiquitination of Cdh1 leading to its degradation and the APC/C^{Cdh1} complex is responsible for degradation of Skp2 (Fukushima et al., 2013).

Use of mouse genetic models have shown that Cdh1 functions as a haploinsufficient tumour suppressor. Complete inactivation of Cdh1 leads to embryonic lethality due to placental defects. Knockout of Cdh1 in MEFs causes defects in proliferation and accumulation of chromosomal aberrations (García-Higuera et al., 2008). Cdh1 is also involved in the degradation of many other cell cycle regulators such as cyclin A, cyclin B and Cdc6 (cell division cycle 6) and therefore the detrimental effect of Cdh1 loss on cells is not only due to dysregulation of Skp2 (García-Higuera et al., 2008). Cdh1 is required to keep Skp2 levels, and other substrate levels, in check during G1 phase in order to control for proper G1/S transition (Figure 1.11) as Cdh1 ablation not only accelerates S-phase entry, but it also lowers the requirement for cyclin E1 for progression through G1 phase (Yuan et al., 2014). The APC/C is regulated by early mitotic inhibitor 1 (Emi1), which binds to the substrate binding regions of Cdh1 and Cdc20 blocking substrate interaction (Miller et al., 2006).

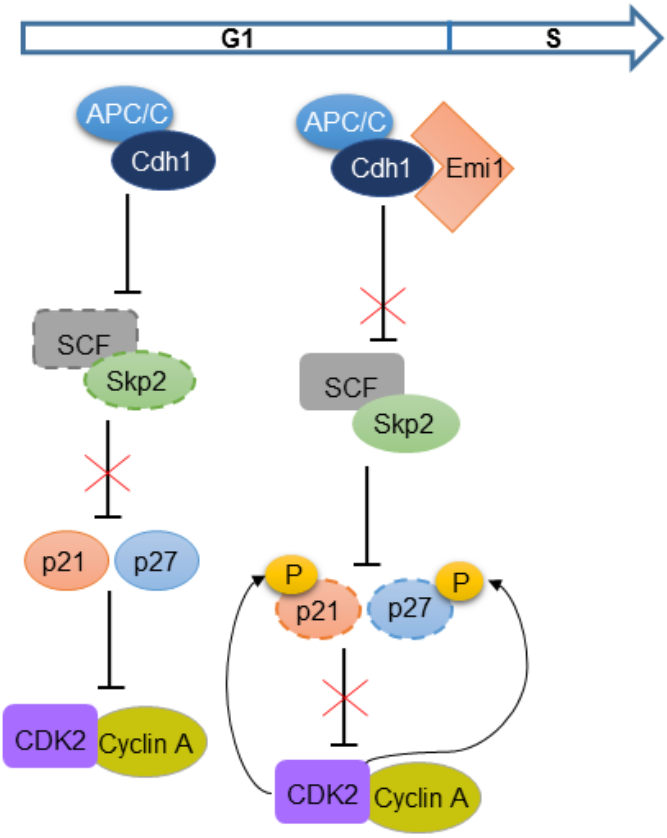

Figure 1.11: Cell cycle transitions are controlled in part by ubiquitin-mediated degradation. During early G1 phase, the APC/C Cdh1 complex is active leading to degradation of Skp2. During mid and late G1, Cdh1 becomes inactive and levels of Skp2 rise leading to degradation of p21 and p27 allowing the cell to progress through to S phase. Skp2 remains active during S- and G2-phases.

1.4 Skp2 gene expression

The *Skp2* gene is found on chromosome 5p13. The expression of *Skp2* changes periodically throughout the cell cycle, however, it is believed that Skp2 protein levels are mainly determined by the rate of Skp2 degradation (Bashir et al., 2004, Wei et al., 2004). Skp2 expression is regulated by multiple transcription factors. These include MYC, FOXO3a, E2F1 and many others (Bretones et al., 2011, Wu et al., 2013, Zhang and Wang, 2006, Schneider et al., 2006). *Skp2* expression increases at the mRNA level in human myeloid leukaemia K562 cells with conditional c-Myc expression. c-Myc binds to the E-box region of the *Skp2* promoter (Figure 1.13) and c-Myc-induced *Skp2* expression leads to reduced p27 levels, demonstrating another mechanism for

c-Myc-dependent transformation (Bretones et al., 2011). Another member of the Myc family of transcription factors, MYCN was also found to be a positive regulator of *Skp2* expression (Evans et al., 2015). MYCN amplification is strongly associated with advanced-stage aggressive neuroblastoma and the relationship of MYCN with Skp2 has been suggested as a likely oncogenic pathway leading to the observed correlation with advanced disease (Bell et al., 2007, Westermann et al., 2007).

In 2012, Wu and colleagues identified FOXO3a as a negative regulator of the *Skp2* gene (Figure 1.13) (Wu et al., 2013). Overexpression of FOXO3a causes cell cycle arrest and apoptosis (Dansen and Burgering, 2008), and loss of FOXO3a expression or cytoplasmic relocalisation has been reported for many human cancers (Yang and Hung, 2009). Interestingly, Wu and colleagues have found that FOXO3a also interacts directly with the SCF complex and inhibits its ubiquitin ligase activity. Further studies will be required to investigate the mechanism by which FOXO3a is inhibiting the SCF^{Skp2} complex.

E2F1 is another key driver of *Skp2* expression (Figure 1.12 and 1.13) (Zhang and Wang, 2006). CDK2/cyclin E activates E2F1 indirectly through inactivation of Rb, Skp2 is therefore able to positively affect its own expression through promotion of the degradation of the CDK2/cyclin E inhibitor, p27 (Figure 1.12). Shortly after the discovery of E2F1 as a key inducer of Skp2 expression, Yung and co-workers investigated whether Skp2 creates an autoinduction loop resulting in high levels of Skp2, low p27 levels and inactivated Rb (Yung et al., 2007). They found that when Skp2 is ectopically overexpressed, there was increased activity on the Skp2 promoter. Conversely, Skp2 knockdown reduced Skp2 promoter activity. They also looked at the rate of S-phase entry and the time to mitogen independence (restriction point), using MEFs derived from a knock-in mouse with a p27 mutation of Thr187 to alanine. They found that MEFs with mutated p27, which would be expected to have a defective autoinduction loop, took much longer than WT MEFs to reach mitogen independence. However, this did not result in a general decrease in the rate of cell cycling, as the time taken to reach S-phase was similar between WT and p27 mutated MEFs when continuously exposed to mitogenic stimuli (Yung et al., 2007).

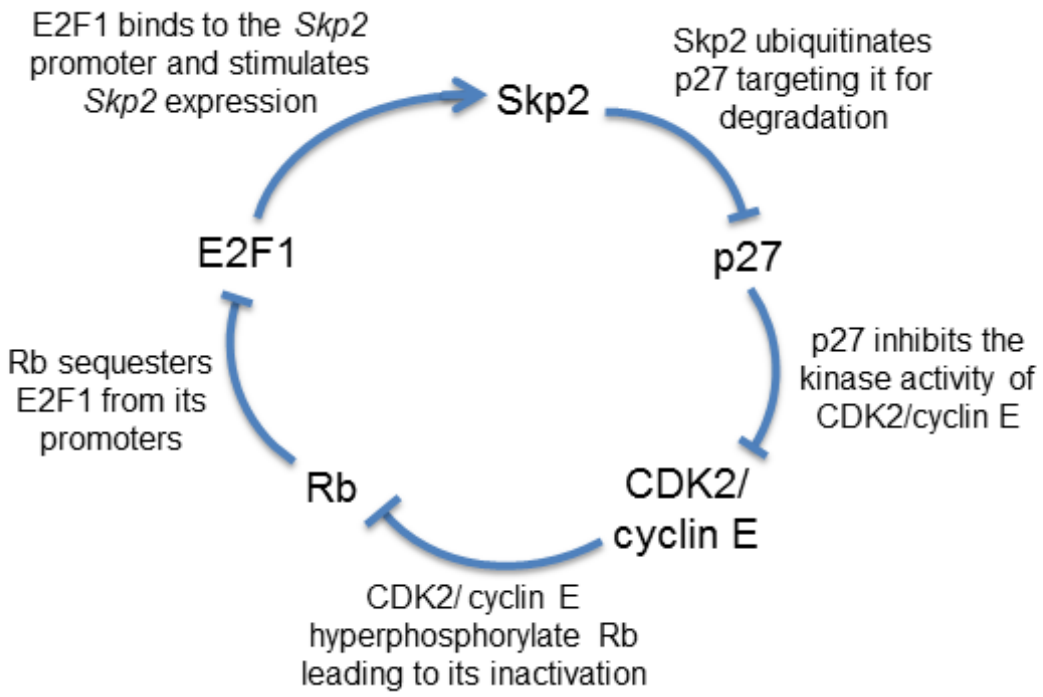

Figure 1.12: The Skp2 autoinduction loop. Skp2 is able to stimulate its own expression without the requirement of exogenous mitogens. Adapted from (Yung et al., 2007)

Schneider and colleagues found that the *Skp2* gene is also regulated by the non-canonical NF-κB pathway upon stimulation by IKKα. They showed that IKKα siRNA treatment leads to down-regulation of Skp2. Increased p27 levels also followed IKKα treatment. They determined that the relB/p52 dimer of the NF-κB family is involved in binding and activating the *Skp2* gene (Schneider et al., 2006).

The mammalian target of Rapamycin (mTOR) has also been found to be involved in *Skp2* gene regulation (Figure 1.13). mTOR is a downstream mediator or the PI3K/Akt pathway. Rapamycin was found to decrease Skp2 both at the transcript and protein levels suggesting that mTOR regulates *Skp2* gene expression. Rapamycin was also found to stabilise p27 levels in breast cancer (Shapira et al., 2006). Consistent with this finding, increased PI3K/Akt pathway activity leads to reduced p27 protein levels (Liang et al., 2002, Yakes et al., 2002).

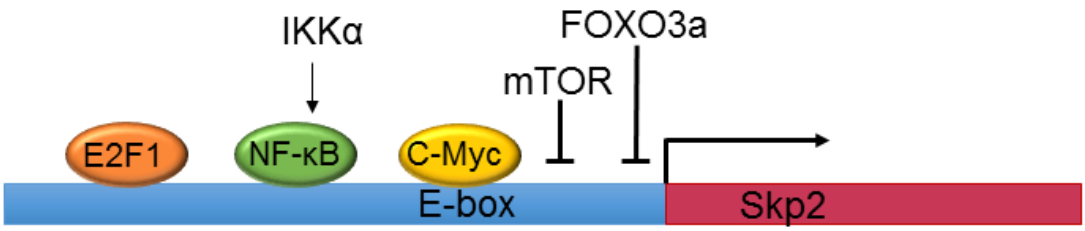

Figure 1.13: Summary of Skp2 gene expression. E2F1, NF-κB and c-Myc are transcription factors which have been found to positively regulate *Skp2*. mTOR and FOXO3a are negative regulators of *Skp2*.

1.5 Regulation of Skp2 by post-translational modification and effects of modification on Skp2 activities

Unlike other subunits of the SCF^{Skp2} complex such as Skp1 and Cul1, the levels of Skp2 change throughout the cell cycle. The most established cause of changes in Skp2 levels is due to ubiquitin-mediated degradation of Skp2. Skp2 is targeted to the APC^{Cdh1} complex during early G1 and mitosis (Lin and Diehl, 2004). However, recent studies have revealed that the phosphorylation state, acetylation state and perhaps even cyclin A-bound state of Skp2 has an effect on its recruitment to the APC^{Cdh1} complex (Rodier et al., 2008, Inuzuka et al., 2012, Gao et al., 2009). Cdh1 binds to two regions within the N-terminal regulatory region of Skp2. The first region is the D-box motif, a motif commonly found in Cdh1 substrates. The consensus sequence for this motif is RXXLXXXXN/D/E (Li and Zhang, 2009). The second region encompasses the NLS (Figure 1.9).

Skp2 is phosphorylated by CDK2/cyclin A on residues 64 and 72 and these phosphorylation events block the association of Skp2 with Cdh1 (Rodier et al., 2008). This modification does not affect the activity of the SCF^{Skp2} complex. However, phosphorylation of Ser64 and to a lesser extent, Ser72, affects the stability of Skp2 by directly affecting Cdh1 binding and subsequent ubiquitination. Consistent with this model, they found that Ser64 phosphorylation occurs in G1 phase when Skp2 is known to be most stable. They then investigated whether a dephosphorylation event is required in order to trigger Skp2 degradation. They found that the phosphatase Cdc14B is responsible for dephosphorylating Skp2 on Ser64 and thus inducing Skp2

ubiquitination and subsequent degradation (Rodier et al., 2008). Therefore, the opposing activities of CDK2 and Cdc14B are crucial for regulating entry into S-phase.

Akt is also able to phosphorylate Skp2 on Ser72 (Gao et al., 2009) Sequence analysis of Skp2 revealed an Akt phosphorylation consensus sequence around Ser72, and phosphorylation of Ser72 was confirmed through an *in vitro* kinase assay. The Akt pathway functions to promote cell growth and cell survival (Song et al., 2005). For many Akt substrates such as p27, p21 and FOXO1, phosphorylation results in masking of their NLS combined with 14-3-3 binding leading to cytoplasmic localisation. Phosphorylation of Skp2 by Akt also leads to masking of its NLS and subsequent nuclear export (Gao et al., 2009). There have been many reports of increased cytoplasmic Skp2 levels in cancers and this study provided a molecular mechanism for this phenomenon (Drobnjak et al., 2003, Radke et al., 2005, Dowen et al., 2003). A concurrent publication with similar findings was that of Lin and co-workers (Lin et al., 2009). They too found that Akt-mediated phosphorylation of Skp2 leads to nuclear export and stabilisation via direct blocking of the Skp2/Cdh1 interaction. The cytoplasmic localisation is stabilised by 14-3-3β binding and this interaction requires phosphorylation of Skp2 at Ser72. Interestingly, Lin and co-workers found that Skp2 binds more tightly to the SCF complex when phosphorylated, suggesting that Akt might mediate SCF complex assembly. In contrast, Bashir et al. (2010) showed that SCF assembly is not affected by either Ser64 or Ser72 phosphorylation.

In 2012, Inuzuka and colleagues identified acetylation sites within the Skp2 NLS/Cdh1-binding site (Inuzuka et al., 2012). They reported that p300 can acetylate Skp2 on residues K68 and K71, and hypothesised that this modification can affect the interaction of Skp2 with Cdh1. Depletion of p300 led to a decrease in Skp2 levels, particularly during G1-phase (Inuzuka et al., 2012). SIRT3 (a deacetylase) was able to deacetylate residues K68 and K71. Members of the Sirtuin family are involved in tumourigenesis and cellular metabolism, and SIRT3 specifically has a tumour suppressive function (Kim et al., 2010, Zhu et al., 2014). In support of this tumour suppressive function, Inuzuka and colleagues found an inverse correlation between Skp2 and SIRT3 immunohistochemical staining in breast cancer samples. They hypothesised that acetylation of residues 68 and 71 might have an effect on the sub-cellular localisation of Skp2 as acetylation of lysines within an NLS often leads to

cytoplasmic accumulation (di Bari et al., 2006, Dietschy et al., 2009). High levels of cytoplasmic Skp2 have been reported in many clinical samples, and is correlated with aggressive malignancy and poor prognosis (Radke et al., 2005, Signoretti et al., 2002).

Akt phosphorylation, but not Akt abundance, fluctuates throughout the cell cycle. Akt1 is a CDK2/cyclin A substrate and its level of phosphorylation mirrors the expression pattern of cyclin A. Phosphorylation of Akt on Ser477 and Thr479 leads to Ser72 phosphorylation of Skp2 by Akt, and subsequent stabilisation of Skp2 (Liu et al., 2014). Phosphorylation of Akt on Ser477 and Thr479 also triggers Ser473 and Thr308 phosphorylation by mTORC2 and PDK1 respectively leading to full activation of Akt (Liu et al., 2014). Therefore CDK2/cyclin A activity indirectly increases Skp2 levels as well as directly affecting Skp2 levels by Ser64 phosphorylation (Rodier et al., 2008).

A

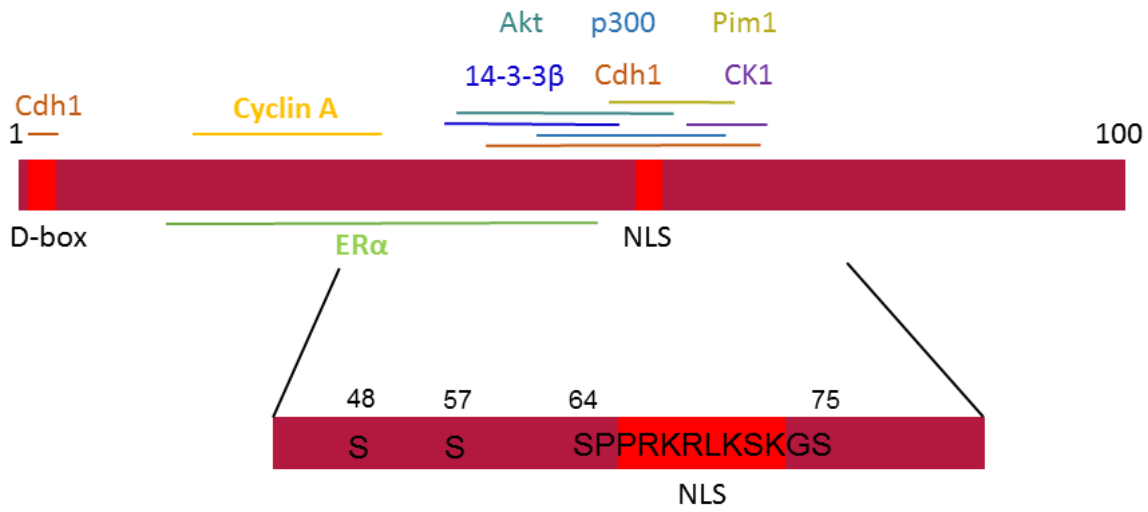

B

Site of modification	Type of modification	Modifier	Effect on Skp2
Ser64	phosphorylation	CDK2/cyclin A, Pim1	Increased stability
Lys68	acetylation	p300	Cytoplasmic localisation, dimerisation
Lys71	acetylation	p300	Cytoplasmic localisation, dimerisation
Ser72	phosphorylation	Akt, Pim1	Increased stability, induction of Ser75 phosphorylation, increased cytoplasmic localisation
Ser75	phosphorylation	CK1	Increased stability, increased cytoplasmic localisation

Figure 1.14: The N-terminus of Skp2 is highly modified and involved in many protein-protein interactions. A) Proteins which interact with Skp2. Lines indicate the approximate interaction site. Ser48 and Ser57 phosphorylation have been identified only by mass spectrometry (Dephoure et al., 2008). B) Kinases and acetylases that modify the Skp2 N-terminus.

In summary, Skp2 is regulated through modifications and protein-protein interactions within its N-terminus (Figure 1.14). The NLS, 14-3-3β binding and acetylation by p300 regulate Skp2 cellular localisation; phosphorylation of residues around and within the Cdh1 binding site regulate the stability of Skp2 and might also regulate SCF^{Skp2} formation; and cyclin A binding within this region may have a regulatory role or may be required for SCF^{Skp2} complex formation. Ser48 and Ser57 phosphorylation has

been identified by MS analysis (Dephoure et al., 2008), however the kinases responsible and the effect, if any, on Skp2 activity have not been determined.

1.6 Skp2B

A splice variant of Skp2 was identified in 2001 (Ganiatsas et al., 2001) originally called Skp2 C-terminal variant (Skp2-CTV), it was later renamed Skp2B. Since its discovery, our knowledge of Skp2B has increased slowly and the majority of the work done on this variant has been carried out by a single group led by Doris Germain. This group have found that Skp2B lacks the last three leucine-rich repeats (LRRs) and the C-terminal tail (Figure 1.15), and is not involved in the degradation of p27 (Radke et al., 2005, Ganiatsas et al., 2001).

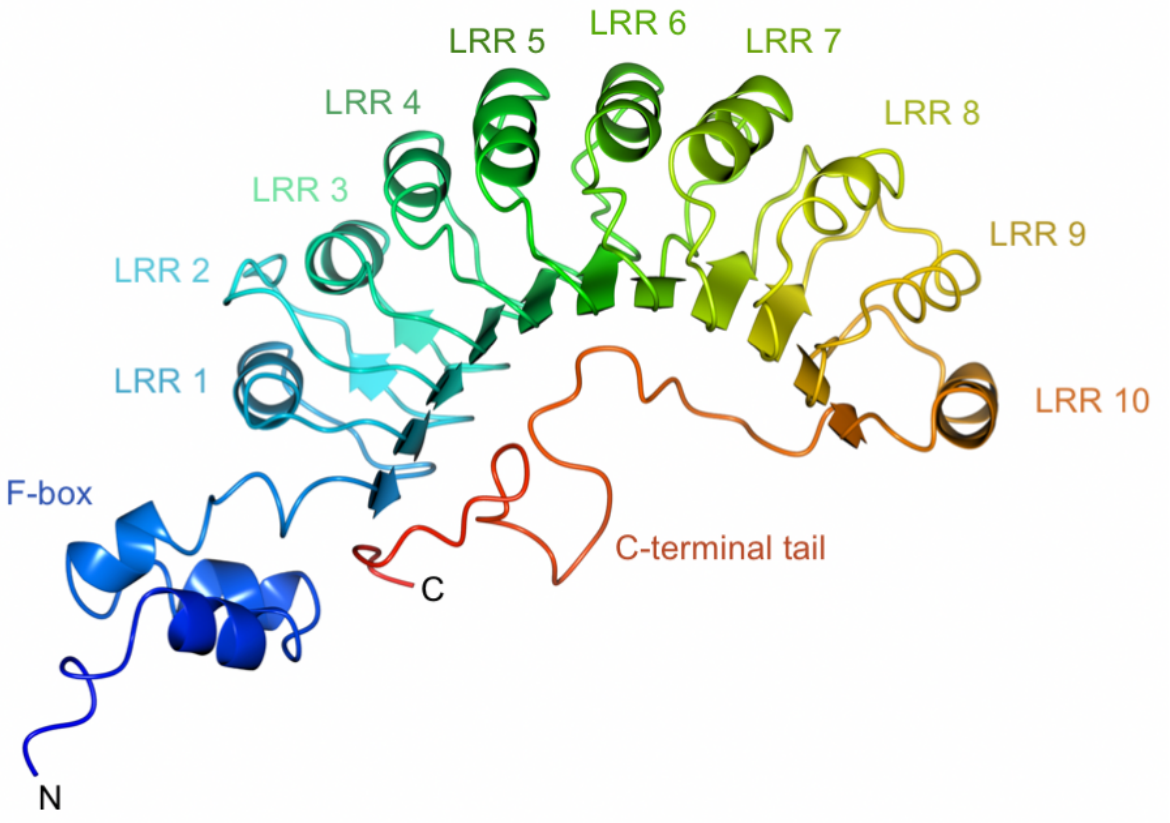

Figure 1.15: Structure of residues 95-424 of Skp2. Skp2 comprises an F-box domain, ten LRRs and a long C-terminal tail. Some of the LRRs are involved in substrate binding (Kobe and Kajava, 2001, Hao et al., 2005).

Skp2B is predominantly cytoplasmic, whereas Skp2 is predominantly nuclear (Ganiatsas et al., 2001). A number of studies have used antibodies that recognise both variants of Skp2 for cellular staining and have reported enriched levels of cytoplasmic Skp2 (Radke et al., 2005). These studies might therefore be measuring Skp2B rather than Skp2. Many studies have reported that high Skp2 levels do not always correlate with low p27 levels in cell lines and primary tissue cultures. This finding might again be due to a high level of Skp2B rather than Skp2, as discussed by Radke and co-workers (Radke et al., 2005).

The levels of Skp2B compared to Skp2 can be quantitated on Western blots due to its lower molecular weight and hence faster migration on SDS-PAGE. When probing for Skp2 there are often two bands; the top band corresponding to Skp2 and the lower one to Skp2B. By identifying this lower band as Skp2B the Germain group were able to show that Skp2B is less stable than Skp2. Using cycloheximide treatment, they determined the half-life of Skp2B to be 30 minutes compared to 90 minutes for Skp2 (Radke et al., 2005).

1.7 The cell cycle inhibitor, p27

p27 (also known as KIP1) is encoded by the *CDKN1B* gene, and belongs to the Cip/Kip family of CDK inhibitor proteins (Polyak et al., 1994a, Polyak et al., 1994b, Toyoshima and Hunter, 1994). p27 inhibits CDK2-, CDK4-, CDK6-, and CDK1/cyclin complexes. The level of p27 oscillates throughout the cell cycle being greatest as the cell moves into G1-phase and then steadily decreases as the cell progresses through G1-phase into S-phase (Pagano et al., 1995). Levels of p27 are high in cells exposed to certain anti-mitogenic signals or differentiation signals such as contact inhibition, TGF-β and serum deprivation (Reynisdottir et al., 1995, Polyak et al., 1994b). The importance of p27 in limiting proliferation is illustrated by the p27 knockout mouse which displayed increased body size, organ hyperplasia and, similar to the Rb knockout mice, these mice developed pituitary gland tumours (Fero et al., 1996). Haploinsufficiency of p27 predisposes to tumours in multiple tissues when challenged with γ-radiation or chemical carcinogens (Fero et al., 1998).

p27 is an intrinsically unstructured protein (IUP, (Lacy et al., 2004)) meaning that it lacks any highly ordered three-dimensional structure (Yoon et al., 2012) and is

proposed to undergo a folding upon binding transition upon incorporation into CDK/cyclin complexes (Wang et al., 2011). The structure of p27 bound to CDK2/cyclin A revealed that p27 binds to CDK/cyclin complexes as an extended structure interacting with both CDK2 and cyclin A (Figure 1.16) (Russo et al., 1996a). It was hypothesised that the disordered structure of p27 provides the opportunity to make diverse interactions (Lacy et al., 2004). Indeed, the regions of p27 that include many sites of post-translational modification lie within these disordered regions allowing for them to be flexible enough to bind diverse partners. For example, within the CDK/cyclin binding region also known as the kinase inhibitory domain (KID), p27 can lose its inhibitory capability through tyrosine phosphorylation (Grimmler et al., 2007). This mechanism of binding is common to IUPs and is believed to increase flexibility in binding and allow access to proteins that introduce modifications (van der Lee et al., 2014).

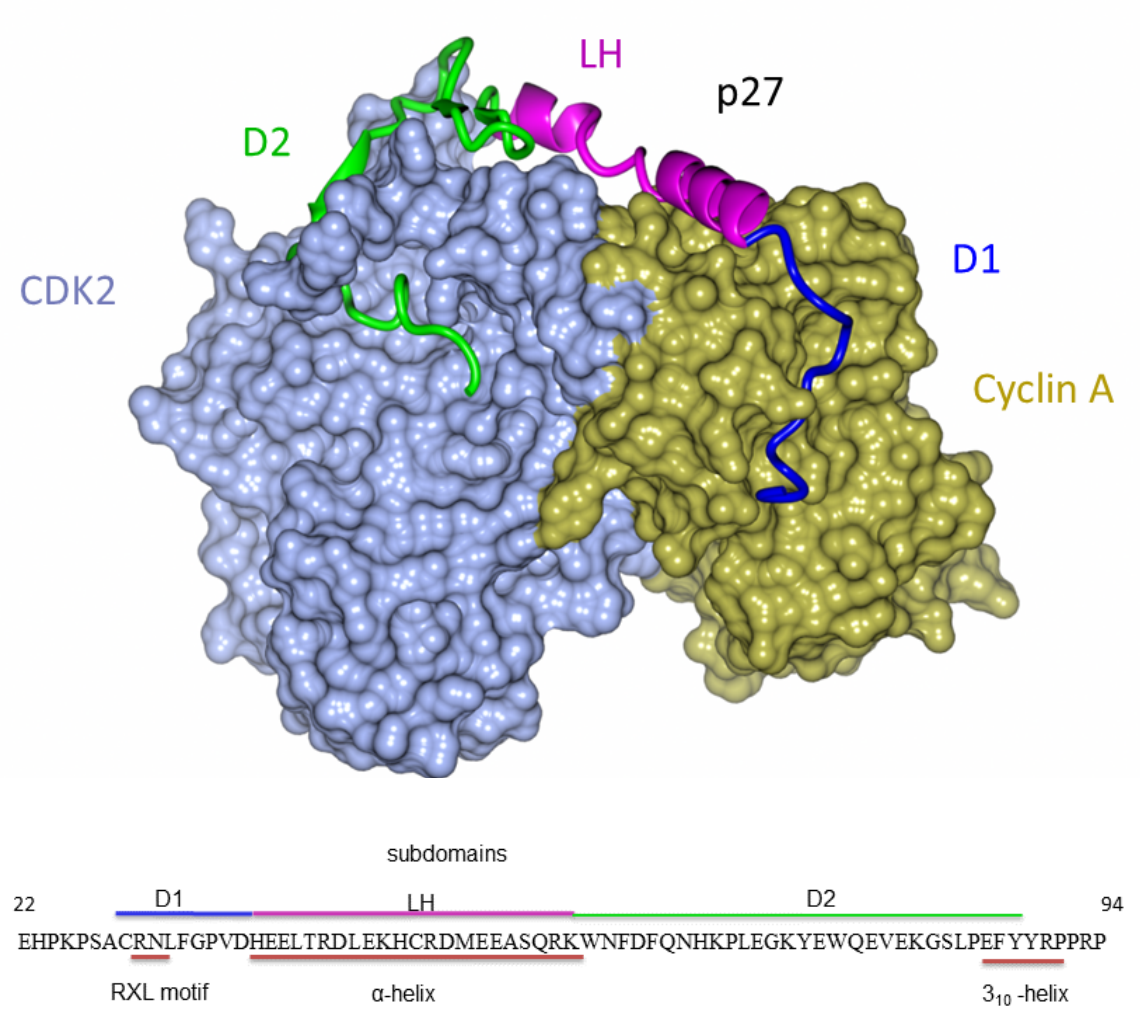

Figure 1.16: **The structure of the p27 KID bound to CDK2/cyclin A**. p27 KID can be divided into subdomains (labelled by bars above the p27 sequence) based on structure and sequence in the region which contacts CDK2/cyclin A. The D1 domain contains the RXL motif, the LH domain is an amphipathic α-helix and the D2 domain binds to the active site of CDK2. Adapted from (Lacy et al., 2004).

1.7.1 p27 mislocalisation in cancer

CDK inhibitors (CKIs) are potent negative regulators of the cell cycle. The INK family of CKIs are frequently mutated or deleted in cancers (Ortega et al., 2002, Asghar et al., 2015). p27, however, is rarely mutated in cancers, and therefore does not behave as a traditional tumour suppressor. Despite this, reduced p27 expression has been associated with development of lung, breast, colon, ovarian, thyroid, prostate and many other cancers (Chu et al., 2008). Hence, the role of p27 in cancer is controversial, and it has been described as a haploinsufficient tumour suppressor

(Fero et al., 1998). This phenotype is demonstrated by the p27 knockout mouse which is not as tumour prone as would be expected, with tumours only occurring in the pituitary gland (Nakayama et al., 1996). In different contexts, p27 can be transferred to alternative complexes or its cellular localisation may be altered. For example, in some cancers which exhibit high p27 levels, p27 is sequestered in CDK4/cyclin D complexes reducing its ability to inhibit CDK2/cyclin E complexes. Her2 overexpression has been reported to upregulate cyclin D and promote CDK4/cyclin D/p27 complex formation (Lane et al., 2000). In contrast, high levels of cytoplasmic p27 are a marker of poor prognosis in many cancers and has been associated with Protein kinase B (Akt) activation (Liang et al., 2002, Viglietto et al., 2002). For example, altered p27 localisation has been reported in prostate (Tsihlias et al., 1998), oesophagus (Singh et al., 1998), thyroid (Baldassarre et al., 1999), ovarian (Duncan et al., 2010, Masciullo et al., 2000) and breast cancers (Catzavelos et al., 1997).

Akt phosphorylates p27 on Ser10, Thr157 and Thr198 and phosphorylation of these residues alone or in combination leads to cytoplasmic accumulation of p27 (Rodier et al., 2001, Fujita et al., 2003, Sekimoto et al., 2004). Phosphorylation of Ser10 occurs during G1 phase in response to growth factor stimulation, perhaps contributing to the inactivation of p27 (Lee and Kay, 2007). This modification creates a binding site for CRM1/Exportin1 suggesting that it may indirectly affect p27 sub-cellular localisation (Rodier et al., 2001). This phosphorylation event was found by Besson and co-workers to be a mechanism of tumourigenesis (Besson et al., 2006). $p27^{S10A/S10A}$ mice are less prone to tumours induced by urethane than WT mice. As $p27^{S10A}$ is unable to undergo Ser10 phosphorylation-induced nuclear export, a larger proportion of $p27^{S10A}$ was found to localise in the nucleus compared to $p27^{WT}$. A possible mechanism of protection from tumour development would be the increased occupation of p27 on CDK2/cyclin complexes within the nucleus (Besson et al., 2006).

Phosphorylation of Thr157 leads to binding of 14-3-3β which blocks binding to importin α and prevents p27 from being imported into the nucleus (Viglietto et al., 2002, Sekimoto et al., 2004). Thr198 of p27 is also phosphorylated by p90 ribosomal S6 kinase (RSK1), which is activated through the MEK/ERK pathway, and 5' AMP activated protein kinase (AMPK) which has a role in energy homeostasis within the cell (Fujita et al., 2003, Liang et al., 2007, Short et al., 2010). When in the cytoplasm, p27 has a role in regulation of the actin cytoskeleton and cell migration through

modulation of RhoA and through this role has been implicated in many cancers (Hsu et al., 2014, Roy et al., 2013). In renal cell carcinoma (RCC), levels of cytoplasmic p27 correlate with tumour grade, and in RCC cell lines PI3K/Akt signalling correlated with Thr157 phosphorylation and cytoplasmic mislocalization (Kim et al., 2009). Phosphorylation of p27 on Thr157 and localisation to the cytoplasm has also been observed to be increased in breast cancer (Viglietto et al., 2002). As a result of the oncogenic nature of cytoplasmic p27, inhibition of its nuclear export has been proposed as a target for therapeutic intervention (Wang et al., 2014, Gravina et al., 2014).

1.7.2 p27 phosphorylation by oncogenic tyrosine kinases

During G1 phase of the cell cycle, p27 is phosphorylated on Tyr74 by Src, and Tyr88 by Src, Abl (and BCR-ABL) and Lyn (a Src family kinase) (Grimmler et al., 2007, Chu et al., 2007). These phosphorylations weaken p27 binding to CDK2/cyclin E. Tyr88 lies in the 3_{10} helix of p27 (Figure 1.16) which occupies the ATP-binding site of CDK2 (Russo et al., 1996b). Phosphorylation of Tyr74 also serves to disrupt hydrophobic interactions and leads to weakening of the CDK2/cyclin E/p27 interaction. Tyr74 and Tyr88 phosphorylated p27 is still able to bind CDK2/cyclin E, but CDK2/cyclin E is partially active in this state and can phosphorylate p27 on Thr187 (Grimmler et al., 2007, Chu et al., 2007). Increase levels of tyrosine-phosphorylated p27 have been reported in leukaemic cells, indicating that increased activity of these tyrosine kinases on p27 might contribute to progression of leukaemia (Kardinal et al., 2006, Grimmler et al., 2007). The Src family kinase inhibitor, AZD0530, and imatinib have been shown to reduce Tyr88 phosphorylation and increase the stability of p27 (Chu et al., 2007).

1.7.3 Transcriptional and translational control of p27

The levels of *Cdkn1b* (the gene encoding p27) transcription remain fairly constant throughout the cell cycle (Hengst and Reed, 1996). Levels of translation of p27 do however change during the cell cycle, with increased translation correlating with exit from the cell cycle. A U-rich region in the 5'-UTR of p27 has been identified that is necessary for efficient translation, and human antigen R (HuR) is a protein which binds to the p27 5' UTR (Millard et al., 2000). The HuR binding site is part of the internal ribosome entry site (IRES). Binding of HuR is therefore inhibitory as it blocks ribosome binding (Kullmann et al., 2002, Coleman and Miskimins, 2009). HuR is

predominantly nuclear in early and mid G1 and then moves out of the nucleus during late G1, S and G2 (Wang et al., 2000). Consistent with this, translation of p27 is regulated during the cell cycle with a decrease at the G1/S transition (Hengst and Reed, 1996). Other factors which bind the p27 5'-UTR are the heterogeneous nuclear ribonuclearproteins (hnRNPs) C1 and C2. C1 and C2 bind to the 5'-UTR of p27 during G2 and M (Millard et al., 2000). hnRNPs C1 and C2 were shown to also bind to the IRES element, however, they are enhancers of p27 translation in contrast to HuR (Cho et al., 2005). Recently, other factors which bind to the 5'-UTR have been identified, such as, Far Upstream Element (FUSE) Binding Protein 1 (FBP1) and urothelial carcinoma-associated 1 (UCA1) (Zheng and Miskimins, 2011, Huang et al., 2014). Recently it has been reported that p27 mRNA is regulated by the miRNA let-7 (Liu et al., 2015). This might in part explain why let-7 is found to be dysregulated in many cancers (Boyerinas et al., 2010). Control of p27 translation is thus emerging as a very complex process, involving multiple proteins which compete to bind to the IRES element and other regions of the 5'-UTR.

1.8 Structures of Skp2-containing complexes

p27 is recognised as a substrate by SCF^{Skp2} when bound to CDK2/cyclin A. Unusually Skp2 requires Cks1 as an accessory protein to bind p27.

1.8.1 The SCFSkp2 structure

In 2000, the first structure of the F-box, LRRs and C-terminal tail of Skp2 (residues 97-424) was published (PDB: 1FQV). The structure revealed the F-box region of Skp2 binding tightly to Skp1 through interlocking helices mediated predominantly by hydrophobic interactions (Figure 1.17) (Schulman et al., 2000). The LRRs of Skp2, which are involved in substrate binding, have a concave structure resembling a sickle. The ~30 amino acid C-terminal tail of Skp2 extends back towards the F-box region packing loosely against its concave LRR region (Schulman et al., 2000).

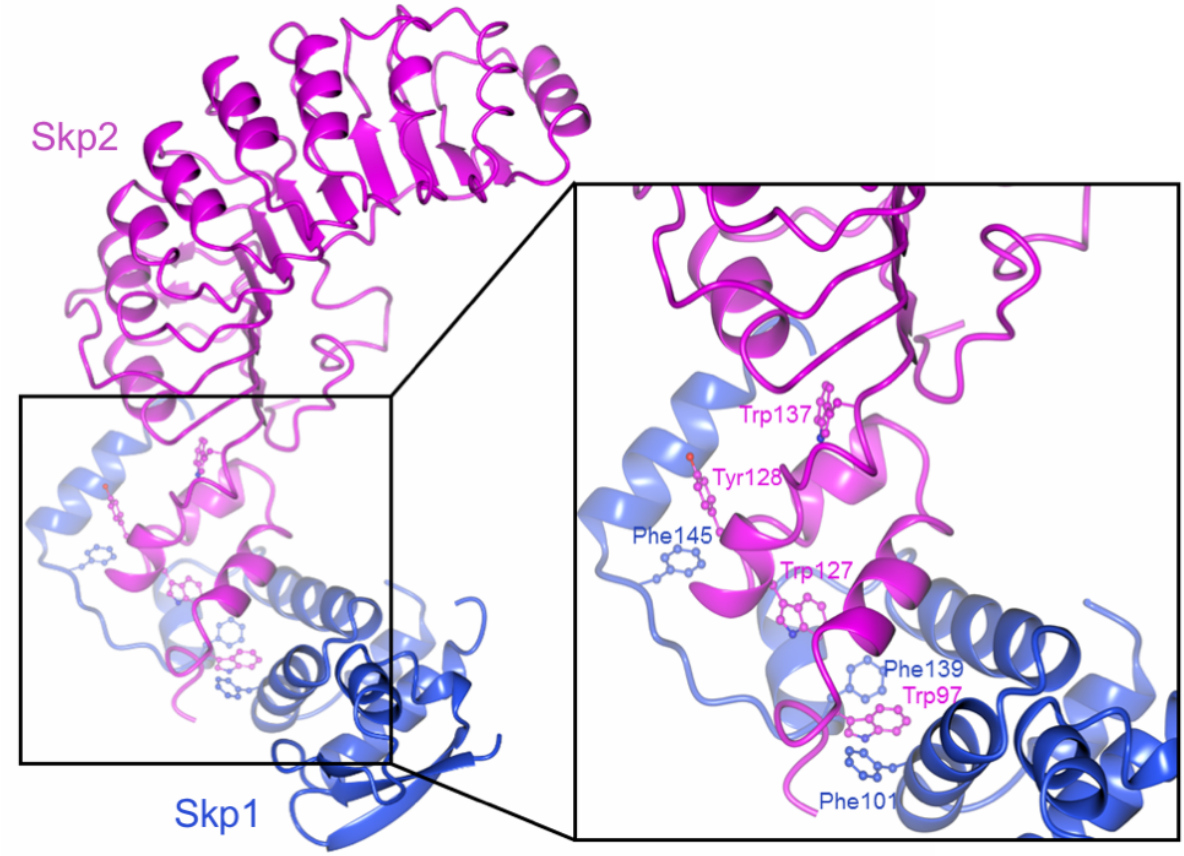

Figure 1.17: The Skp1/Skp2 interface. Skp1 is shown in blue and Skp2 in magenta. Tryptophans, tyrosines and phenylalanines which are oriented toward the core of the Skp1/Skp2 interface are shown in ball and stick conformation. Other hydrophobic residues which contribute to this interaction are not shown for clarity. PDB: 1FQV

Not long after the Skp1/Skp2 structure was solved, the same group published the structure of the Cul1-Rbx1-Skp1-Skp2 complex (PDB: 1LDK). Only the F-box of Skp2 was included in this complex (Zheng et al., 2002). Superimposition of their structure onto the LRR-containing structure revealed the F-box region of Skp2 to be about 100 Å from the zinc-RING finger protein, Rbx1. Docking the structure of an E2 enzyme onto Rbx1, c-Cbl-UbcH7, suggested that the LRRs of Skp2 are orientated toward the catalytic cysteine of the E2, from which they are separated by ~50 Å (Figure 1.18). This distance is determined by the Cul1 scaffold protein. Zheng and co-workers argue that Cul1 serves to separate SCF^{skp2} substrates from their E2 ligase component so as to accommodate substrates of differing sizes and with varying spacing between their ubiquitinated lysines (Zheng et al., 2002). The SCF complex appears to be relatively rigid and therefore this gap opens up new questions concerning the

mechanism of ubiquitination. The structure also revealed that Skp2 does not directly interact with Cul1 (Schulman et al., 2000, Zheng et al., 2002).

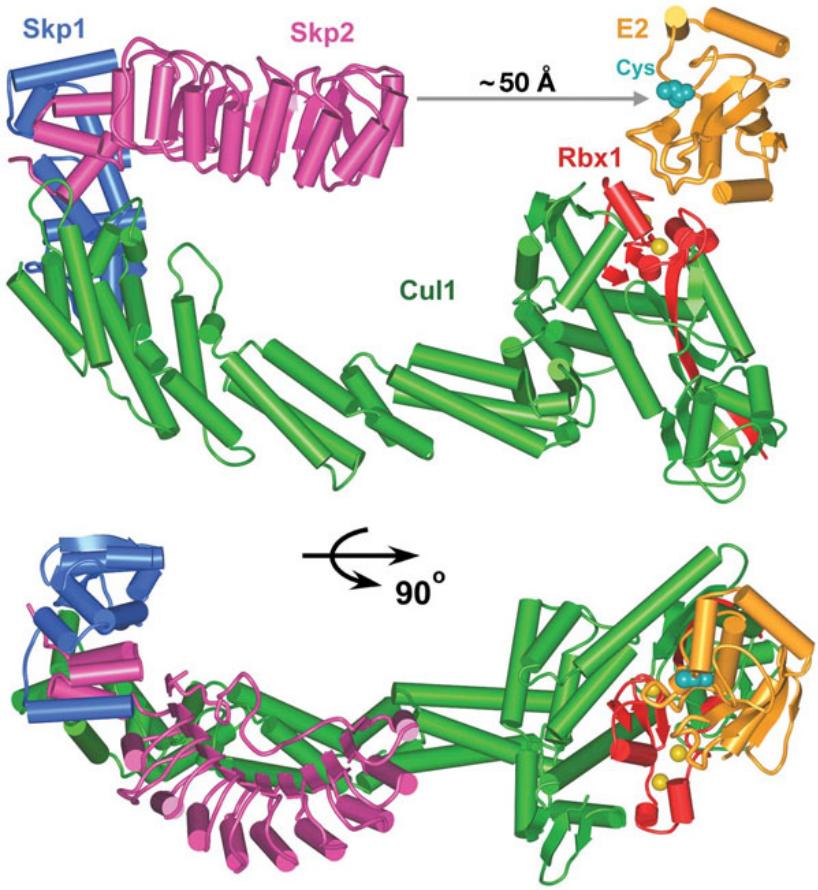

Figure 1.18: Model of the SCF^{Skp2}-E2 complex. A model of the SCF^{Skp2}-E2 complex reveals a *circa* 50 Å gap between Skp2 and the catalytic E2 molecule. The structure appears to be rigid and therefore this gap between Skp2 and the E2 enzyme opens up new questions into the mechanism of ubiquitination. From Zheng et al. (2002).

1.8.2 Skp1/Skp2/Cks1 structure

The structure of Skp1/Skp2/Cks1 bound to a p27 peptide was unexpected in that it showed that Cks1 makes a significant contribution to the p27 binding site and the Skp2 C-terminal tail is only involved in binding substrates indirectly through contacts it makes with Cks1 (Hao et al., 2005). It had been suggested that the Skp2 C-terminal tail might undergo a conformational change in order to accommodate Cks1 (Reed, 2005). However, binding of Cks1 does not cause any significant changes to the Skp2 structure and the structure of Cks1 bound to Skp2 is nearly identical to the structure of unbound Cks1 (Hao et al., 2005).

The Skp1/Skp2/Cks1/p27 peptide structure also confirmed the importance of the phosphorylation at Thr187 to its binding to the SCF^{Skp2} complex, in particular to Cks1. Modelling CDK2/cyclin A into the SCF structure using the CDK2/Cks1 and CDK2/cyclin A structures, showed that CDK2/cyclin A could be accommodated in the SCF complex (Figure 1.19). Therefore this structure provided additional evidence to support a model in which CDK2/cyclin A aids the ubiquitination of p27 independently of its role in Thr187 phosphorylation (Zhu et al., 2004). Within the p27 sequence Glu185 and pThr187 were shown to make a significant contribution to p27 peptide binding (Figure 1.19, (Hao et al., 2005)). The structure of the Skp1/Skp2/Cks1/p27 complex and supporting mutagenesis experiments show that only Glu185 and pThr187 of p27 contribute significantly to the interaction with the SCF^{Skp2} complex (Hao et al., 2005). This result suggests that additional interactions stabilise the complex, for example, Cks1 binding to CDK2. In support of this model, the concentration of Cks1 required to bind a p27 phosphopeptide to the SCF^{Skp2} complex is about tenfold higher than the concentration needed to bind full-length phosphorylated p27 to Cks1 in the presence of CDK2/cyclin E (Hao et al., 2005) and CDK2 binding to Cks1 enhances ubiquitination of p27 (Sitry et al., 2002).

Unexpectedly, the Skp1/Skp2/Cks1/p27 structure showed that Cks1 contributes much of the interface for p27 (Figure 1.19). Only two residues of Skp2, Arg294 and Tyr346, appear to contribute to the interaction with p27. The phosphorylated threonine of p27 (pThr187) binds into an anion binding pocket on Cks1 (Figure 1.19). Cks1 in turn, binds to the concave surface of the LRRs of Skp2 (Hao et al., 2005).

A

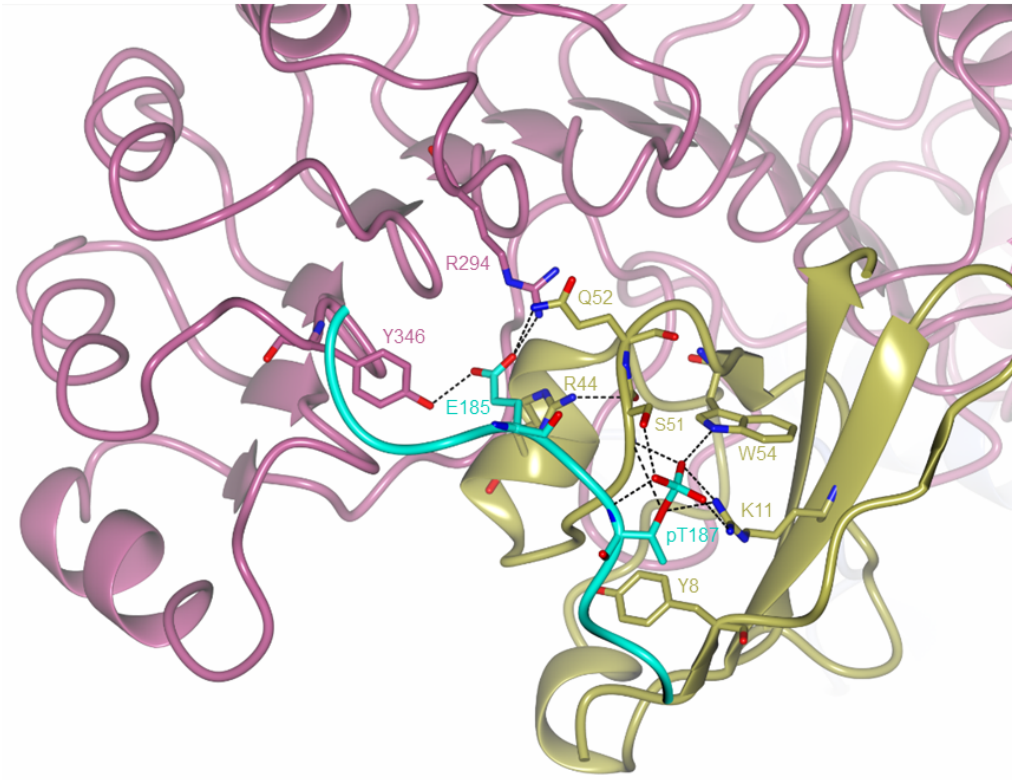

B

p27	176	DGSPNAGSVEQTPKKPGL 193
p57	299	SAAPGVGSVEQTPRKRLR 316
p21	119	LVPRSGEQAEGSPGGPGD 136

Figure 1.19: Residues Glu185 and pThr187 of p27 form key interactions with Skp2/Cks1. A) Structure of Skp2/Cks1/p27. Skp2 is shown in magenta, Cks1 is in gold and p27 is in cyan. Some of the interacting residues are shown as cylinders. B) Crucial residues of p27, such as Glu185 and a phosphorylated residue at position 187 of p27, involved in its interaction with Skp2/Cks1 are conserved between the Cip/Kip family of CDK inhibitors (conserved residues are coloured). PDB: 1AST.

Figure 1.19 shows that a ten amino acid segment of p27 (181-190) binds Skp2/Cks1 in a bipartite manner. Residues 181-184 bind Skp2, residue 185 binds to both Skp2, and Cks1 and residues 186 to 190 bind Cks1. p57 has considerable homology to p27 in the C-terminal region with eight out of ten of the residues equivalent to those contained in the Skp1/Skp2/Cks1/p27 structure being identical to those in p27. It is likely, therefore, that p57 makes similar interactions with Skp2/Cks1 (Hao et al., 2005). p21 has lower sequence homology to p27, however, both p57 and p21 have a glutamate residue at position -2 relative to the phosphorylated residue which, for p27, binds to the anion-binding pocket of Cks1.

1.8.3 The Skp1/Skp2/Cks1/CDK2/cyclin A complex

Skp2 was first identified in a complex with Skp1, Cks1, CDK2 and cyclin A and shown to form a pentameric complex with CDK2/cyclin A (Zhang et al., 1995). CDK2/cyclin A can be docked into the structure of the SCF complex through the interaction of CDK2 with Cks1 (Figure 1.20, (Hao et al., 2005)). The N-terminus of Skp2 interacts with cyclin A through residues 32, 33, 39 and 41 of Skp2 (Ji et al., 2006). Mutating these residues to alanine (termed Skp2 4A) disrupts the Skp2/cyclin A interaction and overexpressing Skp2 4A in U2OS cells leads to p21/p53-mediated cell cycle arrest (Ji et al., 2006).

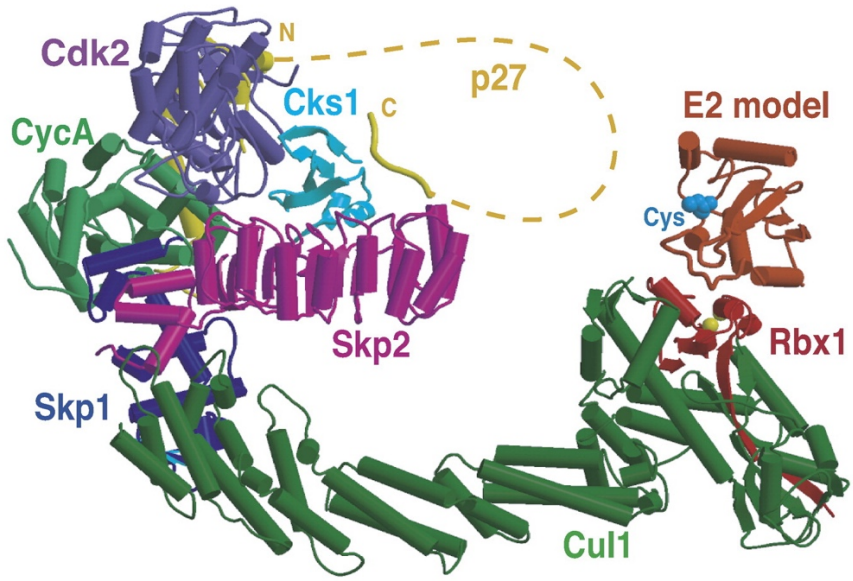

Figure 1.20: Model of the SCF^{Skp2}-Cks1-p27-CDK2-cyclin A structure. Residues 95-424 of Skp2 are shown in ribbon representation. Residues 94-180 of p27 for which no structural information exists is shown as a dashed line. From Hao et al. (2005).

There has been conflicting evidence as to whether CDK2/cyclin A is required for p27 ubiquitination, which might reflect non-overlapping roles for different CDK/cyclin complexes in mediating p27 degradation. It is known that CDK2/cyclin E is required for p27 phosphorylation at Thr187 leading to its degradation, but that there is no significant effect on p27 ubiquitination when CDK2/cyclin E is absent (Spruck et al., 2001). p27 can also be phosphorylated by CDK1/cyclin B, but this does not stimulate its ubiquitination (Montagnoli et al., 1999). The requirement for a direct Cks1/CDK2 interaction for p27 ubiquitination is also controversial. Using a Cks1 mutant which was

shown by biophysical and yeast two-hybrid analyses to be incapable of binding CDK2 (Bourne et al., 1996), one group demonstrated *in vitro* that the Cks1/CDK2 interaction may be redundant for ubiquitination of p27 (Spruck et al., 2001). Whereas, another (Sitry et al., 2002) demonstrated that when Cks1 is mutated, such that it cannot bind CDK2, the ubiquitination of p27 is greatly reduced. This latter study was followed up by another suggesting that CDK2/cyclin A has a non-catalytic role in the turnover of p27 (Zhu et al., 2004). A catalytically inactive CDK2/cyclin A complex was shown to stimulate ubiquitination of phosphorylated p27. In support of the earlier observations (Spruck et al., 2001), CDK2/cyclin E could not promote p27 ubiquitination after phosphorylation. Another study found that CDK2/cyclin E is required for p27 ubiquitination (Ungermannova et al., 2005). However, a comparison of whether CDK2/cyclin A stimulates p27 ubiquitination more effectively than CDK2/cyclin E in their assay was not undertaken.

The structure of the Skp1/Skp2/Cks1/p27 peptide complex supports a model in which CDK2/cyclin A binding to the SCF^{Skp2} complex is mediated by Cks1 as the CDK2-binding interface of Cks1 is accessible, and CDK2/cyclin A can be docked onto the complex without requiring any conformational changes (Figure 1.20). The authors of this paper also showed that a complex assembled from sub-complexes of Cul1/Rbx1, Skp1/Skp2Δ88/Cks1, and CDK2/cyclin A/pThr187p27 is stable to size-exclusion chromatography (SEC) (Hao et al., 2005). As the recombinant Skp2 encoded only the F-box and LRRs and lacked the N-terminal sequence, the Skp2/cyclin A interaction would not be expected to be intact, and therefore, the interaction via the CDK2/Cks1 interaction must be sufficient for complex stability (Hao et al., 2005). The authors suggest that CDK2/cyclin A could strengthen the interaction of p27 with the SCF^{Skp2} complex as the affinity of p27 for Skp2/Cks1 is 10-20 fold lower than that observed for other substrates of the SCF^{Skp2} complex (Nash et al., 2001, Wu et al., 2003).

1.9 The role of Skp2 in cancer

Skp2 has been well-characterised as the substrate recognition component of the SCF^{Skp2} complex, however, it has other functions which often also contribute to cancer progression. In this section, functions of Skp2 involving its role within the E3 ligase will be discussed as well as its other oncogenic functions.

1.9.1 The Skp2/p27 axis

Given the role of Skp2 in promoting cell cycle progression, it is not surprising that it is overexpressed in many cancers such as breast, prostate, non-small cell lung cancer (NSCLC), ovarian and many more (Hershko, 2008). In many of these cancer types, high Skp2 levels correlate with low p27 levels heavily implicating the Skp2/p27 axis in tumourigenesis and/or tumour progression. Counter-intuitively, p27 down-regulation with antisense oligonucleotides has been shown to sensitise cancer cells to chemotherapeutic drugs, for example, flavopiridol and 4-hydroperoxycyclophosphamide (St Croix et al., 1996, Achenbach et al., 2000). In retrospective studies, however, reduced p27 levels correlated with reduced survival after platinum-based chemotherapy for NSCLC and ovarian cancers (Oshita et al., 2000, Masciullo et al., 2000, Korkolopoulou et al., 2002, Hershko, 2010). This is perhaps due to the change in roles of p27 depending on its sub-cellular localisation (see Section 1.7.1). Further investigation is required to evaluate p27 as a predictor of response to chemotherapy and whether attenuation of the Skp2/p27 axis would be beneficial in these patients.

1.9.2 Role of Skp2 in tumourigenesis upon BCR-ABL overexpression

Recent reports have suggested that Skp2 promotes tumourigenesis upon BCR-ABL overexpression and Skp2 loss is also able to counter the effects of BCR-ABL overexpression (Agarwal et al., 2008). Treatment of a leukaemic cell line with Imatinib caused an increase in p27 levels. This was not due to decreased phosphorylation of p27 on Thr187 by CDK2/cyclin E, which would be expected to target p27 for ubiquitination by the SCF^{Skp2} complex. Skp2 mRNA and protein levels on the other hand were reduced following Imatinib treatment, consistent with transcriptional regulation of Skp2 by BCR-ABL (Agarwal et al., 2008). Further investigation into this effect of BRC-ABL on Skp2 suggests that the stability of Skp2 is affected by Imatinib. It was found that BCR-ABL phosphorylates and inactivates Emi1 which leads to increased activity of the APC/C complex (Chen et al., 2011).

1.9.3 Potential for targeting Skp2 in TP53- and Rb1-deficient tumours

Rb and p53 are tumour suppressors frequently lost or mutated in cancers. Combined deletion of *Rb1* (encoding Rb) and TP53 (encoding p53) is effective at inducing tumours in a wide range of tissues in mice. Skp2 loss in Rb-deficient mice blocks

pituitary tumourigenesis (Wang et al., 2010). Skp2 was found to suppress apoptosis in Rb-deficient tumours. These effects are mediated through E2F1-mediated gene expression. The widely accepted mechanism for induction of tumorigenesis by Rb loss is through E2F1 activation. The loss of Skp2 in this context leads to altered E2F1 target gene activation, which switches the E2F1 output from pro-proliferative to pro-apoptotic (Lu et al., 2014). In p53-deficient tumours, Skp2 inactivation can lead to p53-independent senescence when the $p19^{Arf}$-p53 pathway is impaired (Lin et al., 2010a). p53 is activated by oncogenic stress such as the loss of Rb (Sherr, 2012). The activation of the p53 pathway leads to cell cycle arrest, and possibly senescence, or apoptosis. Zhao and co-workers investigated the effect of combined loss of Skp2, Rb and p53 (Zhao et al., 2013). They reported that upon deletion of Skp2 following p53 and Rb loss, p27 levels are increased and safeguard against tumorigenesis. Therefore, inhibition of Skp2 in the context of Rb and p53 loss could be beneficial in cancer therapy.

1.9.4 Skp2 activation of Akt

Skp2 has a role in proliferation through its ubiquitination of many cell cycle regulatory proteins. However, it has also been shown to be involved in many other oncogenic pathways. In the cytoplasm, Skp2 is involved in the ubiquitination of Akt after epidermal growth factor (EGF) stimulation (Chan et al., 2012). This ubiquitination activates Akt through the attachment of Lys63-linked ubiquitin chains. Cytoplasmic Skp2 was also found to have a role in increasing glycolysis through Akt signalling (Chan et al., 2012). Cancer cells develop a mechanism of increasing ATP levels through increased glucose uptake and glycolysis called the Warburg effect (Vander Heiden et al., 2009). This increased ATP synthesis is believed to facilitate increased uptake and synthesis of cellular building blocks (Vander Heiden et al., 2009). Akt has been shown to be a key regulator of the Warburg effect and Akt is often highly active in cancers (Elstrom et al., 2004, Plas and Thompson, 2005). Investigation into the effects of Skp2 activation of Akt on the levels of glucose uptake and tumour size showed that Skp2 does regulate *in vivo* glycolysis, and that knockdown of Skp2 decreases tumour size in a xenograft mouse model bearing Her2-overexpressing breast tumours (Chan et al., 2012).

1.9.5 Role of Skp2 in prostate cancer

Androgens are the primary drivers of prostate cancer cell growth. When androgens are ablated or withdrawn, a proportion of cells undergo apoptosis and the remainder arrest in G1 of the cell cycle. Androgen ablation therapy is the primary treatment for metastatic prostate cancer (Huggins and Hodges, 1941, Katsogiannou et al., 2015), however, 80-90% of patients develop castration-resistant prostate cancer (CRPC) after 12-33 months (Attard et al., 2006). Skp2 has a well-established role in prostate cancer. Expression of Skp2 was found to increase with androgen addition leading to increased degradation of p27 and increased proliferation (Lu et al., 2002, Waltregny et al., 2001). This suggests that Skp2 is involved in a cell's mechanism of overcoming androgen deprivation.

Kokontis and co-workers found that treatment of CRPC cells with an androgen analogue decreased the protein levels of Skp2, CDK2 and cyclin A amongst others (Kokontis et al., 2014). Levels of p27 were found to be significantly increased. As predicted from these findings, they also observed a G1 cell-cycle arrest in response to androgen treatment. This suggests that the Skp2/p27 axis is heavily involved in the anti-proliferative effect of androgen therapy in CRPC (Kokontis et al., 2014).

1.9.6 Role of Skp2 in breast cancer

Skp2 has been reported to be overexpressed in a subset of breast carcinomas with low levels of p27 expression (Signoretti et al., 2002). Emerging evidence suggests that Skp2 plays a key role in cell growth, apoptotic cell death, invasion and metastasis in human breast cancer (Sonoda et al., 2006, Zhang et al., 2005). Furthermore, Skp2 knockdown by RNAi significantly inhibited cell proliferation in MCF-7 breast cancer cells (Sun et al., 2007).

It was found in 2014 that the SCF^{Skp2} complex is one of several E3 ligases which mediate ERα degradation upon oestrogen stimulation (Zhou et al., 2014). CDK2/cyclin E phosphorylation of oestrogen receptor α (ERα) on Ser341 is required for ERα recognition by the SCF^{Skp2} complex. ERα activation by a ligand rapidly stimulates its interaction with Skp2 which leads to its transcriptional activation and subsequent proteasomal degradation of ERα. This coupled process is common among transcription factors (Nawaz and O'Malley, 2004). E2F1 was identified as a late ERα-activated gene regulated by Skp2. As E2F1 is a transactivator of Skp2,

Skp2/ERα-mediated gene expression would be expected to form a feed-forward mechanism to drive S-phase entry. Attenuation of this feed-forward loop perhaps through inhibition of CDK2-mediated phosphorylation of ERα might serve to block proliferation of ERα-positive cancers (Zhou et al., 2014).

1.9.7 Skp2 mediates RhoA expression

Skp2 is also known to be a transcription cofactor. Skp2 cooperates with Miz1, Myc and p300 to induce RhoA expression. RhoA is a member of the Rho family of small GTPases, and has a role in cancer metastasis. Upregulation of RhoA has been documented in many human cancers (Chan et al., 2010, Bellizzi et al., 2008, Horiuchi et al., 2003). Although Skp2 is able to ubiquitinate c-Myc, this ubiquitination is not required for RhoA expression, so this is a novel ubiquitination-independent function of Skp2 (Chan et al., 2010). Skp2 may also act as a cofactor for other Myc target genes (von der Lehr et al., 2003).

1.9.8 Role of Skp2 in migration and metastasis

Skp2 has been found to have a role in migration. $Skp2^{-/-}$ MEFs exhibit decreased ability to migrate to chemoattractants in a transwell assay; and in wound scratch assays, loss of Skp2 severely decreased the wound healing (Lin et al., 2009, Inuzuka et al., 2012). Skp2 was found to be involved in the ubiquitin-mediated degradation of E-cadherin, a transmembrane protein involved in maintaining cell-cell contacts. Upon treatment with the proteasome inhibitor, MG132, E-cadherin levels are increased (Inuzuka et al., 2012).

1.9.9 Summary of the roles of Skp2 in cancer

As Skp2 inactivation is not embryonic lethal in a knockout mouse model, and its oncogenic activity is far-reaching, Skp2 is an attractive target for small-molecule inhibition. An increasing body of data suggests that Skp2 plays essential roles in tumourigenesis induced by loss of PTEN and Rb or by overexpression of BCR-ABL, all of which are common events in human cancers. The role of cytoplasmic Skp2 in migration and metastasis provides further motivation to identify molecules for therapeutic intervention to inactivate Skp2 (Figure 1.21). One well-established mechanism of oncogenesis is the Skp2/ p27 axis, and this appears to be the most penetrative and functionally significant role of Skp2. High Skp2 levels are often

correlated with low p27 levels and p27 is the SCF^{Skp2} substrate which is most increased after Skp2 ablation (Nakayama et al., 2000, Hershko, 2008). However, there are also many tumour types where Skp2 overexpression is not accompanied by decreased p27 levels. Therefore, the role of Skp2 is likely to be tissue, tumour and cell-compartment specific.

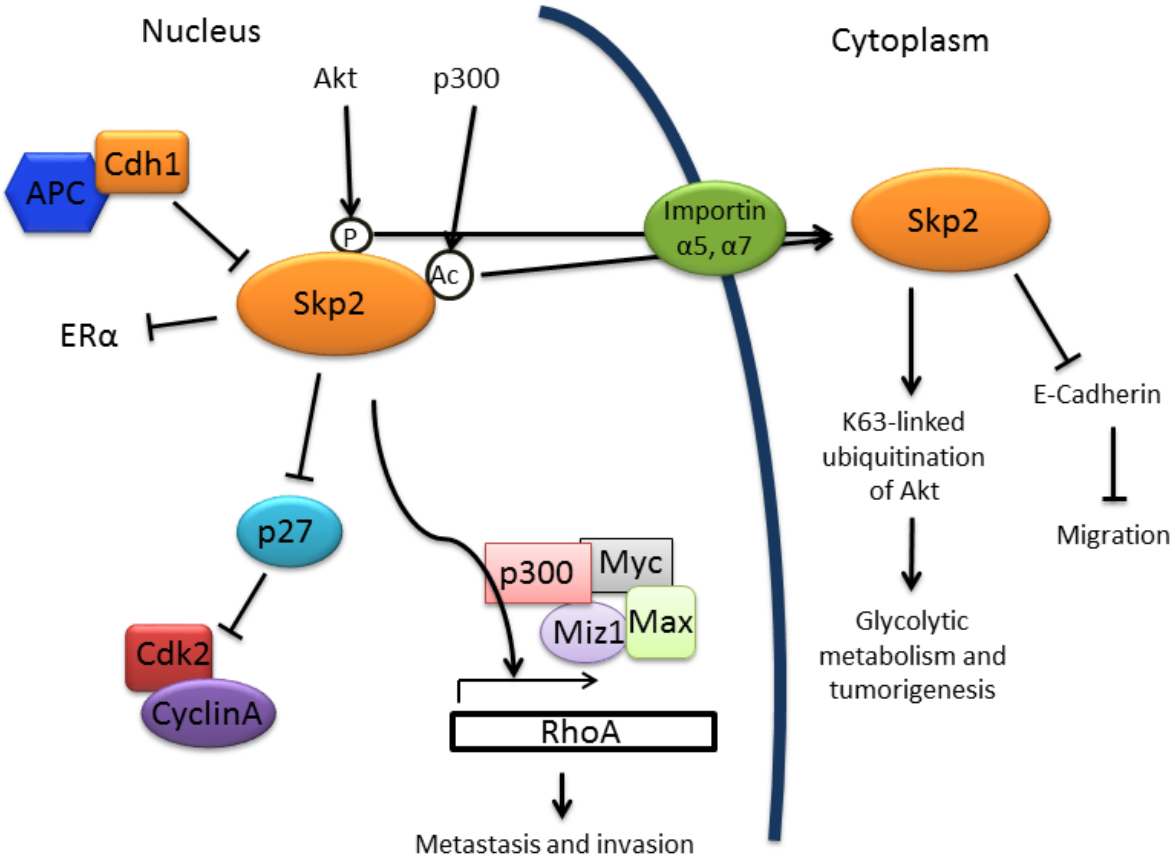

Figure 1.21: Oncogenic roles of Skp2. Skp2 has been implicated in many pro-oncogenic pathways in the nucleus as well as in the cytoplasm to which Skp2 localises after phosphorylation by Akt or acetylation by p300 within the NLS.

The role of Skp2 in tumourigenesis and tumour progression appears to be dependent on acetylation and phosphorylation status, subcellular localisation, and various binding partners (Figure 1.21). A more complete understanding of the roles of Skp2 in cancer would benefit not only basic science, diagnosis and prognosis, but might also highlight pathways and protein targets suitable for drug discovery efforts.

1.10 Targeting the Skp2/p27 interaction for chemotherapeutic intervention

1.10.1 Indirect inhibition of Skp2 activity

Skp2 has emerged as an attractive drug target due to its involvement in cell cycle control, apoptosis and metastasis; as well as emerging roles in the integration of cell signaling pathways involved in oncogenesis. The finding that Skp2 is nonessential for life, but required for cancer progression, has increased expectations of the therapeutic potential of Skp2 (Nakayama et al., 2000). Inhibitors have been developed which indirectly down-regulate Skp2 by targeting the ubiquitin-proteasome system (UPS) or affect Skp2 activity. The Food and Drug Administration (FDA) have approved the use of bortezomib (Velcade) for treatment of multiple myeloma and mantle cell lymphoma (Bross et al., 2004, Kane et al., 2007). Bortezomib is a 26S proteasome inhibitor which prevents degradation of all proteins carrying Lys48-linked ubiquitin chains. Therefore it is unlikely that specifically targeting Skp2 would have a similar effect in multiple myeloma or mantle cell lymphoma. There have been many side effects reported with clinical use of Bortezomib with peripheral neuropathy being one of the most significant (Argyriou et al., 2008, Orlowski and Kuhn, 2008, Swords et al., 2015). This might be due to the wide range of pathways affected by the inhibition of the proteasome.

Another inhibitor which has broad effects is the neddylation activating enzyme (NAE) inhibitor, MLN4924 (Pevonedistat). Pevonedistat was the first reported neddylation inhibitor (Soucy et al., 2009). It blocks the neddylation of cullin proteins, thus preventing their activation. There are seven cullin proteins which make up the cullin-RING E3 ubiquitin ligase (CRL) family and Pevonedistat inhibits the degradation of all CRL substrates, including p27 (Soucy et al., 2009), although much of the activity of Pevonedistat has been attributed to inhibition of SCF- and/or CRL4-mediated ubiquitination of Cdt1 (Soucy et al., 2009, Lin et al., 2010b). Clinical trials of Pevonedistat as a single agent in lymphoma, myeloma and melanoma are ongoing. Results from a recent clinical trial indicate that Pevonedistat has modest clinical activity in patients with acute myeloid leukaemia (AML) and myelodysplastic syndromes (MDS) (Swords et al., 2015). Notably, emergence of resistance to Pevonedistat has been observed *in vitro* (Toth et al., 2012, Milhollen et al., 2012). In

cell lines and xenograft mouse models, mutations in the ATP-binding pocket of NAE were identified as the primary mechanism of resistance to Pevonedistat (Milhollen et al., 2012).

1.10.2 Direct inhibition of Skp2 activity

A number of groups have identified compounds that target Skp2 directly (summarised in Table 1.1 and Figure 1.22). The first compound of this type was reported in 2008, when Chen and co-workers identified a set of inhibitors which were able to disrupt the Skp1/Skp2 complex (Chen et al., 2008). Inhibitors were screened using *in vitro* translated ^{35}S-labeled p27 and an *in vitro* reconstituted system consisting of CDK2, cyclin E, Skp1, Skp2, Cul1, Roc1 and a HeLa cell extract. Their lead compound, compound A (CpdA), was found to decrease p27 ubiquitination in this system. They showed that CpdA induced G1 cell cycle arrest and caspase-independent apoptosis (Chen et al., 2008). No further investigations on CpdA have been published since this initial report.

Other inhibitors have been developed which are reported to disrupt the Skp1/Skp2 interaction (Chan et al., 2013). Using the Skp1/Skp2 crystal structure, two potential pockets where small molecule inhibitors might bind were identified and virtual screening was used to identify hit compounds. The lead compound, compound 25, was hypothesized to bind to a pocket on Skp2 at the interface which contacts Skp1. Compound 25 was found to selectively bind Skp2 without affecting the interaction of Skp1 with the F-box proteins Fbw7 and β-TrCP. Compound 25 is able to prevent complex assembly in an *in vitro* system, however, the Skp1/Skp2 complex could not be disrupted after it had been formed.

Comparing these two studies which identified CpdA and compound 25, there were differences in the mechanisms of action of the compounds, for example, CpdA was found to induce autophagic cell death, whereas compound 25 induced cellular senescence. These differences may be due to where the putative binding sites of the two molecules are located, as compound 25 is believed to bind to Skp2, whilst the CpdA binding site has not been determined. Neither compound has been co-crystallised with Skp1 or Skp2 to confirm their binding sites and as Skp2 requires Skp1 for stability (Li et al., 2005), a structure of compound 25 with Skp2 might be challenging to obtain. Chan and colleagues also investigated the effect of compounds

on glycolysis, as the group had shown in an earlier publication that Skp2 deficiency impairs Glut1 expression, glucose uptake and glycolysis (Chan et al., 2012). They did indeed find that Skp2 inhibition by compound 25 suppressed glycolysis in two prostate cancer cell lines as determined by decreased expression of the glucose transporter 1 (Glut1) (Chan et al., 2013).

The interaction of p27 with Skp2/Cks1 has also been targeted for inhibition with small molecules (Ooi et al., 2013). A high-throughput screening system was used to identify small molecule inhibitors which would displace p27 from the Skp2/Cks1 interface. Skp2 was tagged with a fluorophore and Skp1, Skp2 and Cks1 were co-expressed in insect cells. The complex of Skp1/Skp2/Cks1 was added to a 96 well plate coated with covalently attached p27 phosphopeptide in the presence of small molecules. Two compounds, linichlorin A and gentian violet, were identified as inhibitors of p27 binding to Skp2/Cks1. The compounds have anti-proliferative activity against cancer cells and transformed cells, with IC50 values in the μM range (Ooi et al., 2013). A similar screen was developed in the Liu lab to find inhibitors of the Skp2/Cks1 interaction (Ungermannova et al., 2013). An AlphaScreen assay was used, which is a bead-based proximity assay. With a hit rate of 2.8%, 45 compounds were identified which disrupt the interaction of Skp2 with Cks1. An *in vitro* ubiquitination counterscreen identified two compounds, NSC689857 and NSC681152 which inhibit p27 ubiquitination (Ungermannova et al., 2013).

Another set of inhibitors believed to inhibit the interaction of p27 with Skp2/Cks1 came from the Pagano and Cardozo group (Wu et al., 2012). Using the Skp1/Cks1 crystal structure, a pocket formed by both Skp2 and Cks1 was identified, which is flanked by residues important for the binding of p27. A virtual screen of 315,000 compounds was carried out and mutagenesis was subsequently used to check that the lead compounds bound in the desired pocket. The authors identified four lead compounds, C1, C2, C16 and C20, but were unable to confirm their potential binding modes by co-crystallisation with Skp1/Skp2/Cks1 (Wu et al., 2012). They showed that p27 levels increase upon addition of the compounds, whilst p130 and Cdt1 (which are Cks1-independent substrates) were not affected, suggesting that the compounds might be specific for p27, p21 and possibly also p57. Following on from this initial study, the Cardozo group showed that their inhibitors increase nuclear p27 levels and decrease cytoplasmic levels over time in endometrial carcinoma (ECA) cell lines.

They also tested their compounds *in vivo*. Ovariectomised mice were injected with several doses of estradiol (E2) to induce p27 degradation. The mice were then treated with the C-series inhibitors, and this blocked p27 degradation and inhibited proliferation (Pavlides et al., 2013).

Name of inhibitor	Interaction targeted	Cellular response to inhibitor	Reference
CpdA	Skp1-Skp2	Decreased p27 ubiquitination. G1 arrest and caspase-independent apoptosis observed in myeloma cell lines	(Chen et al., 2008)
Compound #25	Skp1-Skp2	Induces cellular senescence, inhibits proliferation and reduces cancer glycolysis in prostate cancer cell lines.	(Chan et al., 2013)
Linichlorin A and gentian violet	p27 to Skp2/Cks1	Anti-proliferative in HeLa and tsFT210 cells.	(Ooi et al., 2013)
C1, C2, C20, C16	p27 to Skp2/Cks1	Induce p27 accumulation, G1 and G2/M arrest in breast and prostate cancer cell lines. Anti-proliferative *in vivo*.	(Wu et al., 2012, Pavlides et al., 2013)
NSC689857 and NSC681152	Skp2-Cks1	Inhibition of p27 ubiquitination.	(Ungermannova et al., 2013)

Table 1.1: Published small-molecule inhibitors of the SCF^{Skp2}complex.

1.10.3 Can structural studies guide development of small-molecule inhibitors of Skp2?

Structural studies over the past decade and a half have identified a number of potential pockets on Skp2 within the Skp2/Cks1 complex, which appear to be amenable to small-molecule inhibition (Figure 1.22). The most successful inhibitor of the SCF^{Skp2} complex is MLN4924 or Pevonedistat, which is a pan-Cullin inhibitor. The Pagano and Cardozo groups identified novel inhibitors specific to the degradation of

a subset of CKIs. They were able to show that these compounds induced cell cycle arrest (Wu et al., 2012). However, they were unable to obtain a crystal structure of their inhibitors bound to Skp2/Cks1 (Wu et al., 2012). Skp2 on its own is very unstable and therefore compounds which disrupt the Skp1/Skp2 interaction would be expected to render Skp2 unlikely to crystallise. This makes it difficult to define structure-activity relationships for any compounds, and is perhaps the reason for the stalling of SCF^{Skp2} drug discovery efforts over the past few years.

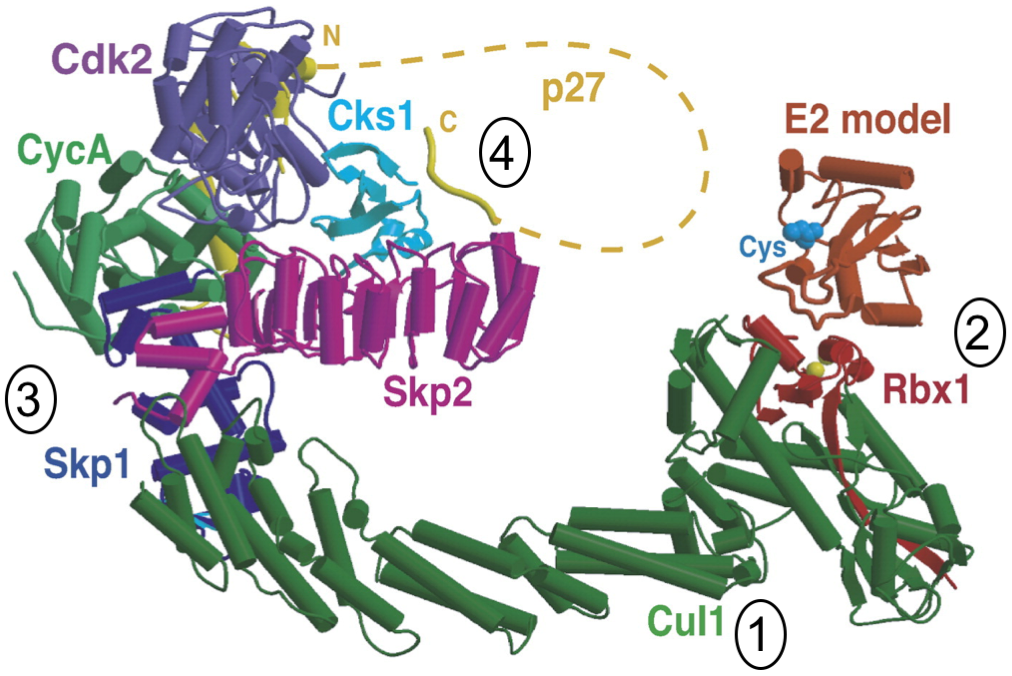

Figure 1.22: Interactions of the SCF^{Skp2} complex which have been targeted for small-molecule inhibitor development. 1) Cul1 activation has been targeted through inhibition of neddylation by MLN4924 (Pavonedistat) (Soucy et al., 2009). 2) The Cdc34 inhibitor, CC0651, has been shown to inhibit the ability of Cdc34 to ubiquitinate substrates (Ceccarelli et al., 2011). 3) Compound A and compound 25 are believed to inhibit the Skp1/Skp2 interaction (Chen et al., 2008, Chan et al., 2013). 4) Compounds have been identified which directly block the interaction of p27 with Skp2/Cks1 (Wu et al., 2012). Figure adapted from Hao et al. (2005).

Overview and aims of thesis

Skp2 was first identified as a component of a CDK2/cyclin A/Skp1/Skp2/Cks1 complex with unknown function (Zhang et al., 1995). Skp2 was later found to be the substrate recognition component of the SCF E3 ubiquitin ligase complex involved in the degradation of a range of substrates that include p27, p21, p57 and cyclin E. Over the past decade, further roles for Skp2 have been reported in areas such as cell cycle control through the indirect inactivation of Rb; metastasis through RhoA gene transactivation; activation of Akt through Lys63-linked ubiquitination; and cell migration through enhanced degradation of E-cadherin.

There is controversy both over the role of cyclin A in both p27 ubiquitination and Skp2 regulation. A number of investigations have shown that the Skp2/cyclin A interaction is required for optimal p27 ubiquitination (Zhu et al., 2004, Montagnoli et al., 1999, Sitry et al., 2002) and others have suggested that this interaction is required for regulation of Skp2 or CDK2/cyclin A kinase activity (Ji et al., 2006, Gao et al., 2009). This investigation first sought to identify the regions of Skp2 that interact with cyclin A and Cdh1. This knowledge would provide novel insights into the binding mechanism of Skp2 to cyclin A, identify potential overlapping sites of Skp2 protein interaction and help to explain how post-translational modifications in the N-terminal region of Skp2 may regulate alternative Skp2 complex assembly. This knowledge might also help to guide the development of small molecules to inhibit Skp2 activity. This work would build on compounds reported in the literature and that are currently in preclinical trials that block Skp2 function. Compound development has been hindered by a lack of appropriate Skp2-containing crystal structures. Despite this drawback, Skp2 remains a key potential target to treat many cancers and other Skp2-protein interactions might offer a better approach to targeting Skp2.

At the start of this project, it was known that Skp2 and p27 compete for binding to CDK2/cyclin A and Skp2 does not bind to CDK2/cyclin E. Although an RXL motif of Skp2 was identified as the putative cyclin A binding site (Sutterluty et al., 1999), it was later determined that Skp2 binds to a separate region of cyclin A as Skp2 binds independently of a RXL-containing short peptide (Ji et al., 2007). Therefore, the Skp2 and p27 binding sites are believed to overlap on the cyclin A surface, but at a site distinct from the RXL recruitment site.

Chapter 3 describes an investigation to identify cyclin A residues that mediate its interaction with Skp2. The Skp2 binding site on cyclin A is a novel site. Mutations at this site do not affect the catalytic activity of CDK2/cyclin A or disturb the cyclin A structure. The binding site of cyclin A on Skp2 is described in Chapter 4. The Skp2 mutant that is unable to bind to cyclin A is a useful tool to study the functional significance of this interaction and to develop further inhibitors that block Skp2 function. Studies to determine the crystal structure of Skp2 bound to CDK2/cyclin A are also described in Chapter 4. The validation of the Skp2 and cyclin A interaction sites *in cellulo* is described in Chapter 5, as well as the potential use of this mutant as a tool for investigating the function of the Skp1/Skp2/CDK2/cyclin A complex.

Chapter 2: Experimental procedures

2.1 Protein expression and purification

2.1.1 Expression of human pThr160 CDK2

The pGEX-6P-1-GST-CDK2-GST-CAK1 DNA construct (Brown et al., 1999) was transformed into chemically competent *E. coli* BL21 (DE3) pLysS cells (Agilent Technologies) according to the manufacturer's instructions. A single colony was picked to grow an overnight culture in 5-10 mL of Luria-Bertani (LB) medium. Ampicillin (Amp, 50 mg/L) and chloramphenicol (Cam, 34 mg/L) were added to maintain the pGEX-6P-1 and pLysS vectors, respectively. The saturated overnight culture was used to inoculate between 1 and 6 litres LB medium supplemented with antibiotics (Amp and Cam), which was incubated at 37°C with vigorous shaking. Once the culture reached an OD_{600} of between 0.8 and 0.9, the temperature was dropped to 18°C and the cells were left to equilibrate to this temperature for one hour. Isopropyl β-D-1-thiogalactopyranoside (IPTG) was then added to a final concentration of 80 μM. The cells were then incubated for 20 hours at 18°C with shaking. The cells were harvested by centrifugation at 4000 rpm (Beckman JLA, 8.1000) at 4°C for 20 minutes. The cell pellet was resuspended in 35 mL ice-cold modified HEPES-buffered saline (mHBS) buffer (Appendix A, Table A1.1) supplemented with a cOmplete™ EDTA-free protease inhibitor cocktail tablet (Roche) and stored at -20°C until use.

2.1.2 Expression of human cyclin A

The pET21d human cyclin A DNA construct (residues 174-432 with a C-terminal hexahistidine tail (Brown et al., 1999)) was transformed into chemically competent *E. coli* BL21 (DE3) pLysS cells (Agilent Technologies) according to the manufacturer's instructions. A single colony was picked to grow an overnight culture in 5-10 mL of LB medium. Amp (50 mg/L) and Cam (34 mg/L) were added to maintain the pET21d and pLysS vectors, respectively. The saturated overnight culture was used to inoculate between 1 and 6 litres of LB medium supplemented with antibiotics (Amp and Cam), which was incubated at 37°C with vigorous shaking. Once the culture reached an OD_{600} of between 0.5 and 0.6, the temperature was dropped to 30°C and the cells were left to equilibrate to this temperature for 15 minutes. IPTG was then added to a

final concentration of 100 µM. The cells were then incubated for 3 hours at 30°C with shaking. The cells were harvested by centrifugation at 4000 rpm (Beckman JLA 8.1000) at 4°C for 20 minutes. The cell pellet was resuspended in 35 mL ice-cold mHBS buffer supplemented with a cOmplete™ EDTA-free protease inhibitor cocktail tablet (Roche) and stored at -20°C until use.

2.1.3 Expression of Skp1/Skp2-N

The pGEX-6P-1-GST-Skp2-Skp1 construct (Figure 2.1) was transformed into chemically competent *E. coli* BL21 (DE3) pLysS cells (Agilent Technologies) according to the manufacturer's instructions. In this expression strategy the GST-Skp2 and Skp1 sequences are transcribed as a single mRNA that includes a second ribosome binding site downstream of the Skp2 stop codon. This construct encodes Skp2 residues 1-140 (Skp2-N) and full-length Skp1 (residues 1-163, Appendix A, Table A1.4). The GST-Skp2 fusion and Skp1 are translated from a single RNA transcript which encodes an internal ribosome binding site (RBS) 3' to the Skp2 stop codon to initiate Skp1 translation (Figure 2.1). A single colony was picked to grow an overnight culture in 5-10 mL of LB medium. Amp (50 mg/L) was added to maintain the pGEX-6P-1 vector. The saturated overnight culture was used to inoculate between 1 and 6 litres of LB medium supplemented with Amp (50 mg/L), which was incubated at 37°C with vigorous shaking. Once the culture reached an OD_{600} of between 0.5 and 0.6, the temperature was dropped to 30°C and the cells were left to equilibrate to this temperature for 15 minutes. IPTG was then added to a final concentration of 100 µM. The cells were then incubated for 3 hours at 30°C with shaking. The cells were harvested by centrifugation at 4000 rpm (Beckman JLA 8.1000) at 4°C for 20 minutes. The cell pellet was then resuspended in 35 mL ice-cold mHBS buffer supplemented with a cOmplete™ EDTA-free protease inhibitor cocktail tablet (Roche) and stored at -20°C until use.

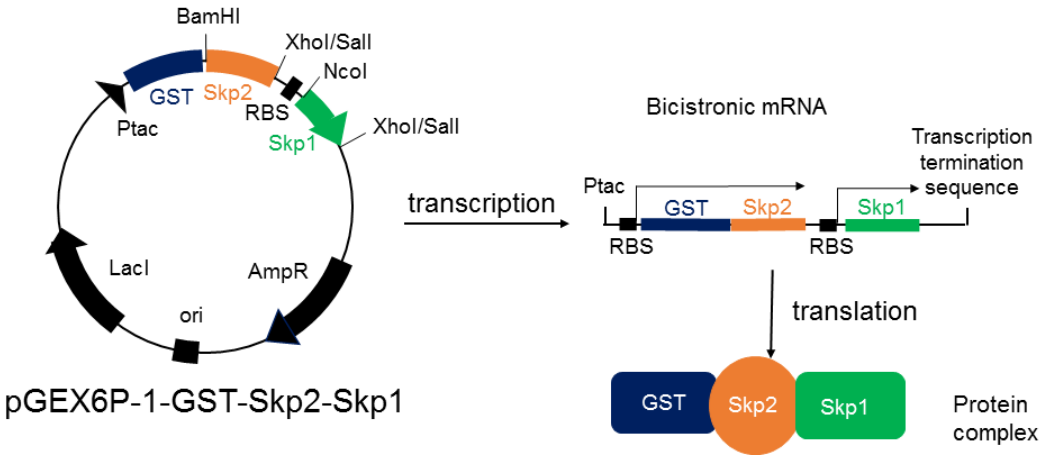

Figure 2.1: GST-Skp2/Skp1 construct. The GST-Skp2 and Skp1 gene sequences are transcribed into a bicistronic mRNA and then translated using separate ribosome binding sites. The GST tag is attached to the Skp2 N-terminus. Figure is from (Schueller, 2001).

2.1.4 Expression of Rb

GST-tagged Rb C-terminal construct encoding Rb residues 792-928 in the pGEX-2T backbone (Adams et al., 1999, Brown et al., 1999) (RbCT) was expressed in chemically competent *E. coli* BL21 (DE3) and purified by glutathione-Sepharose affinity chromatography as described (Brown et al., 1999). The GST-tag was not cleaved. Glycerol was added to the glutathione-Sepharose column eluate to a concentration of 50% and protein was stored at -20°C.

2.1.5 Other proteins required

Monomeric CDK2 was kindly provided by Mathew P. Martin, and p27 proteins were kindly provided by Martyna W. Pastok. All site-directed mutants and truncated versions of the above proteins were prepared using the same protocols as described above. The Skp2-C plasmid construct was a gift from Bing Hao (University of Connecticut). Judith Reeks expressed and purified Skp2-C for experiments described in Chapter 5, Section 4.3.

2.1.6 Lysis of E. coli cells

Lysozyme, DNase I and RNase were added to the resuspended cells (0.25 mg/mL, 10 µg/mL and 50 µg/mL final concentrations, respectively). The cells were lysed on ice by sonication, using pulses of 15 seconds on, separated by 15 seconds rest for a

total of five minutes. Lysates were then spun at 20,000 rpm for 1 hour at 4°C (Beckman Coulter Avanti, JA 25.5). The cleared supernatant was recovered and kept on ice.

2.1.7 GST-affinity purification

The GST-tagged protein complexes were purified by glutathione-Sepharose (GE Healthcare) affinity purification. The gravity-flow column (typically of bed volume 1-5 mls) was equilibrated in mHBS before the lysates were loaded onto the column. The column was run by gravity flow, allowing sufficient time for the GST to bind sufficiently. The column was washed with 10 column volumes (cv) of mHBS and then the complex was eluted with 20 mM glutathione in mHBS pH 7.0. The protein concentration of the eluate was determined using a Nanodrop 2000 (Thermo Scientific™) and GST-3C protease was added at a ratio of 1:50 w/w, protein of interest:3C protease, where cleavage of the GST-tag was required. Cleavage reactions were allowed to proceed overnight at 4°C.

2.1.8 Nickel-affinity purification

His-tagged bovine cyclin A was purified by nickel-affinity purification. The cleared lysate was loaded onto a 5 ml Ni-NTA column (GE Healthcare) pre-equilibrated in mHBS. The column was washed with 5 cv of 15 mM imidazole in mHBS. Elution was then performed with an imidazole gradient up to 300 mM imidazole in mHBS. Eluted fractions were analysed by SDS-PAGE for the protein of interest.

2.1.9 Size-exclusion chromatography

All proteins/ protein complexes were further purified using size-exclusion chromatography (SEC). 2-5 mL of concentrated protein (typically between 1-10 mg/ml) was loaded onto a Superdex 75 (26/60) column (GE Healthcare) which had been pre-equilibrated in mHBS. 2-4 mL fractions were collected and then analysed by SDS-PAGE to identify fractions containing the protein(s) of interest and determine their purity.

2.1.10 Subtractive affinity purification

A second glutathione-Sepharose purification was done in order to eliminate residual cleaved GST, as CDK2/cyclin A and Skp1/Skp2-N elute at the same volume on SEC

columns as GST. The column was again run under gravity-flow. Proteins were recovered in the unbound fraction and concentrated for subsequent experiments in 10, 000 kDa molecular weight cut off (MWCO) VivaSpin filter concentrators (Sartorius), spun at 5,000 rpm (Beckman Coulter Allegra 25R, TA-10-250) and at 4°C.

2.1.11 SDS-PAGE

Unless otherwise stated 12% SDS-PAGE gels were used (Expedeon). LDS sample buffer (Expedeon) was mixed with samples with a ratio of 1:4, before boiling at 100°C for two minutes. InstantBlue gel stain (Expedeon) was used to visualise protein bands.

2.2 Site-directed mutagenesis

2.2.1 Overview

Site-directed mutagenesis (SDM) is a method of creating targeted base changes in double-stranded plasmid DNA. There are several applications of SDM, such as the study of the effect of amino acid changes on protein function, or to remove or insert restriction endonuclease sites. Two synthetic oligonucleotides are designed, both containing the desired mutation. The strands are complementary to each other and the respective strands of the template. These oligonucleotides hybridise with the template after denaturation of the double-stranded DNA (dsDNA). The oligonucleotide primers are extended during incubation at an optimal temperature for the DNA polymerase. Multiple cycles of denaturation, hybridisation and extension generate plasmids with the desired mutations. Following temperature cycling, the product is treated with *Dpn*I endonuclease. *Dpn*I digests methylated and hemimethylated DNA, and thus digests the parental plasmid as DNA from most *E. coli* strains is Deoxyadenosine methylase (dam) methylated. The mutated plasmid can then be transformed into competent cells.

2.2.2 Primer Design

Primers were designed according to the Stratagene Quickchange SDM user manual and purchased from Integrated DNA Technologies (purified using standard desalting methods). The following equation was used to calculate the optimal

sequence of a primer. Primers were designed such that the melting temperature (T_m) was greater than 78°C, when possible.

$$T_m = 81.5 + 0.41(\%GC) – 675/N - \% \text{ mismatch} \qquad \text{(Equation 2.1)}$$

Where N is the number of bases and %GC is the percentage of guanines and cytosines in the primer sequence.

2.2.3 Reaction compositions

Primers were designed with desired mutations (see Appendix A, Table A1.2 for a list of primers used). Mutagenesis was carried out using WT and mutants of human cyclin A (residues 174-432) in pET21d as templates (Ruddick, 2010) according the manufacturer's instructions (Stratagene). The three mutated cyclin A sequences used as templates contained the following mutations: Mutant 5= M246Q, S247EN; Mutant 9= R293T and Mutant 10= T303K, D305R. Cyclin A mutants were subsequently verified by sequencing (Source Bioscience) and transformed into chemically competent E. coli BL21 (DE3) pLysS cells for expression.

All other mutagenesis reactions were carried out using Phusion polymerase according to the Phusion PCR manual (NEB). GC buffer was used, DMSO was added to a concentration of 3% and $MgCl_2$ was added to a final concentration of 2 mM. Primer anneal temperatures and elongation times were altered depending on the primers and templates used, respectively. Reactions were run in an Applied Biosystems GeneAmp PCR system 2700. Methylated template DNA was digested with *Dpn*I (10 units at 37°C for 1 hour) and the reactions were transformed into chemically competent *E. coli* DH5α cells (NEB). The plasmids were amplified in 5 mL overnight cultures of DH5α cells in LB medium supplemented with 50 µg/mL Amp. Plasmids were then purified using the Qiagen Miniprep kit according to the manufacturer's instructions. Sanger sequencing was used to verify the mutations had been correctly created, performed by Source Bioscience or Eurofins MWG.

2.3 DNA, RNA and protein quantitation

DNA, RNA and protein concentrations were determined using a Nanodrop Spectrophotometer 2000 (Thermo Scientific). Extinction co-efficients for proteins and

protein complexes were calculated using the Expasy Protparam program (http://web.expasy.org/protparam/). The extinction co-efficient is related to the residue composition of a protein. Only tryptophans (W), tyrosines (Y) and to a lesser extent cysteines (C) contribute to absorbance at 280 nM. Phenylalanine (F) absorbs at lower wavelengths (240-265).

2.4 Subcloning and plasmid preparation

Unless otherwise stated, InFusion cloning (Clontech) was used to subclone sequences. Primers for InFusion cloning are given in Appendix A, Table A1.3. The InFusion protocol from Clontech was followed throughout. Digested plasmids and PCR products were cleaned up using a PCR clean-up kit (Qiagen) prior to InFusion reaction. Reactions were initially transformed into chemically competent *E. coli* Stellar cells (Clontech) and plasmids purified from overnight cultures using a Miniprep kit (Qiagen).

2.5 Enzyme kinetic analysis of CDK2/cyclin A complexes

2.5.1 Rb phosphorylation assay

9 µL of 1 mg/mL RbCT stock, 6 µL 10x kinase buffer (5 mM ATP, 2 mM $MgCl_2$, 0.5 M Tris-HCl pH 7.5) and 39 µL ddH_2O were mixed in microcentrifuge tubes. Reactions were started with the addition of 6 µL CDK2/cyclin A WT or mutant. Reactions were incubated for 0-10 minutes. The reaction was stopped after each time point by removing a 20 µL aliquot, adding it to a tube containing 4x LDS loading buffer and boiling. Samples were analysed on an 8% gel, which provided a good separation of the variously hyperphosphorylated Rb proteins.

2.5.2 Histone H1 phosphorylation assay using radioisotope-labelled ATP

10 µg of CDK2/cyclin A was mixed in buffer 2 (10 mM Tris, 80 mM NaCl pH 7.5, 20% v/v glycerol, final assay concentration was 10 µg/mL) and 750 µg of Histone H1 was dissolved in buffer 2 (final assay concentration was 883 µg/mL). The reaction was started with the addition of [^{32}P] ATP to a final concentration of 12.5 µM, vortexing and placing in a waterbath at 30ºC. At each time interval, an aliquot of the reaction mix was taken out and spotted onto filter paper. The filter papers were then dried for

20 seconds and transferred to 1% phosphoric acid. [^{32}P] incorporation into histone H1 was measured by liquid scintillation counting. Reactions were carried out by Dr Lan Wang.

2.6 Isothermal titration calorimetry

2.6.1 Isothermal titration calorimetry theory

Isothermal titration calorimetry (ITC) is a biophysical technique used to quantitatively determine properties of bi-molecular interactions (Ladbury and Chowdhry, 1996). It is a useful complementary technique to structural biology as it allows a biochemist to define molecular mechanism in great detail. Every bi-molecular interaction has either an uptake or release of heat associated with it, and ITC is a universal indicator of binding (Ladbury, 2004). The equilibrium binding constant K_b (this is the reciprocal of the dissociation constant, K_d, commonly used as a measure of protein interactions) can be determined by direct measurement of heat exchanged as one component is titrated into the other. Unlike many other techniques, ITC allows the analysis of interactions between proteins in their native forms free from labelling and immobilisation (Cooper, 2003).

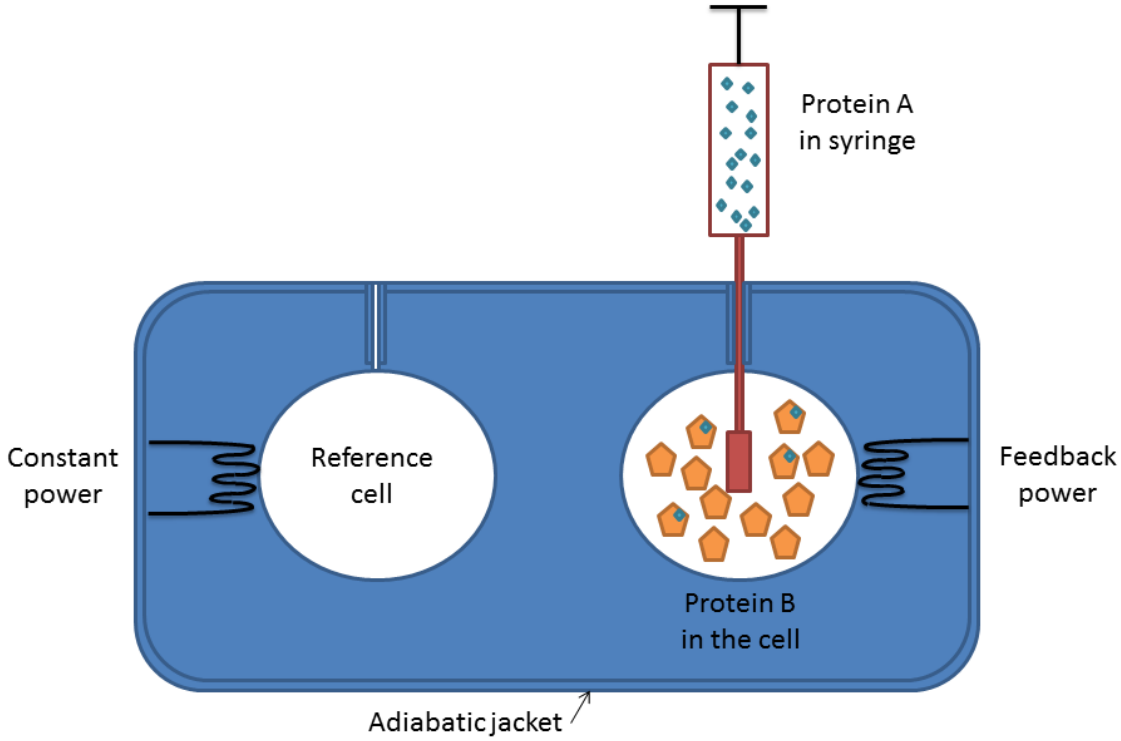

Figure 2.2: Schematic of an isothermal titration calorimeter. The microcalorimeter consists of two cells, the sample cell and the reference cell. One protein is loaded into the cell, the other is titrated into the cell from the syringe, and the heat exchanged upon binding is measured.

A calorimeter has two cells, the reference cell and the sample cell (Figure 2.2). They are in an enclosed adiabatic jacket which stops heat being lost into the surroundings. Constant energy is applied to both cells to keep a constant temperature. As the titrant is injected into the sample cell, this causes heat to either be taken up or be evolved. The change in the input energy to the sample cell to keep a constant temperature with respect to the reference cell is measured. The energy applied to the sample cell is plotted in µcal/sec. Each injection produces a change in the heat applied to the sample cell and then a return to baseline. Integration of these heat pulses gives the total heat exchanged per injection. Thermodynamic parameters can be derived from the heat exchanged. Using the equation below, the entropy of binding (ΔS), Gibbs free energy (ΔG), enthalpy upon binding (ΔH) and the association constant (K) can be calculated (Equation 2.2). The stoichiometry of the interaction (n) can also be determined from the molar ratio of the reactants (protein A/protein B) at the equivalence point of the titration (ITC-200 MicroCalorimeter User's Manual, GE Healthcare).

$$\Delta G = -RT \ln K_a = \Delta H - T\Delta S \qquad \text{(Equation 2.2)}$$

R is the gas constant (8.314 $JK^{-1}mol^{-1}$) and T is the absolute temperature. Enthalpy (ΔH) provides an indication of changes in hydrogen and van der Waal's bonding, whereas TΔS provides an indication of changes in hydrophobic interactions and conformational changes. ΔS is positive for entropically driven reactions.

Another parameter which can be determined by ITC is the stoichiometry (n-value) of the interaction. This is the average number of binding sites per mole of protein. The value for a 1:1 interaction is 1, however this can differ from 1 in an experiment due to many factors. These include miscalculation of protein or ligand concentration; having impurities in the protein or ligand solutions; having binding sites which are not all equally accessible or identical; or the proteins or ligands not being properly folded or active (ITC-200 MicroCalorimeter User's Manual, GE Healthcare).

In order to design an ITC experiment, a unitless c-value is used to describe the practical window over which the instrument can accurately determine the binding constants (Equation 2.3). A working c-value of 10-500 is preferable (Wiseman et al., 1989). It is recommended that the molar concentration of protein A (syringe) is 10 times greater than the molar concentration of protein B (cell). Given the volume of the cell (200 µl) and the syringe (40 µl), these starting conditions will ensure that at the end of the titration, there is a 2-fold molar excess of the titrant.

$$c = [M]/K_D \qquad \text{(Equation 2.3)}$$

[M] is the molar concentration of the protein in the cell (protein B in Figure 2.2).

2.6.2 ITC experiments

Protein concentration was determined using a Nanodrop 2000 spectrophotometer (see Section 2.3). CDK2/cyclin A could not be concentrated to as high a concentration as Skp1/Skp2, so Skp1/Skp2 or p27 peptides were injected from the syringe into CDK2/cyclin A in the cell. Proteins were adjusted to the correct concentration using mHBS. To avoid buffer mismatch, proteins were purified using the same SEC column in the same buffer. The temperature was kept at 25°C. There was an initial delay of 60 seconds. The titrations consisted of 18 injections, an initial injection of 0.5 µL and then 17 injections of 2 µL with 180 seconds between injections. The stirring speed in

the reaction cell was 1000 rpm. Heats of Skp1/Skp2 or p27 dilution were determined in independent control experiments by diluting the syringe content into buffer.

2.6.3 ITC data analysis

The ITC data were analysed using non-linear least squares regression in the Origin® software (OriginLab®). Drifts in the baseline were corrected during data analysis. The heats of dilution caused by the addition of the syringe content into buffer in the cell were subtracted from the addition of the syringe contents into the sample in the cell for all sets of data apart from the initial cyclin A mutant data (Figure 3.14). Origin 7.0 (OriginLab Corp.) was used for all data analysis, including ligand dilution subtractions and data fitting to the one-set-of-sites model.

2.7 Skp1/Skp2 pull-down assay

Compounds were dissolved in DMSO to a concentration of 100 mM and 10 mM. 200 µL of IgG-binding magnetic beads (Novex, Life Technologies) were washed twice with 200 µL IP lysis buffer (Pierce). 20 µL of magnetic IgG binding bead suspension were added to microcentrifuge tubes (1.8 mL) followed by 200 µL of lysis buffer containing 5 µg of anti-Skp2 antibody (8D9, 32-3300 Life Technologies) and this mixture was then rotated gently for 30 minutes. 20 µg of purified, untagged Skp1/Skp2 was added and a 2 µg sample was taken for the 10% inputs. The microcentrifuge tubes were rotated at 4ºC for one hour. The tubes were placed on a magnet to sediment the beads. The supernatant was removed, and 198 µL lysis buffer with 2 µL inhibitor was added. The final concentrations of inhibitor were 1 mM and 100 µM. The tubes were then left rotating overnight at 4ºC. The following morning, the magnetic beads were washed twice with 200 µL IP lysis buffer. 30 µL of Laemmli buffer (6.25 mM Tris/HCl, 2% w/v SDS, 10% v/v glycerol, 5% v/v β-mercaptoethanol, 0.0025% w/v bromophenol blue, pH 6.8) was then added. The sample was split to run two SDS-PAGE gels followed by Western blot in order to probe for Skp1 and Skp2-N separately as they have similar molecular weights.

2.8 Circular dichroism

The integrity of the CDK2/cyclin A mutant folds were assessed by circular dichroism (CD). CDK2/cyclin A complexes were buffer exchanged using a PD-10 column (GE

Healthcare) into 10 mM potassium phosphate pH 7.0. The final concentration of protein was 0.1 mg/mL. All CD experiments were taken on a Jasco J-810 spectropolarimeter at 20°C. A buffer base-line was subtracted from the protein spectrum for each experiment. The far-UV CD spectra (190-250 nm), was measured using a 0.2 mm Hellma quartz cuvette, a 2nm bandwidth, and a scan speed of 20 nm/min with a response time of 4s. The spectra were recorded as three averaged accumulations, and displayed as Δε ($M^{-1}cm^{-1}$) calculated using the mean residue concentration. In order to test the stability of the proteins, the melting temperature was calculated following the CD experiments. The CDK2/cyclin A complexes were slowly heated from 20ºC to 80 ºC causing the proteins to denature. When proteins unfold, they lose their highly ordered structures and the CD spectra is changed (Greenfield, 2006). Thereby, the melting temperature is given by the temperature at which there is a change in the CD spectra to one characteristic of an unfolded protein.

2.9 Analytical SEC and SEC-MALLS

When light passes through a solvent, interaction with molecules in the solvent leads to scattering of the light. This scattered light is detected at many angles to the beam. Changes in solute lead to changes in the scattering and these are dependent on the concentration and molar mass of the solute. In a suitably calibrated system, this information can be used to determine the molar mass of the solute. For large proteins of greater than 200 kDa, this method can be used to determine protein size by deriving the radius of gyration. The SEC-MALLS instrument typically consists of a size-exclusion column followed by a scattering detector and refractive index monitor.

The SEC-MALLS instrument was calibrated with BSA immediately prior to this experiment. The instrument was run at 0.5 ml/minute in mHBS pH 7.0, 1 mM DTT which had been filtered twice to remove any small particles. Protein samples (100 µl) were loaded onto a Superdex 200 10/300 GL SEC column (GE Healthcare). The column output was analysed by a DAWN HELEOS II MALLS detector (Wyatt Technology), in which light scattered from a polarized laser source of 664 nm is detected by eight fixed angle detectors. The sample is then analysed by an Optilab T-rEX differential refractometer (Wyatt Technology), which measures absolute and differential refractive index using a 664 nm LED light source at 25°C. Data were

collected and analysed using ASTRA 6 software (Wyatt Technology). Data analysis was performed by Dr Owen R. Davies.

2.10 X-ray crystallography

2.10.1 Introduction to X-ray crystallographic methods

X-ray crystallography is a technique for obtaining atomic resolution structures of proteins. To obtain X-ray diffraction data, the molecules must be in an ordered crystalline array. One commonly used method of crystallisation is vapour diffusion, in which the protein solution is allowed to equilibrate in a closed container with a larger aqueous reservoir (Figure 2.3). Crystallisation requires high protein purity, usually greater than 95%. Commercial sparse matrix screens of various precipitants and conditions are generally used for initial screens. If crystallisation is successful, resulting crystals are tested for diffraction using X-rays.

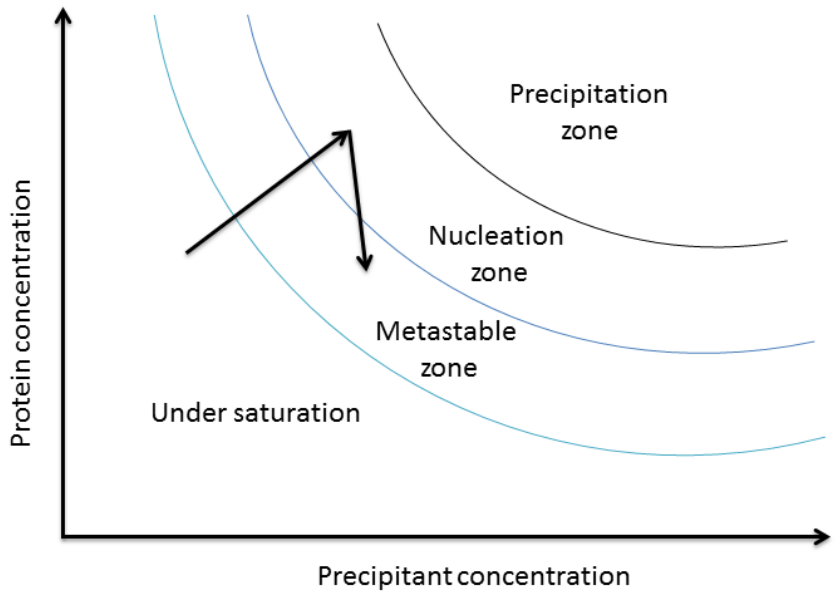

Figure 2.3: Protein crystallisation phase diagram. The protein solution increases in precipitant due to vapour diffusion. Crystal formation is initiated when the protein and precipitants are optimal within the nucleation zone window. The process of crystallisation decreases the concentration of the protein in the solution leading to crystal growth in the metastable zone.

2.10.2 The unit cell

The simplest repeating unit of a crystal, which is repeated to form the crystal lattice, is called the unit cell. The translations in a three-dimensional lattice may be described in terms of three vectors a, b and c; and angles α, β and γ between them (Figure 2.4). A crystal is assigned a space group, which is classed based on the operations which described the crystalline periodicity.

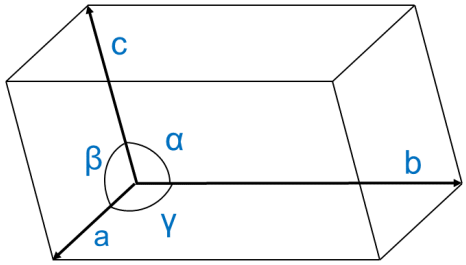

Figure 2.4: The unit cell of a crystal lattice. A primitive unit cell and parameters are illustrated. The dimensions of the unit cell are described with the vectors a, b and c and angles α, β and γ.

2.10.3 Bragg's Law

Exposure of a protein crystal to X-ray radiation leads to diffraction of the X-ray by the lattice planes which satisfy Bragg's Law (Equation 2.4).

$$2d\sin\theta = n\lambda \qquad \text{(Equation 2.4)}$$

Where d is the interplanar distance, θ is the scattering angle, n is the order of the reflection and λ is the wavelength of the incident wave.

2.10.4 Structure factors

Each reflected wave can be described by a structure factor, which is a mathematical function describing the amplitude (F) and phase of a wave (α) diffracted from crystal lattice planes. The structure factor equation (Equation 2.5) describes how structure factors can be calculated from the distribution of atoms in the unit cell.

$$\boldsymbol{F}(hkl) = F(hkl).exp[i\alpha\,(hkl)]$$

$$= \sum_j^N f_j.\exp\,(B_j.\exp\,[2\pi i\,(hx_j + ky_j + lz_j)] \qquad \text{(Equation 2.5)}$$

Where $\boldsymbol{F}(hkl)$ is the structure factor for the reflections of Miller indices $h\ k\ l$; $F(hkl)$ is the structure factor amplitude; $\alpha\ (hkl)$ is the phase; f is the atomic scattering factor; B is the temperature factor (or B-factor); and x, y and z are the fractional coordinates of atoms j giving rise to the scattering.

The structure factors can then be used to derive the electron density $\rho(xyz)$ using Fourier Transform (Equation 2.6).

$$\rho(xyz) = \frac{1}{V}\ \Sigma_h \Sigma_k \Sigma_l\ F(hkl).\exp\left[2\pi i\left(hx_j + ky_j + lz_j\right)\right] \qquad \text{(Equation 2.6)}$$

Where V is the unit cell volume.

2.10.5 Molecular Replacement

As X-ray detectors can only record intensities but not phases, the phase information is lost. This is known as the 'phase problem'. This phase problem can be solved using a number of methods. When a highly homologous molecule has been structurally characterised, the phases of the known structure can be used in order to solve the unknown structure. In order to solve the CDK2/cyclin A mut 7 structure, the method of molecular replacement was used starting from a high resolution CDK2/cyclin A WT structure (PDB code 2C5O) as the search model.

Molecular replacement uses the Patterson method (Equation 2.7), which consists of three steps, a search for the rotation function [C]; a search for the translation t and finally a refinement of the position molecule(s).

$$X_2 \approx [C]X_1 + t \qquad \text{(Equation 2.7)}$$

First, the Patterson function, P_c, calculated from the model is compared to the observed data, P_o, for all orientations of the data. This gives a rotation function, R which is a statistical quantity of the correctness of the molecular replacement solution.

The Patterson function (Equation 2.8) is a Fourier transform of the square of the structure factor amplitudes, and can therefore be used to produce a density map. Peaks in the Patterson function indicate interatomic vectors.

$$P(\underline{u}) = \Sigma_v \rho(\underline{x}).\rho(\underline{x}+\underline{u})\, dV = \frac{2}{V}\, \Sigma_h \Sigma_k \Sigma_l\, F(hkl)^2.\cos[2\pi\,(hu+kv+lw)]]$$

and $F_h^2 = I(hkl)$ (Equation 2.8)

Where $P(\underline{u})$ is the value of the Patterson function at a point specified by the vector $\underline{u}(u,v,w)$; $\rho(\underline{x}+\underline{u})$ is the electron density at positions $\underline{x}$ and $\underline{x}+\underline{u}$; and V is the unit cell volume.

2.10.6 Crystallisation and structure determination of CDK2/cyclin A mutant 7

CDK2/cyclin A mut 7 was concentrated to 5.6 mg/mL in mHBS. As the mutant complex did not crystallise in conditions previously shown to support crystal growth of the CDK2/cyclin A WT complex, the mutant complex was re-screened in sitting drop 96-well trays (MRC two-well plate, Hampton Research) using a Mosquito liquid handler (TTP Labtech). Drops were 300 + 300 nL and 300 + 600 nL (protein + mother liquor). Crystals were first obtained from a Morpheus (Molecular Dimensions) commercial screen. A hit was obtained from condition H11, which corresponds to 0.1 M Tris/Bicine pH 8.5, 0.1 M amino acids, 20% v/v glycerol, 10% w/v PEG 4K at 4°C. An optimisation screen was designed based on this condition. The optimisation screen was set up using a Biomek NXP automated workstation (Beckman Coulter). Stock solutions were 1 M Buffer 3 (Tris/bicine), 1 M amino acids, 100% glycerol and 60% PEG 4K. Due to the high glycerol concentration, cryoprotectant was not required. Conditions which yielded crystals were Morpheus buffer 3 (Tris/bicine) pH 9.0, 20% v/v glycerol, 10% w/v PEG 4K, drop ratio 2:1; and Morpheus buffer 3 (Tris/bicine) pH 9.0, 22.7% v/v glycerol, 11.3% w/v PEG 4K, 50 mM amino acids, drop ratio 1:1. Crystals were harvested using fibre loops and flash-cooled in liquid nitrogen. X-ray diffraction data were collected at the Diamond Light Source (Didcot, UK) on the I-24 microfocus beamline. The automatic molecular replacement program MOLREP (CCP4 suite (Vagin and Teplyakov, 1997)) was used to calculate molecular replacement solutions and the correlation coefficients (the agreement between observed and calculated Patterson functions). Model building was done using Coot (CCP4 suite (Emsley et al., 2010)).

2.11 Cell based assays

2.11.1 Maintenance of HeLa and HEK293T cell lines

Human HeLa and HEK293T cells were grown in RPMI 1640 media (Gibco ®, Thermo Fisher Scientific) supplemented with 10% v/v foetal calf serum (FCS). Cells were grown at 37°C in 5% CO_2 in a humidified incubator and passaged when confluency reached around 80%. Cell lines used in this study were routinely confirmed to be mycoplasma negative using the Mycoalert detection kit (Lonza) by Elizabeth Matheson.

2.11.2 Transfection of HeLa and HEK293T cells

Cells were seeded onto 6-well plates or 10 cm dishes 18-20 hours prior to transfection at a density of about 5 x 10^4 cells/mL so that they achieved 60-70% confluency at the time of transfection. Transfection was carried out using LT1 (Mirius Bioscience) transfection reagent according to manufacturer's instructions. Briefly, 0.75 µg (for 6-well plates) or 4.5 µg (for 10 cm dishes) of each of the pcDNA3 Myc-Skp2 and pcDNA5/FRT/TO Flag-cyclin A vectors (prepared using an EndoFree Plasmid Maxi Kit, vector maps are shown in Figure 2.5) was added to Opti-MEM reduced serum media (ThermoFisher Scientific). 3 µL of LT1 was added for every 1µg of DNA. The mixture was swirled gently and incubated at room temperature for 20 to 30 minutes before adding dropwise to different areas of the wells or plate to evenly distribute the LT1:DNA complexes. Cells were placed in the 37°C incubator for 24 hours before harvesting (Section 2.11.3). For the IP experiments, two 10 cm dishes were used for every co-transfection (plasmid combination) in order to have excess amounts of protein for the IP experiments.

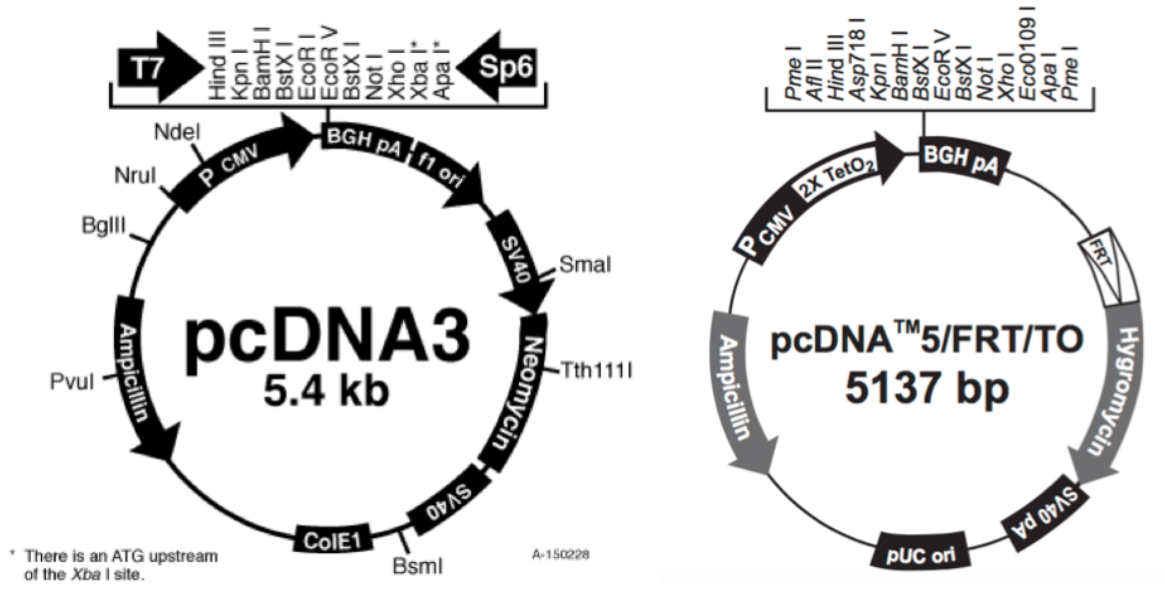

Figure 2.5: Plasmid maps of pcDNA3.1 and pcDNA5/FRT/TO. (Reproduced from Life Technologies pcDNA3.1 and pcDNA5/FRT/TO manuals).

2.11.3 Lysis of HeLa and HEK293T cells

HeLa and HEK293T cells in 6-well plates were lysed by addition of 30 µL 6.25 mM Tris-HCl pH 6.8, 10% glycerol 2% SDS for the expression tests using the BCA assay (Section 2.11.4). For the immunoprecipitation experiments (Section 2.11.5) cells were scraped off the 10 cm dishes in ice-cold PBS and then spun down at 500 rpm (Eppendorf microcentrifuge) for five minutes. The supernatant was discarded and the cell pellet was resuspended in IP lysis buffer (Pierce). After lysis buffers were added, samples were stored at -20°C until use.

2.11.4 BCA assay

A BCA assay kit (Pierce ThermoFisher) was used according to the manufacturer's instructions to determine protein concentrations of whole cell lysates for measurement of expression levels of transfected proteins. Briefly, cells were thawed and sonicated for 15 seconds on ice. 2.5 µL were taken and mixed with 22.5 µL MilliQ water and added to wells of a flat-bottom 96-well plate. Reagent A and B were mixed according to the Manufacturer's instructions and 200 µL was added to each diluted lysate in the 96-well plate. The plate was incubated at 37°C for 30 minutes and then absorbance was measured at 570 nm using a Model 680 Microplate Reader (BioRad). Standard BSA concentrations were measured for every separate reading.

2.11.5 Immunoprecipitation

Immunoprecipitation experiments were carried out using the Classic IP Kit (Pierce) with anti-Flag antibody (Sigma F1804), anti-Myc-tag antibody (9E10, SantaCruz sc40) or anti-Cdh1/FZR1 antibody (Life Technologies 34-2000). HeLa and HEK293T cells were suspended in IP lysis buffer (Pierce) supplemented with Halt Protease and Phosphatase Inhibitor Cocktail (Life Technologies) and transferred into microcentrifuge tubes. For each co-transfection (plasmid combination), two 10 cm dishes of cells were lysed per IP reaction. Cells were mixed for one hour at 4°C to allow cell lysis. The lysates were then passed through a 22 gauge needle, and spun down at 13,000 rpm (Beckman Coulter microfuge® 22R) for 15 minutes at 4°C. 80 µL of the supernatant was removed and retained as the whole cell lysate (WCL) fraction. The rest of the supernatant was added to the Control Agarose Resin. The supernatant and resin were mixed for 30 minutes and then the column flow-through was collected and 8 µg of antibody was added. The mixture was incubated on ice with occasional mixing for two hours and then the antibody-lysate mixture was added to prewashed Protein A/G Agarose, and mixed end-to-end for a further hour. The column was then washed according to the Classic IP Kit protocol. Anti-Flag antibody-immobilised and anti-Myc tag antibody-immobilised proteins were eluted with Flag (M2 peptide, Sigma) and Myc (M2435, Sigma) peptides, respectively. Cdh1 antibody-immobilised proteins were eluted by addition of 40-60 µL Laemmli sample buffer.

2.11.5.1 Western immunoblotting

Proteins were separated on a 4-20% Criterion gel (Biorad) using SDS-PAGE, and then transferred to a polyvinylidene difluoride (PVDF) membrane using Biorad wet electroblotting equipment. Blots were blocked in Tris-buffered saline with 0.05% v/v Tween 20 (TBST) supplemented with 5% w/v dehydrated milk for one hour. Blots were incubated overnight at 4°C with primary antibody in TBST supplemented with 5% w/v dehydrated milk at a dilution recommended by the manufacturer. Blots were washed for a total of 15 minutes in TBST. Stabilised peroxide-conjugated goat anti-mouse (Dako) or goat anti-rabbit (Dako) antibody was added at a 1:1000 dilution and incubated for one hour at 4°C in TBST supplemented with 5% w/v dehydrated milk. Blots were washed again for a total of 40 minutes in TBST. Enhanced chemiluminescence (ECL, Pierce) was used as the Western blotting developing reagent and blots were exposed onto film (Kodak).

2.11.6 Antibodies

Anti-cyclin A2 (BF683, 4656) was purchased from Cell Signalling. Anti-Skp2 (32-3300) and anti-Cks1 (37-0200) were purchased from Life Technologies. Anti-Cdh1 (ab3242) was purchased from Abcam. Anti-Flag (F3165) was purchased from Sigma. Anti-Myc (05-419) was purchased from Merck Millipore. Anti-CDK2 (sc-6248), anti-p27 (sc-528) and anti-GAPDH (sc-25778) were purchased from Santa Cruz Biotechnology.

Chapter 3: Identification of the cyclin A Skp2 binding site

3.1 Creation of cyclin A mutants to identify the Skp2-binding site on cyclin A

3.1.1 Cyclin A is unique amongst cyclins in its interaction with Skp2

CDK2/cyclin A has a role in the ubiquitination of p27 by the SCF^{Skp2} complex. As outlined in Chapter 1, Skp2 binds to cyclin A and this event may help to stabilise the interaction between CDK2/cyclin A and the SCF^{Skp2} complex. However, is not clear to what extent the Skp2/cyclin A interaction is required for p27 ubiquitination and whether the only function of the Skp2/cyclin A interaction is to assist the ubiquitination of p27. It has been demonstrated that the direct interaction between Skp2 and CDK2 is very weak (Ji et al., 2006) suggesting that the major interaction between CDK2/cyclin A and Skp2 is through the cyclin subunit. The same group demonstrated that Skp2 does not interact with CDK2/cyclin E, which, given that the two cyclins are very similar in structure (Figure 3.1), suggests surface sequence differences that might define a cyclin A-specific Skp2 binding site (Ji et al., 2006, Jeffrey et al., 1995, Honda et al., 2005).

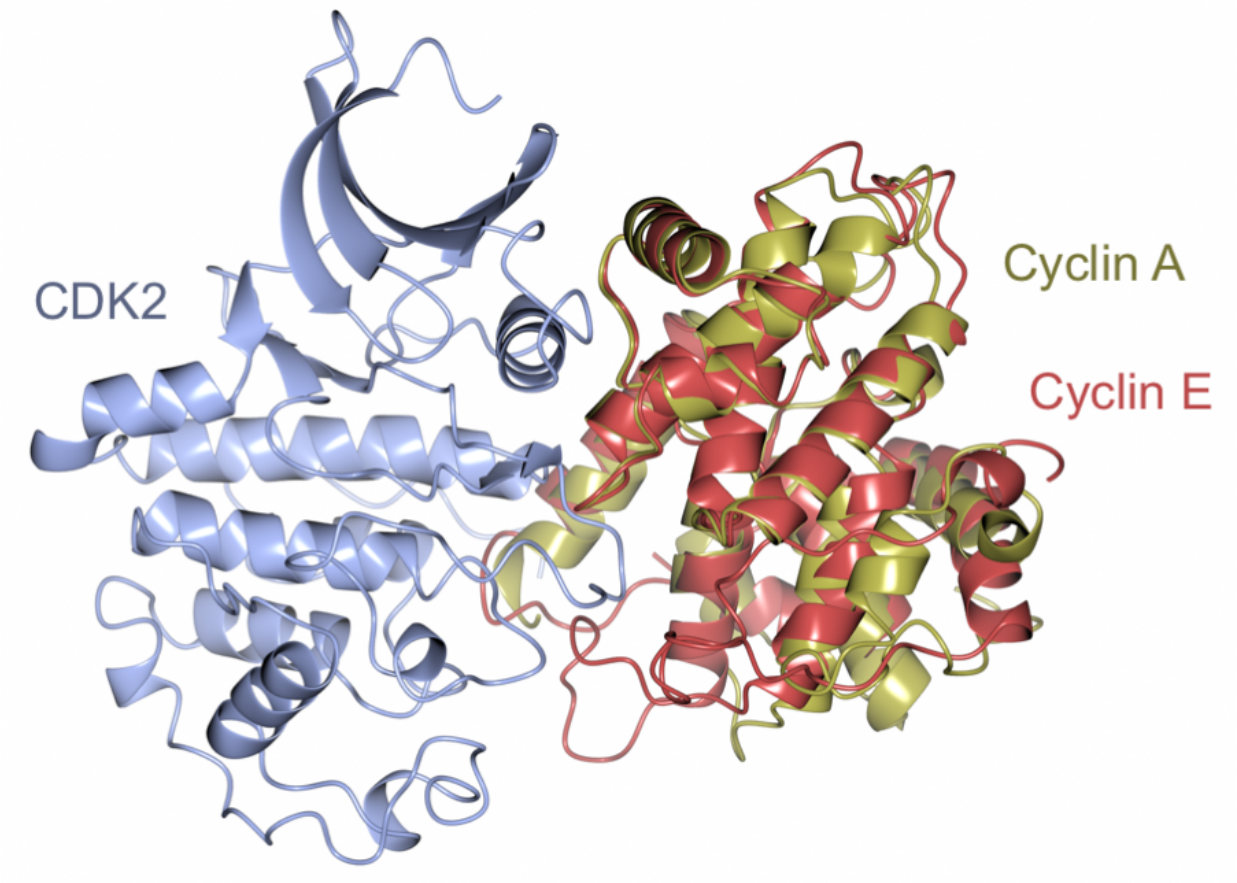

Figure 3.1: CDK2 with superposed cyclin A and cyclin E. PDB codes 1JST (cyclin A) and 1W98 (cyclin E). CDK2 from 1W98 is shown.

As expected for two cyclins that both partner CDK2 and bind to recruited substrates and p21/p27 inhibitors, cyclins A and E share a high degree of sequence similarity at the CDK2 interface and recruitment site, respectively (Jeffrey et al., 1995, Honda et al., 2005). Outside this region, the N-terminal CBF (N-CBF) is relatively well conserved (Figure 3.2). The sequence identity between cyclin E1 and cyclin A N-CBFs (residues 126-225 and 207-305, respectively) is 42% and the r.m.s.d. in Cα carbons is 0.8 Å for 100 atoms. The C-terminal CBFs (C-CBFs) of cyclin E1 and cyclin A share a fairly high degree of structural homology with an r.m.s.d in Cα of 1.4 Å (PDB 1W98 and 1JST, respectively). However, the C-CBFs are poorly conserved at the sequence level with 13% homology (residues 226-330 of cyclin E1 and residues 306-401 of cyclin A). In addition to differences in sequence, CDK2/cyclin E and CDK2/cyclin A differ in their relative dispositions of the cyclin subunit. The C-terminal domain of cyclin E makes additional contacts with CDK2 particularly in the activation loop. Overall, the interface between CDK2 and cyclin E is 14% larger than that between CDK2 and cyclin A. Both

the cyclin sequence and its interactions with the associated CDK2 subunit might contribute to the observed difference in binding affinity between Skp2 and CDK2/cyclin A vs CDK2/cyclin E. However both cyclins have similar activating effect on CDK2 (Honda et al., 2005, Brown et al., 1995, Jeffrey et al., 1995).

Figure 3.2: Alignment of the sequences of cyclin A and cyclin E showing the regions which are in close contact with p27. Orange bars indicate residues within 5 Å of p27. Cyclin A is the upper sequence. Adapted from Lacy et al. (2005). An asterisk indicates positions which have a fully conserved residue. A colon indicates conservation between groups of strongly similar properties, scoring >0.5 in the Gonnet PAM 250 matrix. A full stop indicates conservation between groups of weakly similar properties, scoring =<0.5 in the Gonnet PAM 250 matrix. Figure was created using Clustal Omega (Sievers et al., 2011), uniprot codes P20248 (cyclin A) and P24864 (cyclin E).

Additional insights into where cyclin A might bind Skp2 have been provided by competition studies with other known CDK2 regulators. CDK2/cyclin A was found to be associated with Skp2 in transformed cell lines, but associated with p21 in untransformed cell lines raising the possibility that Skp2 and p21 could be mutually exclusive in their binding to CDK2/cyclin A (Xiong et al., 1993b, Zhang et al., 1995). Further support for overlapping p21/p27 and Skp2 binding sites on cyclin A came from

the discovery that p21 and p27 can both disrupt the CDK2/cyclin A/Skp2 interaction (Yam et al., 1999, Ji et al., 2006). However, Skp2 does not contain a solvent-accessible RXLF motif (Figure 3.3) and a RXLF motif-containing peptide can bind to cyclin A in the presence of Skp2 (Ji et al., 2006). Taken together these results suggest that Skp2 may bind to a site on the upper surface of the N-CBF (relative to the orientation of Figure 3.3).

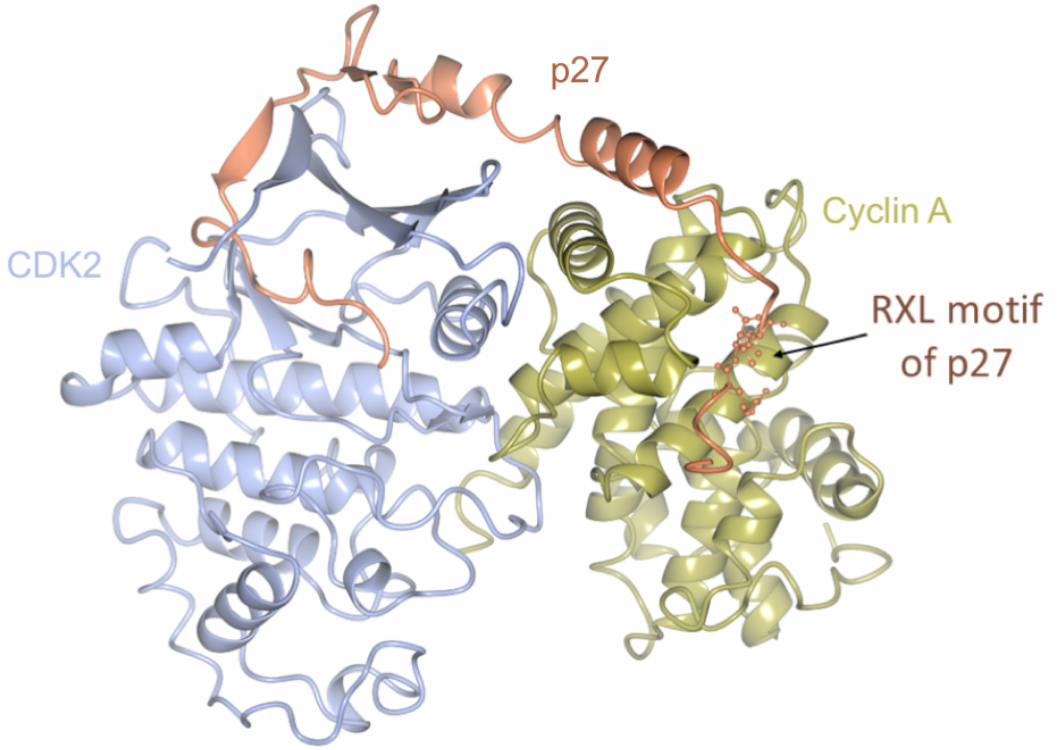

Figure 3.3: The RXL motif of p27 binds to the cyclin recruitment site. Skp2 does not contain an RXL motif and is believed to compete with p27 for binding to the upper surface of the N-CBF. CDK2 is in ice-blue, cyclin A is in yellow and p27 is in coral.

3.1.2 Skp2 is a CDK2/cyclin A substrate

CDK2/cyclin A substrates often bind to the RXL recruitment site of cyclin A. Cyclin binding to the substrate can confer specificity as changing a CDK's cyclin partner alters the substrates phosphorylated by the complex (Brown et al., 2007, Loog and Morgan, 2005). The interaction of Skp2 with cyclin A is not required for Skp2 phosphorylation (Ji et al., 2006). Skp2 is phosphorylated by CDK2/cyclin A and a Skp2 mutant that shows decreased binding to cyclin A is still a CDK2/cyclin A substrate.

3.1.3 Skp2 may be a regulator of CDK2/cyclin A

Ji and co-workers investigated the activity of a Skp2 blocking peptide, consisting of residues 28 to 45 of Skp2 (Ji et al., 2007). They found that this peptide was able to block the Skp2/cyclin A interaction, and the peptide was small enough that it did not block the p27 interaction. Therefore, the peptide and p27 could bind simultaneously keeping CDK2/cyclin A in an inactive state. This observation, together with their earlier work that showed that p27 could be competed off CDK2/cyclin A by an increasing concentration of Skp2, led to the hypothesis that Skp2 protects CDK2/cyclin A from p27 inhibition (Ji et al., 2006). Figure 3.4 shows the possible binding site of the Skp2 blocking peptide which is predicted to be near the p27 binding site, but does not overlap with it. Therefore, other residues of Skp2, not included in this peptide, must mediate the interaction with cyclin A which does overlap with p27.

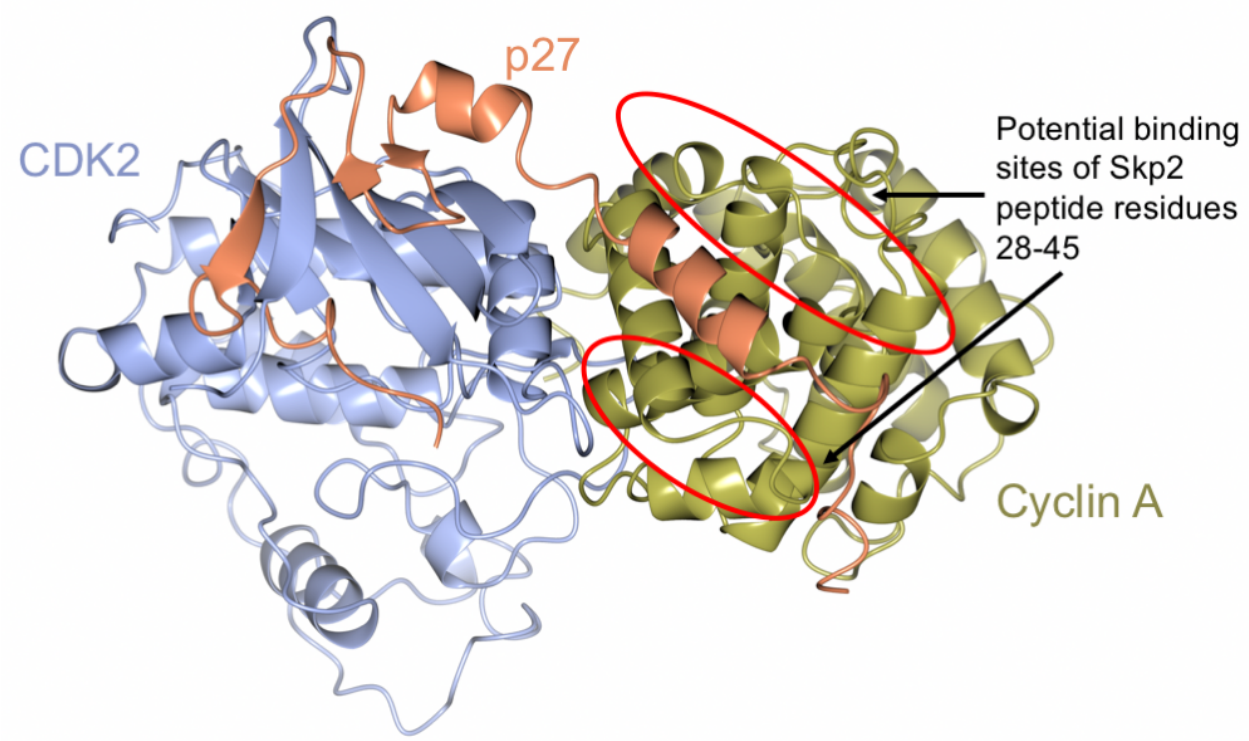

Figure 3.4: Structure of CDK2/cyclin A with p27 showing the potential binding sites of a peptide of Skp2. Skp2 and p27 compete for binding to cyclin A, however a peptide of residues 28-45 of Skp2 is able to bind in combination with p27.

In contrast, Yam and colleagues found that binding of the Skp1/Skp2 complex itself to CDK2/cyclin A inhibits kinase activity (Yam et al., 1999). In the original paper identifying Skp1 and Skp2 as CDK associated proteins, Skp2 was not found to

significantly affect CDK2/cyclin A kinase activity *in vitro* (Zhang et al., 1995). These differences might be explained by differences in experimental design, as Ji and co-workers found Skp2 to be protective when p27 is present, whereas the other two studies were performed *in vitro* in the absence of p27.

3.2 p27 competes with Skp2 for CDK2/cyclin A

To confirm the observation that Skp2 and p27 binding to CDK2/cyclin A is mutually exclusive *in vitro* using purified proteins, Nicole Schueller demonstrated that at equimolar concentrations, CDK2/cyclin A preferentially partitions into a complex with p27 rather than Skp2 (Figure 3.5 (Schueller, 2001)).This observation supports the earlier experiments of Sitry and co-workers (Sitry et al., 2002) that demonstrated that although Skp2 can remove p27 from the CDK2/cyclin A complex at high concentrations, the binding of p27 to CDK2/cyclin A is much tighter than Skp2 to CDK2/cyclin A.

A

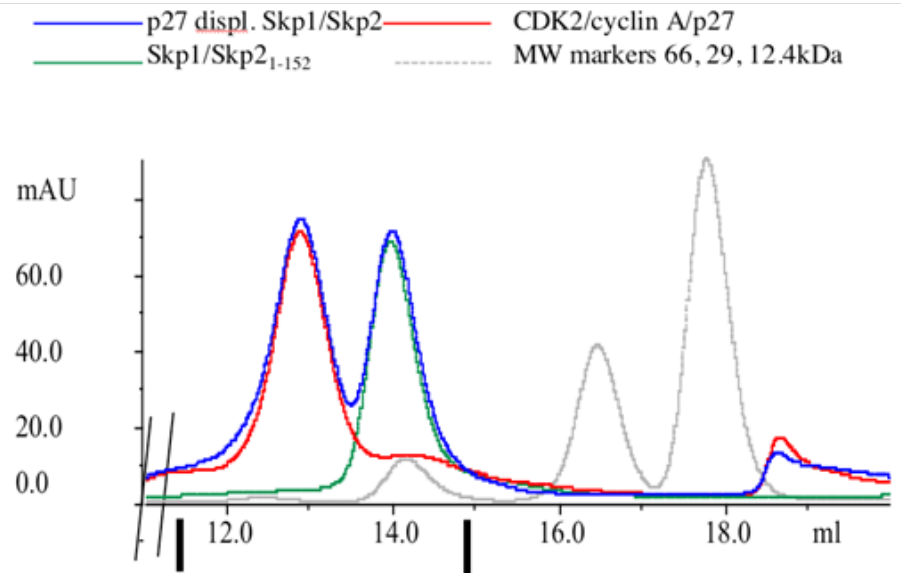

B

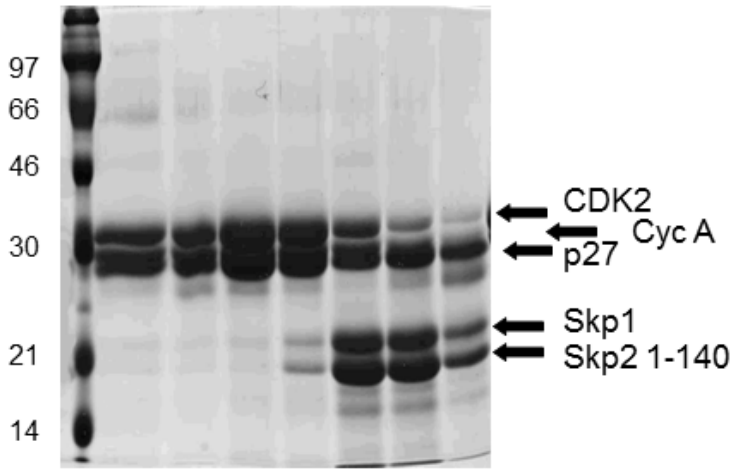

Figure 3.5: CDK2/cyclin A preferentially binds to p27 over Skp1/Skp2. A) Elution profiles of different complexes, as indicated in the key. B) Fractions from the p27 displacement of Skp1/Skp2 experiment (between black bars of panel A) were run on an SDS-PAGE gel. Experiment was carried out by Nicole Schueller.

3.3 Overview of chapter

This chapter describes experiments to identify the Skp2 binding site on cyclin A. A mutant cyclin A is described that shows negligible binding to Skp1/Skp2. Structural and kinetic analysis was performed on this cyclin A mutant in order to determine whether these mutations might affect cyclin A function or binding to other proteins. The mutant defines a novel protein binding site on the cyclin A N-CBF that is highly conserved across cyclin A orthologues and is not found in other cyclins that regulate the cell cycle.

3.4 Characterisation of the Skp2 binding interface of cyclin A

3.4.1 Generation of cyclin A mutants and their incorporation into CDK2/cyclin A complexes

A first set of cyclin A mutants were designed and tested for their interaction with Skp2 (Appendix A Table A1.2, (Ruddick, 2010)). The mutations encompass the p27 binding site but exclude residues at the RXL recruitment site. The residues were mutated from the sequence of cyclin A to that of cyclin E as cyclin A but not cyclin E binds to Skp2. This approach would decrease the likelihood of large conformational changes occurring to cyclin A as a result of mutation. It was also reasoned that mutations to alanine might not yield a mutant that blocked Skp2 binding. An alignment of the cyclin A and cyclin E sequences (Figure 3.2 and Figure 3.6) showed that the highest levels of conservation between cyclin A and cyclin E are within the p27 and CDK2 binding regions.

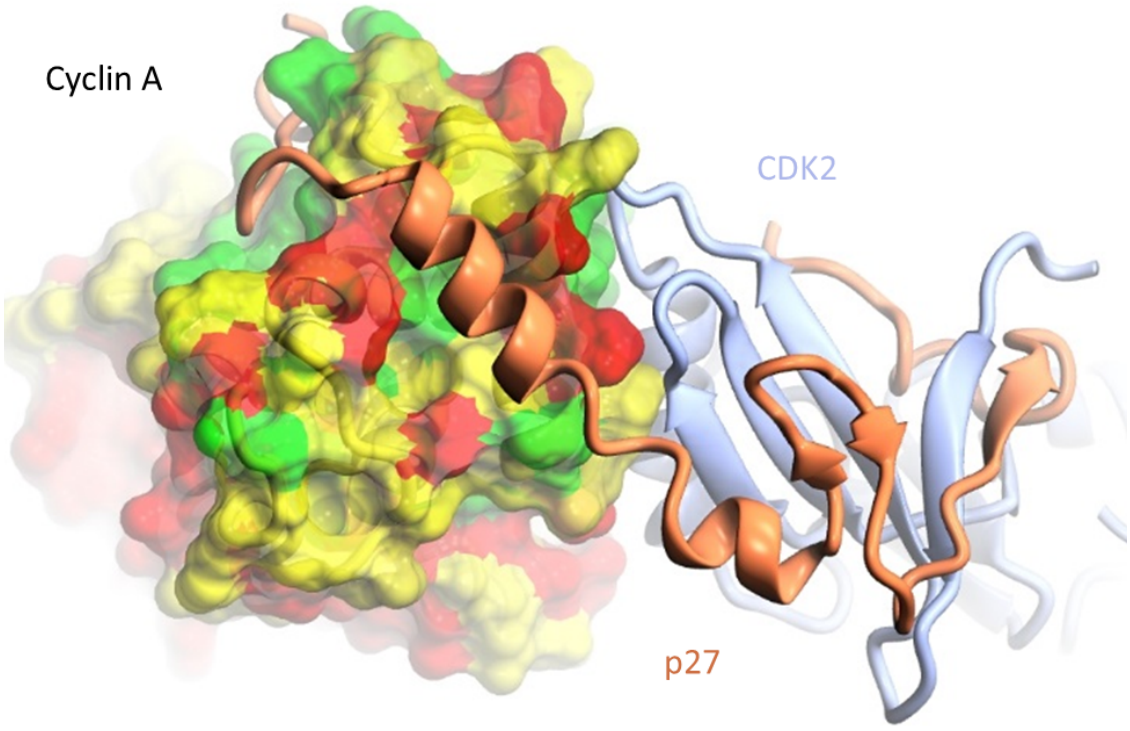

Figure 3.6: Residues conserved between cyclin A and cyclin E are predominantly in the p27 and CDK2 binding regions. Cyclin A is coloured according to whether the region is conserved, green indicates conserved regions, red indicates non-conserved regions and yellow indicates regions that are moderately well-conserved. CDK2 is coloured ice-blue and p27 is in coral. PDB: 1JSU

Building on this work further mutations were made to cyclin A (Table 3.1). The cyclin A construct used as a template to generate the mutants encodes the tandem CBFs, residues 173-432 in the pET21d vector backbone and is suitable for subsequent cyclin A expression in *E. coli* cells. The structure of this cyclin A fragment (referred to as cyclin A hereafter) was first described in Brown et al. (1999) and has since been used in a large number of structural studies. Cyclin A mutants (Table 3.1 and Figure 3.7) were designed based on the proximity of the residues to p27 (Figure 3.2), the conservation of the residues between cyclin A and cyclin E (Figure 3.6) and the understanding that Skp2 does not bind to the RXL recruitment site of cyclin A (Ji et al., 2006). The position of the mutated regions in relation to p27 are shown in Figure 3.7. Mutagenesis was carried out using a QIAGEN Quickchange kit according to the Manufacturer's instructions and is described in detail in Chapter 2 Section 2.

Mutant name	Residues mutated	Residue changes
Cyclin A mut 2	284-289	DTYTKK to GACSGD
Cyclin A mut 3	290-299	QVLRMEHLVL to EILTMELMIM
Cyclin A mut 6	299-305	LKVLTFD to MKALKWR
Cyclin A mut 7	244-247	SSMS to ATQEN

Table 3.1: Cyclin A residues mutated to investigate the Skp2 binding interface. The residues mutated and residue changes are shown in the table. A list of primers used in the mutagenesis of cyclin A is provided in Appendix A, Table A1.2.

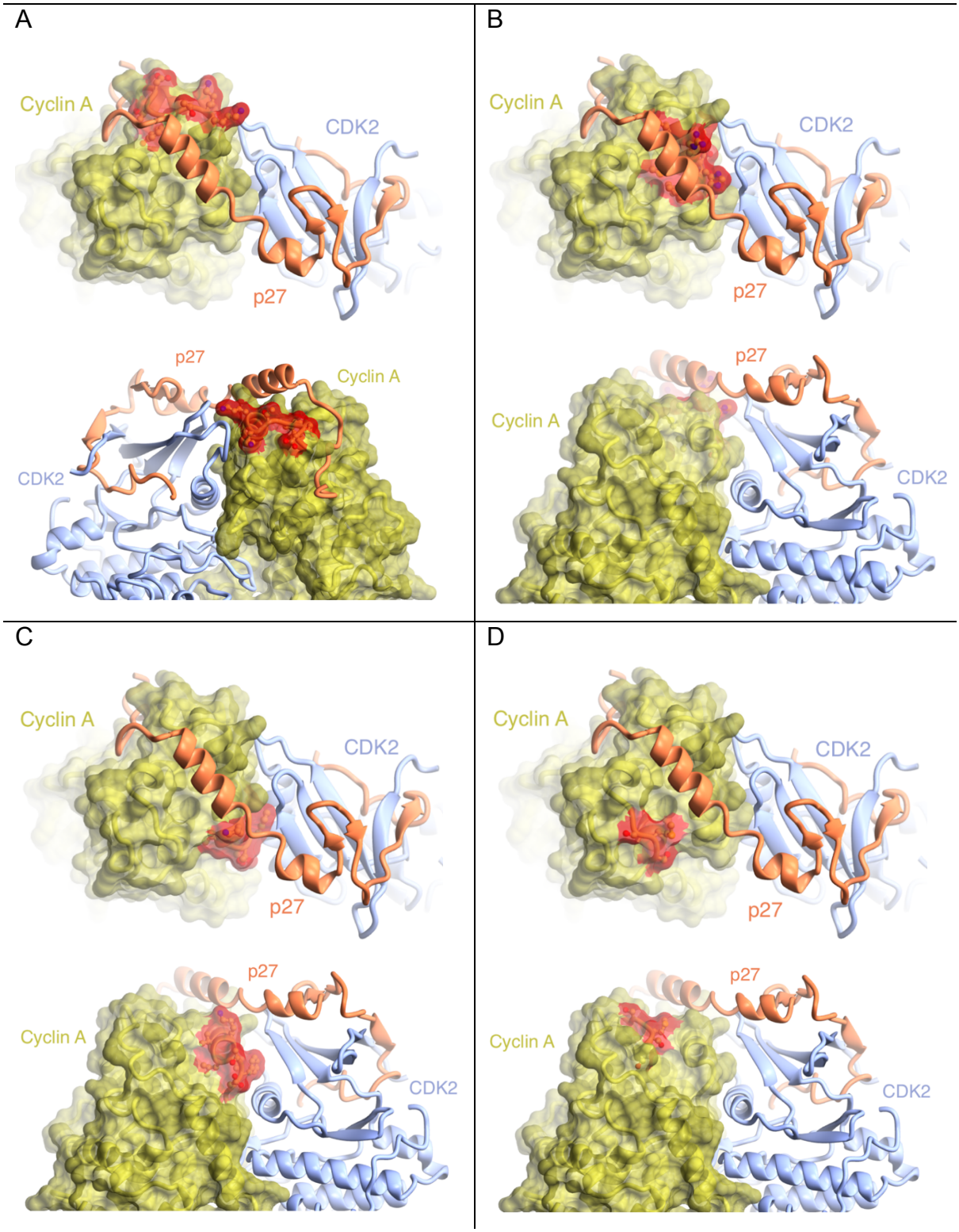

Figure 3.7: Regions of cyclin A mutated and their proximity to p27. CDK2/cyclin A mut 2 (A) mut 3 (B) mut 6 (C) and mut 7 (D) regions where mutations were made from a top view (looking down on p27) and from a side view (either front or back). CDK2 is in ice-blue, cyclin A is in yellow and p27 is in coral. The regions mutated (in red) were in close proximity to the p27 binding site but distant from the RXL binding site based on knowledge of the Skp2/cyclin A interaction. PDB: 1JSU.

To check that introducing these mutations is not detrimental to the integrity of the cyclin A, expression tests were performed. Briefly, constructs were transformed into *E. coli* strain BL21 (DE3) pLysS and cyclin A expression was induced at 30°C for three hours upon addition of 1 mM IPTG once the culture had reached an OD_{600} of between 0.5 and 0.6. A detailed description of the E. coli transformation and subsequent protein expression protocols can be found in Chapter 2, Section 1.2.

Unlike bovine cyclin A (Brown et al., 1995), human cyclin A is not stable in the absence of CDK2. As a result, human cyclin A is purified as a CDK2/cyclin A complex (Brown et al., 1999). CDK2 is expressed as a cleavable GST fusion from the pGEX-6P-1 vector backbone. Alternatively, to generate CDK2 phosphorylated on Thr160, this CDK2 expression cassette is co-expressed from the same vector with GST-CAK1 (*S. cerevisiae* CDK-activating kinase (Kaldis et al., 1996, Brown et al., 1999)). Briefly, GST-tagged CDK2 expressed from recombinant *E. coli* cells was affinity purified on a glutathione-Sepharose column. This column then acted as an affinity column for the untagged cyclin A, exploiting the tight binding between the two proteins (Figure 3.8A). The complex was eluted by excess glutathione, cleaved with 3C protease (to remove the GST tag from the CDK2) and subsequently purified by size-exclusion chromatography (SEC, Figure 3.8B). An excess of CDK2 is sometimes observed in the CDK2/cyclin A purification as CDK2 expresses very well. This is illustrated in Figure 3.8B where the shoulder on the peak at around 190 ml is excess CDK2. As the GST dimer and CDK2/cyclin A co-elute, the major peak was re-applied to a glutathione-Sepharose column and the CDK2/cyclin A collected in the flow-through (Figure 3.8C).

Figure 3.8 shows that all cyclin A mutants express well although there is some variation, but this is within the margin of variation seen for cyclin A WT expression and purifications. Typical yields for CDK2/cyclin A WT and mutants are *circa* 8 mg/L. This analysis also confirms that each of the cyclin A mutants retains the ability to bind to CDK2. Authentic and mutant CDK2/cyclin A complexes could be successfully concentrated to *circa* 12 mg/mL and stored in aliquots (400 µL) at -20°C/-80°C. However, for isothermal titration calorimetry (ITC) experiments (Sections 3.6 and 3.7.3), protein samples were freshly prepared.

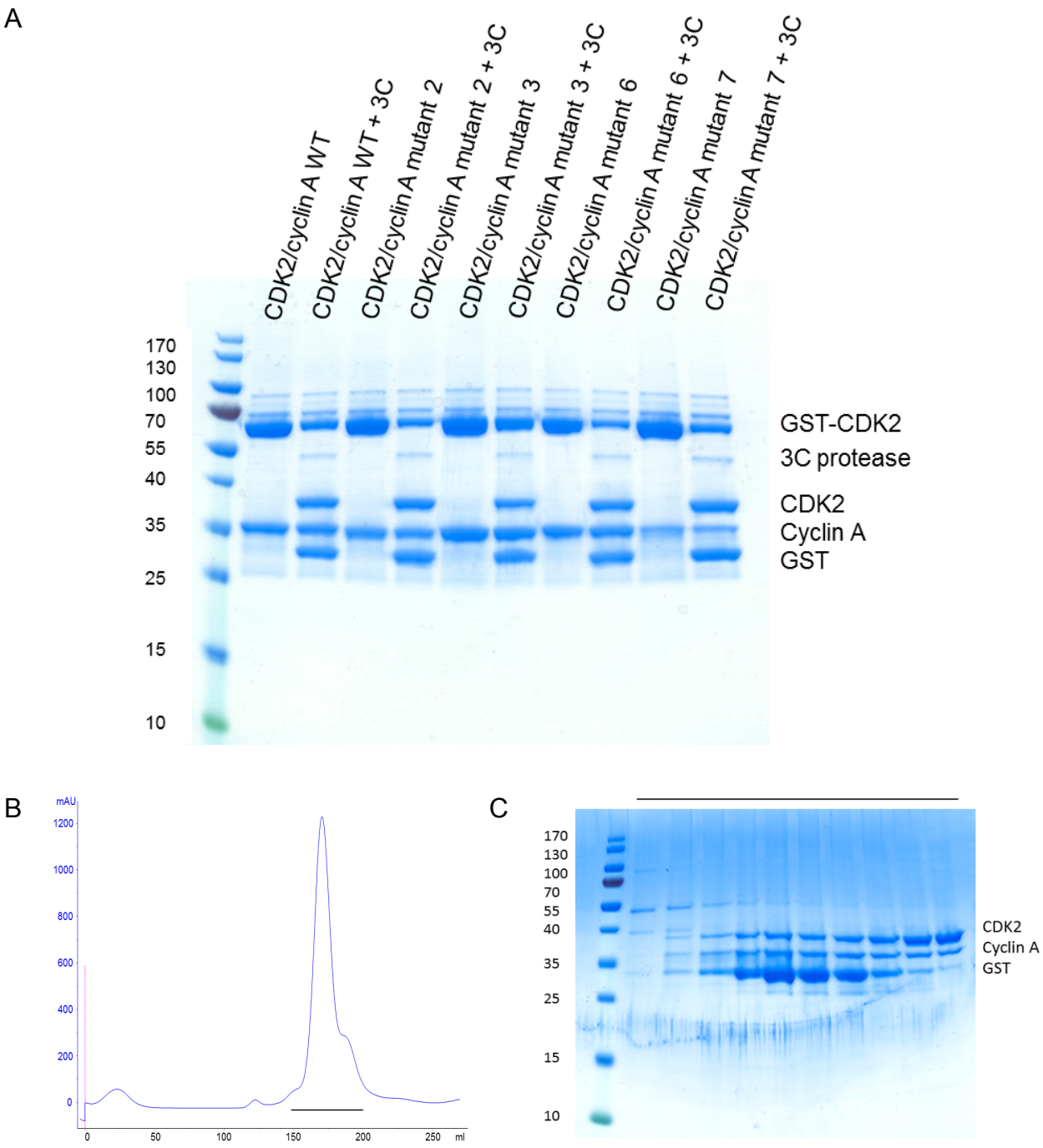

Figure 3.8: Purification of CDK2/cyclin A. A) CDK2/cyclin A WT and mutants after glutathione- Sepharose affinity purification and after 3C protease was added B) Size-exclusion chromatogram of CDK2/cyclin A WT after 3C cleavage of the GST tag on the N-terminus of Skp2. C) SDS-PAGE analysis of CDK2/cyclin A selected fractions from the region of the peak indicated by the black bar on the chromatogram (B).

3.4.2 Generation of a Skp2/Skp2 complex to characterise Skp2 association with CDK2/cyclin A

Skp2 is unstable when monomeric, which is thought to be due to the hydrophobic nature of the F-box region. To overcome this difficulty, the N-terminal sequence of Skp2 that encodes the N-terminal regulatory region and the F-box (residues 1-140, Figure 1.9), was co-expressed as a GST fusion with Skp1 (Figure 2.1).

E. coli BL21 (DE3) pLysS cells were transformed with the vector pGEX-6P-1-GST-Skp2-N-Skp1 and the complex was successfully expressed following a 3 hour induction at 30°C. It was subsequently purified by GST affinity chromatography, cleaved with 3C protease and then loaded onto a size-exclusion column. It was found that the Skp1/Skp2-N complex co-elutes with GST (Figure 3.9). Consistent with a model in which Skp2 is unstable without Skp1, an excess of Skp2 was not observed. The complex expresses well and typical yields were *circa* 40 mg from 1 L of cell culture.

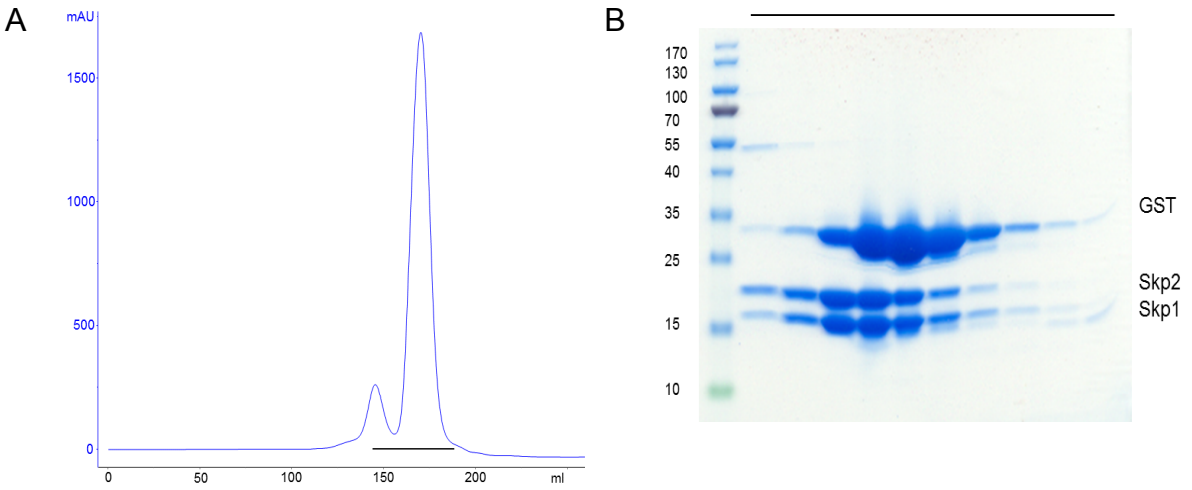

Figure 3.9: Purification of Skp1/Skp2-N. A) Size-exclusion chromatogram of Skp1/Skp2-N after 3C cleavage of the GST tag on the N-terminus of Skp2. B) SDS-PAGE analysis of Skp1/Skp2-N selected fractions from the region of the peak indicated by the black bar on the chromatogram (A).

The Skp1/Skp2-N complex elutes earlier than would be expected from its molecular weight. Skp1/Skp2-N co-elutes with CDK2/cyclin A, which is a globular protein complex of *circa* 65 kDa. This result suggests that Skp1/Skp2 might exist as a dimer

of dimers $(Skp1/Skp2\text{-}N)_2$ in solution. To unambiguously assess the Skp1/Skp2-N oligomeric state, the complex was analysed by size-exclusion chromatography-multi-angle laser light scattering (SEC-MALLS, methods described in Chapter 2, Section 10). This analysis showed that the complex does not oligomerize from which it can be inferred that it has a highly asymmetric shape in solution (Figure 3.10). As the structure of all but the N-terminal tail of Skp2 has been determined (Figure 1.17) (Schulman et al., 2000, Hao et al., 2005), it can be hypothesised that the N-terminal sequence may be very elongated causing the apparent molecular weight to be nearly twice its calculated molecular weight.

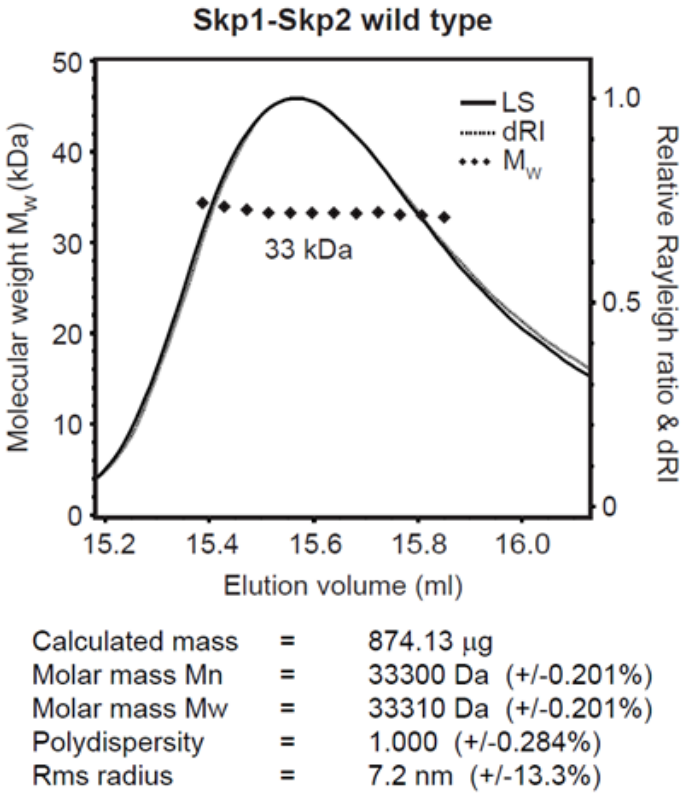

Figure 3.10: SEC-MALLS data for Skp1/Skp2-N. The calculated molecular weight of Skp1/Skp2-N is about 32700 kDa.

3.5 CDK2/cyclin A mutants identify a cyclin A surface that is required for stable association with Skp2

SEC was used to test the binding of the CDK2/cyclin A mutant complexes to Skp1/Skp2-N. The chromatograms showed that every cyclin A mutant tested could form a quaternary complex with CDK2 and Skp1/Skp2-N on a Superdex 200 10/30

column, but the chromatograms were difficult to interpret (data not shown). However it seemed that the mutants might be weakening the binding to some degree. It is possible that Skp2, like p27 binds to a large extended surface of cyclin A and knockout of one site might not block binding completely. A mutant cyclin A was therefore designed that incorporated all the 4 sets of mutations present in cyclin A mutants 2, 3, 6 and 7. This cyclin A sequence was gene-synthesized (IDT) and supplied in the IDTsmart vector. It was then amplified by PCR and subsequently inserted into the pET21d vector by InFusion cloning (Chapter 2, Section 4).

Figure 3.11 shows that the CDK2/cyclin A global mutant does not form a complex with Skp1/Skp2-N that is stable to gel filtration. Each of the complexes was sequentially applied to the same column (Superdex 200 10/30). There is a marked shift in the peak elution position when CDK2/cyclin A WT is mixed with Skp1/Skp2-N, but there is only a slight shift when the CDK2/cyclin A global mutant is mixed with Skp1/Skp2. The SDS-PAGE gel shows that the CDK2/cyclin A global mutant and the Skp1/Skp2-N complex elute at very similar volumes, to generate a very broad elution profile. The CDK2/cyclin A WT/Skp1/Skp2-N peak is not very far shifted from the binary complex peaks, so one might infer that Skp1/Skp2-N has become less elongated with the quaternary complex being more globular. The CDK2/cyclin A global mutant mixed with Skp1/Skp2-N runs as a single peak, but this peak nearly overlays completely with the binary Skp1/Skp2-N and CDK2/cyclin A global mutant complex peaks, indicating that this a quaternary complex is not being formed or is binding weakly. The small shift in the elution profile from what should be a peak to overlay the binary Skp1/Skp2-N and CDK2/cyclin A global mutant complexes might be due to non-specific binding caused by the proteins co-eluting on this column.

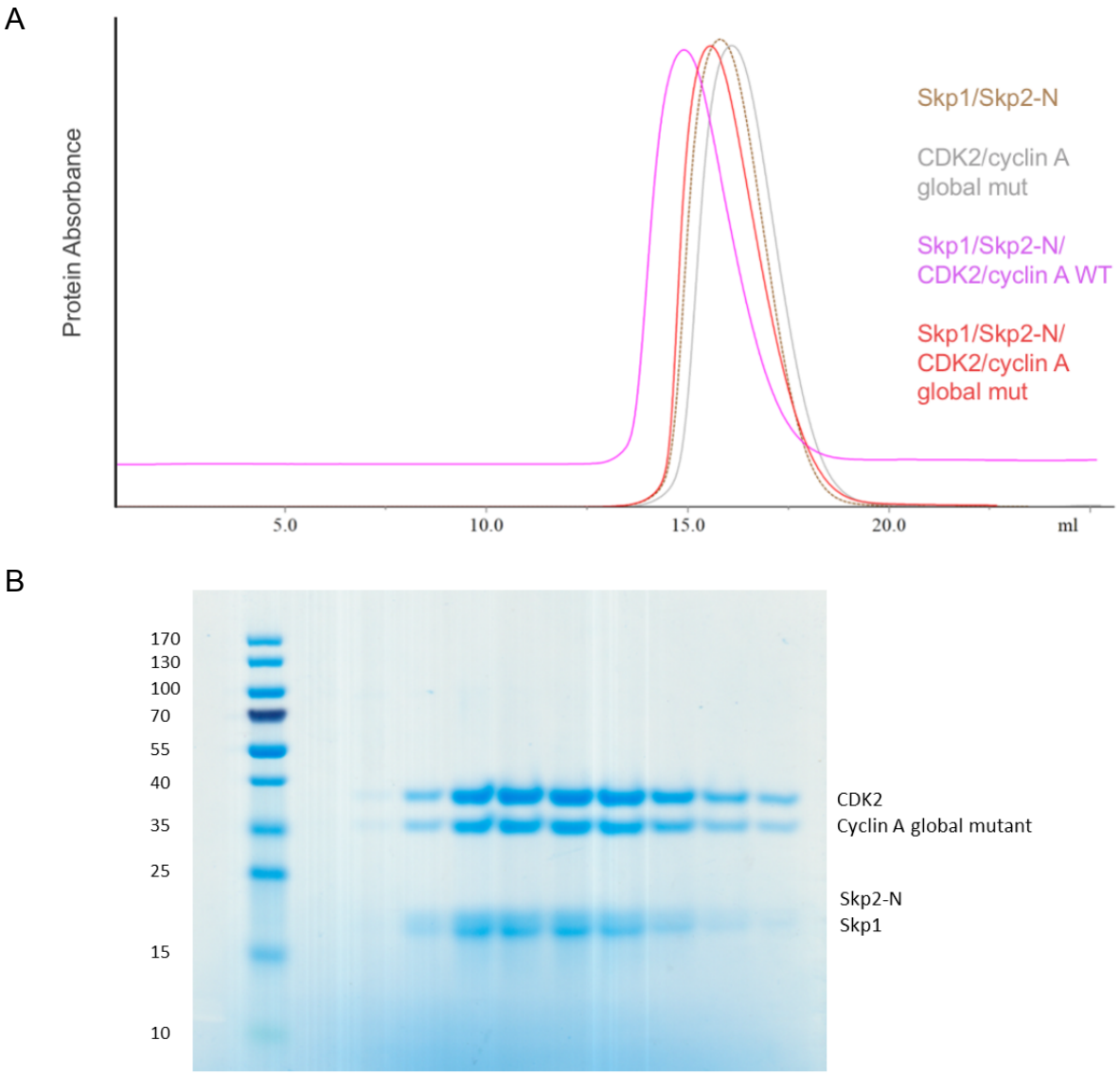

Figure 3.11: CDK2/cyclin A global mut/Skp1/Skp2-N complex is not stable to gel filtration. A) The protein complexes were mixed after concentrating and left to form a complex for one hour. They were then run on the Superdex 75 10/30 column. The curves were normalised to the Skp1/Skp2-N/CDK2/cyclin A WT trace to account for differences in absorbance and concentration. B) SDS-PAGE gel of the CDK2/cyclin A global mutant/Skp1/Skp2-N run.

CDK2/cyclin A mut 2 and mut 6 were analysed by analytical SEC on a Superdex 75 10/30 column which gave better resolution of the binary and quaternary complex peaks (Figure 3.12). This would show the individual contributions of these CDK2/cyclin A mutants to the binding of Skp1/Skp2-N. The elution profile of CDK2/cyclin A mut 6 is shown as an example in Figure 3.12 (red trace) and compared to that generated when authentic CDK2/cyclin A was mixed with Skp1/Skp2 (blue trace). Skp1/Skp2-N and CDK2/cyclin A elute at similar volumes on a Superdex 75 26/60 column (compare

elution volumes of each complex in Figures 3.8B and C and 3.9), such that quaternary complex formation would be favoured. There were, however, some indications that the mutant cyclin A-containing complex might not be as stable as that containing WT cyclin A, indicated by the shoulder on the quaternary complex (red trace, Figure 3.12). A more quantitative method of analysing this interaction was sought in order to determine the contributions of regions of cyclin A to its interaction with Skp1/Skp2-N.

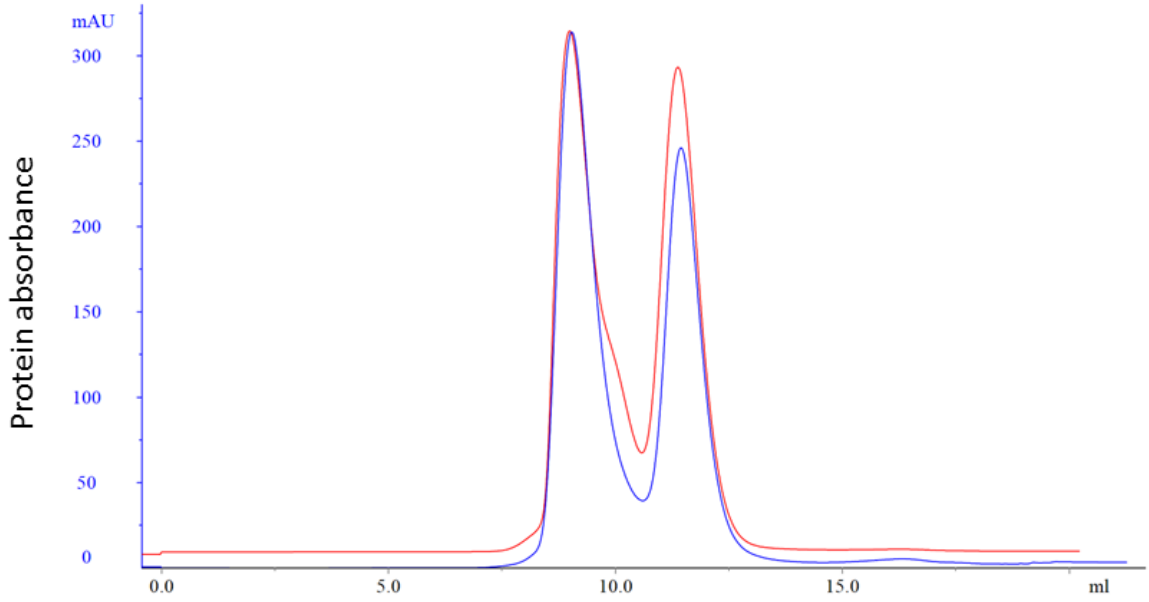

Figure 3.12: Analytical gel filtration elution profile of CDK2/cyclin A mut 6/Skp1/Skp2. The proteins were mixed after concentrating and left to form a complex for one hour. They were then run on the Superdex 75 10/30 column. The blue trace is CDK2/cyclin A mixed with Skp/Skp2-N. The red trace is CDK2/cyclin A mut 6 mixed with Skp/Skp2-N. The curves were normalised to the Skp1/Skp2-N/CDK2/cyclin A WT trace to account for differences in absorbance and concentration.

3.6 Use of ITC for analysis of the Skp2 binding site on cyclin A

3.6.1 CDK2/cyclin A global mut is unable to bind Skp1/Skp2-N

Although analytical gel filtration offers several advantages for studying protein-protein interactions, there are limitations to this technique. In order to provide a more quantitative measure of the interaction between CDK2/cyclin A and Skp1/Skp2-N, more sensitive techniques to analyse protein-protein interaction were attempted. Both surface-plasmon resonance (SPR) and isothermal titration calorimetry (ITC) were

pursued, but ITC gave more reproducible and reliable results. ITC is a useful method for analysing binding affinities and thermodynamics of protein-protein interactions. Following optimisation of the experimental conditions (described in Chapter 2, Section 6.2), comparative ITC experiments were performed with CDK2/cyclin A in the cell and the Skp1/Skp2-N complex in the syringe as the Skp1/Skp2-N complex proved to be more amenable to concentrating. The binding of CDK2/cyclin A global mut to Skp1/Skp2-N was determined (Figure 3.13), in order to validate the findings of the analytical SEC experiment (Figure 3.11).

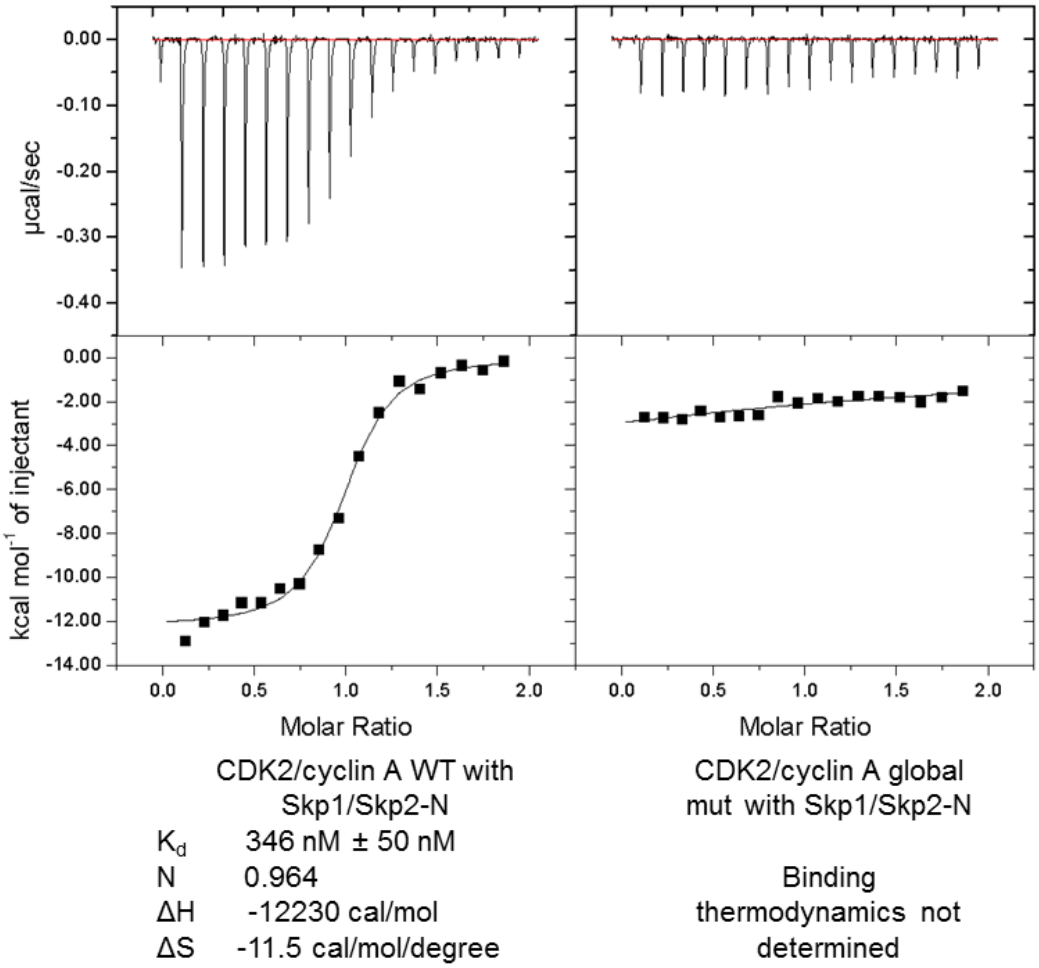

Figure 3.13: CDK2/cyclin A global mutant does not bind to Skp1/Skp2-N as determined by ITC. Binding isotherms determined by ITC with thermodynamic parameters and binding constant shown below. ITC experiment was carried out at 25°C. 20 µM CDK2/cyclin A in the cell and 180 µM Skp1/Skp2 in the syringe.

3.6.2 Analysis of the contribution of individual cyclin A residues to the Skp2/cyclin A interaction

The interaction between CDK2/cyclin A and Skp1/Skp2-N can be measured by ITC. A strong response was seen with little background noise (Figure 3.13). As expected, CDK2/cyclin A WT and Skp1/Skp2-N bind tightly and a K_d value of *circa* 300 nM was measured for their interaction. In contrast, the binding of the CDK2/cyclin A global mutant to Skp1/Skp2-N was so weak that a K_d value could not be determined (Figure 3.13).

These ITC results (Figure 3.13) confirmed that the cyclin A global mutant does not bind to Skp1/Skp2-N, from which it was concluded that the authentic residues at these positions together make a substantial contribution to the Skp2 binding site on cyclin A. Next, the mutants with fewer mutations were assessed for their binding to Skp1/Skp2 in order to identify the contributions from the different sites on cyclin A (Figure 3.14).

A

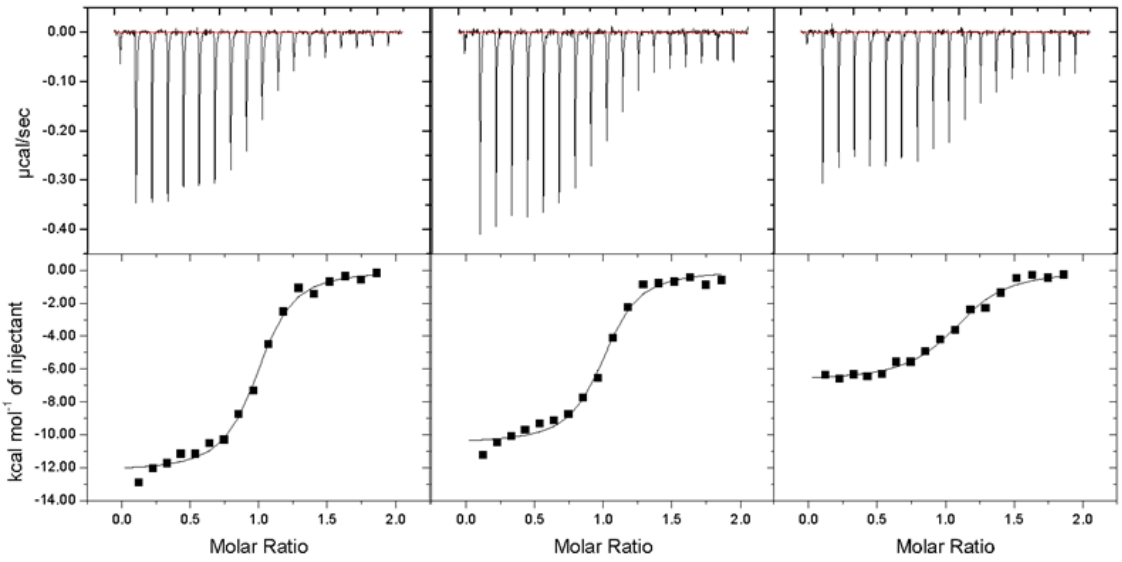

CDK2/cyclin A WT with Skp1/Skp2-N
K_d 346 ± 50 nM
N 0.964
ΔH -12230 cal/mol
ΔS -11.5 cal/mol/degree

CDK2/cyclin A mut 2 with Skp1/Skp2-N
K_d 340 ± 60 nM
N 0.973
ΔH -10520 cal/mol
ΔS -5.71 cal/mol/degree

CDK2/cyclin A mut 3 with Skp1/Skp2-N
K_d 658 ± 101 nM
N 1.07
ΔH -6732 cal/mol
ΔS 5.7 cal/mol/degree

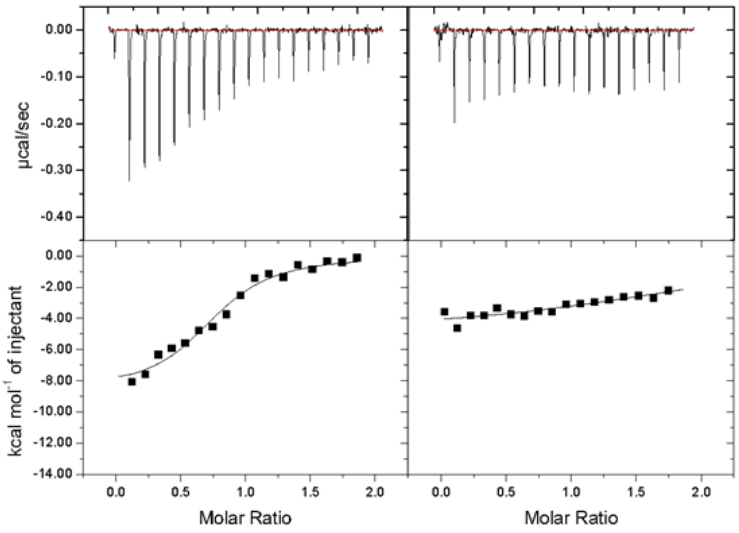

CDK2/cyclin A mutant 6 with Skp1/Skp2-N
K_d 1.69 ± 0.34 µM
N 0.763
ΔH -8603 cal/mol
ΔS -2.45 cal/mol/degree

CDK2/cyclin A mutant 7 with Skp1/Skp2-N

Binding thermodynamics not determined

B

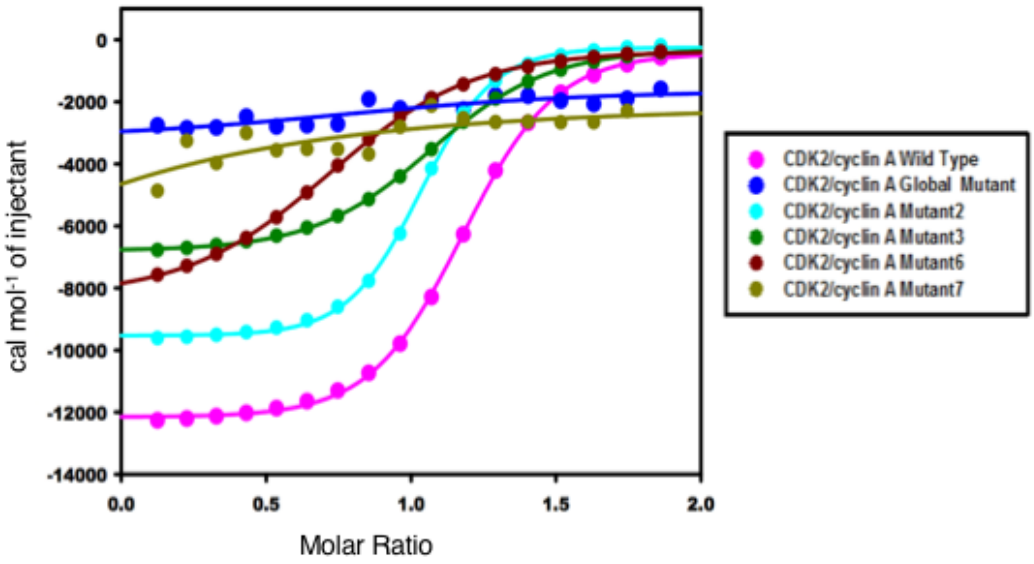

C

Cyclin A	residues mutated	residue changes	Kd (nM)
WT	none	none	346 ± 50
mut 2	284-289	DTYTKK to GACSGD	340 ± 60
mut 3	290-299	QVLRMEHLVL to EILTMELMIM	658 ± 101
mut 6	299-305	LKVLTFD to MKALKWR	1 690 ± 340
mut 7	244-247	SSM-S to ATQEN	CBD

Figure 3.14: CDK2/Cyclin A mutants display a range of binding affinities to Skp1/Skp2-N. A) Binding isotherms determined by ITC with thermodynamic parameters and binding constant shown below. ITC experiment was carried out at 25°C. 20 μM CDK2/cyclin A in the cell and 180 μM Skp1/Skp2 in the syringe. B) Titration plots of the integrated data from (A). C) Table to show residue changes made to cyclin A and their resulting effects on binding affinity.

ITC was used to characterise the contribution of the other cyclin A mutants to the Skp1/Skp2-N interaction. The protein samples were analysed by SDS-PAGE after each experiment to confirm that a lack of apparent binding between Skp1/Skp2-N and the various CDK2/cyclin A complexes was not a result of protein degradation (Figure 3.15).

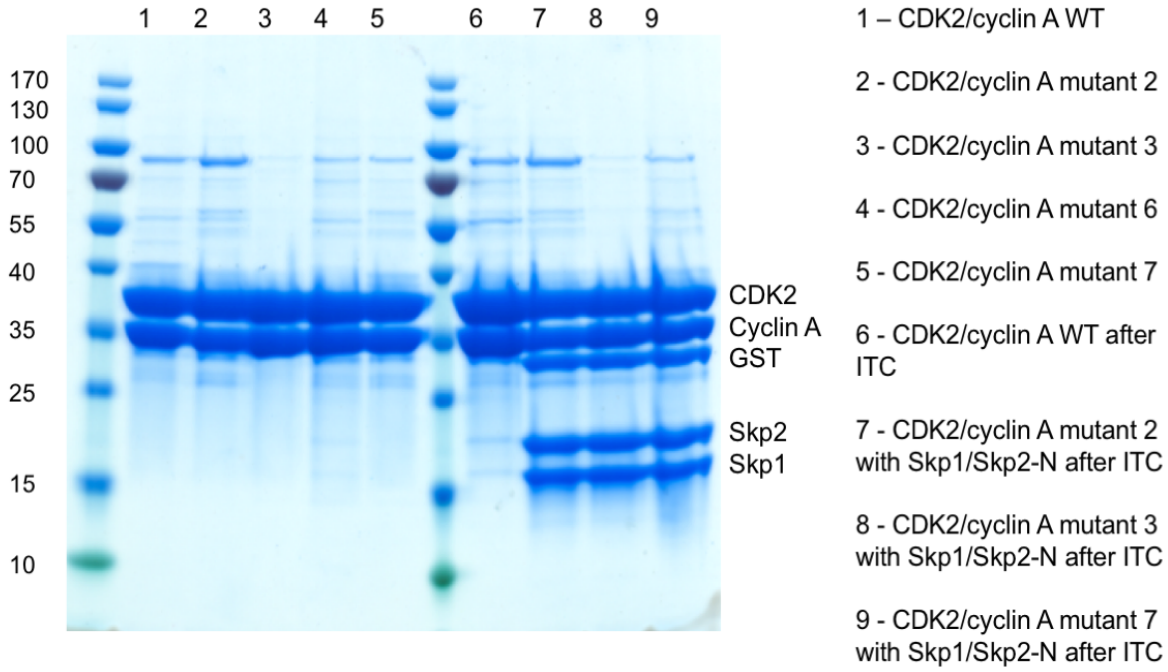

Figure 3.15: CDK2/cyclin A WT and mutants before and after ITC experiments. Lanes 1-5 show CDK2/cyclin A WT and mutant samples before the ITC experiment, lanes 7-9 show samples recovered from the cell after the ITC experiment indicating that there was GST contamination from the Skp1/Skp2 purification.

The ITC analysis revealed that most of the sites which were modified contribute somewhat to the binding. Residues 284-289 (sequence DTYTKK) of cyclin A do not interact with Skp2 as CDK2/cyclin A mut 2 is able to bind Skp1/Skp2 with an affinity the same as determined for CDK2/cyclin A WT. However, the thermodynamics of the CDK2/cyclin A/Skp1/Skp2-N interaction have altered somewhat. For example, the ΔH value is greater (less negative) than for the cyclin A WT complex, indicating that there is less heat exchanged upon binding. The amino acid changes introduced into cyclin A in CDK2/cyclin A muts 3 and 6, significantly reduced the binding affinity to K_d values of 0.66 and 1.7 μM, respectively. Mutation of residues 244-247 (mut 7) had the greatest effect on the interaction with Skp2- an interaction could not be measured between the two proteins (Figure 3.14A and B). These residues are on a loop region (Figure 3.7). Whether these residues in the cyclin A sequence make a significant direct contribution to the Skp2 interaction, or whether the bulge introduced into the cyclin A structure disrupts a larger interface is not known. The ITC experiment was repeated

for CDK2/cyclin A global mut and CDK2/cyclin A mut 7 binding to Skp1/Skp2-N using new protein preparations (see Appendix A2 for replicate experiments).

To dissect the effect of this insertion, an intermediate in the construction of this mutant in which MS (residues 246 and 247) of the cyclin A sequence were mutated to QEN (called mut 5). This mutant was then tested for its binding to Skp1/Skp2-N (Figure 3.16). Like cyclin A mut 7, cyclin A mut 5 has a much weaker binding affinity than cyclin A WT.

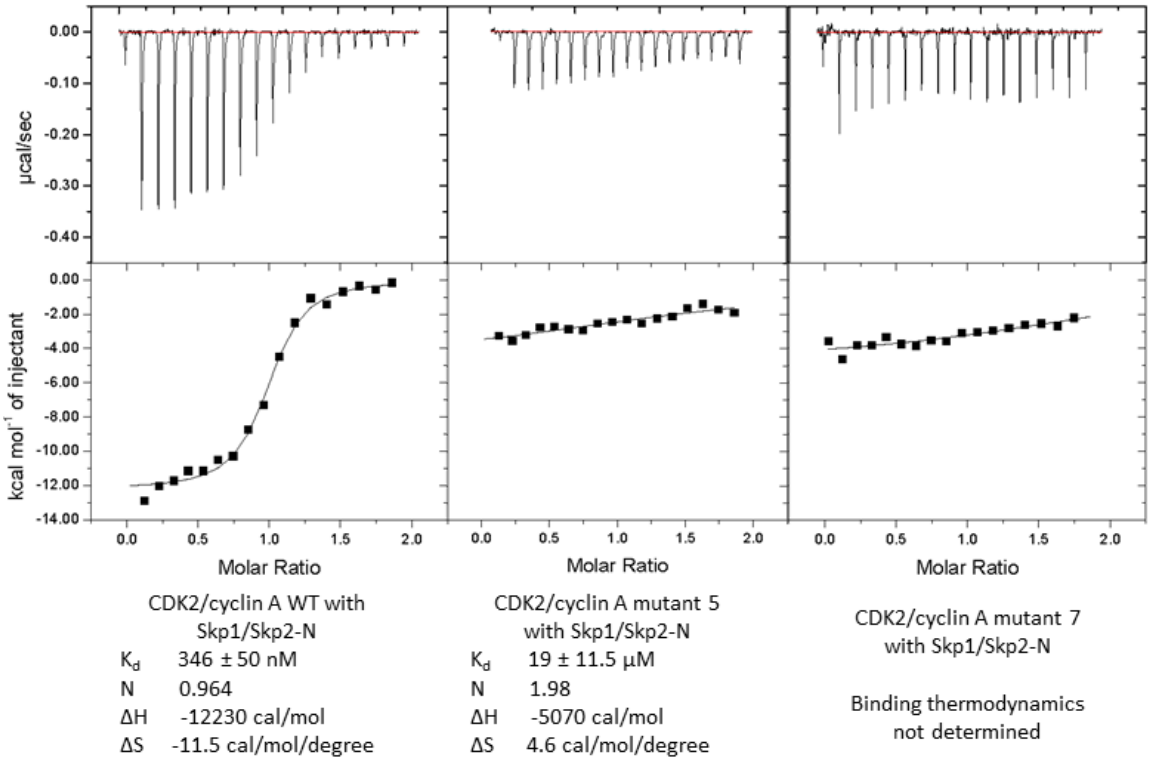

Figure 3.16: The binding between CDK2/cyclin A mut 5 and Skp1/Skp2 is very weak. Binding isotherms determined by ITC with thermodynamic parameters and binding constant shown below. ITC experiment was carried out at 25°C. 20 µM CDK2/cyclin A in the cell and 180 µM Skp1/Skp2 in the syringe.

The mutations of cyclin A mut 5 have a large effect on the Skp2-cyclin A interaction despite being a change of only two residues. It is hypothesised that the extra residue is having an effect by ejecting Skp2 from the binding site rather than the loss of key interacting residues. A comparison of the molecular surfaces of cyclin A and cyclin E at this site highlight the extra bulk present in the cyclin E structure that changes the surface shape. When the surface is coloured by electrostatic potential, the region that is mutated to create cyclin A mut 7 (circled in Figure 3.17), becomes negatively

charged due to the introduction a glutamate residue. A charge at this site might be incompatible with Skp2 binding.

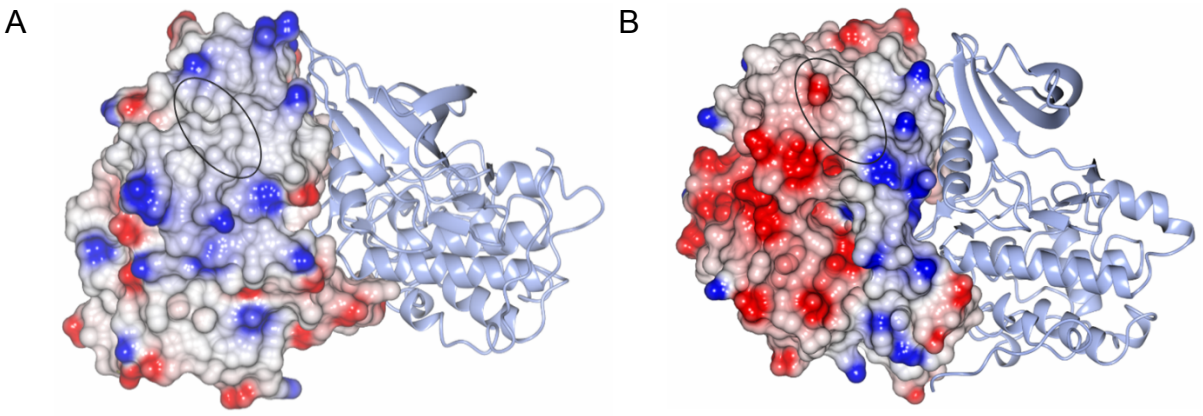

Figure 3.17: Differences in electrostatic potential between cyclin A and cyclin E. A) Cyclin A, PDB: 1JST. B) Cyclin E, PDB 1W98. The region mutated to create mut 7 is indicated by the black rings.

Taken together, binding data obtained for these mutants suggests that Skp2 might bind across the mut 3, 6 and 7 sites. However, mutation of the mut 7 site alone is sufficient to block the interaction. The minimal change to the cyclin A sequence, which impairs Skp1/Skp2-N binding, is made in mut 5 where residues 246 and 247 are mutated from MS to QEN, introducing an extra residue to the cyclin A sequence. Figure 3.18 shows an overlay of the cyclin A and cyclin E structures at this loop region where the cyclin A mut 7 mutations were made. The inserted glutamate residue derived from the cyclin E sequence protrudes out from the loop into the solvent before the sequences return into register at cyclin A residue 249.

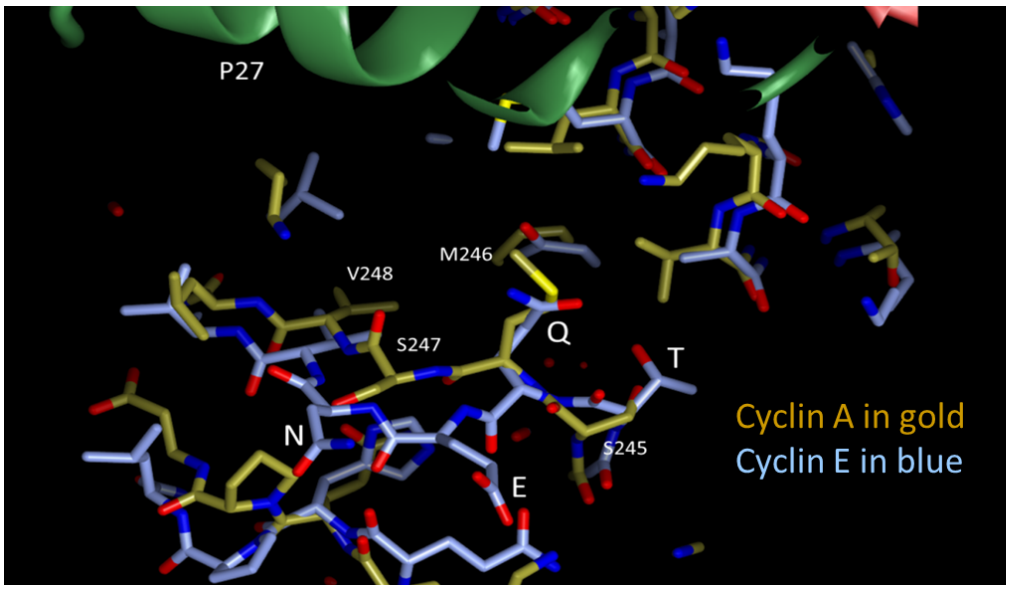

Figure 3.18: Overlay of the cyclin A and cyclin E structures in the region which has been mutated to create cyclin A muts 5 and 7. Cyclin E has an extra residue in this loop region.

3.7 Characterisation of cyclin A mut 7

The ITC results revealed that the Skp2 interaction can be blocked by making a few mutations to a loop region of cyclin A. This region is not known to be involved in any other interactions of cyclin A suggesting this a Skp2-specific interaction site. It is important to initially validate the structure of the mutant to check that the lack of binding to Skp2 is not simply due to a change in the overall secondary structure or loss of structure altogether. As very few mutations of cyclin A were required in order to cause a loss in binding to Skp2, this mutant could potentially be a useful reagent to investigate the Skp2/cyclin A interaction in cell-based assays.

3.7.1 CDK2/cyclin A mut 7 exhibits similar secondary structure features to CDK2/cyclin A WT

As cyclin A mut 5 and mut 7 bind very weakly to Skp1/Skp2-N, it is possible that they might not be properly folded. In order to confirm their secondary structure content, they and cyclin A WT were analysed by circular dichroism (CD). CD results from the unequal absorption of right-handed and left-handed circularly polarized light by a protein. CD spectra between 260 and 180 nm can be analysed for several secondary structure types, such as alpha helices, beta strands, turns and others (Sreerama and

Woody, 1994). The cyclins were analysed in solution in potassium phosphate buffer to minimise background absorption at these wavelengths. The CD data obtained show that cyclin A mut 7 is folded and has a similar secondary structure to the WT protein (Figure 3.19). The spectrum is characteristic of an alpha-helical protein with two characteristic negative minima at 208 and 222 nM. The lower minima at 208 nM compared to 222 nM for CDK2/cyclin A WT suggests the presence of a significant proportion of random coils in the structure (Zhou et al., 1992). The minima values for CDK2/cyclin A mut 7 are more similar. The alpha helical content of both WT and mutant cyclin A is around 40%. As a further measure of protein integrity, the melting temperatures of WT and mutant cyclin A were also determined using differential scanning fluorimetry (DSF, Figure 3.19). Melting temperature is an indicator of a protein's native stability (Kumar et al., 2000). Both proteins showed co-operative unfolding, whereby the unfolding occurs in a single transition. The melting temperatures were similar with a ΔT_m of 3.1°C.

Finally, in order to determine whether these mutations affect the structure of CDK2/cyclin A, the CDK2/cyclin A mut 7 structure was determined. Initially, conditions which had previously been used to crystallise CDK2/cyclin A (0.8 to 1.35 M ammonium sulphate versus 0.6 to 0.95 M potassium chloride in 0.1 M HEPES pH 7.0) were used. However, no crystals were obtained from this screen, which usually has a high success rate. It was concluded that the mutant cyclin A might not allow for the same crystal form as CDK2/cyclin A WT to be created and therefore the CDK2/cyclin A mut 7 complex was tested against commercial screens. The purity of the CDK2/cyclin A mut 7 protein prior to crystallisation trials was confirmed by SDS-PAGE (Figure 3.20). The best hit was in a MORPHEUS screen (Molecular Dimensions). The conditions were 0.1 M Tris/Bicine pH 8.5, 0.1 M amino acids, 20% v/v glycerol, 10% w/v PEG 4K at 4°C. An optimisation screen was then designed and crystals suitable for data collection were obtained (Figure 3.21).

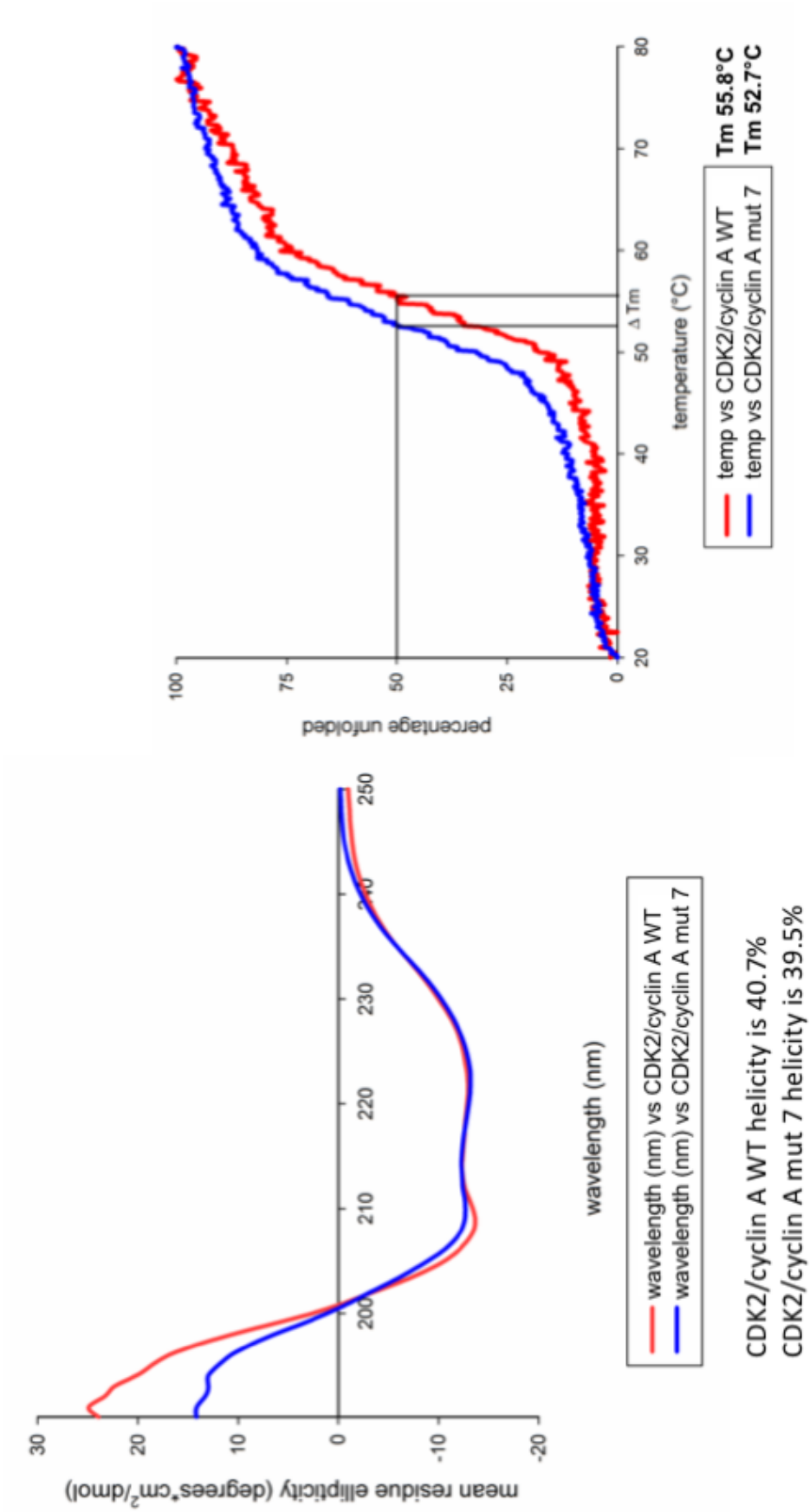

Figure 3.19: CD data of CDK2/cyclin A WT and CDK2/cyclin A mut 7. CDK2/cyclin A complexes were in potassium phosphate buffer pH 7.0. Left is the CD spectra and on the right is the loss of secondary structure with increase in temperature.

3.7.2 The crystal structure of CDK2/cyclin A mut 7

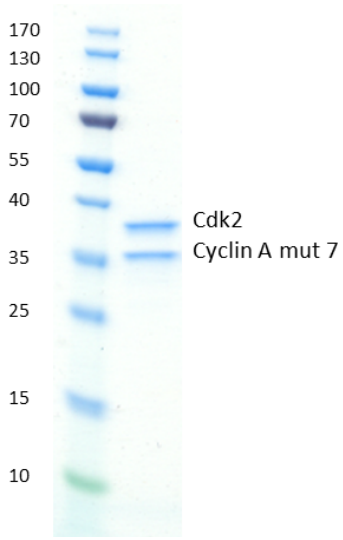

Figure 3.20: Purity of CDK2/cyclin A mut 7 before setting up crystal trays.

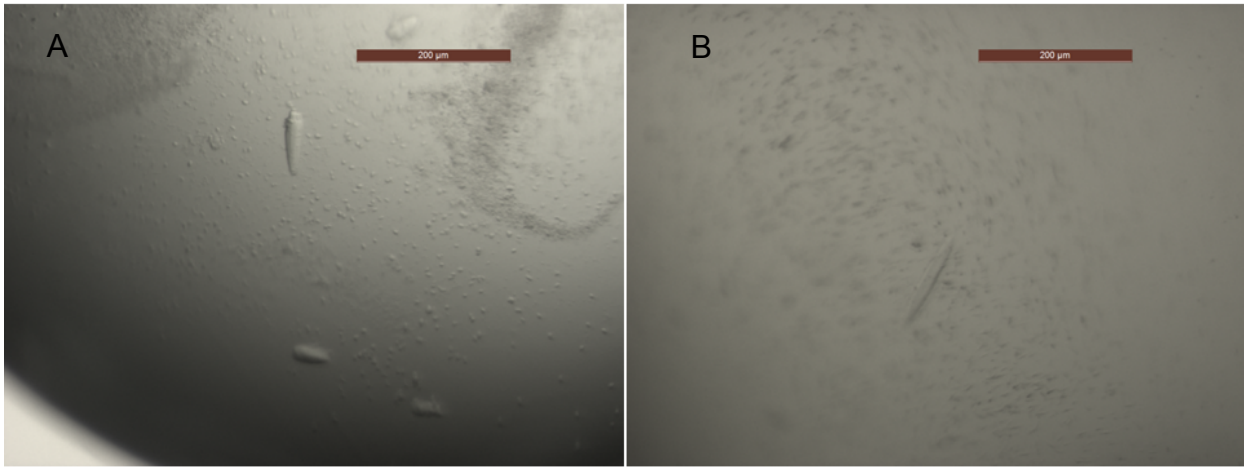

Figure 3.21: Crystals of CDK2/cyclin A mut 7. Protein concentration was 5.6 mg/mL CDK2/cyclin A mut 7. A) Crystals obtained in Morpheus buffer 3 (Tris/bicine) pH 9.0, 20% v/v glycerol, 10% w/v PEG 4k at 4°C. Drop ration 2:1 B) Crystal obtained in Morpheus buffer 3 (Tris/bicine) pH 9.0, 22.7% v/v glycerol, 11.3% w/v PEG 4k, 50 mM amino acids at 4°C. Drop ratio 1:1 Bars are 200 µm.

Crystals grown in the conditions described in Figure 3.21 were harvested by Dr Mathew Martin. Due to the high glycerol content, cryoprotectant was not required. Despite the small size of the crystals, a data set was collected for one of the crystals. It diffracted to 3.6 Å with a P31 2 1 space group. This is a different space group to that observed with CDK2/cyclin A WT crystals and is at lower resolution than might have been expected from previous CDK2/cyclin A WT studies. The dataset was collected at the Diamond Light Source (Didcot, UK) on beamline I24, by the Facilities Manager, Dr. Arnaud Baslé. Data were collected using a Pilatus3 6M detector with a detector

distance of 61.05 cm and an exposure time of 9 milliseconds. The oscillation range was 0.1º, for a total oscillation of 119.9º. Data were processed using Xia2 (Winter, 2009) and programmes from the CCP4 suite (Winn et al., 2011, 1994) as implemented in CCP4i2. Data collection and processing statistics are given in Table 3.2.

The data analysis was done with the help of Dr Julie A. Tucker. The structure of CDK2/cyclin A mut 7 was solved by molecular replacement (Molrep (Vagin and Teplyakov, 1997)) using a high resolution structure of CDK2/cyclin A (PDB code 2C5O chains A and B) as a search model after removing the residues that had been mutated. The crystal asymmetric unit contains two copies of the CDK2/cyclin A mut 7 heterodimer. Chains A, B, and D are well defined, whilst chain C shows very poor electron density for the kinase N-terminal lobe. The model was manually completed in Coot (Emsley et al., 2010) following an initial refinement in Refmac5 (with map sharpening, jelly body restraints, TLS and overall B-factor restraints (Murshudov et al., 1997), followed by Buster (with TLS and autoNCS restraints (Blanc et al., 2004)). Omit maps were calculated using Buster from the final model after removal of residues 244 to 248 from chains B and D. Figures were prepared using CCP4MG (Winn et al., 2011). Details of the refinement statistics and final model quality are given in Table 3.2.

The electron density around the mutated region of cyclin A was analysed to determine the positions of the residues within the structure (Figure 3.22), and the density is strong around the backbone of the chain and around the side chains of most residues. The direction of the Gln246 side chain can be determined from the density. However, there was little density for Glu247, suggesting that this side chain is in a flexible conformation. As would be expected, this mutated region of cyclin A is similar to cyclin E (Figure 3.22). An obvious difference between cyclin A WT and mut 7 is the space occupied by Glu247. This residue may sterically clash with residues of Skp2, thus preventing key interactions of Skp2 with cyclin A.

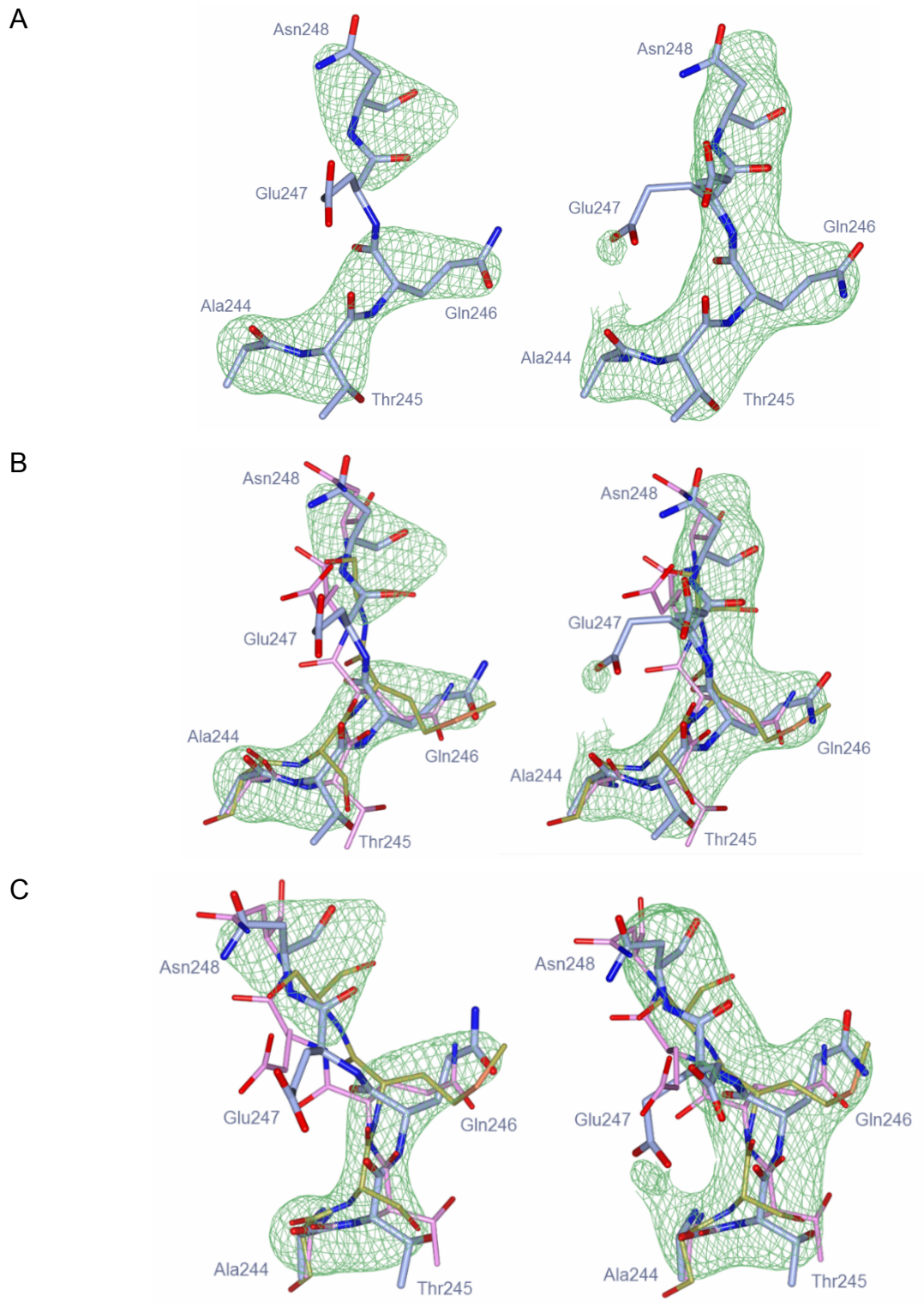

Figure 3.22: F_o-F_c OMIT maps for cyclin A mutated region of mut 7. Maps are contoured at 3 σ and are drawn as a green mesh. On the left is chain B and on the right is chain D. A) Residues 244-248 of cyclin A mut 7 are shown. B) cyclin E (PBD: 1W98) and cyclin A (PDB: 2C5O) are superimposed onto cyclin A mut 7 shown in pink and gold, respectively. C) Another view of B. Figure was created using CCP4MG.

A superimposition of cyclin A WT and cyclin A mut 7 shows good agreement between the two structures and the only effect of the mutations to cyclin A are limited to the mutated region itself (Figure 3.23). This suggests that Skp2 forms an interaction with this region of cyclin A and the decreased binding is not due to loss of structural features elsewhere in the protein.

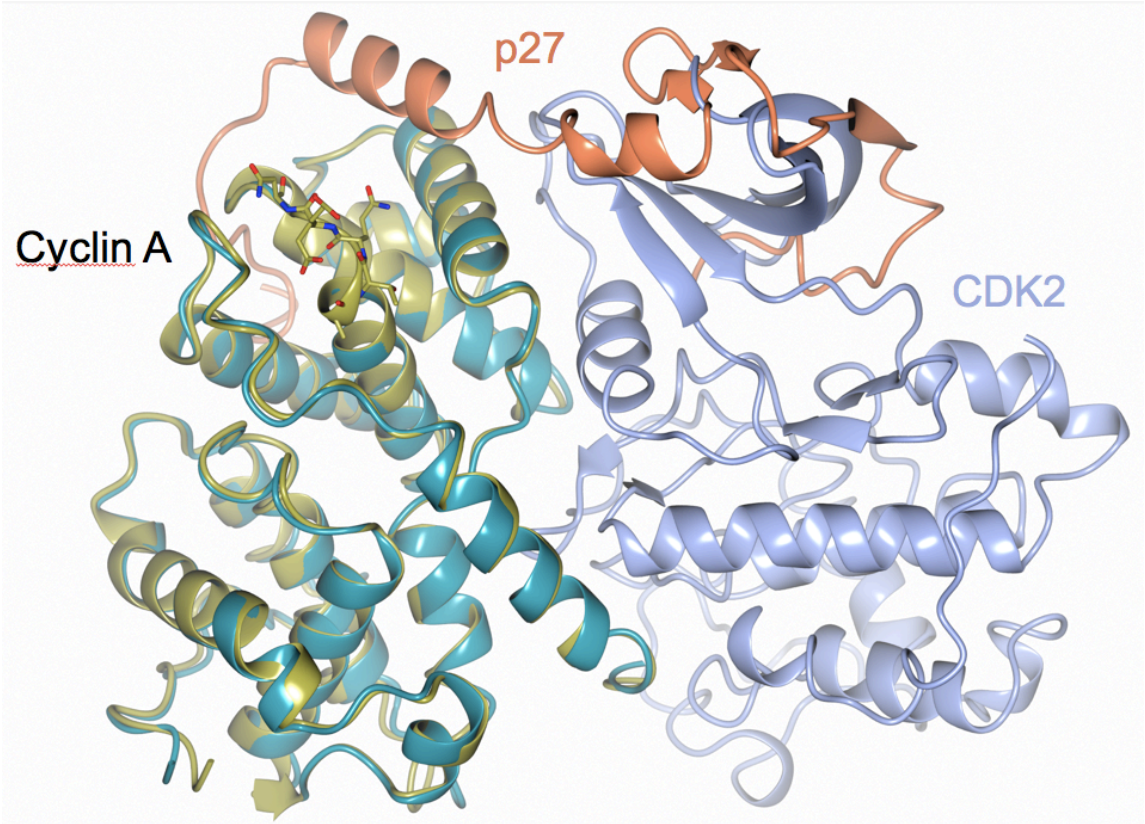

Figure 3.23: Superimposed cyclin A WT and cyclin A mut 7. CDK2 is in ice-blue, p27 is in coral, cyclin A WT is in turquoise and cyclin A mut 7 is in gold. CDK2 and p27 are shown to show the orientation of cyclin A. Residues 244-248 of cyclin A mut 7, which encompass the mutated region of cyclin A are shown in cylinder conformation. Figure was created using CCP4MG.

Table 3.2: Crystallographic parameters for CDK2/cyclin A mut 7 structure

Beam-line	Diamond Light Source I24
Wavelength (Å)	0.979
Detector type	PILATUS3 6M
Data collection date	10 May 2015
Space group	P 31 2 1
Cell constants a; b; c (Å)	105.6; 105.6; 294.1; 90; 90; 120
Resolution range (Å) [1]	49.47-3.61 (3.9-3.61)
Completeness overall (%)[1]	99.6
Reflections, unique	22577
Multiplicity[1]	6.4
Mean(I)/sd(I)[1]	4.8
*R*merge $_{overall}$ [2]	0.395
*R*value $_{overall}$ (%) [3]	21
*R*value $_{free}$ (%)[1]	27
Non hydrogen protein atoms (A;B;C;D)	4683; 4148;4706;4107
Solvent molecules	7

R.m.s. deviations from ideal values

Bond lengths (Å)	0.015
Bond angles (°)	1.7

Average *B* values (Å^2)

Average B values for protein (Å^2 A;B;C;D)	32.6; 26.2; 34.5; 30.6
Average B values for water (Å^2)	31.9

Φ, Ψ angle distribution for residues [4]

In favoured regions (%)	95.4
In allowed regions (%)	3.9
In outlier regions (%)	0.64

1 Values in parentheses refer to the outer resolution shell

2 $R_{merge} = S_{hkl} [(\Sigma_i |I_i - \langle I \rangle|)/ \Sigma_i I_i]$

3 $R_{value} = S_{hkl} ||F_{obs}| - |F_{calc}|| / S_{hkl} |F_{obs}|$

R_{free} is the cross-validation *R* factor computed for the test set of 5% of unique reflections

4 Ramachandran statistics as defined by Coot

3.7.3 p27 binds to cyclin A mut 7 with similar affinity to WT cyclin A

As the cyclin A surface identified by mut 7 has not been reported as a site of cyclin A-protein interaction, this mutant might be useful as a probe to investigate the functional significance of the Skp2/cyclin A interaction. Before exploiting the mutant in this way, its ability to bind to other cyclin A partners was investigated. From the SEC analysis, the cyclin A mutations do not affect their interaction with CDK2.

One of the criteria for designing the cyclin A mutations was proximity to the p27 binding site as Skp2 and p27 compete for binding to CDK2/cyclin A. However, it was mutation of the more distant residues that produced a CDK2/cyclin A complex that was unable to bind Skp1/Skp2-N. Therefore, it was hypothesised that by disrupting the Skp2 interaction through mutation of residues 244-247, the interaction of cyclin A with p27 might not be affected. ITC was again used to test whether this is the case. Two p27 fragments were expressed in *E. coli* and purified by Dr Martyna W. Pastok (Figure 3.24). p27S consists of amino acids 23-106 and p27XS is slightly smaller and includes residues 34-106. These two fragments were chosen as p27S includes the RXLF sequence at residues 30-33 and so binds to the cyclin A recruitment site, whereas p27XS does not (Russo et al., 1996b).

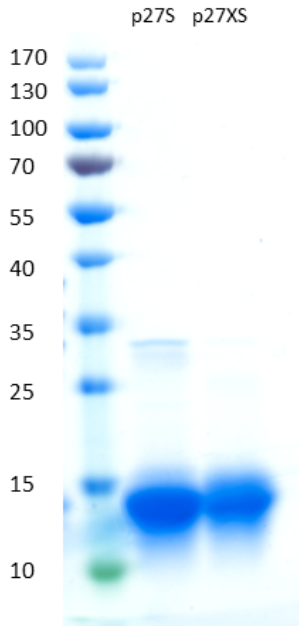

Figure 3.24: Purity of the p27 peptide fragments p27S and p27XS. These fragments were expressed in *E. coli* and purified by Martyna W. Pastok.

The binding of p27 to CDK2/cyclin A mut 7 was determined in order to assess whether these mutations have affected the ability of cyclin A to carry out its known functions. Figure 3.25 shows that the binding affinities were only very slightly weaker for both

p27S and the smaller fragment, p27XS. The difference in the binding affinities between WT and mut 7 were within the error of the ITC experiment. This large error is commonly seen for very tight interactions as they are difficult to accurately measure by ITC. Due to limited amounts of proteins and time restraints, the binding of p27 to CDK2/cyclin A WT and CDK2/cyclin A mut 7 was not optimised. The thermodynamic parameters for the interaction are also similar for cyclin A WT and mut 7. Therefore, the introduction of these mutations should be able to provide a readout of the Skp2/cyclin A interaction and any effects on p27 will not be directly due to the binding of p27 to cyclin A. The calculated K_d values are higher than those reported by the Kriwacki group (Lacy et al., 2004). Again, using ITC, this group measured the K_d of a peptide of residues 22-105 of p27 to be 3.5 nM ± 1.2 nM (Lacy et al., 2004). This could possibly be due to the experimental conditions as the concentrations in the cell and syringe were kept at a ratio of about 1:10 (as they were for the CDK2/cyclin A Skp1/Skp2-N experiments). However, this interaction might be better analysed with a lower ratio as it is a very tight interaction. The enthalpy (ΔH) associated with this interaction is very large and this is most likely due to the amount of hydrogen bonds created over the large surface area of CDK2/cyclin A contacted by p27. The enthalpy observed is consistent with what has been observed in previous investigations (Ou et al., 2011).

A

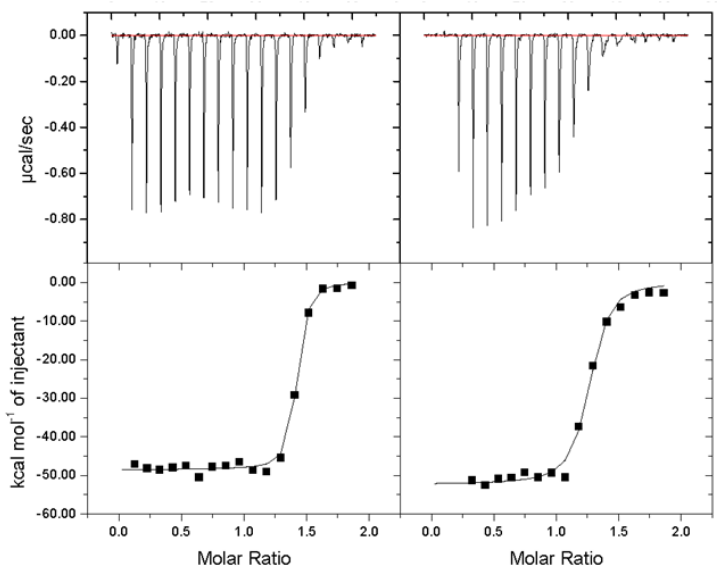

CDK2/cyclin A WT with p27 S
K_d 10.25 nM ± 46.9 nM
ΔH -48510 cal/mol
ΔS -126 cal/mol/deg

CDK2/cyclin A mut 7 with p27 S
K_d 47.6 nM ± 222.2 nM
ΔH -52300 cal/mol
ΔS -142 cal/mol/deg

B

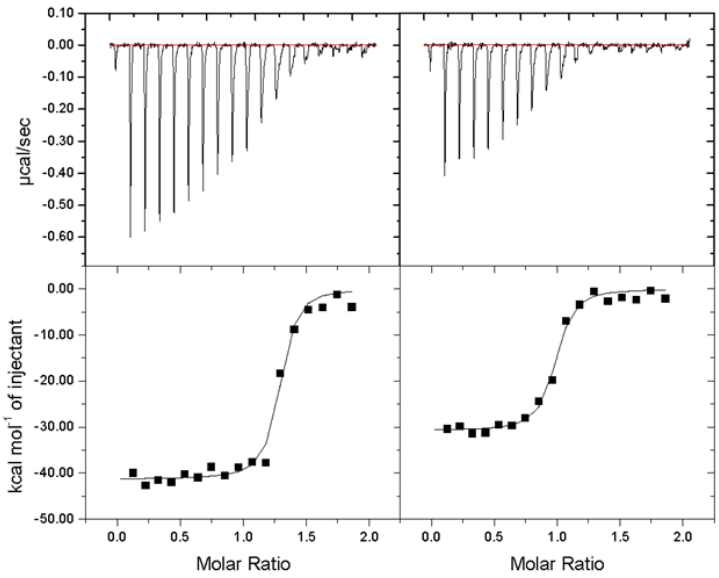

CDK2/cyclin A WT with p27 XS
K_d 31.8 nM ± 95.2 nM
ΔH -41330 cal/mol
ΔS -104 cal/mol/deg

CDK2/cyclin A mut 7 with p27 XS
K_d 52.9 nM ± 197.2 nM
ΔH -30780 cal/mol
ΔS -70 cal/mol/deg

Figure 3.25: CDK2/cyclin A WT and mut 7 interaction with p27 peptides. Binding affinity and thermodynamic data shown underneath calorimetry data. A) CDK2/cyclin A WT binding to p27S. B) CDK2/cyclin A mut 7 binding to p27S. C) CDK2/cyclin A WT binding to p27XS. D) CDK2/cyclin A mut 7 binding to p27XS. ITC experiment was carried out at 25°C. 20 µM CDK2/cyclin A in the cell and 180 µM p27 peptide in the syringe.

p27, p21 and p57 are well conserved in their CDK2/cyclin A binding domains (Figure 3.26), so it would be expected that they would bind in a similar way to p27 and therefore the interaction of p21 and p57 with CDK2/cyclin A is unlikely to be affected by the mutations. The relative binding affinities of Skp2 and p27 to CDK2/cyclin A are in agreement with the analytical gel filtration data which showed that p27 can displace Skp2 from CDK2/cyclin A/Skp1/Skp2 (Figure 3.5).

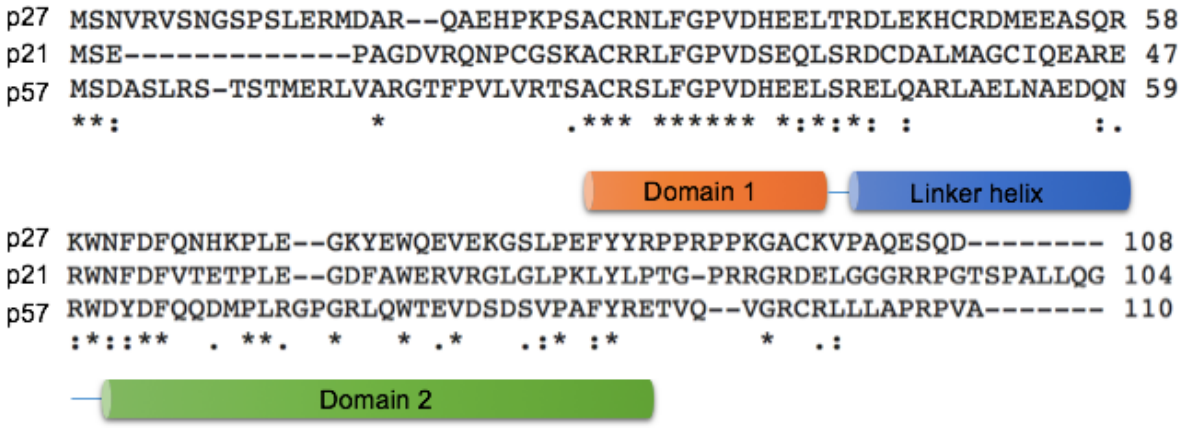

Figure 3.26: Sequence alignment of the kinase inhibitory domains of p27, p21 and p57. Within the domains of p27 that bind to CDK2/cyclin A there is good conservation with other CDK2 inhibitory proteins. Adapted from Lacy et al. (2004). An asterisk indicates positions that are fully conserved. A colon indicates conservation between groups of strongly similar properties, scoring >0.5 in the Gonnet PAM 250 matrix. A full stop indicates conservation between groups of weakly similar properties, scoring =<0.5 in the Gonnet PAM 250 matrix. Figure was created using Clustal Omega (Sievers et al., 2011).

3.7.4 CDK2/cyclin A global mut and mut 7 are catalytically active

Cyclin A is involved in the recruitment of substrates to CDK2. These substrates include, Skp2 (Rodier et al., 2008), p53 (Wang and Prives, 1995), pRb (Mittnacht et al., 1994), Histone H1b (Contreras et al., 2003), and BRCA1 (Ruffner et al., 1999). Substrates are selected by binding to the cyclin protein (Roberts, 1999), therefore it is important that when mutating cyclin A, its role as a substrate recruiter has not been compromised. CDK2/cyclin A activity was tested against two substrates, histone H1 and Rb. Histone H1 is not part of the nucleosomal core, however, it is important for maintaining chromatin higher-order structure. CDK2 phosphorylates histone H1 during the G1-S transition and S-phase (Talasz et al., 1996). Phosphorylation increases or

decreases transcription of certain genes (Bhattacharjee et al., 2001, Dou and Gorovsky, 2000). Phosphorylation occurs on the N- and C-terminal tails of histone H1 with the consensus sequences K [S/T]PXK and K[S/T]PK being recognised by CDK1 and CDK2 (Meijer et al., 1989, Maller et al., 1989). Phosphorylation of histone H1 was assayed by a radiometric phosphorylation assay (methods are described in Chapter 2, Section 5.2). The results showed that CDK2/cyclin A global mutant and mut 7 are able to phosphorylate histone H1 with an activity similar to CDK2/cyclin A WT (Figure 3.27).

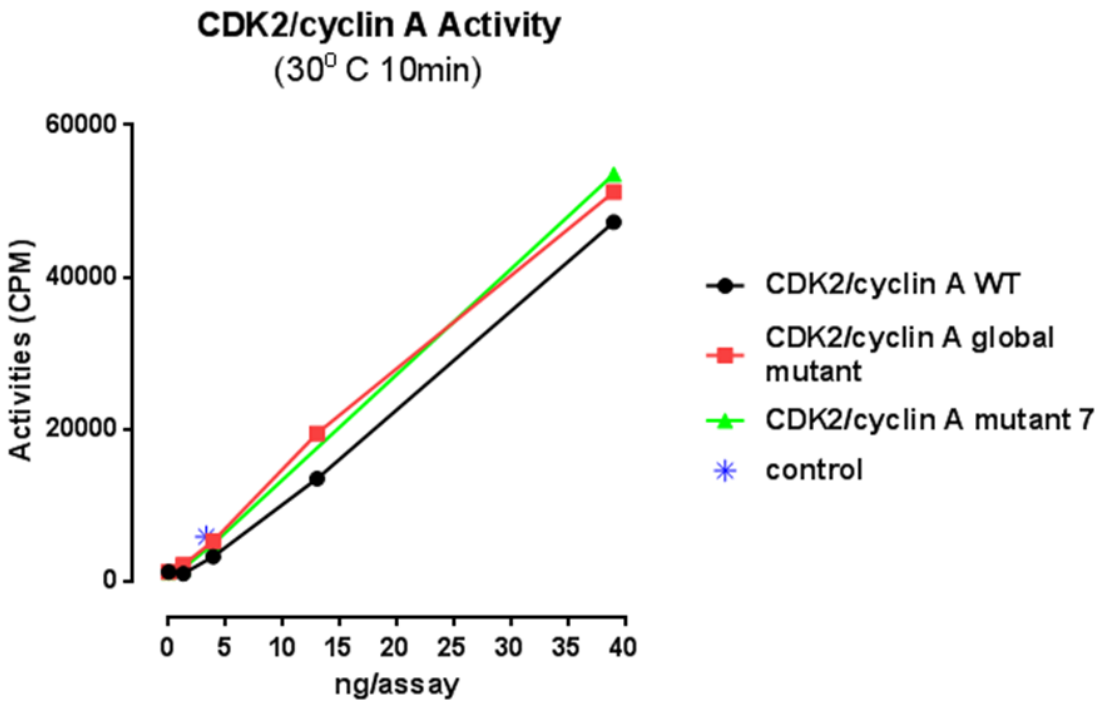

Figure 3.27: CDK2/cyclin A mutant 7 is able to phosphorylate histone H1. A radioactive *in vitro* kinase assay was carried out by Lan-Zhen Wang. Values are derived from one experiment. The control is the reaction solution without any CDK2/cyclin A added.

The C-terminal domain of Rb is phosphorylated at many sites by CDK2/cyclin A during the G1-S transition (Zarkowska and Mittnacht, 1997). This phosphorylation inactivates Rb leading to transcription factors such as E2F1 being released from repression by Rb and is required for the cell to pass through the restriction point (Weinberg, 1995). CDK2 phosphorylation can be visualised on an SDS-PAGE gel as the phosphorylation causes the Rb to migrate more slowly (Chapter 2, Section 5.1). Figure 3.28 shows that the global mutant and mut 7 are able to phosphorylate the C-terminal domain of Rb as effectively as the authentic complex.

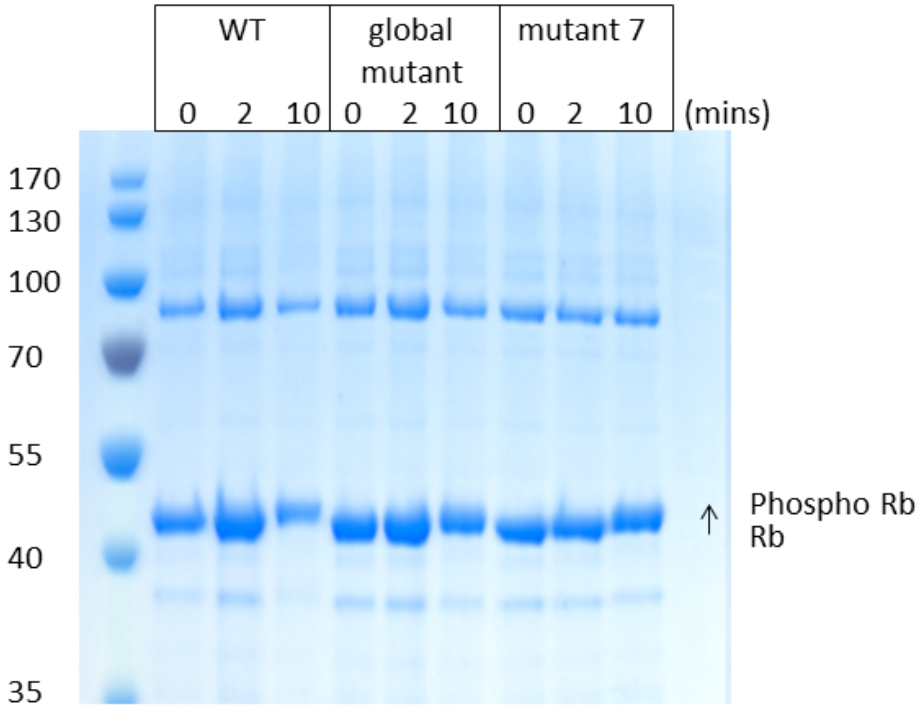

Figure 3.28: CDK2/cyclin A mut 7 is able to phosphorylate Rb. CDK2 with indicated cyclin A variants were incubated with a C-terminal construct of Rb for the indicated times. The reaction was stopped by adding SDS loading buffer and boiling. Samples were subjected to SDS-PAGE and phosphorylation monitored by mobility shift. The band at *circa* 90 kDa is a contaminant protein.

Many of the substrates of CDK2/cyclin A are also substrates of CDK2/cyclin E, including Rb and histone H1. Therefore, it might be expected that mutating cyclin A residues to the cyclin E sequence would not have an effect on substrate binding. By exploiting the difference in the Skp2-binding abilities between these two cyclins, the other interactions of cyclin A have not been affected.

3.8 Discussion

Deletion of cyclin A2 in mice is lethal with mice dying at E5.5. This phenotype suggests that other cyclins are not able to compensate for loss of cyclin A2 during early embryogenesis (Murphy et al., 1997). It is interesting, therefore, to determine the features of the cyclins which make them unique. This investigation has determined the answer to how Skp2 is specific for cyclin A, but the question of why it is specific to cyclin A requires more investigation.

A novel cyclin A protein interaction site located on the cyclin A N-terminal CBF has been identified. This site is required for CDK2/cyclin A to form a stable complex with Skp1/Skp2-N and does not affect the association of CDK2/cyclin A with other known regulators. Work in this chapter also confirms the earlier observations that Skp2 binding to CDK2/cyclin A is mutually exclusive with p27 and that the association of p27 with CDk2/cyclin A is tighter than that of Skp2. Mutation of cyclin A residues 244-247 is not injurious to other cyclin A functions as it is folded properly; it does not affect the kinase activity of CDK2/cyclin A against Rb (C-terminal domain) or Histone H1; and cyclin A mut 7 is able to interact with CDK2, p107 and p27. Therefore, the cyclin A residues identified here as required for the binding of Skp1/Skp2-N will be a very useful tool to identify the function of the Skp2/cyclin A interaction in cell-based assays.

3.8.1 Conservation of the cyclin A mut 7 site

Analysis of the conservation of the region which was mutated to create cyclin A mut 7 indicates that there is high sequence conservation in this region (Figure 3.29). The N-CBF of cyclin A is well conserved, indicating the essential role of this lobe in mediating protein-protein interactions.

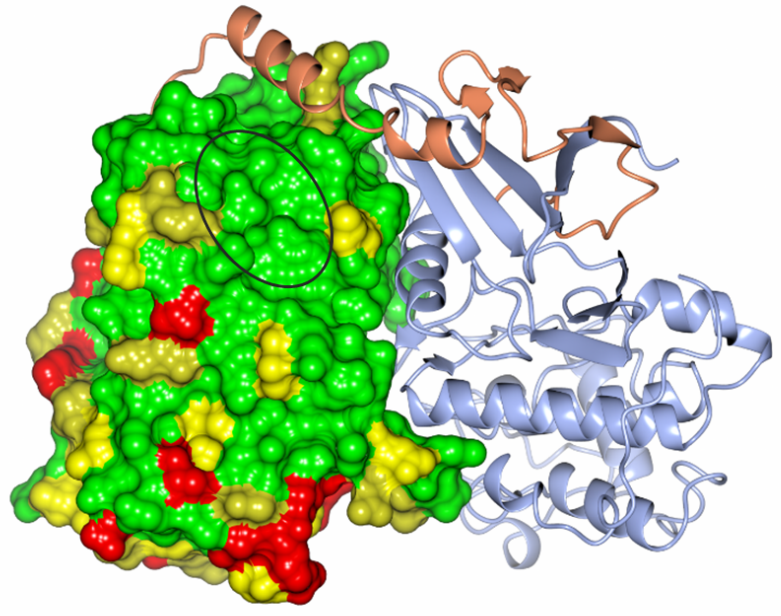

Figure 3.29: Sequence conservation across species of cyclin A. Cyclin A is coloured according to whether the region is conserved, green indicates conserved regions, red indicates non-conserved regions and yellow indicates regions that are moderately well-conserved. CDK2 is coloured ice-blue and p27 is coral. PDB: 1JST. A black ring indicates residues 244-247 of cyclin A, which have been shown to be involved in its interaction with Skp2. Uniprot codes P20248 (*Homo sapian*), P51943 (*Mus musculus*), P30274 (*Bos taurus*), P43449 (*Gallus gallus*), P47827 (*Xenopus laevis*) and P37881 (*Mesocricetus auratus*) were used for the sequence alignment.

3.8.2 The Skp1/Skp2-N structure is elongated producing a higher apparent molecular weight when analysed by SEC

This investigation determined that the Skp1/Skp2-N complex is a single heterodimer. When Skp1/Skp2-N binds to CDK2/cyclin A, the quaternary complex runs at a similar elution volume as the two binary complexes. This suggests that the large apparent molecular weight of Skp1/Skp2-N by SEC is a shape effect and is due to the elongated and unstructured N-terminus of Skp2. The non-additive effect when Skp1/Skp2-N binds to CDK2/cyclin A suggests that the N-terminus of Skp2 binds along the surface of cyclin A to create a more compact and globular complex.

3.8.3 Regulation of CDK/cyclin complexes through interactions with the N-terminal and C-terminal CBFs of the cyclin

The Zhu lab demonstrated that Skp2 in excess is able to compete p27 from CDK2/cyclin A and protect CDK2/cyclin A from inhibition by p27 (Ji et al., 2006). In contrast, a former member of the Endicott lab, Nicole Schueller, was able to show that CDK2/cyclin A preferentially binds to p27 over Skp2 (Figure 3.5, (Schueller, 2001)). The ITC data shown here are in agreement with the latter finding. p27 was found to bind to CDK2/cyclin A about tenfold tighter than Skp1/Skp2-N, suggesting that Skp2 would not be able to compete p27 from CDK2/cyclin A unless it were in great excess over p27. As p27 binds more weakly to CDK2/cyclin A after phosphorylation on Tyr74 and Tyr88, which partially activates CDK2/cyclin A, it is possible that Skp2 is then the preferred binding partner (Chu et al., 2007, Grimmler et al., 2007). If this were the case, then you would expect that the full activation of the CDK2/cyclin A complex would result from binding to Skp2, perhaps in the context of the SCF^{Skp2} complex.

Investigations into cyclin substrate recruitment have found that the cyclin recruitment site which binds to RXL motifs present in substrates is required for docking. Rb, p53, p107, p21, p27 are substrates of CDK2/cyclin A which bind to the recruitment site on the N-terminal CBF (Lowe et al., 2002). This recruitment site is shared with cyclins A, B, D and E that regulate the cell cycle. Cyclins C, H and T bind to CDK8, CDK7 and CDK9, respectively and collectively regulated early events in the initiation of eukaryotic transcription (reviewed in (Loyer et al., 2005)). These cyclins do not share sequence features with the cell cycle cyclins in the region of the recruitment site and in the case of the cyclin H structure, the recruitment site location is obscured by an extended C-terminal sequence (Kim et al., 1996, Lolli, 2010). These observations suggest that the substrate recruitment function of the N-CBF is not conserved in the transcriptional CDKs.

Recent reports have shown that the cyclin T C-CBF is involved in binding regulatory proteins, such as human immunodeficiency virus 1 (HIV-1) Tat protein. Through binding CDK9/cyclin T1 (P-TEFb), HIV Tat (Zhu et al., 1997) and AFF4 (Schulze-Gahmen et al., 2013) promote the synthesis of viral transcripts. The binding of the inhibitory protein hexamethylene bisacetamide-inducible protein (HEXIM) 1 is mutually exclusive with HIV Tat binding, and it has been recently shown (S. Baumli, A. Hole and R. Heath, unpublished results) that HEXIM1 and BRD4 bind to the cyclin

T C-CBF. Taken together these observations suggest that cyclin T has a novel substrate and regulatory protein binding site that can accommodate multiple interactions on the C-CBF rather than the N-CBF. This emerging view of cyclins promotes the idea that the cyclin is not only for substrate recognition and docking, but that there are regulatory interactions occurring at multiple sites offering the possibility of cross-talk between signalling pathways. This model is an extension of the established model of CDK activation by the cyclin and cyclin recruitment at one specific site. The implications for this work might be that this would suggest a regulatory role for Skp2 binding to cyclin A. The finding from the Zhu lab that the Skp2/cyclin A interaction is not required for Skp2 phosphorylation at Ser64 (Ji et al., 2006), suggests this novel binding site is not an alternative substrate recruitment site and therefore it might be to allow for regulatory interactions.

Chapter 4: Identifying residues of Skp2 which mediate its interaction with Cyclin A

4.1 The Skp2 N-terminal regulatory region

The N-terminus of Skp2 is unstructured with multiple residues subject to post-translational modification and involved in protein-protein interactions. A disordered structure is typical of a region with multiple binding and post-translational modification sites, as it can allow for flexibility and folding-upon-binding (Dyson and Wright, 2005). Over the past decade, multiple studies have been published describing the complex regulatory networks that are involved in modification of, and protein interactions made within the first 80 residues of Skp2. There have been accounts of phosphorylation and acetylation in this region (Figure 4.2B) leading to cytoplasmic localisation and influencing the migration-inducing potential of Skp2 (Gao et al., 2009, Inuzuka et al., 2012); Skp2 stabilisation through phosphorylation (Rodier et al., 2008, Cen et al., 2010, Inuzuka et al., 2012); and Skp2 ubiquitination through interaction with the APC^{Cdh1} complex, and subsequent degradation (Bashir et al., 2004, Lin et al., 2009).

Skp2 was first identified as part of a CDK2/cyclin A/Skp1/Skp2/Cks1 complex (Zhang et al., 1995). However, since this discovery, little further knowledge has been gained as to whether this interaction is an important mechanism in the function of Skp2. Cyclin A interacts with the disordered N-terminal region of Skp2. A SDM study in 2006 aimed to determine the function of the Skp2/cyclin A interaction (Ji et al., 2006). Skp2 mutations were made within the N-terminal region and tested for their ability to bind to cyclin A through co-immunoprecipitation experiments. WT Skp2 and mutated Skp2 were also overexpressed in cell lines and cell cycle analysis was carried out. Due to the study design, where Skp2 WT or mutant was being overexpressed, they were determining how well the mutations made to Skp2 countered the effects of Skp2 overexpression. They reported that disruption of the Skp2/cyclin A interaction did not have an effect on p27 or p21 expression, however, a higher proportion of cells entered G1 arrest. They also showed using recombinant proteins that GST-Skp2 does not pull down CDK2 (Ji et al., 2006). In agreement with this observation, Skp2 was shown not

to bind CDK2/cyclin E suggesting that the specificity is primarily driven by cyclin A. Although CDK2 cannot form a stable complex with Skp2 on its own, it might bind to Skp2 in the context of a ternary CDK2/cyclin A/Skp2 complex. The role of Skp1 in complex formation with CDK2/cyclin A is less controversial. Despite the proximity of Skp1 to cyclin A in the proposed SCF-Skp2-Cks1-CDK2-cyclin A model (Figure 4.1), there is no evidence to support a direct interaction between Skp1 and CDK2/cyclin A (Ji et al., 2006).

It is possible to superpose the Skp1/Skp2/Cks1 structure with that of CDK2/Cks1 and CDK2/cyclin A/p27 (Figure 4.1). This structure reveals that the furthest N-terminal residue which has been structurally characterised, residue 97, is distant from the proposed Skp2 binding site, consistent with the data suggesting this N-terminal tail is extended and unstructured (see Chapter 3, Section 4.2).

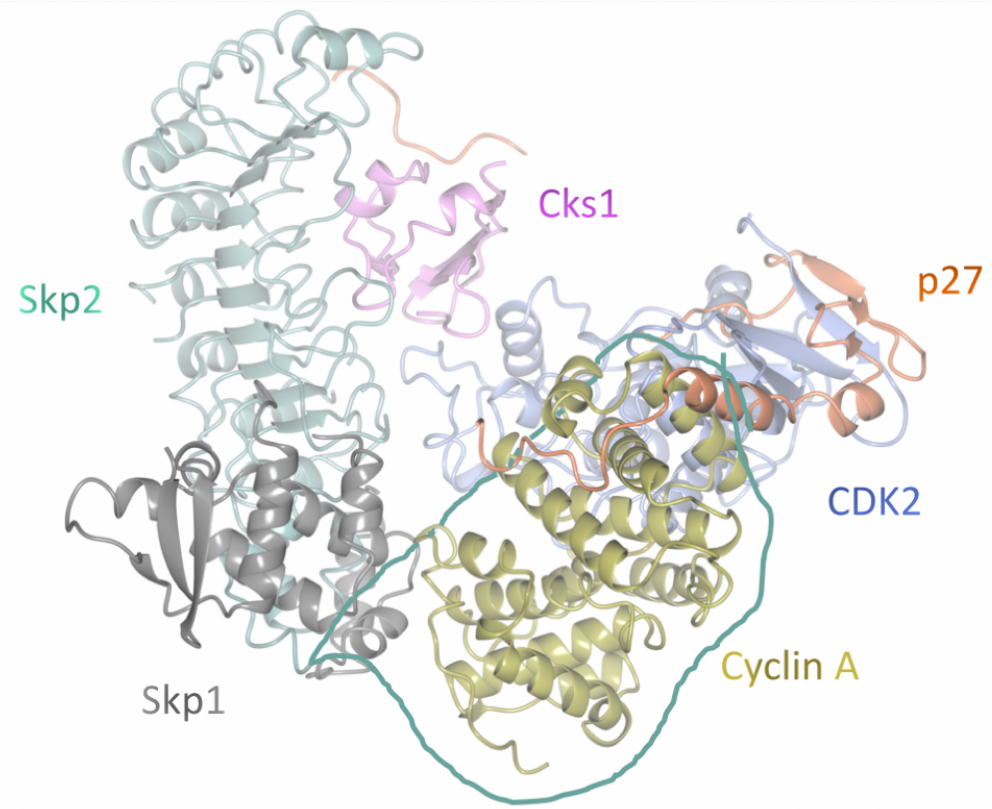

Figure 4.1: Model of the Skp1/Skp2/CDK2/cyclin A/Cks1/p27 complex. The N-terminus of Skp2 is modelled to show the possible routes that it could take to reach the proposed Skp2 binding site which overlaps with part of the p27 binding site.

Due to the predicted disordered structure of the Skp2 N-terminus (Figure 4.2), determination of the structure of this region by X-ray crystallography may not be possible, and there are no crystal structures that include this region of Skp2 to date. Computational methods, such as secondary structure prediction, can provide an estimation of secondary structure. Secondary structure prediction algorithms take into account the preference of amino acids for α-helices or β-sheets. For example, alanines and leucines have high α-helical propensity, whereas tryptophans and threonines prefer to form beta sheet structures. The PSIPRED secondary structure prediction server (Buchan et al., 2013) suggests the Skp2 N-terminus has very few structural elements, with no secondary structure predicted within the cyclin A binding site (Figure 4.2, (Ji et al., 2006)).

A

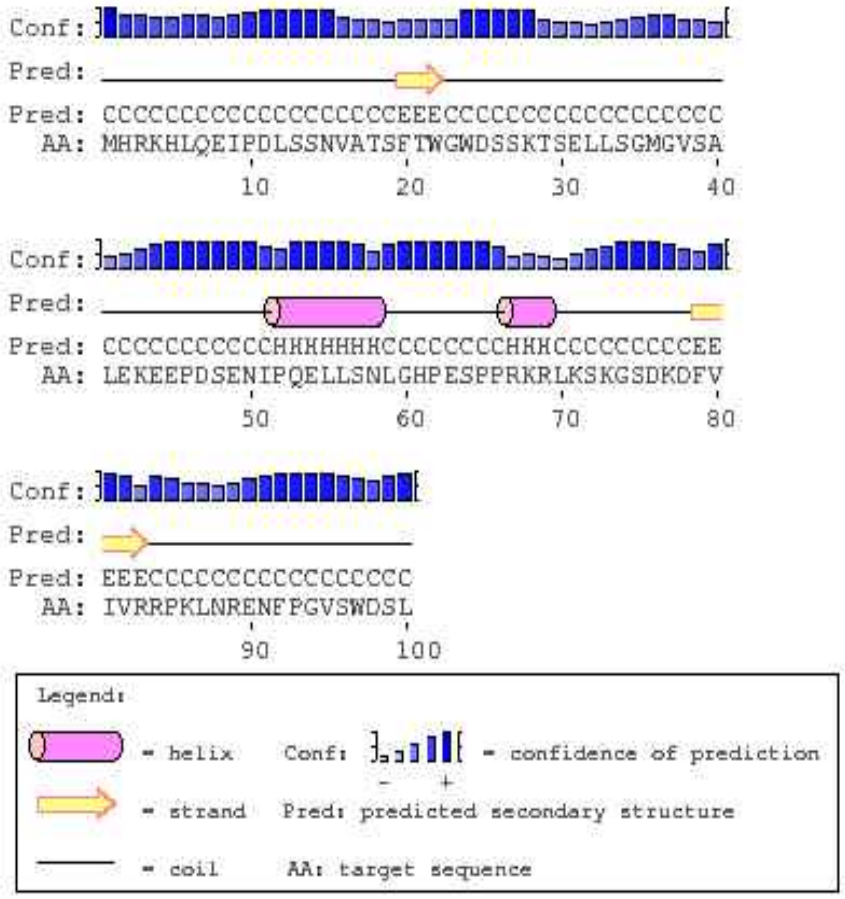

B

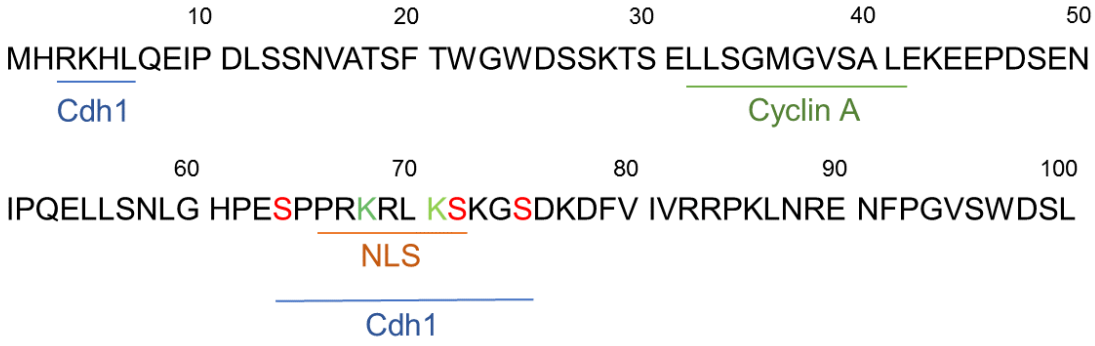

Figure 4.2: The Skp2 N-terminal regulatory region. A) Secondary structure prediction for Skp2 residues 1-100 using PSIPRED server (Buchan et al., 2013). B) Binding sites within the Skp2 N-terminus. Akt, 14-3-3β and many other proteins have been found to bind to this region of Skp2. Residues 32, 33, 39 and 41 have been shown to be required for cyclin A binding (Ji et al., 2006, Chan et al., 2013). The D-box motif of Skp2 which binds Cdh1 comprises residues 3-7 of Skp2, however Cdh1 binding is also believed to involve additional residues further along the sequence, and phosphorylation of residues 64, 72 and 75 has been shown to compromise Skp2 binding to Cdh1 (Rodier et al., 2008, Lin et al., 2009, Hao et al., 2005). Residues subject to phosphorylation are shown in red, and residues subject to acetylation are shown in green. Residues 66-72 comprise the Skp2 nuclear localisation signal (Hu et al., 2011).

In the preceding Chapter, details of the Skp2-binding site of cyclin A were presented. This chapter describes experiments to determine the cyclin A-binding site of Skp2. A model for the binding of Skp2 to cyclin A is presented, and the possible functions of this interaction are discussed. Identifying residues of Skp2 which are involved in this interaction might allow for crystallisation of the CDK2/cyclin A/Skp1/Skp2 complex.

4.3 The cyclin A-binding site is located towards the Skp2 N-terminus

4.3.1 Skp2 4A is impaired in its binding to CDK2/cyclin A

A Skp2 construct containing residues 1-140 was mutated to alanine at residues Leu32, Leu33, Ser39 and Leu41, (hereafter referred to as Skp2-N 4A), in order to confirm the finding of Ji et al. (2006) that these residues are required for binding cyclin A. These residues are not part of a structured region (Figure 4.2), therefore, changing this sequence would not be expected to create structural changes. The primers for this mutagenesis are listed in Appendix A, Table A1.2. The SEC elution profile of this mutant looks very similar to that of Skp1/Skp2 WT (compare Figures 3.8 and 4.3) indicating that the mutations have not had a detrimental effect on protein stability or binding to Skp1.

A

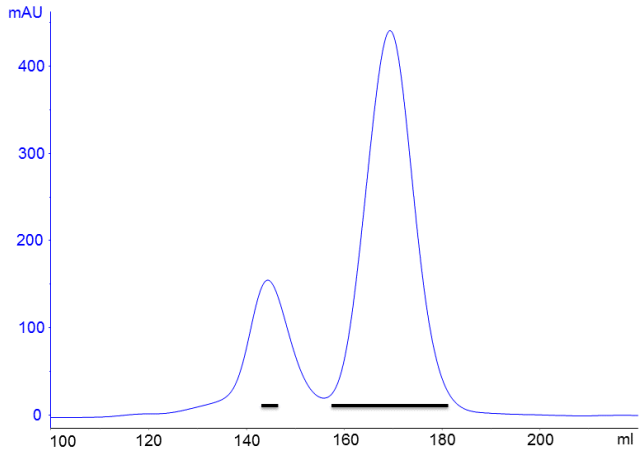

B

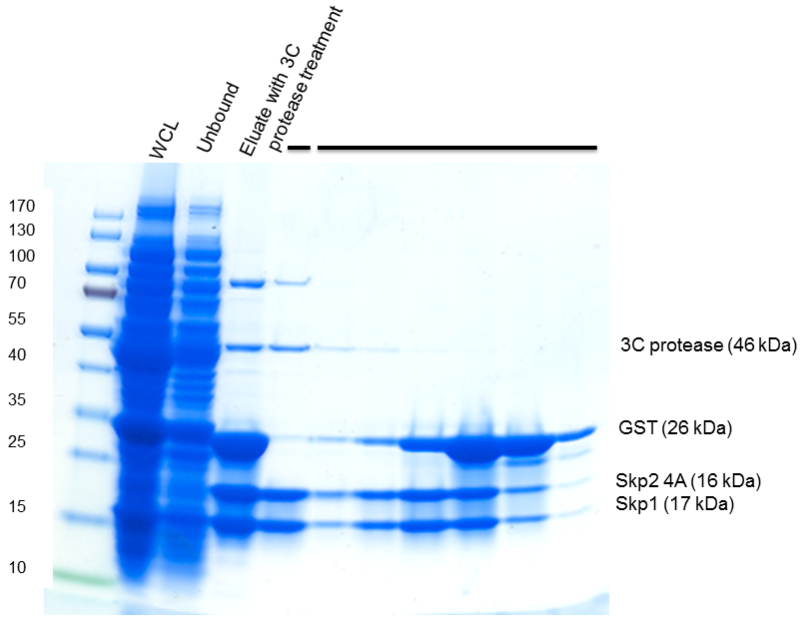

Figure 4.3: Purification of Skp1/Skp2-N 4A A) Skp1/Skp2-N 4A gel filtration chromatogram. B) SDS-PAGE gel showing whole-cell lysate (WCL), the unbound fraction from the glutathione-Sepharose column, eluate after 3C protease treatment and fractions from the regions of the peaks indicated by the black bars.

Skp1/Skp2-N 4A expressed well and ITC was used again to assess its interaction with CDK2/cyclin A (Figure 4.4). Skp1/Skp2-N 4A was found to form a weak interaction with CDK2/cyclin A. This result was repeated and a similar binding affinity of 5.5 ± 0.61 μM was measured.

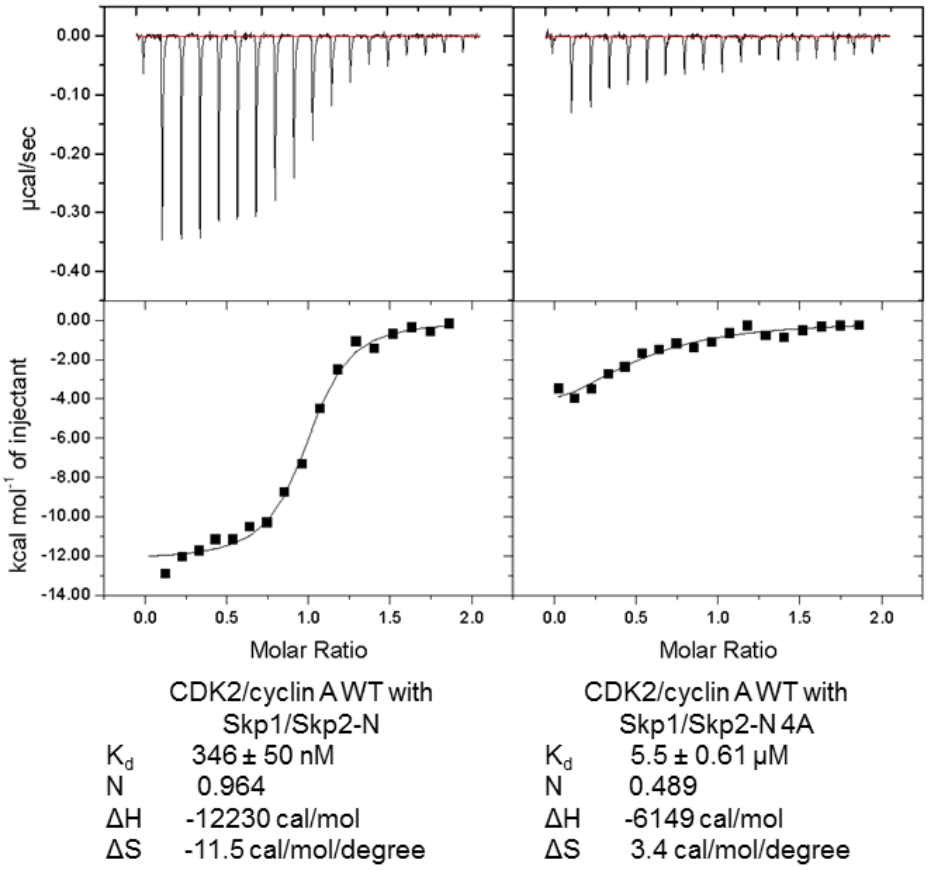

Figure 4.4: Binding isotherms for Skp2-N WT and 4A binding to CDK2/cyclin A. ITC experiment was carried out at 25°C. 20 µM CDK2/cyclin A in the cell and 180 µM Skp1/Skp2 in the syringe.

4.3.2 Residues between Phe20 and Ser30 of Skp2 also contribute to the interaction with cyclin A

The binding affinity of the Skp2-N 4A mutant for CDK2/cyclin A is over 10-fold weaker than that of WT Skp2 (Figure 4.4). Ji and co-workers confirmed this binding site by immunoprecipitation from a HEK293T WCL, and it has been shown here in an *in vitro* reconstituted system that mutating these residues has a direct effect on complex formation (Ji et al., 2006). The predicted secondary structure (PSIPred (Buchan et al., 2013)) for Skp2-N 4A is the same as for the WT sequence (data not shown) suggesting that these residues are directly involved in the cyclin A interaction rather than contributing to the integrity of the secondary structure. Skp2-N 4A still retained some ability to bind to CDK2/cyclin A, suggesting that the cyclin A-binding site of Skp2 might be a fairly extended one. Previous work in the Endicott lab found through pull-down

experiments that Skp2 residues 20-48 are required for binding to cyclin A (Schueller, 2001). In order to determine whether residues 20-30 are involved in a direct interaction with cyclin A, constructs consisting of Skp2 residues 20-140 ($Skp2_{20-140}$) and residues 30-140 ($Skp2_{30-140}$) were created. Both constructs include all of the residues mutated to create the Skp2-N 4A mutant. Skp2 residues 1-19 and 1-29 were removed in a deletion mutagenesis reaction using primers that annealed to either side of the deleted region. The truncations were not injurious to Skp2 and protein yields and the elution profiles following SEC were similar to Skp2-N (1-140) (Figure 4.5).

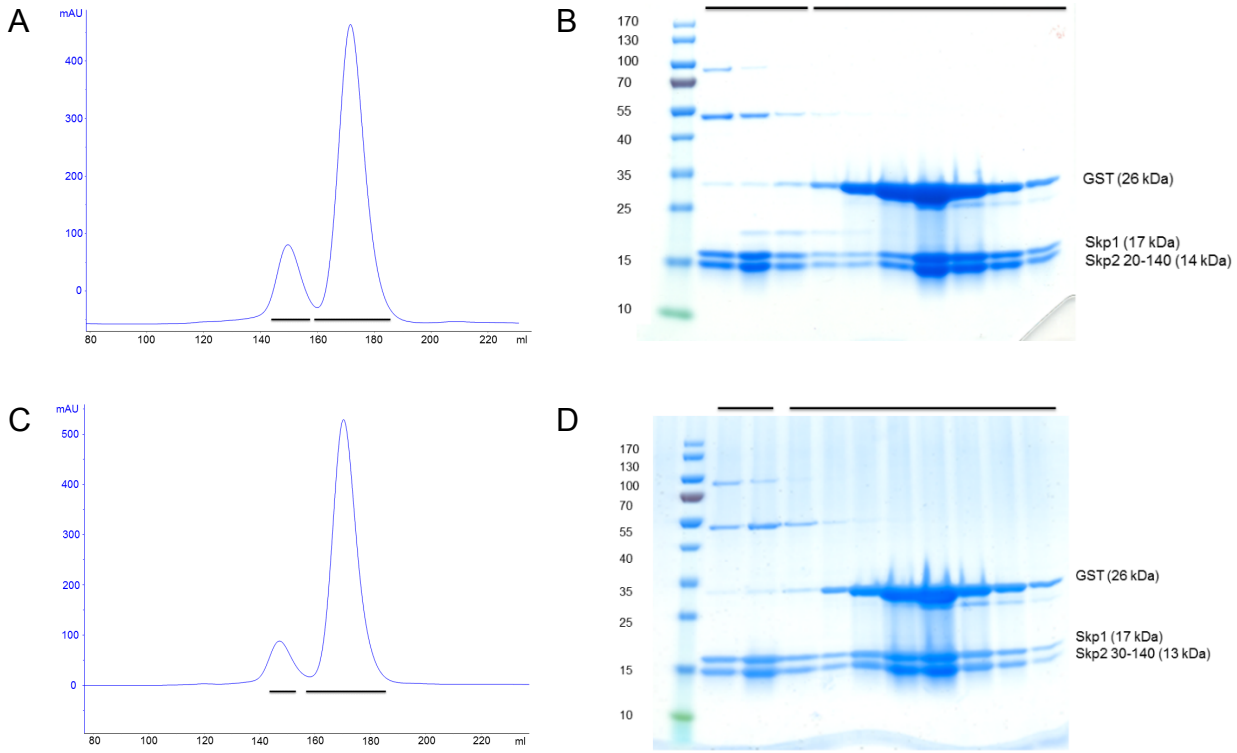

Figure 4.5: Purification of $Skp1/Skp2_{20-140}$ and $Skp1/Skp2_{30-140}$. A) SEC elution profile of $Skp1/Skp2_{20-140}$. B) SDS-PAGE gel of fractions from the SEC elution of $Skp1/Skp2_{20-140}$. C) SEC elution profile of $Skp1/Skp2_{30-140}$. D) SDS-PAGE gel of fractions from the SEC elution of $Skp1/Skp2_{30-140}$.

The association of these two truncated Skp2-N complexes with CDK2/cyclin A was also tested by ITC (Figure 4.6) These experiments revealed that residues within the range Phe20 to Ser30 are required for binding to CDK2/cyclin A. Removing the first 19 residues did not have an effect on binding affinity, however, removing the first 29 residues decreased the binding affinity from around 300 nM to 5.8 μM.

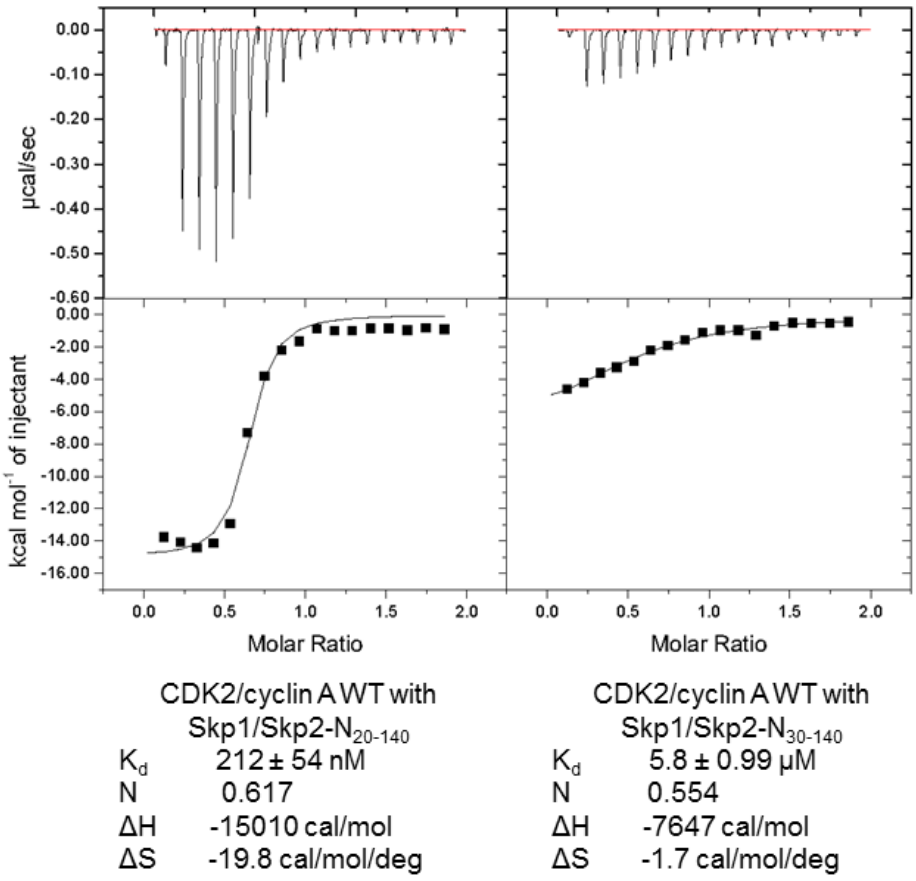

Figure 4.6: Analysis of the binding of Skp1/Skp2$_{20\text{-}140}$ and Skp1/Skp2$_{30\text{-}140}$ to CDK2/cyclin A. ITC analysis was carried out using the same stock of CDK2/cyclin A for both binding analysis of Skp1/Skp2$_{20\text{-}140}$ and Skp1/Skp2$_{30\text{-}140}$. For comparison, the K_d for CDK2/cyclin A binding to Skp1/Skp2 (1-140) was 346 nM. ITC experiment was carried out at 25°C. 20 µM CDK2/cyclin A in the cell and 180 µM Skp1/Skp2 in the syringe.

There is a large decrease in binding affinity for Skp1/Skp2-N$_{30\text{-}140}$ binding to CDK2/cyclin A considering the Skp2 fragment still contains the four residues previously shown to be involved in the interaction with cyclin A (residues 32, 33, 39 and 41 (Ji et al., 2006)). One explanation for these observations could be that there is a mechanism of folding-upon-binding which creates a secondary structure which requires residues within the range Phe20 to Ser30 for stabilisation. Alternatively, Skp2 might form part of its interaction with cyclin A through residues within the range Phe20 to Ser30. Within this sequence, there are charged and hydrophobic residues which might be involved in the interaction with CDK2/cyclin A. Residues within this region are fairly well conserved across species (Figure 4.7), some of which might be involved in the interaction with cyclin A.

```
                          21        30
Homo sapians              TWGWDSSKTS
Mus musculus              TWGWDSSKTS
Bos taurus                TWGWDSSKTS
Gallus gallus             SWDWDSSKTS
Xenopus laevis            MWCWDSNKPS
```

Figure 4.7: Sequence alignment of Skp2 residues 21-30 across species. Highly conserved residues are shown in red.

4.3.3 Mutation of residues 22 and 24 weakens the binding affinity of Skp2 for CDK2/cyclin A.

To identify which residues within this sequence might be important for the Skp2/cyclin A interaction, two double mutants were created, and paired due to proximity to one another. These mutants were W22A W24A and D25A K28A. They were subsequently expressed and purified from recombinant *E. coli* cells (Figure 4.8).

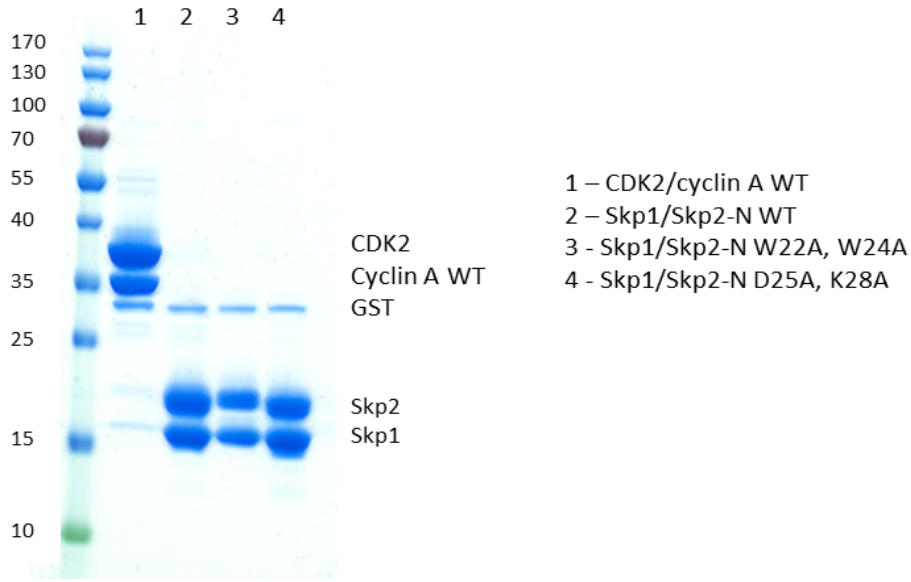

Figure 4.8: Purified CDK2/cyclin A WT and Skp1/Skp2 WT and mutants before ITC. SDS-PAGE gel of CDK2/cyclin A and Skp1/Skp2 complexes before ITC. Small amounts of GST were still present in the purified samples.

Residues Trp22 and Trp24 of Skp2 were found to contribute to its interaction with cyclin A (Figure 4.9). Their individual contribution to the binding affinity was not tested. The cyclin A binding surface on Skp2 is therefore extensive with a stretch of over 20

residues contributing to the interaction. This might suggest that Skp2 extends over the surface of cyclin A in a similar way to p27. Alternatively, Skp2 could fold-upon-binding to create a globular domain in this region. The two tryptophans are part of a region of Skp2 predicted to form a short beta-sheet (Figure 4.2A).

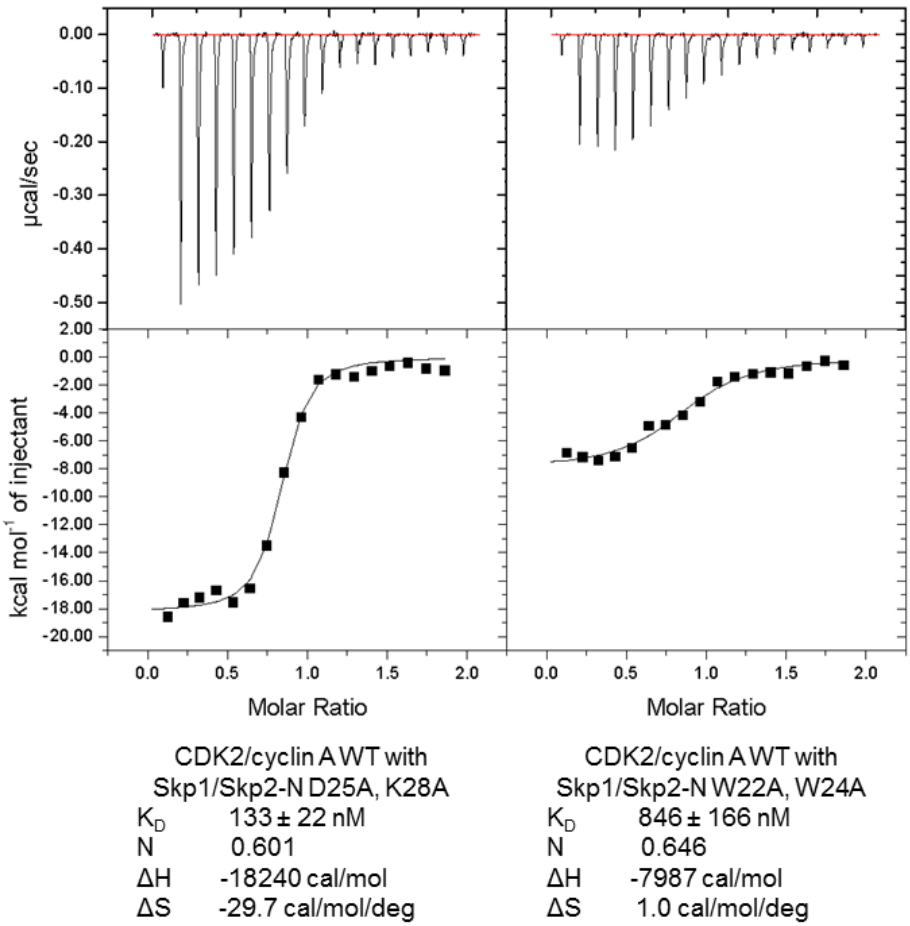

Figure 4.9: Binding isotherms for Skp2 double mutants D25A, K28A and W22A, W24A binding to CDK2/cyclin A WT. ITC experiment was carried out at 25°C. 20 µM CDK2/cyclin A in the cell, and 180 µM Skp1/Skp2-N in the syringe.

4.3.4 Further mutation of Skp2 4A to include W22A and W24A mutations leads to loss of binding

Taken together, the experiments to test the binding of Skp1/Skp2-N 4A and Skp2 truncations to CDK2/cyclin A WT suggested that Skp2 residues Trp22 and Trp24 contribute to its interaction with cyclin A. Skp2 4A was further mutated to include the W22A and W24A mutations. This mutant (hereafter referred to as Skp2-N 6A) was

expressed and purified and found to be stable and able to associate with Skp1 (Figure 4.10). A comparison of the relative mobilities of the different Skp1/Skp2-N mutant complexes by SDS-PAGE shows that the introduction of different mutants can make a substantial change in their electrophoretic properties (Figure 4.10). When running Skp2-N 6A on an SDS-PAGE gel, the introduction of the six mutations causes a change in the electrophoretic mobility of Skp2 (Figure 4.10). The Skp2-N 4A mutation also causes a less noticeable shift in electrophoretic mobility. Comparing the mobilities of the various Skp2 mutants indicates that there is a band shift when mutating Leu32 and Leu33 to alanines and a further band shift when Trp22 and Trp24 are mutated to alanines (Figure 4.10). This could be due to Skp2-N 4A and 6A not being able to bind as much SDS as the WT protein causing a slower migration through the acrylamide gel (Rath et al., 2009). The change in electrophoretic mobility could also be due to insufficient unfolding upon boiling of Skp2 when certain residues are mutated. Mass spectrometry could be used to determine whether Skp2-N 4A and 6A are being modified by enzymes in *E. coli*, thus increasing their molecular weight.

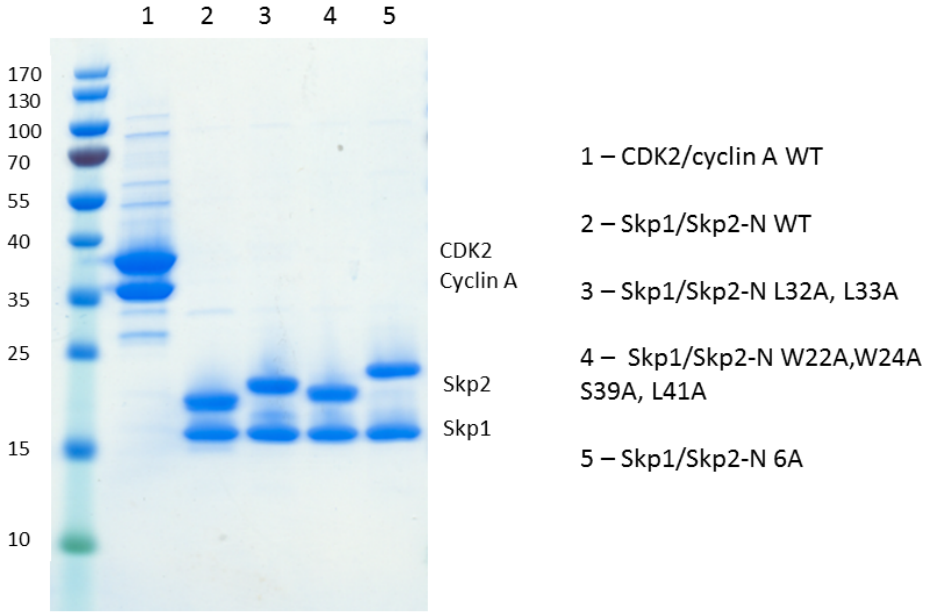

Figure 4.10: SDS-PAGE analysis of purified CDK2/cyclin A WT, Skp1/Skp2 WT and Skp1/Skp2-N mutants. SDS-PAGE of protein complexes before ITC. Mutation of some residues causes a change in electrophoretic mobility of Skp2.

Skp1/Skp2-N 6A was analysed for its binding to CDK2/cyclin A and binding was found to be unable to bind CDK2/cyclin A (Figure 4.11). For this experiment, the binding of CDK2/cyclin A WT to Skp1/Skp2-N WT was measured again using the same stock of CDK2/cyclin A for the experiments shown in 4.11 and 4.12). The K_d obtained was 45

nM, which is a much higher binding affinity than previously determined (K_d of 346 nM, Figure 3.14). The samples for this ITC experiment were purer than the last one (compare Figures 3.15 and 4.10) suggesting that this is a reliable experiment. However, the binding affinity would not be affected by the presence of contaminants as this would merely change the concentration and alter the binding stoichiometry. The error measurements shown with the binding affinity are errors of the fit of the curve to the data. This is at the lower end of all binding affinities measured for CDK2/cyclin A WT binding to Skp1/Skp2-N, a binding affinity of around 200 nM is the average for all measurements (see appendix A, section A2).

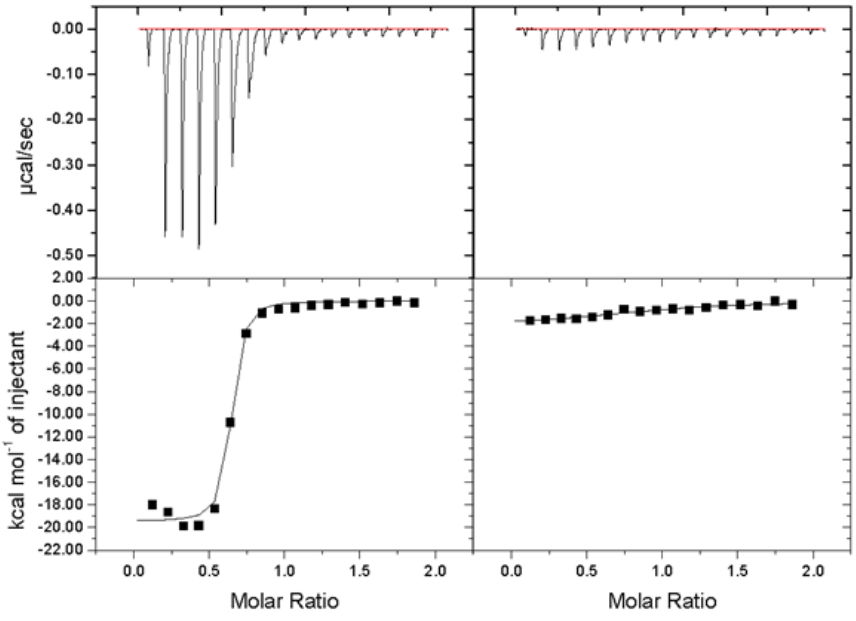

Figure 4.11: Skp1/Skp2-N 6A is unable to bind to CDK2/cyclin A. ITC experiment was carried out at 25°C. 20 µM CDK2/cyclin A in the cell, and 180 µM Skp1/Skp2-N 6A in the syringe

4.3.5 Analysing the contributions of the cyclin A-binding regions on Skp2 to overall binding affinity

The observation that the cyclin A-binding region of Skp2 is extended over 19 residues suggests that these sites might have secondary structure. To test this hypothesis, a

Skp2 peptide of residues 21-43 was synthesised and tested using CD (Chapter 2, Section 8). It was found that to have no secondary structure (data not shown). However, this region could be folding-upon-binding, or require more of the sequence in order to form a stable secondary structure.

Three clusters of residues have been identified as forming the Skp2 interaction site with cyclin A. The individual contributions of each of these three sites were then interrogated in order to determine whether these sites bind co-operatively or whether they act independently. From the ITC experiments that tested the interactions of the Skp2 double mutants with CDK2/cyclin A (Section 4.3.3), it was clear that Trp22 and Trp24 together contribute to the interaction with cyclin A. The contribution of L32A and L33A; and W22A, W24A, S39A and L41A to the observed loss of binding, were then assessed for their binding to determine the contribution of the three clusters of binding sites (Figure 4.12 and Appendix A, Section A2).

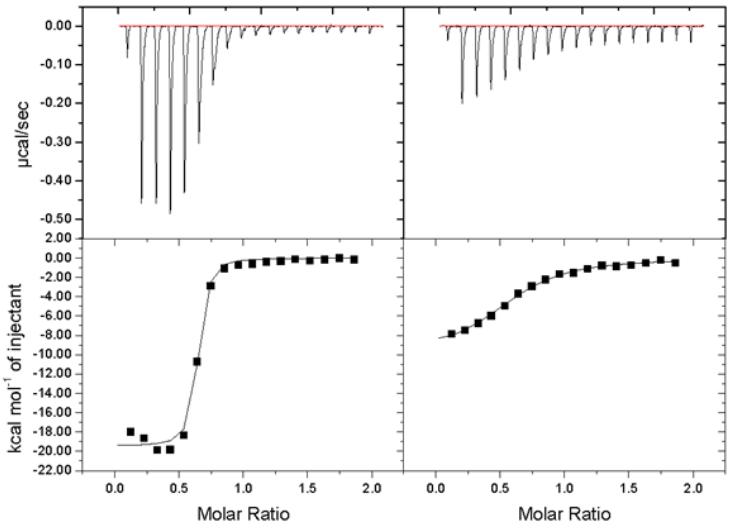

CDK2/cyclin A WT with Skp1/Skp2-N WT		CDK2/cyclin A WT with Skp1/Skp2-N L32A, L33A	
K_d	45 ± 11 nM	K_d	2.2 ± 0.18 µM
N	0.604	N	0.598
ΔH	-19460 cal/mol	ΔH	-9851 cal/mol
ΔS	-31.7 cal/mol/deg	ΔS	-7.2 cal/mol/deg

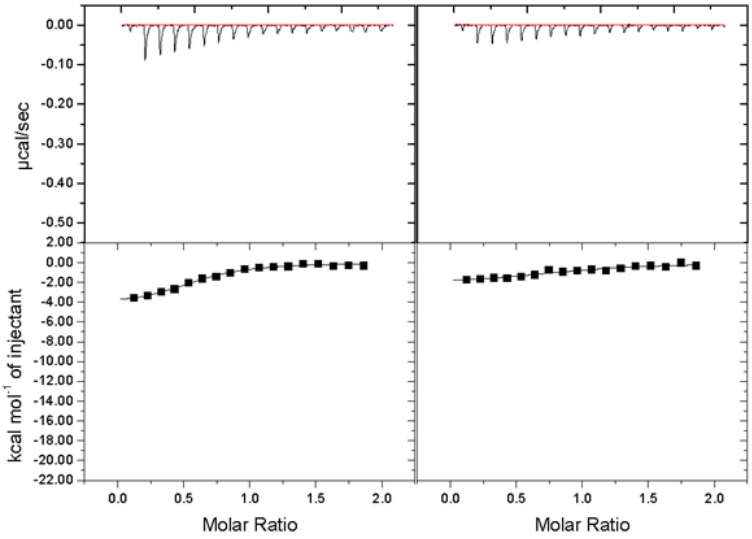

CDK2/cyclin A WT with Skp1/Skp2-N W22A, W24A, S39A, L41A		CDK2/cyclin A WT with Skp1/Skp2-N W22A, W24A, L32A, L33A, S39A, L41A (6A)
K_d	2 ± 0.31 µM	
ΔH	-4372 cal/mol	
ΔS	11.4 cal/mol/deg	Binding thermodynamics not determined

Figure 4.12: Binding isotherms for CDK2/cyclin A binding to Skp1/Skp2-N mutants with various mutations within the cyclin A-binding region. CDK2/cyclin A WT binding to Skp1/Skp2-N WT; L32A, L33A; W22A, W24A, S39A, L41A; and W22A, W24A, L32A, L33A, S39A, L41A (6A). The same stock of CDK2/cyclin A was used for all four experiments. See Figure 4.9 for sample purity. ITC experiment was carried out at 25°C. 20 µM CDK2/cyclin A in the cell, and 180 µM Skp1/Skp2 in the syringe.

Within the Skp2 N-terminus, three clusters of residues (Trp22 and Trp24; Leu32 and Leu33; and Ser39 and Leu41) were identified as being involved in the interaction with cyclin A (Figure 4.4 and 4.11). All sites seem to be contributing to the interaction. The ITC experiment of Skp1/Skp2-N 6A binding to CDK2/cyclin A was repeated and is shown in Appendix A2. Knocking out any one site reduces the cyclin A-binding capacity of Skp2 and knocking all out causes near complete loss of binding, suggesting that the three sites bind independently of one another. Alternatively, one of the sites may dock to cyclin A making it easier for other parts of Skp2 to subsequently bind. Mutation of cyclin A residues 244 to 247 to residues of the cyclin E sequence caused loss of Skp2 binding (Chapter 3). The mutations included an insertion of a glutamate residue, and analysis of the cyclin E structure shows that the glutamate points out into solution (Chapter 3, Section 3.7.2). Although an extended region of Skp2 was found to bind cyclin A, this sequence can be displaced by this insertion suggesting that the bulge in the surface of cyclin A caused by the mutations prevents docking of the three binding sites by extending the area of the cyclin A surface which Skp2 residues 22 to 41 spans.

4.4 CDK2 does not form an interaction with Skp1/Skp2

4.4.1 Role of CDK2 in the interaction of CDK2/cyclin A with Skp2

The finding that the cyclin A-binding site of Skp2 is fairly extended opens up the possibility that CDK2 may contribute to the interaction with Skp2. There is some discrepancy in the literature as to whether CDK2 contributes to the CDK2/cyclin A interaction with Skp2. Yam and co-workers found that Skp1 and Skp2 are pulled down by CDK2 in an *in vitro* GST pull-down assay, where CDK2 was GST tagged (Yam et al., 1999). However, Ji and co-workers were unable to pull down CDK2 in a similar GST pull-down assay, where Skp2 was GST tagged (Ji et al., 2006). An explanation for this might be found by considering the binding of p27 to CDK2/cyclin A and CDK2/cyclin E. p27 binds to CDK2/cyclin A and CDK2/cyclin E through a sequential mechanism which involves an initial interaction with the cyclin at the RXL recruitment site, and then folding of the p27 around cyclin A/E onto CDK2 (Lacy et al., 2004). Skp2 might, therefore, bind to CDK2/cyclin A in a similar manner. However, as CDK2/cyclin E does not bind to Skp2, it seems unlikely that Skp2 forms a significant interaction with CDK2 without cyclin A.

Figure 4.13 shows the CDK2/cyclin A surface structure with p27 in coral and the region of cyclin A identified as contributing to the interaction with Skp2 (Chapter 3) in yellow with a red surface. Skp2 also binds to the p27 binding site of cyclin A as p27 and Skp2 binding to cyclin A is mutually exclusive. In order to determine the role of CDK2 in binding of the CDK2/cyclin A complex to Skp1/Skp2-N, monomeric CDK2 was expressed in *E. coli* and purified by Dr Mathew P. Martin.

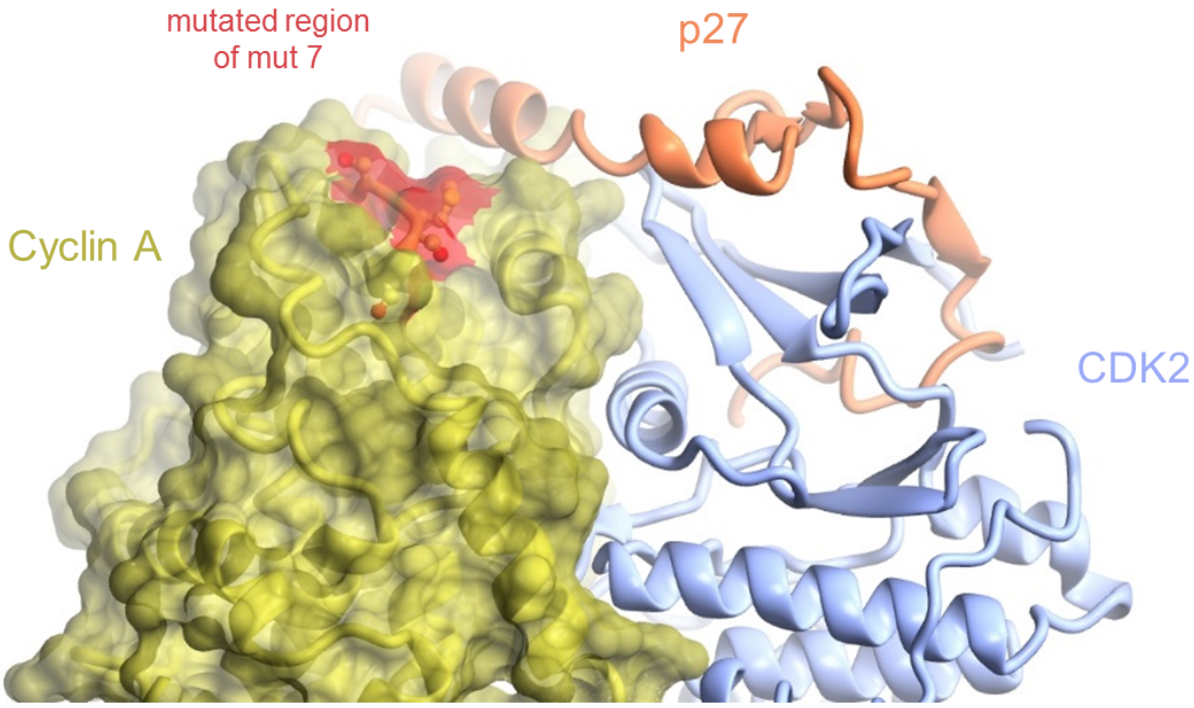

Figure 4.13: Mutated residues of cyclin A mut 7 are in close proximity to CDK2. CDK2 is in ice-blue, cyclin A is in yellow with mutated region in red (cyclin A mut 7), p27 in coral. PDB: 1JSU

4.4.2 Monomeric CDK2 does not bind to Skp1/Skp2-N

ITC was used to quantitate the interaction between CDK2 and Skp1/Skp2-N (Figure 4.14). The ITC experiment showed that monomeric, unphosphorylated CDK2 does not bind to Skp1/Skp2-N.

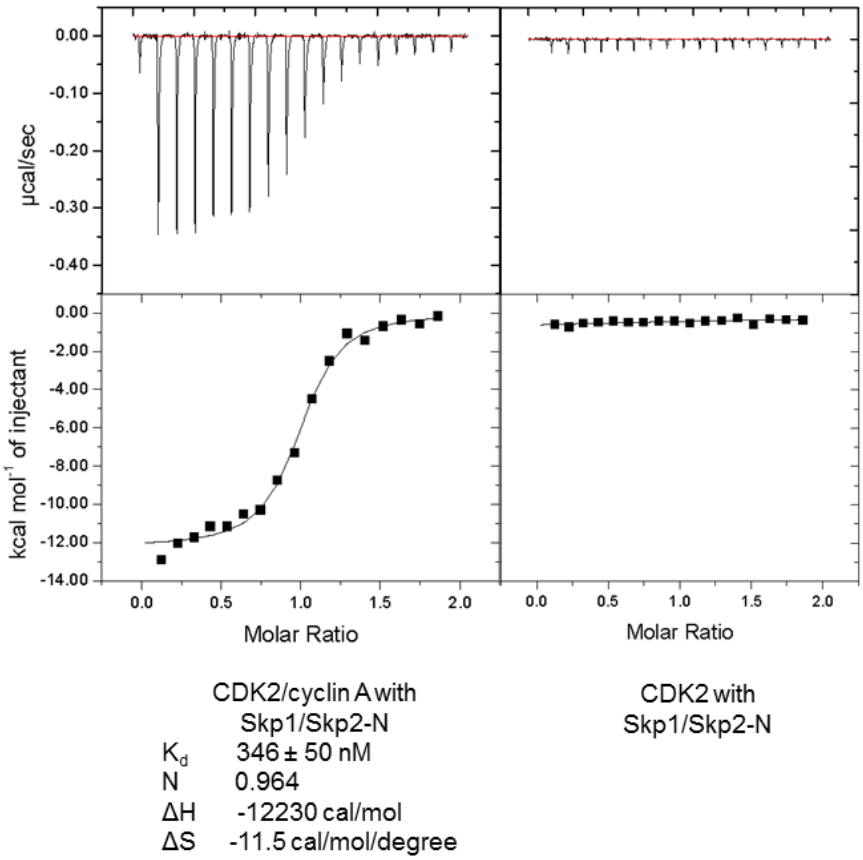

Figure 4.14: Binding isotherms of CDK2/cyclin A binding to Skp1/Skp2-N compared with monomeric CDK2 binding to Skp1/Skp2-N. ITC experiment was carried out at 25°C. 20 µM CDK2 or CDK2/cyclin A in the cell, and 180 µM Skp1/Skp2-N in the syringe.

This result could arise if the CDK2 were unstable and had aggregated in the cell. When the contents of the cell were recovered after the experiment, there were no signs of cloudy precipitate. SDS-PAGE analysis of the proteins after the experiment showed that CDK2 was intact and had the expected stoichiometry with Skp1/Skp2-N (Figure 4.15).

Another control which could have been done would be to use cyclin E1 as a surrogate for cyclin A to determine the contribution of CDK2 to the binding of Skp2 as cyclin E cannot bind Skp2. This would ensure CDK2 was stable and in a conformation which supports protein-protein interactions. However, in contrast to cyclin A, cyclin E does not express well in *E. coli* and a protocol had not been established in the lab for producing cyclin E recombinantly, so it was not possible at the time to do this experiment. Other temperatures and conditions could have been used to establish

whether CDK2 does bind slightly as the conditions used were those used for CDK2/cyclin A binding to Skp1/Skp2-N.

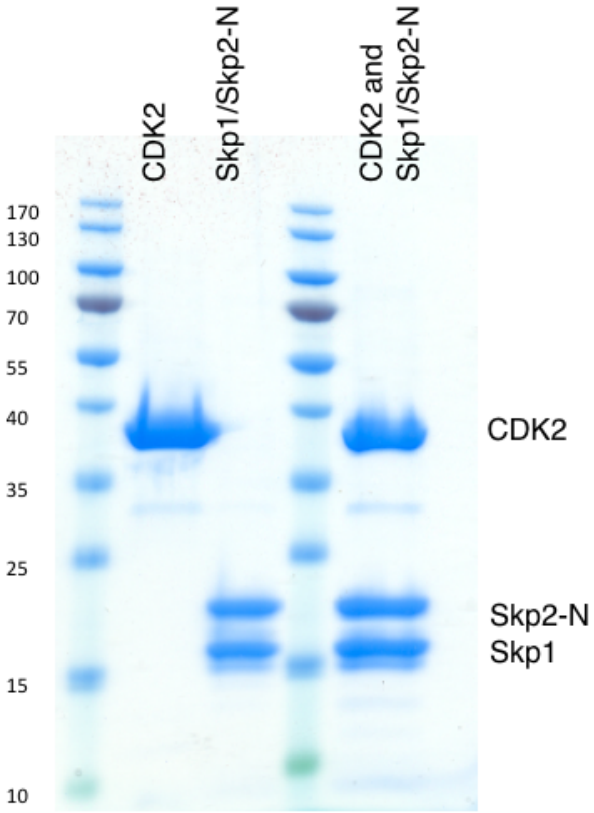

Figure 4.15: SDS-PAGE analysis of CDK2 and Skp1/Skp2-N before and after the ITC experiment. On the left are the individual protein samples before the ITC experiment, and on the right is the protein mixture recovered from the ITC cell.

The Skp2 construct used in this experiment comprised residues 1-140. Ji and co-workers also used an N-terminal construct of Skp2 in their study, whereas Yam and co-workers used full-length Skp2. Full-length phosphorylated Skp2 binds to CDK2 indirectly through Cks1, an interaction which is mediated through the C-terminus of Skp2 (Hao et al., 2005). This difference in Skp2 constructs could explain the discrepancy in the published studies. In agreement with Ji and co-workers, our results confirm that monomeric CDK2 does not form an interaction with the Skp2 N-terminus.

4.4.3 Thermodynamics of binding are different between CDK2/bovine cyclin A and bovine cyclin A binding to Skp1/Skp2-N

In order to investigate the binding of CDK2/cyclin A to Skp1/Skp2-N further, bovine cyclin A was expressed as a surrogate for monomeric human cyclin A. Bovine cyclin A was used in these experiments as human cyclin A is not stable in a monomeric form,

and must be co-purified with CDK2. Bovine and human cyclin A are similar in sequence (Figure 4.16) and structure (Brown et al., 1995, Jeffrey et al., 1995). The sequence is identical between residues 164 and 302 of human cyclin A, which encompasses the Skp2 binding site identified around residues 244 to 247 of human cyclin A. Therefore, it would be expected that binding of Skp2 to bovine cyclin A and human cyclin A would be equivalent.

```
Human cyclin A2  MLGNSAPGPATREAGSALLALQQTALQEDQENINPEKAAPVQQPRTRAALAVLKSGNPRG 60
Bovine cyclin A2 MLGSSAHGPAAREAGSAV-TLQQTAFQEDQENVNPEKAAPAQQPRTRAGLAVLRAGNSRG 59
                 ***.** ***:******: :*****:******:*******.*******.****::** **

Human cyclin A2  LAQQQRPKTRRVAPLKDLPVNDEHVTVPPWKANSKQPAFTIHVDEAEKEAQKKPAESQKI 120
Bovine cyclin A2 PA-PQRPKTRRVAPLKDLPINDEYVPVPPWKANNKQPAFTIHVDEAEEEIQKRPTESKKS 118
                  *  ***************:***:* *******.*************:* **:*:**:*

Human cyclin A2  EREDALAFNSAISLPGPRKPLVPLDYPMDGSFESPHTMDMSIILEDEKPVSVNEVPDYHE 180
Bovine cyclin A2 ESEDVLAFNSAVTLPGPRKPLAPLDYPMDGSFESPHTMEMSVVLEDEKPVSVNEVPDYHE 178
                 * **.******::********.****************:**::*****************

Human cyclin A2  DIHTYLREMEVKCKPKVGYMKKQPDITNSMRAILVDWLVEVGEEYKLQNETLHLAVNYID 240
Bovine cyclin A2 DIHTYLREMEVKCKPKVGYMKKQPDITNSMRAILVDWLVEVGEEYKLQNETLHLAVNYID 238
                 ************************************************************

Human cyclin A2  RFLSSMSVLRGKLQLVGTAAMLLASKFEEIYPPEVAEFVYITDDTYTKKQVLRMEHLVLK 300
Bovine cyclin A2 RFLSSMSVLRGKLQLVGTAAMLLASKFEEIYPPEVAEFVYITDDTYTKKQVLRMEHLVLK 298
                 ************************************************************

Human cyclin A2  VLTFDLAAPTVNQFLTQYFLHQQPANCKVESLAMFLGELSLIDADPYLKYLPSVIAGAAF 360
Bovine cyclin A2 VLAFDLAAPTINQFLTQYFLHQQPANCKVESLAMFLGELSLIDADPYLKYLPSVIAAAAF 358
                 **:*******:*********************************************.***

Human cyclin A2  HLALYTVTGQSWPESLIRKTGYTLESLKPCLMDLHQTYLKAPQHAQQSIREKYKNSKYHG 420
Bovine cyclin A2 HLALYTVTGQSWPESLVQKTGYTLETLKPCLLDLHQTYLRAPQHAQQSIREKYKNSKYHG 418
                 ****************::*******:*****:*******:********************

Human cyclin A2  VSLLNPPETLNL 432
Bovine cyclin A2 VSLLNPPETLNV 430
                 ************:
```

Figure 4.16: Sequence alignment of human and bovine cyclin A2 to illustrate sequence conservation between the two cyclin orthologues. Uniprot accession numbers P20248 (*Homo sapian*) and P30274 (*Bos taurus*). An asterisk indicates positions that are fully conserved. A colon indicates conservation between groups of strongly similar properties, scoring >0.5 in the Gonnet PAM 250 matrix. A full stop indicates conservation between groups of weakly similar properties, scoring =<0.5 in the Gonnet PAM 250 matrix. Figure was created using Clustal Omega (Sievers et al., 2011).

Bovine cyclin A was purified using nickel affinity purification (Figure 4.17A), through binding of a C-terminal hexahistidine tag to the nickel resin. SEC was then used as a

final purification procedure (Figure 4.18). CDK2/bovine cyclin A was purified following the same protocol as used to purify CDK2/human cyclin A (Figure 4.17B).

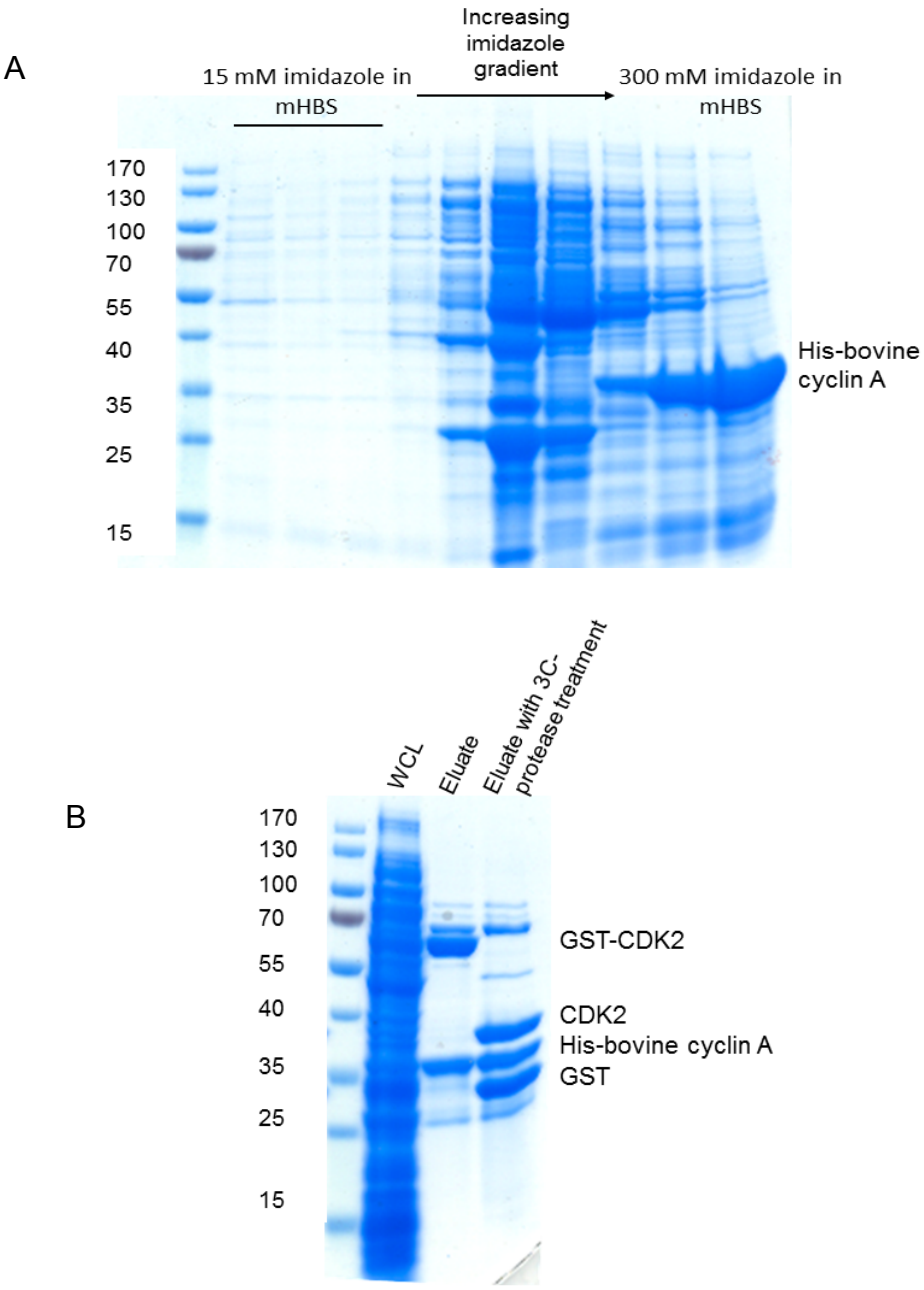

Figure 4.17: Affinity purification of bovine cyclin A (A) and CDK2/bovine cyclin A (B). A) His-tagged bovine cyclin A was purified using nickel-affinity chromatography. The column was washed with 15 mM imidazole in mHBS. Bovine cyclin A was eluted by increasing the imidazole concentration. Only the final fraction was used for the subsequent SEC purification. B) CDK2/bovine cyclin A was purified using the protocol for purification of CDK2/human cyclin A (see Chapter 2, Sections 1.7 to 1.9). WCL (whole cell lysate) was derived from the bovine cyclin A *E. coli* cell lysate.

Bovine cyclin A expresses well in *E. coli* under the same conditions as are used to successfully express human cyclin A (Figure 4.17). Only the last fraction shown in Figure 4.17A was concentrated and loaded onto the size-exclusion column for further purification (Figure 4.18) as high amounts of contaminating proteins co-eluted with bovine cyclin A at the lower imidazole concentrations.

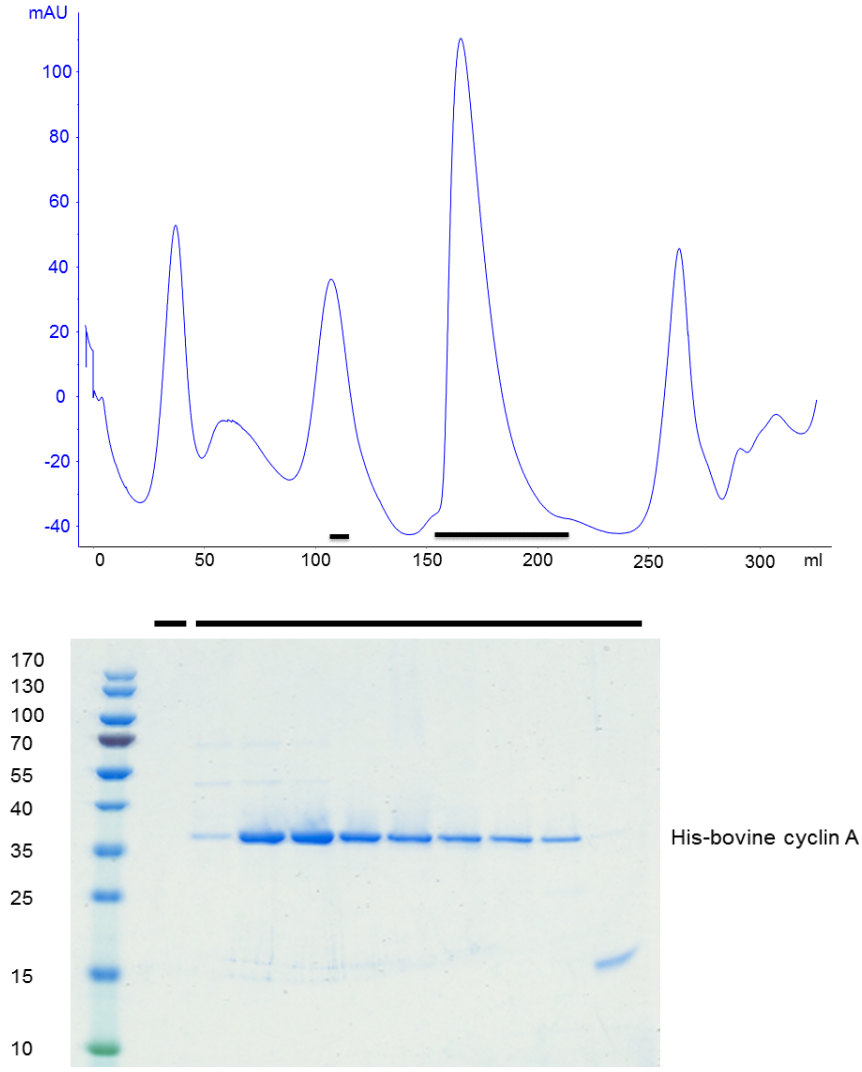

Figure 4.18: Purification of bovine cyclin A was achieved by nickel-affinity chromatography followed by SEC. Fractions corresponding to the parts of the chromatogram with the black bars underneath were analysed by SDS-PAGE. A high level of purity of bovine cyclin A was achieved after nickel-affinity purification and SEC.

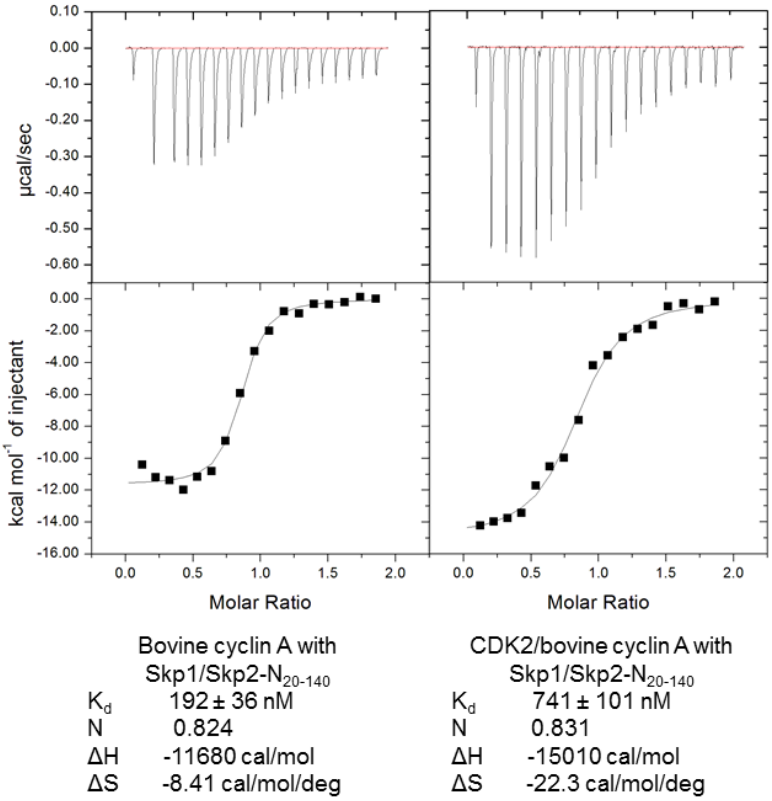

Figure 4.19: Binding isotherms for bovine cyclin A and CDK2/bovine cyclin A binding to Skp1/Skp2-N_{20-140}. The ITC experiment was carried out at 25°C. 20 µM CDK2 or CDK2/cyclin A in the cell and 200 µM Skp1/Skp2 in the syringe.

Monomeric bovine cyclin A was then tested for binding to Skp1/Skp2-N_{20-140} by ITC (Figure 4.19). Bovine cyclin A binds tightly to Skp1/Skp2-N, with a measured K_d of 192 ± 36 nM. This value compares to the affinity of Skp1/Skp2-N_{20-140} to CDK2/bovine cyclin A of 741 ± 101 nM. The relatively tight association suggests that the complex is sufficiently stable for crystallisation trials. It might, therefore, be possible to obtain the structure of bovine cyclin A bound to a Skp2 peptide or Skp1/Skp2-N. Interestingly, the K_d for CDK2/bovine cyclin A binding to Skp1/Skp2-N was weaker than bovine cyclin A binding to Skp1/Skp2-N by about fourfold (Figure 4.19). However, the enthalpy (ΔH) was much greater for CDK2/bovine cyclin A than monomeric bovine cyclin A binding to Skp1/Skp2-N_{20-140}. Bovine cyclin A and human cyclin A are very similar, and therefore, it would be expected that the Skp1/Skp2 binding affinities would be similar. However, the binding to bovine cyclin A could be weaker as this is not the physiological binding partner of Skp2. In this case, you would expect that monomeric human cyclin A would then also bind tighter than CDK2/human cyclin A, which is around 200 nM binding affinity.

The bovine cyclin A versus CDK2/bovine cyclin A binding to Skp1/Skp2-N experiment (Figure 4.19) and the monomeric CDK2 versus CDK2/human cyclin A experiment (Figure 4.14) have given similar results; they both show that Skp1/Skp2-N does not make a significant interaction with monomeric CDK2. But the two experiments are slightly different and the binding profiles of CDK2/bovine cyclin A and CDK2/human cyclin A look slightly different (compare Figure 4.19, right panel, to Figures 3.13 and 4.11, left panels), with a weaker K_d for CDK2/bovine cyclin A-Skp1/Skp2-N. Hence, the binding might be altered by the subtle differences in either the way CDK2 binds bovine cyclin A compared to human cyclin A; or the way CDK2/bovine cyclin A compared to CDK2/human cyclin A binds to Skp1/Skp2-N.

4.5 Stoichiometry of the CDK2/cyclin A interaction with Skp1/Skp2-N

ITC experiments described in Chapters 3 and 4 revealed an unexpected N-value for CDK2/cyclin A binding to Skp1/Skp2. This value was expected to be 1, indicative of a 1:1 stoichiometry, however, the N-value has been found to be around 0.6 for the CDK2/cyclin A interaction with Skp1/Skp2-N (Figure 4.4 left panel and 4.11, left panel). This suggests either an overestimation of the protein concentration in the cell or an underestimation of the protein concentration in the syringe. When this result was first noticed, protein concentrations were re-calculated rigorously. However, the N-value remained around 0.6. Therefore, it is possible that a proportion of CDK2/cyclin A is in a state which cannot undergo an interaction. For some of the ITC experiments, there was a proportion of contamination from GST in the sample (see Figures 3.15 and 4.8). The initial ITC experiments on the cyclin A mutants gave an N-value of about 1 for CDK2/cyclin A WT binding to Skp1/Skp2-N. However, this sample contained some GST (Figure 3.15). Repeating the ITC experiment with no GST gave an N-value of 0.6 (Figure 4.11). Therefore, it appears that GST is not causing the N-value to differ from its expected value. It would appear, therefore, that a proportion of the CDK2/cyclin A in these experiments is unable to form an interaction with Skp1/Skp2-N. This stoichiometry has also been observed for CDK1 binding to cyclin B, and therefore might be something inherent to the CDK (Brown et al., 2015). Another change in the ITC binding isotherm when GST had been fully removed, was that the affinity of Skp1/Skp2 for CDK2/cyclin A was measured at about 10-fold tighter than for previous experiments (compare Figures 3.13 and 4.11). As the samples were very pure for the ITC experiment shown in Figure 4.11 (compare Figures 3.15 and 4.10), the result

seems to be the more reliable experiment. However, the binding affinity should not be affected by the purity of the sample. The binding affinity of CDK2/cyclin A and Skp1/Skp2-N has been measured several times (See Appendix Section A2) and this high binding affinity appears to be unusually tight.

In this chapter and the previous one, the binding interfaces of the Skp2/cyclin A interaction have been described and the literature suggests that inhibition of this interaction might prevent tumour growth. It would be useful to build on the current literature describing small molecule drug developments which target Skp2. As Skp2 has been found to be upregulated in many cancers and to have many roles in cancer (see Chapter 1, Section 9), it has been widely accepted as a valid target for drug development. The crystallisation of the SCF^{Skp2} complex has helped this drug discovery effort. Addition of structural information for the Skp2/cyclin A interaction would also aid drug discovery efforts to inhibit the SCF^{Skp2} complex. The following section describes efforts to obtain a structure of CDK2/cyclin A bound to Skp1/Skp2 or a Skp2 peptide.

4.6 Structural investigations of the Skp1/Skp2/CDK2/cyclin A complex

Taken together, the data outlining the binding site of cyclin A on Skp2 show that there are about 55 residues between the N-terminus of Skp2, which is visible in the Skp1/Skp2-C crystal structure (Figure 1.17), and the region of Skp2 that mediates the interaction with cyclin A. It is likely that these residues form an elongated structure to bridge the interaction of Skp2 with cyclin A. The first 19 residues of Skp2 were shown to be external to the cyclin A binding site (Figure 4.6). Using the biophysical data indicating the Skp2 N-terminal residues involved in the interaction with cyclin A, peptides were synthesised with the aim of obtaining a co-crystal structure with CDK2/cyclin A. The synthesised peptides are shown in Table 4.1.

Peptide number	Residues of human Skp2	Sequence
1	31-43	ELLSGMGVSALEK
2	21-43	TWGWDSSKTSELLSGMGVSALEK
3	18-43	TSFTWGWDSSKTSELLSGMGVSALEK

Table 4.1: Skp2 peptides synthesised for co-crystallisation with CDK2/cyclin A.

Crystal trays were initially set up using peptide 1 at 1.8 mM mixed with 5.8 mg/mL CDK2/cyclin A WT, and hits were obtained in a MORPHEUS screen (Molecular Dimensions). Large flat plate crystals were obtained in condition G7 (0.1 M buffer system 2 (Sodium HEPES, MOPS (acid)) pH 7.5, 0.1 M carboxylic acids, 50% v/v precipitant mix 3 (40% v/v glycerol, 20% w/v PEG 4000), with a 1:1 drop ratio of protein to well solution. The crystals were cryocooled and taken to Diamond Light Source (Didcot, UK) for data collection. When the data were analysed and the structure solved, the peptide was found to be absent from the structure.

It appeared that the lack of success with the co-crystallisation of peptide 1 with CDK2/cyclin A could have been due to two factors. The first is that the crystal contacts don't accommodate the Skp2 peptide. And secondly the peptide might not be binding tight enough. Peptide 2, which is more extended than peptide 1 and contains Trp22 and Trp24 which were identified as contributing to the interaction with cyclin A (Figure 4.9), was designed. Crystal trays were set up using peptide 2 as with peptide 1. The MORPHEUS screen was not used as CDK2/cyclin A crystallises readily from this screen in a crystal form incompatible with peptide binding, and new conditions more optimal for the growth of the peptide-bound complex were desired. In order to disrupt the crystal contacts observed in the CDK2/cyclin A crystal lattice and allow the peptide to bind within an alternative lattice, a key leucine residue of CDK2 (Leu25) was mutated to an aspartate. Commercial screens were set up using peptide 2 with CDK2 WT/cyclin A and CDK2 L25D/cyclin A. Crystals with CDK2/cyclin A WT, but not CDK2 L25D/cyclin A formed after one month at 4°C from an Index screen condition (Hampton Research) with CDK2/cyclin A WT rather than the CDK2 L25D mutant (Figure 4.20). Data collection was carried out at Diamond Light Source (Didcot, UK)

and the crystals diffracted to 2.8 Å. The data were analysed and structure solved, and it was found again that the peptide was not present. The crystallization trials of the Skp2 peptides with the CDK2 L25D/cyclin A mutant complex did not yield any crystals. This result suggests that CDK2/cyclin A does not crystallise readily in alternative lattices, but confirms the importance of the Leu25 contact. This work did, however, identify alternative conditions which yield CDK2/cyclin A crystals.

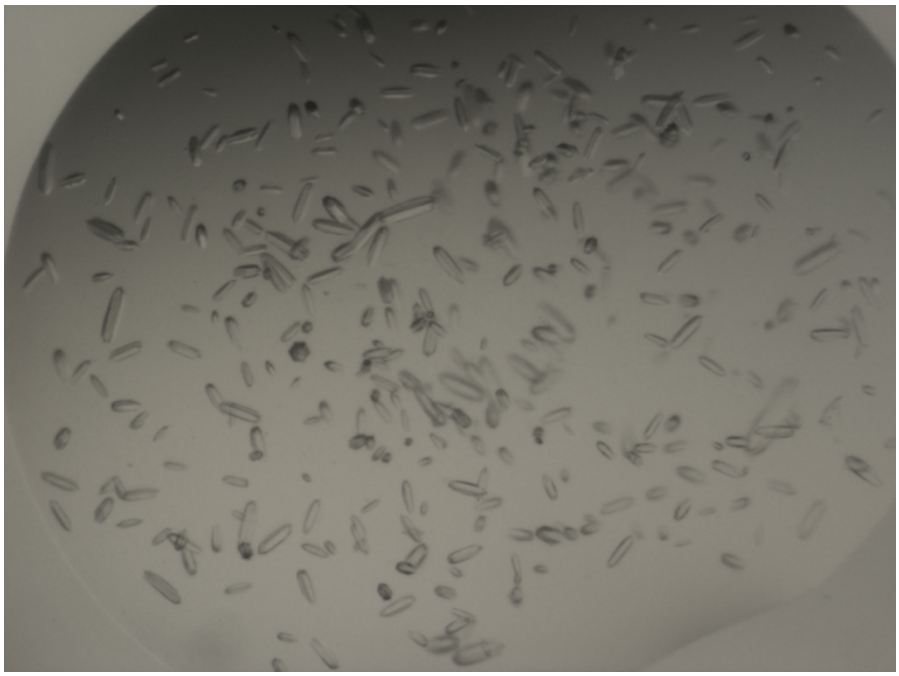

Figure 4.20: Crystals obtained by co-crystallisation of CDK2 (WT)/cyclin A with Skp2 peptide 2. Crystals grew in Index screen condition C12 (15% v/v Tacsimate pH 7.0, 0.1 M HEPES pH 7.0, 2% w/v PEG 3350). Drop shown is 2:1 protein: mother liquor.

Finally, peptide 3 was purchased. This peptide contains an additional three residues at the N-terminus to encompass a potentially structured region around residue 20 (Figure 4.2) which is required for proper orientation of Skp2 to the cyclin A binding site. In addition, the greater number of residues might increase the binding affinity, albeit, it might increase the flexibility. Peptide 3 has not yet been put into crystallisation trials. Due to the lack of success with peptides 1 and 2, the binding of peptide 3 to CDK2/cyclin A should be confirmed before continuing with the crystallisation trials.

4.7 Discussion

4.7.1 Model of the cyclin A binding site of Skp2

These data have allowed for a clearer understanding of the interactions within the CDK2/cyclin A/Skp1/Skp2/Cks1 complex. There are 56 residues between the N-terminus of Skp2 which has been structurally characterised (residues 97 to 424) and the sequence of Skp2 identified here as being involved in the interaction with cyclin A (Trp22 to Leu41). This result is represented in Figure 4.21, which is a superimposed structure of Skp1/Skp2/Cks1 (PDB: 2AST), CDK2/Cks1 (PDB: 1BUH) and CDK2/cyclin A/p27 (PDB: 1JSU), created by Dr Julie A Tucker. The Figure hypothesises that the N-terminus of Skp2 loops around cyclin A to dock at the Skp2-binding site. Further interactions cannot be used to map the binding as the residues of Skp2 that compete with p27 for binding to cyclin A are not known, and therefore which region of Skp2 might bind along the top (relative to figure orientation of Figure 3.3) of cyclin A cannot be located. It might be possible to obtain a crystal structure of CDK2/cyclin A/Skp1/Skp2-N with the Skp2 region which spans the gap from the N-terminus to the identified binding site of cyclin A truncated such that only the minimum amount of residues required to cross this gap were present. This might be more amenable to crystallisation as it would mean that this region would be less flexible.

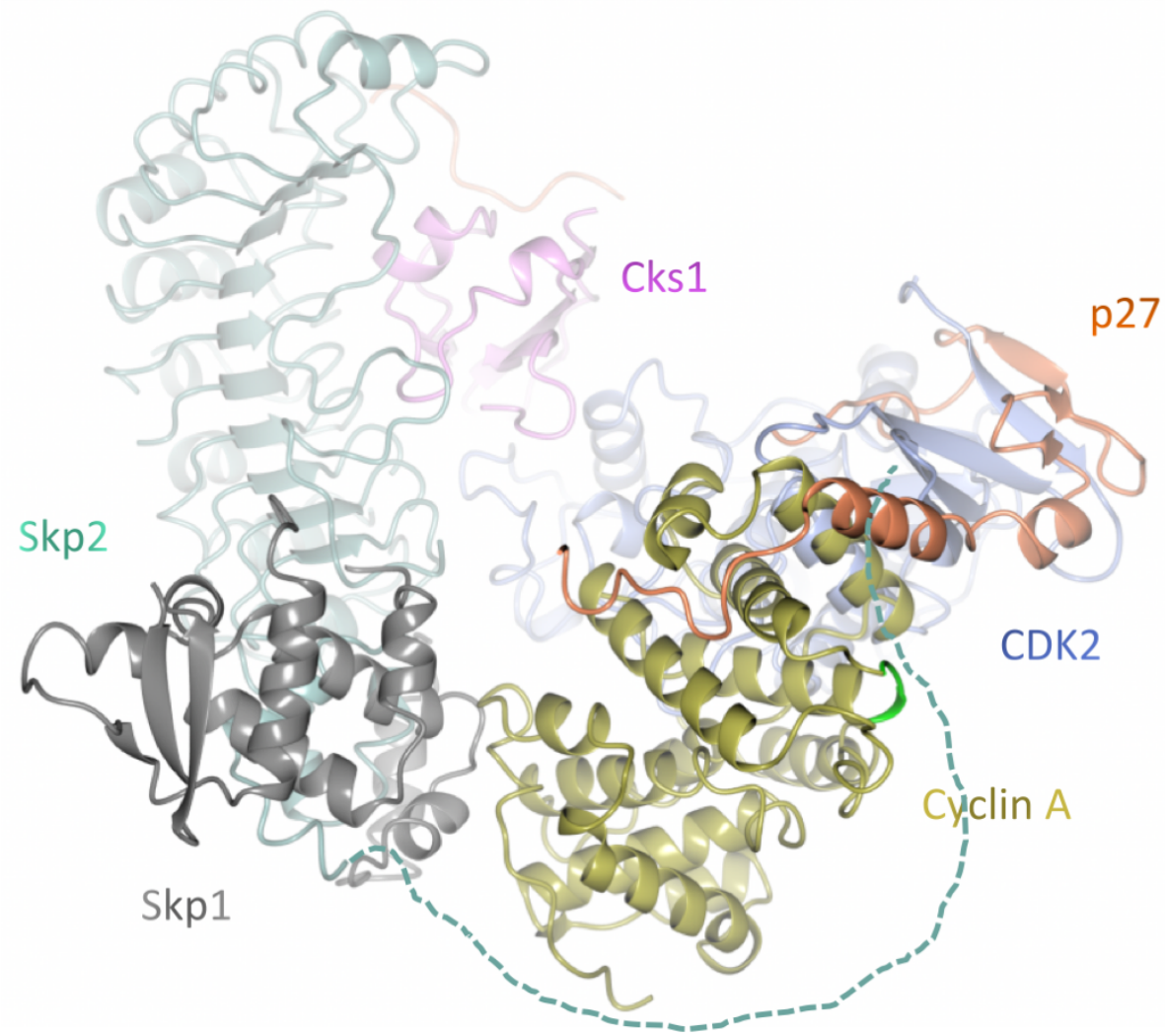

Figure 4.21: Structural model of the CDK2/cyclin A/Skp1/Skp2/Cks1 complex. A dashed line illustrates the N-terminus of Skp2 which has not been structurally characterised. The loop region of cyclin A which has been identified as being involved in the interaction with Skp2 is shown in green (cyclin A mut 7). The superimposed structure was created by Dr Julie A. Tucker using CCP4MG. Skp1/Skp2/Cks1 (PDB: 2AST), CDK2/Cks1 (PDB: 1BUH) and CDK2/cyclin A/p27 (PDB: 1JSU).

4.7.2 Hydrophobic residues of Skp2 are key to its interaction with cyclin A

The Skp2-binding site on cyclin A does not have features suggestive of a binding pocket. Five of the six residues shown in this Chapter to influence Skp2 binding to cyclin A are hydrophobic. The separation of the residues along the Skp2 sequence would be compatible with them adopting a helical structure that might form a hydrophobic face that could dock on cyclin A. The p27 structure is helical as it binds to the upper surface of the cyclin A N-CBF and a number of residues are hydrophobic. A comparison of this region of the p27 sequence with that of Skp2 between residues

22 to 41 shows little homology between the two (Figure 4.22), suggesting that Skp2 and p27 do not share many cyclin A residue interactions. Rather than following the same path along the 'top' of cyclin A, perhaps Skp2 crosses the path of the p27 binding site causing their mutually exclusive binding. This upper region of the cell cycle cyclins may be able to mediate diverse interactions. On cyclin A, this site is involved in its interaction with p27 and it was recently reported that the upper region of cyclin B can support helix binding. The CDK1 C-terminal tail forms an amphipathic helix and this helix was identified in the CDK1/cyclin B structure to bind to a symmetry-related cyclin B molecule at the site which on cyclin A is the upper p27 binding site. This helix mimics interactions which p27 makes with cyclin A. It is probable that it is at this site that Skp2 and p27 compete for binding to cyclin A.

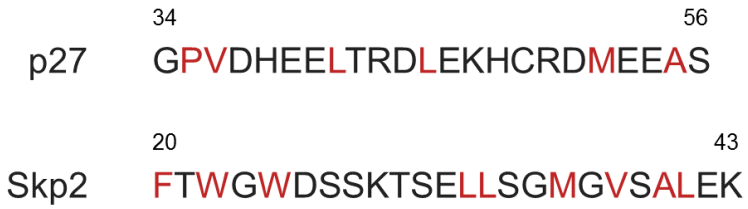

Figure 4.22: Comparison of cyclin A binding regions of Skp2 and p27. Skp2 residues W22, W24, L32, L33, S39 and L41 were identified as contributing to the interaction with cyclin A. The cyclin A-binding region (with the exception of the RXL motif at residues 30-32) of p27 is shown. Hydrophobic residues are in red. Skp2 contains many hydrophobic residues within this region including many residues involved in the interaction with cyclin A, whereas p27 has a higher proportion of charged residues.

As many of the Skp2 residues identified as contributing to the interaction with cyclin A are hydrophobic, the hydrophobic surface of cyclin A was analysed. There is a hydrophobic groove next to the cyclin A loop which was identified as involved in the interaction with Skp2. The hydrophobic side chain of Met246 of cyclin A points out towards this groove (Figure 4.23). The structure of CDK2/cyclin A mut 7 revealed that Gln246 of cyclin A mut 7 points out towards this groove (Chapter 3, Section 7.2). As glutamine is polar, this would be expected to decrease the hydrophobicity of this groove (Figure 4.23B). Glu247 of cyclin A mut 7 points out into solution and might sterically clash with residues of Skp2.

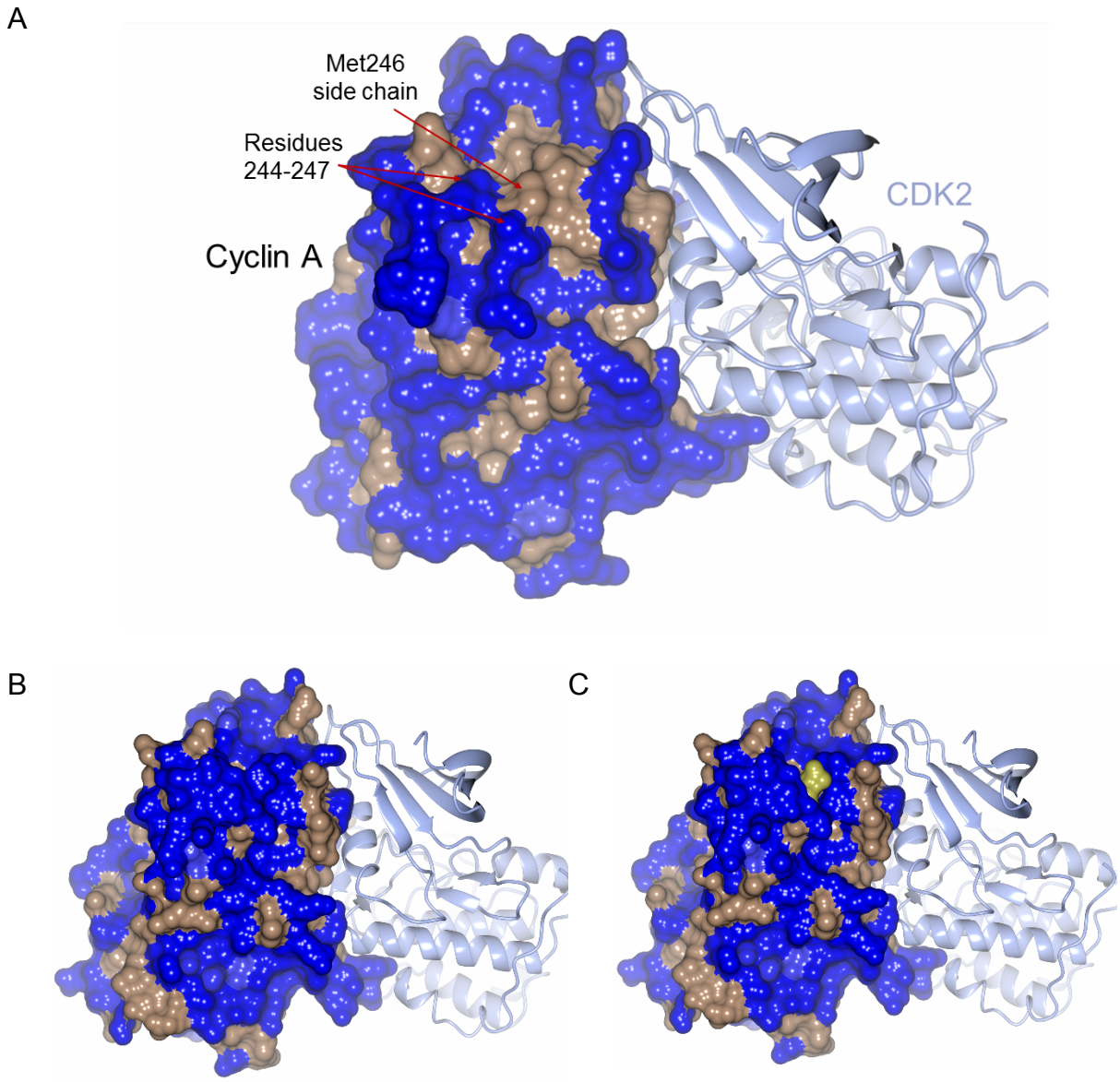

Figure 4.23: Hydrophobic residues of Skp2 which contribute to its interaction with cyclin A might bind to a hydrophobic groove on cyclin A. CDK2/cyclin A WT (A) and CDK2/cyclin A mut 7 (B and C) are shown with cyclin A in surface representation with hydrophobic regions shown in dark fawn with polar and charged regions shown in blue. A) Cyclin A residues 244-247 which contribute to the interaction with Skp2 are in close proximity to a hydrophobic groove. C) Gln246 of cyclin A mut 7 is shown in gold to illustrate its position in this groove. CDK2 is coloured ice-blue.

4.7.3 Identification of Skp2 residues which contribute to its interaction with cyclin A

Mutations made to cyclin A in order to disrupt the Skp2 interaction (Chapter 3) lie on a loop region that is not believed to be involved in any other interaction of cyclin A.

This cyclin A mutant might therefore be useful as a probe to investigate the function of the Skp2/cyclin A interaction and to gain further insights into whether it would be beneficial to inhibit this particular interaction. Reports from other labs using the Skp2 4A mutant, which is impaired for binding to cyclin A, suggest that the Skp2/cyclin A interaction is important for Skp2 function, and that blocking this interaction could lead to G1 cell cycle arrest or apoptosis (Ji et al., 2006, Ji et al., 2007, Lu et al., 2014). By identifying the Skp2 interaction site on cyclin A, it will be possible to determine whether the effects of the mutations made to Skp2 are due to inhibition of the cyclin A interaction specifically. The mutations made to Skp2 are in a region involved in multiple protein-protein interactions, and thus this site may not function exclusively in the binding of cyclin A and it would be useful to tease out the exact role. Identifying the significance of this interaction might also allow for the explanation of the role that cyclin A plays in protecting or promoting Skp2 interactions with other proteins.

The Skp2/cyclin A interaction has been shown by the Zhu group to be a useful target for therapy through the engineering of a Skp2 peptide (Ji et al., 2007). The peptide comprised residues 28-45 of Skp2 and thus included the four residues Ji and co-workers identified as mediating the interaction of Skp2 with cyclin A in their earlier paper (Ji et al., 2006). This peptide was tagged with HIV Tat to allow for its entry into cells. Using an MTS cell proliferation assay, they found that introducing this peptide blocked the Skp2/cyclin A interaction and decreased the proliferation of U20S cells, with an IC_{50} of 35 μM. They also found that the peptide was able to bind to cyclin A in the presence of p27, suggesting that the overlap of the Skp2 and p27 binding sites on cyclin A lies outside Skp2 residues 28-45 and therefore the tryptophan residues at 22 and 24 might share a binding site with p27.

4.7.4 Might Skp2 act as a regulator of CDK2/cyclin A?

Regulators of CDK/cyclin complexes tend to bind to both the CDK and cyclin subunits. Examples include, p27 binding to CDK2/cyclin A/E and HIV-Tat binding to CDK9/cyclin T1 (Chapter 1, Section 1.4 (Russo et al., 1996a, Gu et al., 2014)). As Skp1/Skp2-N does not interact with monomeric unphosphorylated CDK2, and Skp1/Skp2-N binds equivalently to monomeric bovine cyclin A and CDK2/human cyclin A (Figures 4.14 and 4.19), it is likely that CDK2 does not make a contribution to the interaction of CDK2/cyclin A with Skp2. Therefore, it seems unlikely that Skp2 would be able to regulate CDK2 activity in a similar way to other regulators of CDK/cyclin complexes.

4.7.5 Implications of the work described in this chapter

In this investigation, Skp2 residues within the region of Trp22 to Leu41 were identified as being involved in the interaction of Skp2 with cyclin A (specifically residues Trp22, Trp24, Leu32, Leu33, Ser39 and Leu41). The residues identified in this work have not been directly linked to binding of any other proteins to Skp2, however, they are within a region implicated in many protein-protein interactions, and cyclin A binding to Skp2 might have an effect on the binding of other proteins. Therefore, it is likely that this site is not solely involved in the cyclin A interaction. Being able to study the Skp2/cyclin A interaction from both sides in functional studies will allow for the specificity of either site for this interaction to be determined.

Chapter 5: Functional characterisation of the Skp2/cyclin A interaction

5.1 Overview of chapter

This chapter describes cell-based experiments to validate the mutations identified in Chapters 3 and 4 that block the interaction of Skp2 with cyclin A. Cyclin A mut 7 has been shown to be properly folded; the mutations do not cause any structural rearrangements in distal parts of the protein; it is able to bind CDK2, p107 and p27; and is equivalent to WT cyclin A in its ability to activate CDK2. Cyclin A was shown to bind to an extended region of the Skp2 N-terminus. It was also found that Skp1/Skp2-N does not bind to monomeric CDK2. Cyclin A mut 5 and mut 7, and Skp2 4A and 6A were tested in the following *in cellulo* experiments (Figure 5.1).

A cyclin A mutant, which cannot bind Skp2, will allow for the specificity of any phenotypic effects to be assessed, due to the specificity of the interaction site for Skp2. The mutations made to Skp2 are within a region involved in multiple protein-protein interactions and therefore might give rise to off-target effects. In contrast, the Skp2-binding site on cyclin A appears to be in a region not known to be involved in any other interactions of cyclin A. It would, therefore, be expected that the phenotype associated with the cyclin A mutations would be cleaner than that associated with the Skp2 mutants.

It has been demonstrated that mutation of residues 244 to 247 on a loop of cyclin A causes a complete loss of cyclin A binding to Skp2 with a K_d too low to be determined by ITC (Figures 3.14 and 3.16). Skp1/Skp2-N 4A retained some binding to cyclin A, with a K_d value about 10 times weaker than WT (Figure 4.4). Skp2 4A will be used in *in cellulo* experiments to confirm the experiments of Ji and co-workers (Ji et al., 2006). Skp1/Skp2-N 6A showed very weak binding to CDK2/cyclin A (Figure 4.11). Therefore, both Skp2 6A and cyclin A mut 7 would be expected to be mutants which would cause a noticeable phenotype when assayed *in cellulo* (binding affinity are summarised in Figure 5.1B).

A

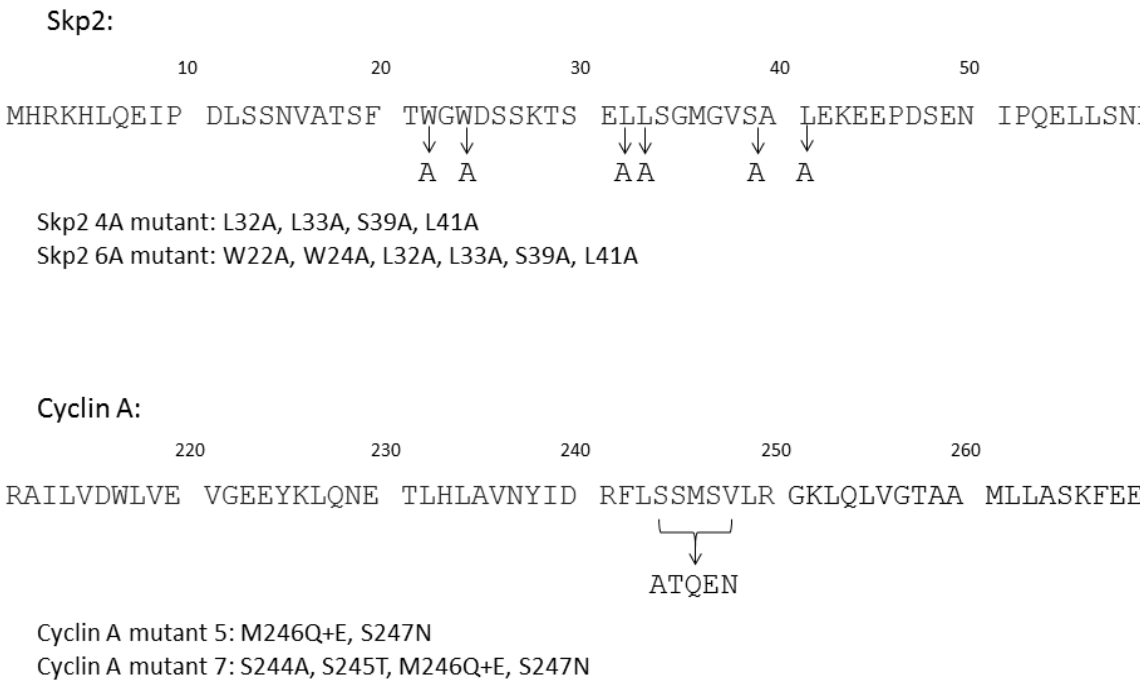

B

Interaction	**Kd**
Skp1/Skp2 WT binding to CDK2/cyclin A WT	346 ± 50 nM
Skp1/Skp2 WT binding to CDK2/cyclin A mut 5	19 ± 11.5 μM
Skp1/Skp2 WT binding to CDK2/cyclin A mut 7	unable to determine
Skp1/Skp2 4A binding to CDK2/cyclin A WT	5.5 ± 0.61
Skp1/Skp2 6A binding to CDK2/cyclin A WT	unable to determine

Figure 5.1: Mutations made to Skp2 and cyclin A. A) Partial Skp2 and cyclin A sequences and mutated regions are shown. B) Summary table of binding affinities determined by ITC.

5.2 Putative functions of the Skp2/cyclin A interaction

5.2.1 Role of the Skp2/cyclin A interaction in degradation of p27

The finding that CDK2/cyclin A binds to the SCF complex and that there is a non-catalytic role of CDK2/cyclin A in the ubiquitination of p27 has led to additional research into the Skp2/cyclin A interaction. Using the Skp1/Skp2/Cks1 (Hao et al.,

2005, Rodier et al., 2008) and CDK2/Cks1 (Bourne et al., 1996) structures, CDK2/cyclin A can be superimposed onto the SCF complex. This model reveals that the Skp2/cyclin A interaction would be expected to be intact in the SCF-Skp2-Cks1-CDK2-cyclin A complex due to the predicted proximity of the N-terminus of Skp2 to cyclin A (Figure 4.21). Seeliger and co-workers used ITC to determine that the binding affinity of p27 for Skp2/Cks1/CDK2 is 150 nM, whereas the binding affinity for Skp2/Cks1 is 470 nM, showing that CDK2 enhances the binding affinity of p27 to the SCF^{Skp2} complex (Seeliger et al., 2003). When the structure of Cks1 bound to Skp1/Skp2 was solved two years later, it was apparent that CDK2 has no role in contacting the C-terminus of p27. Therefore, any effect it might have on the binding affinity would be allosteric or through the anchoring of the p27 N-terminus. The structure of CDK2/Cks1 revealed no change in Cks1 structure upon CDK2 binding. Further investigations are therefore required to determine whether this difference is significant, and if so, why p27 binds tighter to Skp2/Cks1/CDK2 than Skp2/Cks1.

Despite expectations that the Skp2/cyclin A interaction might be important for p27 ubiquitination, Ji and co-workers found that p27 levels were unaffected by the introduction of the 4A mutations to Skp2 (Ji et al., 2006). However, this might have been due to the presence of the endogenous Skp2 and therefore knocking down the endogenous Skp2 might achieve an effect. This could be achieved by transiently knocking down Skp2 or cyclin A and transfecting in relevant Skp2 or cyclin A functional mutant constructs.

There are several possible roles for CDK2/cyclin A within the SCF complex to contribute to the ubiquitination of p27. One is the recruitment of p27 to the complex. Secondly, CDK2/cyclin A could have a role in the stabilisation of the complex. And finally, perhaps the role of CDK2/cyclin A is to retain p27 within the SCF^{Skp2} complex until it is competed off of CDK2/cyclin A by Skp2. Previous investigations into the role of the Skp2/cyclin A interaction indicate a role for the Skp2/cyclin A interaction in regulation of the cell cycle and apoptosis. Increased levels of p27 could lead to cell cycle arrest at G1 phase, however, it is unclear whether increased p27 levels might lead to apoptosis.

5.2.2 Role of the Skp2/cyclin A interaction in Skp2 phosphorylation

CDK2/cyclin A phosphorylates Skp2 at Ser64 (Yam et al., 1999). Phosphorylation at Ser64 leads to stabilisation of Skp2 by interfering with its interaction with Cdh1. Skp2 is dephosphorylated by Cdc14B during M phase and early G1 phase (Rodier et al., 2008). Ji and co-workers investigated whether the association of Skp2 with cyclin A is required for phosphorylation of Skp2 and found that Skp2 4A can be phosphorylated by CDK2/cyclin A at Ser64 (Ji et al., 2006). They concluded that a stable interaction between Skp2 and cyclin A is not required for Skp2 phosphorylation.

5.2.3 Role of the Skp2/cyclin A interaction in Cdh1 association

Cdh1 is a substrate recognition component of the APC/C, involved in the ubiquitination of Skp2 which leads to its degradation via the 26S proteasome (Bashir et al., 2004, Wei et al., 2004). It was established that phosphorylation of Skp2 at Ser64, Ser72 and Ser75 by CDK2/cyclin A, Akt, Pim1, casein kinase I (CKI) and possibly other kinases protects Skp2 from binding to Cdh1 and therefore stabilises Skp2 (Rodier et al., 2008, Cen et al., 2010, Inuzuka et al., 2012, Gao et al., 2009). The findings of Gao et al. (2009) were conflicting as they found that although these phosphorylation events stabilise Skp2 levels, they do not directly block Cdh1 binding. Gao and co-workers also reported that the Skp2/cyclin A interaction is required for recruitment of Skp2 to the APC^{Cdh1} complex. They transfected a Skp2 4A construct into HEK293T and found that as well being unable to bind cyclin A, it was also unable to pull down Cdh1. This result suggests that Skp2 binds to Cdh1 in complex with cyclin A (Gao et al., 2009). However, this seems contradictory as Skp2 was found to be stabilised by phosphorylation by CDK2/cyclin A and hence the Skp2/cyclin A interaction would be believed to promote stabilisation of Skp2 (Rodier et al., 2008).

5.3 Mutagenesis and sub-cloning to create Skp2 and cyclin A mutant constructs in mammalian vectors

A pcDNA3 plasmid containing the Skp2 gene sequence was purchased from Addgene (Plasmid number 19947). The Skp2 6A mutant sequence with 3'UTR was synthesised by IDT. A SDM reaction was used to mutate Ala22 and Ala24 back to tryptophans, thus creating the 4A mutant. After sequencing the insert, both the Skp2 4A and Skp2 6A mutants were then PCR amplified and inserted into a pcDNA3 vector

from Addgene from which WT Skp2 had been removed by *EcoR*I and *Hind*III restriction digestion. The primers for the InFusion cloning are shown in Appendix A, Table A1.3.

A pcDNA5/FRT/TO/NEO plasmid containing the cyclin A gene sequence was provide by Keiko Yata (Gurdon Institute, Cambridge). Mutations were made to the plasmid sequence to create cyclin A mut 5 and mut 7 and these constructs were then confirmed by sequencing. The cyclin A sequences were then PCR amplified and re-inserted via InFusion cloning into a non-mutated vector stock which had been digested with *Hind*III and *Bam*H1. This step was to control for the possibility of the vector backbone being altered during the mutagenesis reaction. Primers for the InFusion cloning are shown in Appendix A, Table A1.3. Different methods were used to make the Skp2 and cyclin A mutant plasmids because of a delay in delivery of the synthetic Skp2 6A sequence. The plasmids generate Myc-tagged Skp2 and Flag-tagged cyclin A, respectively.

5.4 Validating the Skp2 and cyclin A mutants in HeLa cells

5.4.1 Cyclin A and Skp2 test expression in HeLa cells

HeLa cells were chosen to transiently express the mutant cyclin A and Skp2 constructs as a HeLa cell line in which the *CDKN1B* gene that encodes p27 had been replaced with a gene to express p27 T187D mutant protein, was available in the lab. This cell line would be useful in distinguishing any possible effects of the Skp2/cyclin A interaction on phosphorylation of p27.

Initially, a co-transfection was done with varying concentrations of the Skp2 and cyclin A plasmids to determine their expression levels (Figure 5.2). All of the constructs were expressed well, even at the lowest concentration of 0.375 µg plasmid DNA per well. 0.75 µg/well was chosen as an appropriate concentration for subsequent transfection experiments. For the subsequent co-immunoprecipitation experiments, cells were seeded onto 10 cm dishes. 4.5 µg/dish of each plasmid were used for these experiments (scaled up from 6-well plates according to the Mirius Bioscience LT-1 transfection protocol).

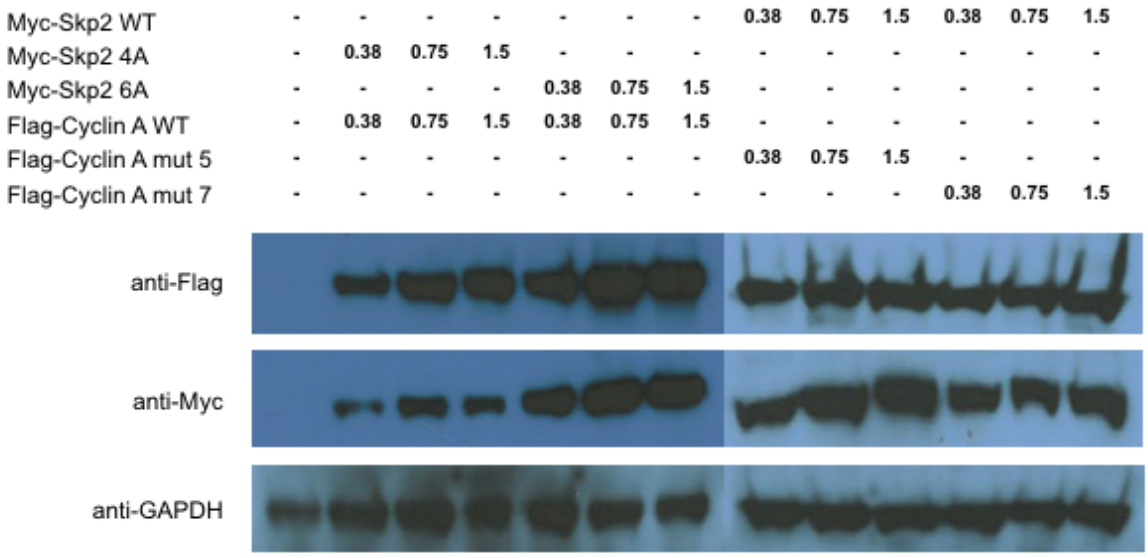

Figure 5.2: Expression of Flag-cyclin A and Myc-Skp2 constructs in HeLa cells. Flag-cyclin A and Myc-Skp2 were transiently co-transfected into HeLa cells using the indicated amounts of DNA. Cells were seeded in a 6-well plate. Cells were lysed after 24 hours, and 20 ng total protein was loaded into each well of the gel. GAPDH was used as a loading control.

5.4.2 Analysis of Skp2 and cyclin A mutants' binding capabilities in HeLa cells

A co-immunoprecipitation experiment was then carried out (Figure 5.3) using anti-Flag antibodies to pull-down cyclin A interacting proteins and using anti-Myc and anti-Skp2 to detect Myc-Skp2 in the eluate. This and the following co-immunoprecipitation experiments were carried out as described in Chapter 2, Section 12.5. The co-immunoprecipitation data seemed to suggest that the Skp2 and cyclin A mutants retain their ability to bind to each other (Figure 5.3). However, there was no change in the electrophoretic mobility of Skp2 4A and 6A in the immunoblot whilst there was a mobility change in the whole-cell lysate (WCL) sample. It is possible that the anti-Myc antibody could be binding to endogenous c-MYC, but a c-MYC/cyclin A interaction has not been reported. As Skp2 was originally identified in an anti-cyclin A immunoprecipitation in HeLa cells (Zhang et al., 1995), one would assume that the CDK2/cyclin A/Skp2 complex is the principal cyclin A containing complex particularly when Skp2 is overexpressed. The lysate was incubated with control agarose resin for 30 minutes as per the Pierce classic IP protocol (Thermo Fisher) in order to remove any agarose binding proteins before the immunoprecipitation experiment. You would not expect, therefore, that Myc-Skp2 was being co-immunoprecipitated non-specifically.

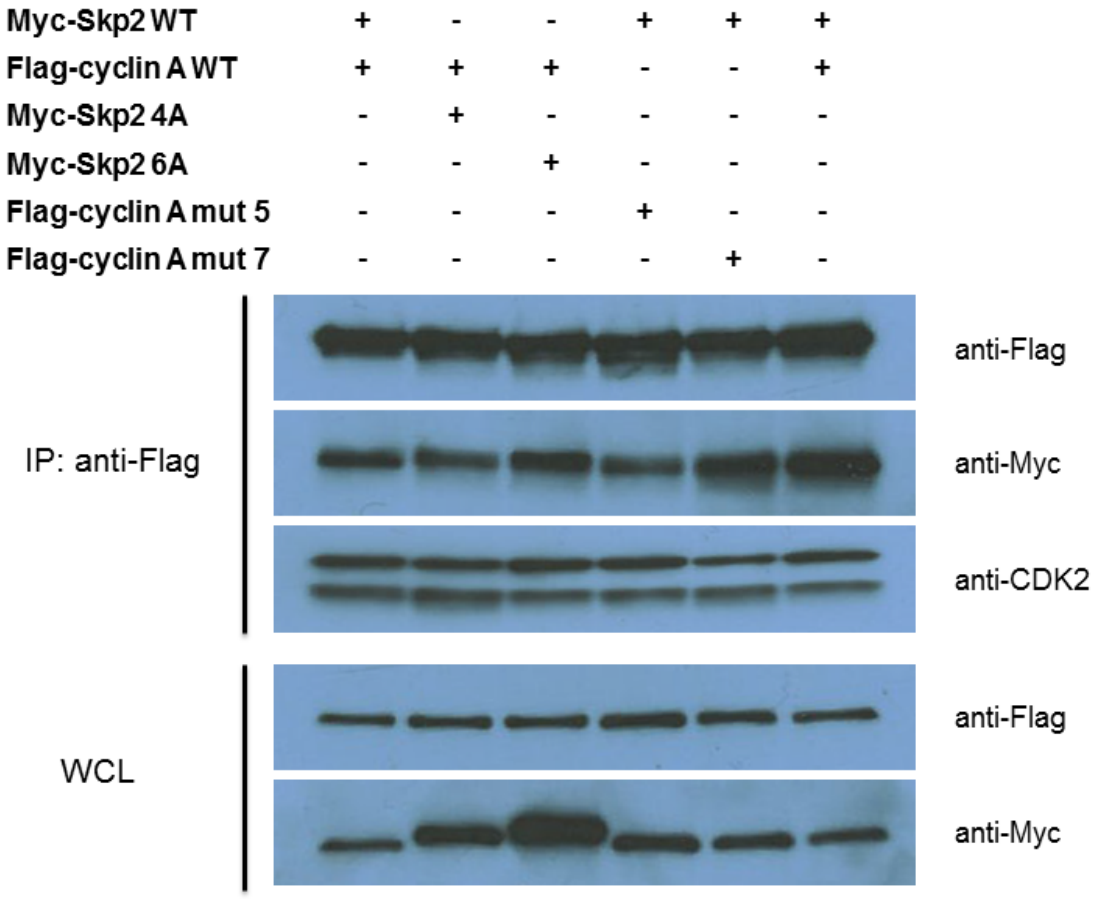

Figure 5.3: The mutations made to Skp2 and cyclin A do not appear to block their interaction in HeLa cells. HeLa cells were transfected with the indicated Myc-Skp2 and Flag-cyclin A constructs. Cells were lysed 24 hours after transfection.

Figure 5.4 shows that Skp2 is being co-immunoprecipitated by cyclin mut 5 and mut 7 and Skp2 4A and Skp2 6A are being co-immunoprecipitated with WT cyclin A. The weak binding to one another might be sufficient for complex formation in this experiment. In order to test this hypothesis further, both Skp2 6A and cyclin A mut 7 were co-transfected together in order to further decrease the stability of the complex (Figure 5.4).

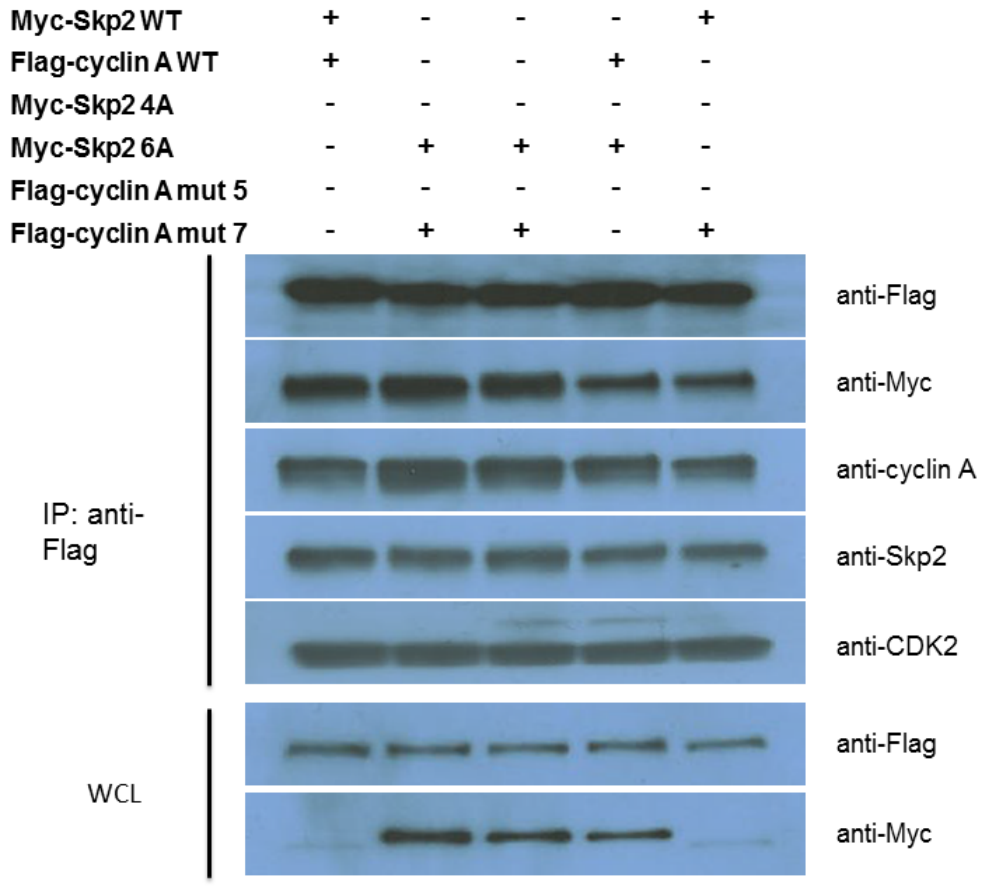

Figure 5.4: Blocking the Skp2/cyclin A interaction by mutation of both Skp2 and cyclin A does not appear to disrupt CDK2/cyclin A/Skp2 complex formation in HeLa cells. HeLa cells were transfected with the indicated Myc-Skp2 and Flag-cyclin A constructs. Cells were lysed 24 hours after transfection.

5.4.3 Determining the role of Cks1 in CDK2/cyclin A/Cks1/Skp2 complex formation

5.4.3.1 Generation of a Skp2 mutant deficient in Cks1 binding

A second co-immunoprecipitation experiment was carried out in HeLa cells. The most effective Skp2 mutant (Skp2 6A) was co-transfected with the most effective cyclin A mutant (cyclin A mut 7) in order to see if the combined effect of knocking out binding sites on both interacting partners would block the interaction. Again, no reduction in binding was observed between Skp2 and cyclin A (Figure 5.4). Furthermore, cyclin A and Skp2 were probed using anti-cyclin A and anti-Skp2 antibodies and this confirmed that Skp2 was being pulled down. It is possible that the interaction between Skp2 and cyclin A is being bridged via CDK2 and Cks1 (Figure 5.5). Cks1 was probed in the co-immunoprecipitation-Western blots and bands were visible in all lanes at

approximately 25 kDa (data not shown). This value is an unexpectedly high molecular weight for Cks1 which has a calculated molecular weight of 9 kDa. A search of Cks1 antibodies led to the finding that many of the antibodies available against Cks1 also bind to a protein of about 25 kDa, but the antibody suppliers identify Cks1 as a lower molecular weight band. As there were no bands on the Western blot below that at 25 kDa, it seemed that Cks1 was not in fact being pulled down in the HeLa cell co-immunoprecipitations.

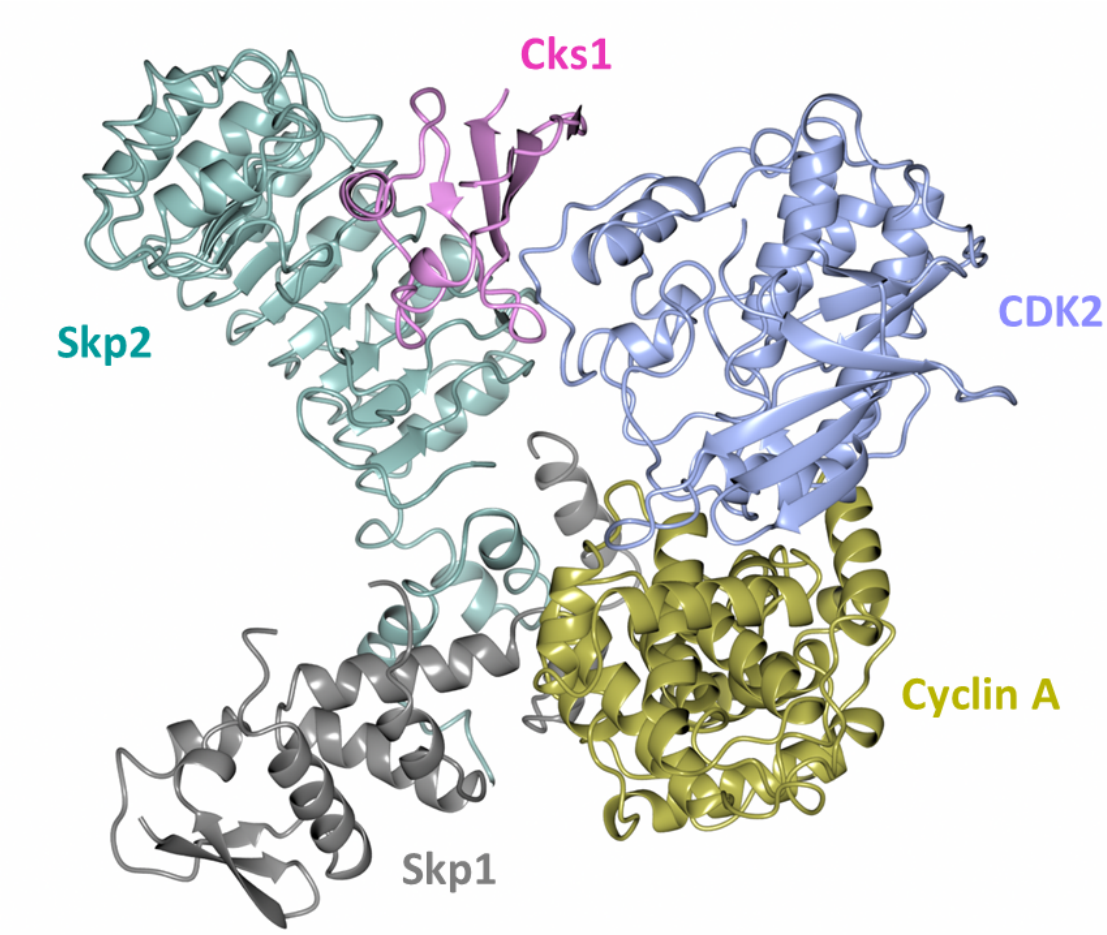

Figure 5.5: Model of the Skp1/Skp2/CDK2/cyclin A/Cks1 complex. Pairwise interactions which form this complex are Skp1-Skp2, Skp2-Cks1, Cks1-CDK2, CDK2-cyclin A and Skp2-cyclin A. This is a superimposed structure of Skp1/Skp2/Cks1 (PDB: 2AST), CDK2/Cks1 (PDB: 1BUH) and CDK2/cyclin A/p27 (PDB: 1JSU), created by Dr Julie A Tucker.

5.4.3.2 Use of a HTRF assay to assess the interactions between Skp2 mutants and Cks1

In order to further test whether the interaction with Cks1 bridges Skp2 and cyclin A, a mutant of Skp2 was identified which is unable to bind to Cks1. A Homogenous Time Resolved Fluorescence (HTRF) assay was developed to test the effect of mutations

on the Skp2/Cks1 interaction (Figure 5.6). This work was carried out by Judith Reeks, who developed the assay, carried out the site-directed mutagenesis, purified the protein and ran the assay. A GST-tagged C-terminal construct of Skp2 (residues 96-424, N-terminally GST-tagged) was used without cleavage of the GST tag. This C-terminal Skp2 fragment (Skp2-C) is only soluble when bound to Skp1, so again the two proteins were co-expressed in *E. coli*. The GST tag binds to a terbium-labelled anti-GST antibody. Cks1 was N-terminally Avi-tagged, which allows for its biotinylation. A dye-labelled streptavidin binds to Cks1-biotin. When Skp2 and Cks1 are in close proximity due to interaction between them, fluorescence energy transfer is observed and fluorescence is emitted at 665 nm.

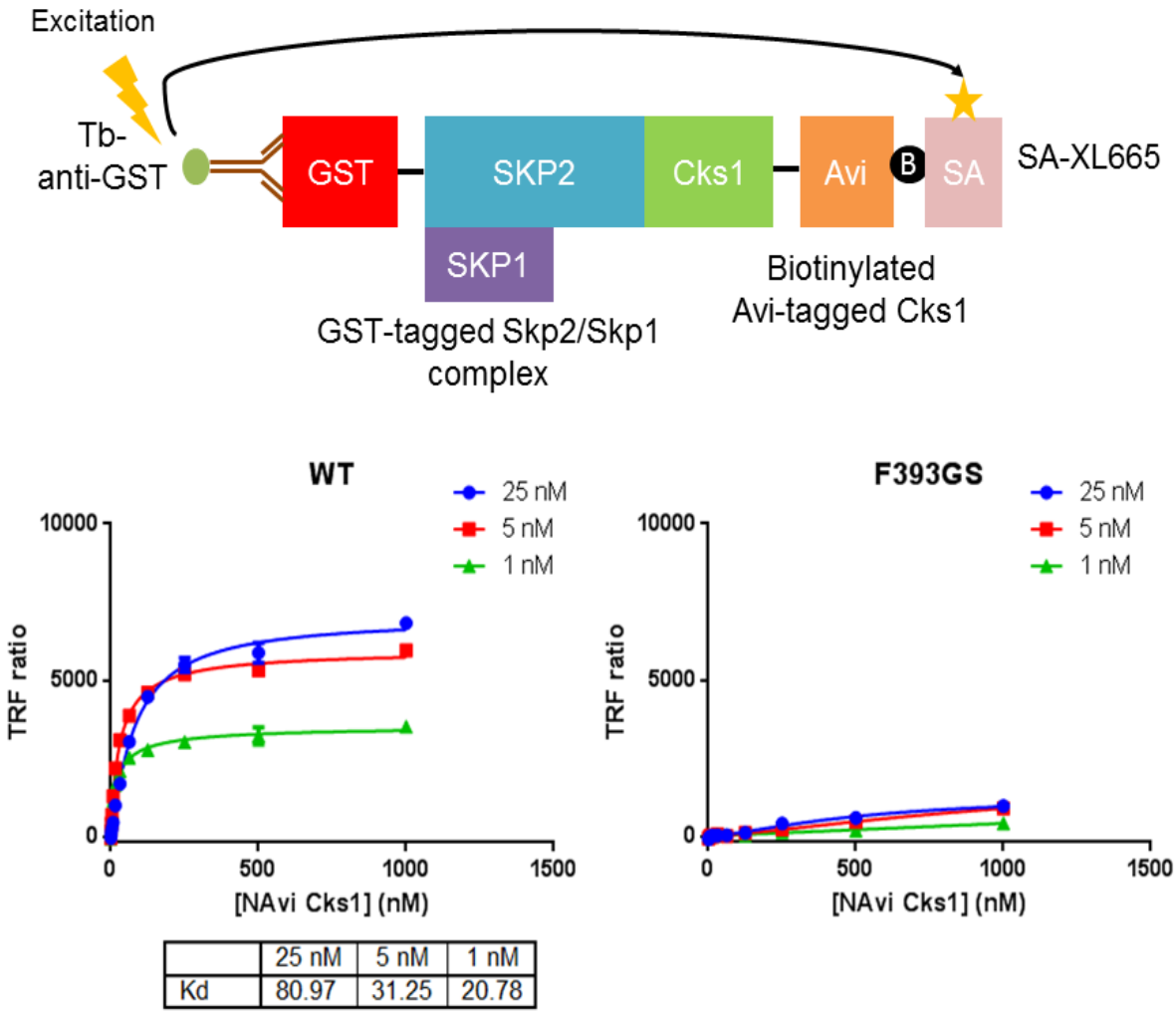

	25 nM	5 nM	1 nM
Kd	80.97	31.25	20.78

Figure 5.6: Use of an HTRF assay to identify a mutation which leads to inhibition of the Skp2/Cks1 interaction. The assay format is shown in the upper panel. Skp2 binds to Cks1 with a K_d in the 10s of nanomolar range. When Phe393 of Cks1 is mutated to Gly and Ser, the interaction with Skp2 is lost.

The binding affinity of Skp2 WT for Cks1 was measured at around tens of nanomolar (Figure 5.6), which is in close agreement with the published K_d of 14 nM (Seeliger et al., 2003). Analysis of the Skp2/Cks1 interface suggested that Phe393 might be required for Cks1 binding and mutation might block the Skp2/Cks1 interaction (Figure 5.7). Mutation of Phe393 to arginine or aspartate did not affect binding (data not shown). Mutation of Phe393 to glycine and serine, however, resulted in total loss of binding (Figure 5.6). This is perhaps through a similar mechanism as seen with cyclin

A mut 5 and mut 7, where the introduction of an extra residue creates a bulge which blocks the interaction.

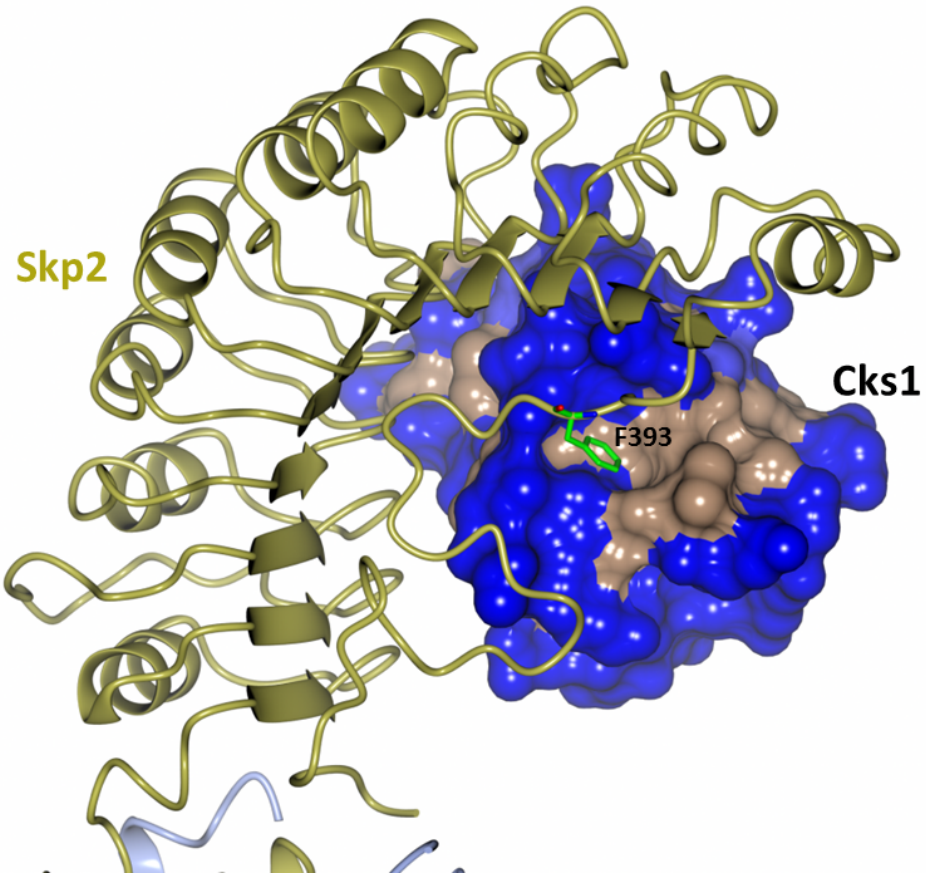

Figure 5.7: Phe393 of the C-terminal tail of Skp2 sits in a pocket of Cks1. Phe393 is shown as sticks with carbon atoms in green and interacts with a pocket on the surface of Cks1. The Cks1 surface is colour coded according to hydrophobicity. PDB:2AST, figure created using CCP4MG.

5.4.3.3 Blocking both cyclin A and Cks1 binding to Skp2 does not appear to block Skp2/CDK2/cyclin A complex formation in HeLa cells

The F393GS mutation was made in the Skp2 WT and Skp2 6A constructs in order to investigate the role of Cks1 in mediating the binding interaction between Skp2 and cyclin A. However, the CDK2/cyclin A/Skp2 complex was still formed (Figure 5.8). There are two bands in lane 2 of the anti-Skp2 blot. The lower band is likely to be endogenous Skp2 which does not have a Myc-tag. Skp2 6A + F393GS might therefore show slightly reduced binding as it might be binding less WT cyclin A, allowing WT endogenous Skp2 to be co-immunoprecipitated. The lack of a band for endogenous Skp2 in lane 3 suggests that the mutants might be working somewhat

as predicted from the *in vitro* work (Chapter 3). Flag-cyclin A mut 7, which is immobilised on the beads in this case, does not bind any endogenous Skp2 (no lower band for Skp2 in lane 3). Although the F393GS mutant of Skp2 did not provide an unambiguous answer as to whether Cks1 plays a role in the maintenance of the Skp2/cyclin A interaction in HeLa cells, it provides an additional tool mutation to investigate the potential effect of blocking the Skp2/Cks1 interaction in cell-based assays.

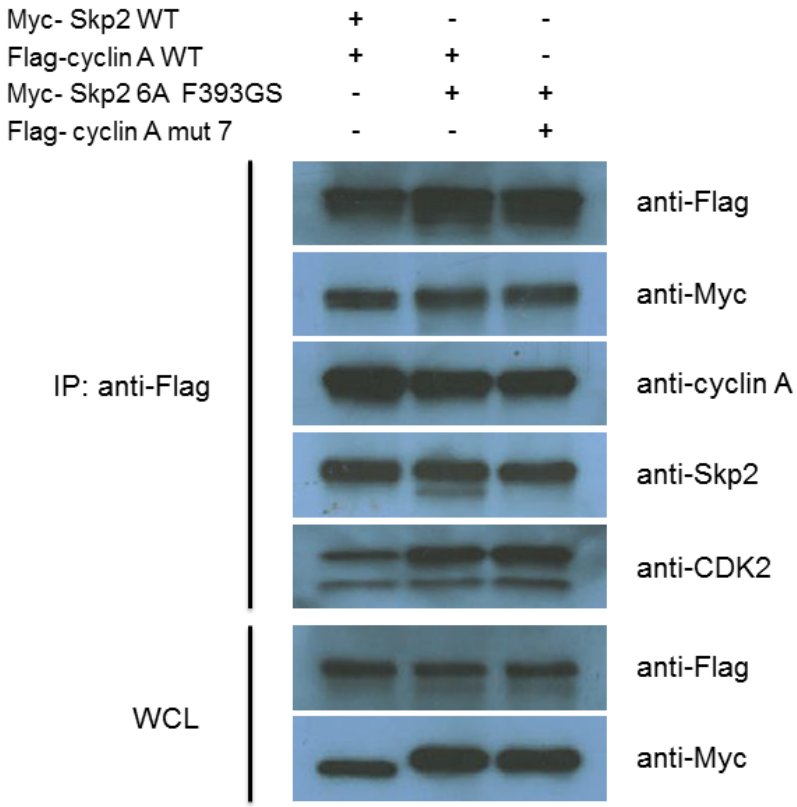

Figure 5.8: Introducing the Skp2 F393GS mutation to Skp2 6A does not disrupt the CDK2/cyclin A/Skp2 interaction in HeLa cells. HeLa cells were transfected with the indicated Myc-Skp2 and Flag-cyclin A constructs. Cells were lysed 24 hours after transfection.

5.5 Validating the Skp2/cyclin A interaction in HEK293T cells

5.5.1 Cyclin A and Skp2 test expression in HEK293T cells

As the results obtained from the HeLa co-immunoprecipitation experiments were unexpected from the published results (Ji et al., 2006) and *in vitro* characterisation of the Skp2 and cyclin A mutants (Chapter 3 and 4), other cell lines were explored in

order to validate the *in vitro* results. As the Skp2 4A mutation had been validated in cell-based assays using HEK293T cells (Ji et al., 2006), a co-immunoprecipitation experiment was carried out in these cells in an effort to reproduce the literature and validate cyclin A mut 5 and 7 and Skp2 6A. An expression test was first carried out, and again there were good expression levels (Figure 5.9). Again, 4.5 µg/10 cm dish of each plasmid were transfected.

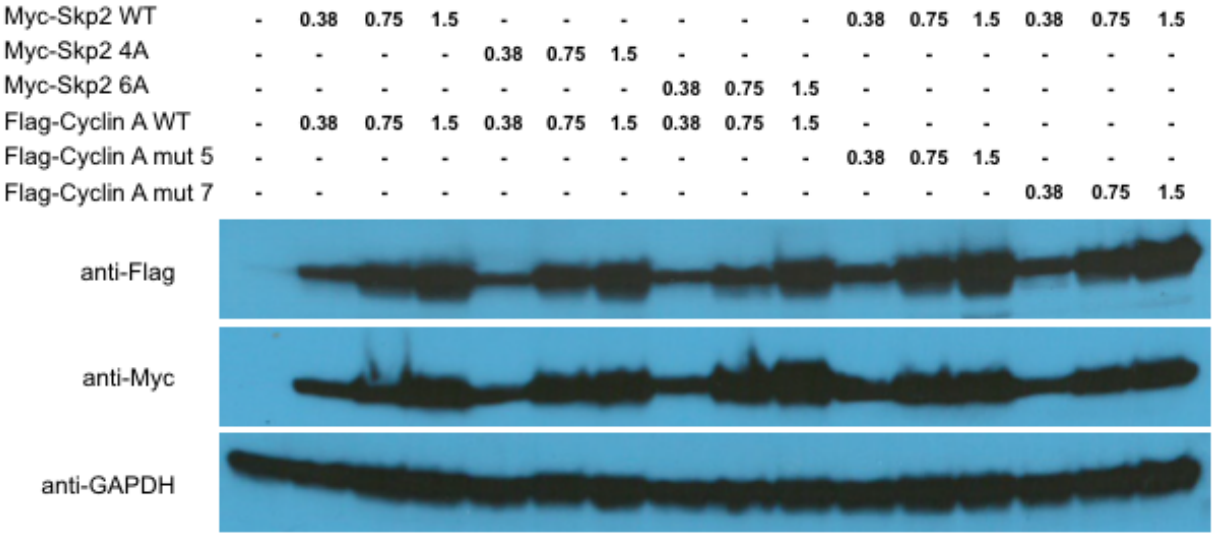

Figure 5.9: Expression levels of Flag-cyclin A and Myc-Skp2 constructs in HEK293T cells. Flag-cyclin A and Myc-Skp2 were transiently co-transfected into HEK293T cells using the indicated amounts of DNA. Cells were seeded in a 6-well plate. Cells were lysed after 24 hours. GAPDH was used as a loading control.

5.5.2 Mutation of Skp2 and cyclin A at the identified binding sites blocks their interaction in HEK293T cells

In contrast to what was seen in HeLa cells, when co-immunoprecipitation was carried out in HEK293T cells, using anti-Flag antibody to pull down Flag-cyclin A interacting proteins, there was a marked reduction in the binding of Skp2 4A and 6A to WT cyclin A and cyclin A mut 5 and 7 to WT Skp2 (Figure 5.10). Despite the apparent lack of effect of binding interface mutations on formation of the Skp2/cyclin A complex in HeLa cells, in HEK293T cells, the blot clearly shows reduced complex formation (Figure 5.10). Here, a change in the electrophoretic migration for Skp2 4A and 6A is observed in both the WCL and the immunoprecipitates. Lanes 2 and 3 show that there is some endogenous Skp2 binding to the Flag-cyclin A WT. This is not seen in

lanes 4 and 5 as Flag-cyclin A mut 7, which is deficient in Skp2-binding, is immobilised on the beads. There is less Skp2 4A and Skp2 6A being immunoprecipitated with cyclin A WT, which is in agreement with the literature (Ji et al., 2006) and with the ITC results (Chapter 4).

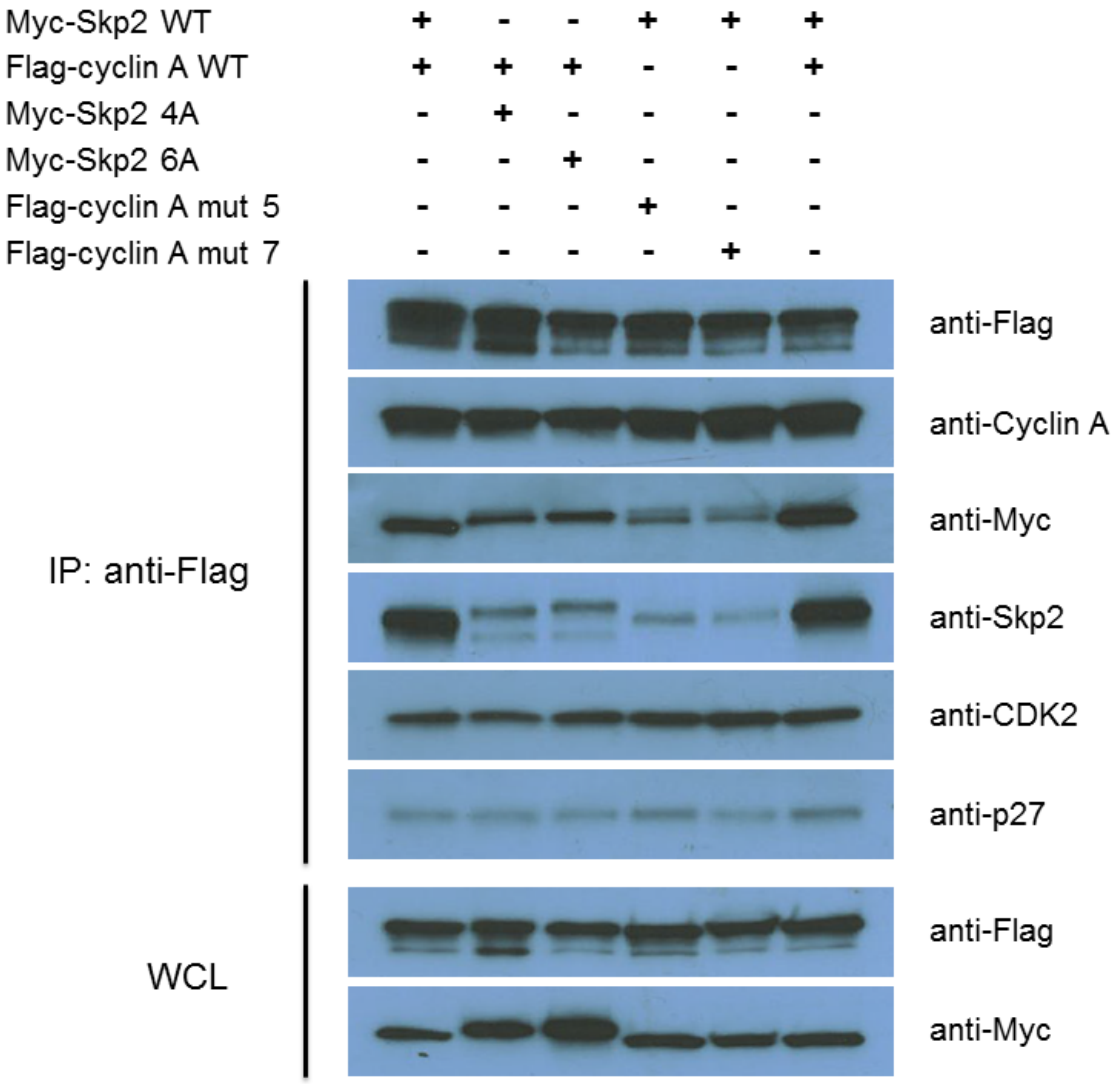

Figure 5.10: In HEK293T cells, the Skp2/cyclin A interaction is blocked by introduction of mutations at the putative Skp2/cyclin A binding interface. HEK293T cells were transfected with indicated Myc-Skp2 and Flag-cyclin A constructs. Cells were lysed 24 hours after transfection.

5.6 Cyclin A binding to Skp2 is not required for Skp2 recognition by the APC^{Cdh1} complex

As the effect of the binding interface mutations on Skp2/cyclin A complex formation has been validated in HEK293T cells, the functional significance of the interaction

could then be probed. Initially, another co-immunoprecipitation was carried out in order to investigate the effects of the mutations on the ability of Skp2 to bind to Cdh1. In this investigation, the most effective mutants were used, Skp2 6A and cyclin A mut 7. Endogenous Cdh1 was immobilised onto beads via an anti-Cdh1 antibody. It was found that Skp2 does not require cyclin A in order to bind to Cdh1 (Figure 5.11). This immunoprecipitation experiment suggests that Skp2 and cyclin A bind to Cdh1 independently of one another. The levels of Cdh1 immobilised in lane 3 are less than in the other lanes in Figure 5.11. Cdh1 was too dilute in the WCL to be detected and therefore it couldn't be determined whether this was due to lower total levels of Cdh1 for this sample compared to the others. The levels of Skp2 appear to be decreased in this sample, and cyclin A levels appear to be decreased when probing with an anti-Flag antibody, but not when probed with an anti-cyclin A antibody.

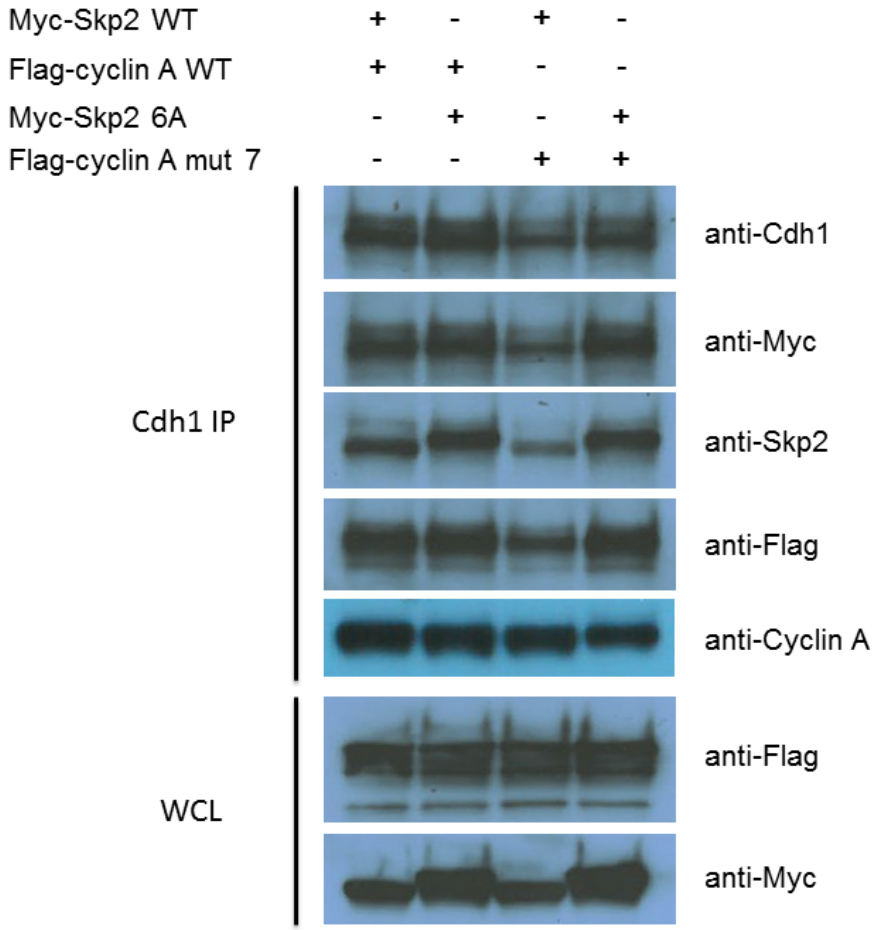

Figure 5.11: Skp2 does not require cyclin A to bind Cdh1. Cdh1 antibody was immobilised on agarose resin. HEK293T cells were transfected with the indicated Myc-Skp2 and Flag-cyclin A constructs. Cells were lysed 24 hours after transfection.

5.7 Discussion

5.7.1 Validation of mutations at the Skp2/cyclin A interface

Using the mutants of Skp2 and cyclin A defective in complex formation as judged by *in vitro* experiments (see Chapters 3 and 4) a co-immunoprecipitation was carried out in order to determine whether disruption of these sites are sufficient to disrupt complex formation *in cellulo*. As the constructs which were expressed in cell lines were of the full-length proteins, this validates that other regions of Skp2 (C-terminus) and cyclin A (N-terminus) are not contributing towards the interaction with each other.

Co-immunoprecipitation was used to determine the effectiveness of the cyclin A and Skp2 mutations at disrupting complex formation in HeLa and HEK293T cells. The Skp2/cyclin A interaction appeared to be intact in HeLa cells when the mutants were introduced. Despite further investigations into the potential role of Cks1, which binds to both Skp2 and CDK2 and therefore could allow for complex formation, an explanation for this result has not been found as Cks1 could not be detected in the samples. One explanation is that the Cks1 antibodies used in the immunoprecipitation experiments are not very efficient. One way of overcoming this difficulty with the Cks1 antibody would be to transfect in exogenous tagged Cks1 and probe for the tag. When the co-immunoprecipitation experiment was carried out in HEK293T cells, the Skp2 and cyclin A mutants did show reduced binding to one another and the amount of protein pulled down was consistent with the *in vitro* ITC data. These data are consistent with that of Ji et al. (2006).

The high level of expression in HeLa cells could mean that the concentrations of the interacting partners were so high that they were still able to form an interaction when either binding partner were mutated. In order to control for this, Skp2 6A was cotransfected with cyclin A mut 7 such that the binding sites on either protein would be deficient for binding to each other. This should disrupt the interaction even in the context of overexpression. However, the interaction between Skp2 6A and cyclin A mut 7 appeared to be intact (Figures 5.3 and 5.4). Alternatively, the antibody could bind non-specifically to the overexpressed proteins. A control such as a non-specific isotype control antibody would allow for any non-specific background binding to be detected.

5.7.2 Role of cyclin A in Skp2 recognition and ubiquitination by the APC^{Cdh1} complex

The interaction between Skp2 and Cdh1 was then investigated in HEK293T cells. Gao and co-workers found that Skp2 requires cyclin A for binding to Cdh1 in HEK293T cells (Gao et al., 2009). However, the data presented here show that a Skp2 mutant which is unable to bind cyclin A, can bind to Cdh1. Equal amounts of Skp2 6A and Skp2 WT were pulled down, and similarly cyclin A mut 7 can be pulled down just as effectively as WT cyclin A (Figure 5.11). However, this method is unable to show whether Skp2 and cyclin A bind simultaneously or mutually exclusively to Cdh1.

There is considerable interplay between Cdh1 and cyclin A. Cyclin A contains a D-box motif which interacts with Cdh1 (Geley et al., 2001) and cyclin A has a role in dissociating Cdh1 from the APC/C complex. Cdh1 binds to cyclin A through the RXL motif within the Cdh1 C-terminal domain (Sørensen et al., 2001, Mitra et al., 2006). By mutating the RXL site of Cdh1, its interaction with the APC is stabilised. CDK2/cyclin A is able to phosphorylate Cdh1, and this phosphorylation is inhibitory and may serve to release Cdh1 from the APC/C core (Lukas et al., 1999, Sorensen et al., 2000). Phosphorylation of Cdh1 is an additional mechanism which could lead to the stabilisation of Skp2 by CDK2/cyclin A. Cdh1 is also involved in the ubiquitin-mediated degradation of cyclin A (Sørensen et al., 2001). In summary, there are many mechanisms which could lead to the discrepancy between the results presented here and that of Gao and co-workers, such as the phosphorylation status of Cdh1 and/or Skp2. There are also differences in the way in which this experiment was done compared to the study reported by Gao and co-workers (Gao et al., 2009). Firstly, they used an anti-Flag antibody which would recognise their Flag-Skp2 constructs as the immobilised ‘bait’, whereas here an anti-Cdh1 antibody and endogenous Cdh1 was the immobilised ‘bait’. Secondly, in the published investigation, only Skp2 constructs were transfected whereas here Skp2 and cyclin A constructs were co-transfected such that both proteins would be overexpressed.

It is reported in this chapter that the Skp2/cyclin A interaction is not required for binding of Skp2 to Cdh1. There is controversy in the literature over the role of CDK2/cyclin A in the recognition of Skp2 by the APC^{Cdh1} complex. It was reported that Ser64 phosphorylation by CDK2/cyclin A stabilises Skp2 suggesting that

phosphorylation can protect Skp2 from degradation via the APC^{Cdh1} complex. Others have reported, however, that phosphorylation of Ser64 might not block the direct Skp2/Cdh1 interaction as incubation of Skp2 with Pim1 which phosphorylates Skp2 on Ser64, Ser72 and Ser417 did not disrupt the Skp2/Cdh1 interaction (Cen et al., 2010).

There may be many routes of indirect CDK2/cyclin A stabilisation of Skp2. For example through CDK2/cyclin A activity on Akt. Akt phosphorylation, but not Akt abundance, fluctuates throughout the cell cycle. A recent report from the Pandolfi and Wei groups (Liu et al., 2014) found that Akt phosphorylation mirrors the expression pattern of cyclin A. Decreased CDK2/cyclin A, but not cyclin E, results in decreased Akt phosphorylation and Akt1 was identified as a CDK2/cyclin A substrate. Phosphorylation of Akt by CDK2/cyclin A is mediated through the RXL motifs of Akt. Phosphorylation of Akt by CDK2/cyclin A at Ser477 and Thr479 leads to increased Ser72 phosphorylation of Skp2, Skp2 stabilisation and increased proliferation. They further showed that Akt phosphorylation at Ser477 and Thr479 triggers Ser473 and Thr308 phosphorylation by mTORC2 and PDK1, respectively, leading to full activation of Akt, and therefore increased phosphorylation of Ser72 of Skp2 (Liu et al., 2014). Therefore it is possible that an increased CDK2/cyclin A activity would lead to increased stabilisation through Akt rather than directly through Ser64 phosphorylation. Another route to Skp2 stabilisation by CDK2/cyclin A is through CDK2/cyclin A phosphorylation of Cdh1 at Ser36, Ser40 and Thr121 which promotes β-TrCP-mediated ubiquitination and subsequent degradation of Cdh1 (Fukushima et al., 2013).

5.7.3 Final comments

Due to time constraints, the effects on ubiquitination of p27 when Skp2 and cyclin A are replaced with binding interface mutants were not investigated. Ji and co-workers tested whether their Skp2 4A mutant retained its ability to ubiquitinate p27 (Ji et al., 2006). They found that p27 ubiquitination was unaffected by the introduction of these mutations. Their assay involved the use of proteins purified from HEK293T cell lysates and an *in vitro* ubiquitination assay. Other investigations which would be useful for identifying the functional significance of the Skp2/cyclin A interaction are discussed in Chapter 6.

Validation in HEK293T cells of the mutations that block the Skp2 and cyclin A interaction is a starting point from which to investigate the functional significance of this interaction.

Chapter 6: Concluding remarks and future directions

6.1 The Skp2/cyclin A interaction

Mutation of cyclin A residues 244 to 247 is sufficient to block the Skp2/cyclin A interaction. The mutations do not cause structural rearrangements as determined by X-ray crystallography and circular dichroism; do not destabilise the CDK2/cyclin A complex as shown by thermal stability analysis; do not affect CDK2/cyclin A kinase activity; and do not disrupt its interaction with CDK2 or p27. Taken together, these results show that this is a novel interaction site on cyclin A. This result is also in agreement with the finding that Skp2 does not bind to the RXL recruitment site of cyclin A (Ji et al., 2006).

This work has built on the findings of Ji and colleagues, who identified four residues of Skp2 which contribute to the interaction with cyclin A (Ji et al., 2006) with two additional tryptophan residues of Skp2 being shown to contribute to the interaction of Skp2 with cyclin A (Chapter 4). Mutating all six residues leads to nearly complete loss of binding. Monomeric CDK2 was shown not to bind to Skp2, showing that although the physiological complex incorporates CDK2, cyclin A alone interacts with Skp2.

The Skp2 and cyclin A mutations have been created in Skp2 and cyclin A constructs in mammalian vectors (Chapter 5), and therefore, this interaction is primed to be interrogated *in cellulo*. Analysis will include characterising the effects of the mutations on cellular localisation of Skp2, cell cycle and p27 ubiquitination. Ji and co-workers characterised the effect of Skp2 4A overexpression in U2OS cells and found that this caused a higher proportion of cells to accumulate in G1 phase. The authors also reported an unexpected finding that there was no change in p27 ubiquitination and degradation upon Skp2 4A overexpression (Ji et al., 2006). Future work will aim to confirm this observation in a wider range of cell lines and to extend it to characterise the functions of Skp2 6A.

Cyclin A acts as a substrate recruiter for CDK2. It is required for CDK2 activation and certain substrates are selected by cyclin A through binding to the RXL recruitment site, however, Skp2 is not recruited to CDK2/cyclin A through the RXL site. It has

been shown that Skp2 does not need to bind cyclin A in order to be phosphorylated on Ser64 by CDK2/cyclin A, through use of the Skp2 4A mutant (Ji et al., 2006). This finding could be confirmed using cyclin A mut 7 in a kinase assay against Skp2. A kinase assay could also be employed to determine whether Skp2 might have a regulatory role when it binds to CDK2/cyclin A. For example, Skp2 might affect the phosphorylation of other substrates of CDK2/cyclin A.

Cyclin A is closely related to cyclin E and both are involved in the activation of CDK2, however Skp2 cannot bind to cyclin E (Ji et al., 2006). There is disagreement in the literature as to whether CDK2/cyclin E and CDK2/cyclin A are equivalent in their ability to stimulate p27 ubiquitination. Zhu and co-workers have found that CDK2/cyclin A stimulates the ubiquitination of p27 to a greater extent than CDK2/cyclin E when p27 is already phosphorylated (Zhu et al., 2004). Whereas, Montagnoli and co-workers found that there is no difference in the ability of CDK2/cyclin A and CDK2/cyclin E to stimulate the ubiquitination of unphosphorylated p27 (Montagnoli et al., 1999). This experiment measured both the ability of CKD2/cyclin A to phosphorylate p27 and stimulate its ubiquitination, which may be the cause of the discrepancy in the findings. Phosphorylation of p27 at Thr187 is often attributed to CDK2/cyclin E rather than CDK2/cyclin A, due to this event primarily occurring in G1 phase. A further understanding of the roles of CDK2/cyclin E and CDK2/cyclin A in the ubiquitination of p27 would be aided by knowing whether cyclin A binds to the Skp2 N-terminus in order to facilitate ubiquitination of p27 or whether there is an alternative role of the Skp2/cyclin A interaction. Therefore, the cyclin A and Skp2 mutants described in this thesis could be used to further investigate the role of cyclin A in p27 ubiquitination.

6.1.1 The functional significance of the Skp2/cyclin A interaction

The Skp2 and cyclin A mutants described in this thesis are reagents which can be used to probe the functional significance of the Skp2/cyclin A interaction in cells. Some studies have hypothesised that cyclin A has a role in p27 ubiquitination within the SCF^{Skp2} complex through its interaction with Skp2 (Sitry et al., 2002, Zhu et al., 2004, Montagnoli et al., 1999);, which is consistent with CDK2/cyclin A, and not CDK2/cyclin E, having a kinase-independent role in p27 ubiquitination. whereas others have suggested that the Skp2/cyclin A interaction is not required for the ubiquitination of p27. Instead it has been proposed that this interaction is required for proper cell cycle progression, and that attenuation of this interaction leads to

dysregulation of the cell cycle and apoptosis in Rb-deficient cells (Ji et al., 2006, Ji et al., 2007, Lu et al., 2014). The role of the CDK2/cyclin A complex in the ubiquitination of p27 could be deciphered using the cyclin A and Skp2 mutants described in our investigation. The mutants could additionally be used to determine whether attenuation of the Skp2/cyclin A interaction causes a G1 block or leads to apoptosis. As the cellular distribution of Skp2 is regulated by its N-terminus, it would also be possible to see whether cyclin A binding might affect the subcellular distribution of Skp2 in the cell.

6.2 Is Skp2 and p27 mutually exclusive binding to CDK2/cyclin A functional?

p27 is able to bind to cyclin A mut 7 and the mutations do not have an effect on the kinase activity of the CDK2/cyclin A complex (Chapter 3, Sections 7.3 and 7.4). Ji and co-workers reported that Skp2 is able to protect CDK2/cyclin A from p27-mediated inhibition (Ji et al., 2006). However, p27 was found to bind more tightly than Skp2 to CDK2/cyclin A (Chapter 3, Sections 6 and 7.3). Taken together, these results suggest that only when Skp2 is in large excess can the inhibition of CDK2/cyclin A by p27 be disrupted by Skp2.

p27 is phosphorylated by oncogenic tyrosine kinases on Tyr74 and Tyr88, such as cSrc, prior to Thr187 phosphorylation by CDK2/cyclin A (Grimmler et al., 2007). Tyrosine phosphorylation of p27 weakens the binding of p27 to CDK2/cyclin A, and leads to its partial activation. Skp2 and p27 compete for binding to cyclin A, and this investigation has found that p27 binds about 10 times stronger than Skp2 (compare Figures 3.13 and 3.25 and see Appendix A, Section A2 for replicates of this experiment). Furthermore, the binding of p27 might be measured at a stronger binding affinity with optimisation, as the K_d has previously been reported at 3.5 nM (Lacy et al., 2004). Both Tyr74 and Tyr88 are in the region of p27 which contacts CDK2, with Tyr88 occupying the ATP-binding pocket. p27 would be expected to bind to the SCF^{Skp2} complex when phosphorylated at Tyr74, Tyr88 and Thr187 as the interaction of p27 with cSrc occurs predominantly during G1 phase (Chu et al., 2007). Tyr88 phosphorylation is also expected to precede phosphorylation of p27 at Thr187 and p27 ubiquitination as mutation of Tyr88 of p27 to phenylalanine leads to stabilisation of p27 in mouse embryonic fibroblasts (MEFs) (Grimmler et al., 2007). It might be

possible, therefore, that Skp2 can compete p27 off the CDK2/cyclin A complex after p27 is phosphorylated at Tyr74 and Tyr88 and recruited to the SCF^{Skp2} complex. One way of testing whether Skp2 can compete off Tyr74 and Tyr88 phosphorylated p27 would be through creation of a phosphomimetic mutant and assessing whether this mutant binds to CDK2/cyclin A less tightly than WT Skp2. If p27 binding to CDK2/cyclin A were reduced to the point it was weaker than Skp2, this would suggest that when p27 is recruited to the SCF^{Skp2} complex, there is a handover of CDK2/cyclin A. Competition binding assays such as pull-down assays or biophysical methods, such as ITC, could be employed in order to determine whether Skp2 is able to compete off Tyr74 and Tyr88-phosphorylated p27.

6.3 Role of Ser72 phosphorylation in Skp2 regulation and cyclin A binding

Studies over the past seven years have increasingly pointed towards the importance of the phosphorylation and acetylation state of Skp2 within and around the NLS (PRKRLKS, residues 66-72, Figure 6.1) being important for its activity and regulation (Gao et al., 2009, Inuzuka et al., 2012, Rodier et al., 2008, Lin et al., 2009). These models would suggest that Skp2 activity may be attenuated by inhibition of the kinases responsible. A number of Akt substrates interact with 14-3-3 proteins after Akt-mediated phosphorylation, which in turn results in a change in phosphoprotein localisation (Brunet et al., 2002, Fujita et al., 2003, Sekimoto et al., 2004). Skp2 interacts with 14-3-3β and Akt phosphorylation of Skp2 significantly enhances this interaction (Lin et al., 2009, Gao et al., 2009). Gao and colleagues found that suppression of Akt led to increased levels of p27, but observed that this resulted from reduction in Skp2 Ser72 phosphorylation which would otherwise stabilise Skp2 through reducing its binding to Cdh1 (Gao et al., 2009). Lin and co-workers reported that Ser72 phosphorylation promoted SCF^{Skp2} complex formation and enhanced the ubiquitination of p27 (Lin et al., 2009). The result from Lin and colleagues is surprising as it has been shown that the Skp2 N-terminus is dispensable for SCF^{Skp2} complex formation as assessed by SEC (Hao et al., 2005). Furthermore, they found that suppression of the Akt pathway led to impaired SCF^{Skp2} complex formation and although Skp2 WT and Skp2 S72D readily complex with endogenous Skp1 and Cul1, the binding of Skp2 S72A was found to be significantly impaired. Inhibition of PI3K by

LY294002 also prevented SCF^{Skp2} formation. In contrast to Akt inhibition, however, PI3K inhibition also prevented Skp1 binding to Cul1 suggesting that this is a broad effect on Cul1-containing SCF complexes (Lin et al., 2009).

Determining whether these phosphorylation events affect the interaction of Skp2 with Cdh1 or affect the stability of Skp2 through another mechanism could be relevant to identifying alternative routes of inhibition of Skp2. For example, upregulation of Akt results in stabilisation of Skp2 and increased degradation of p27 (Gao et al., 2009), and therefore Akt inhibitors might be indicated for tumours with increased levels of Skp2.

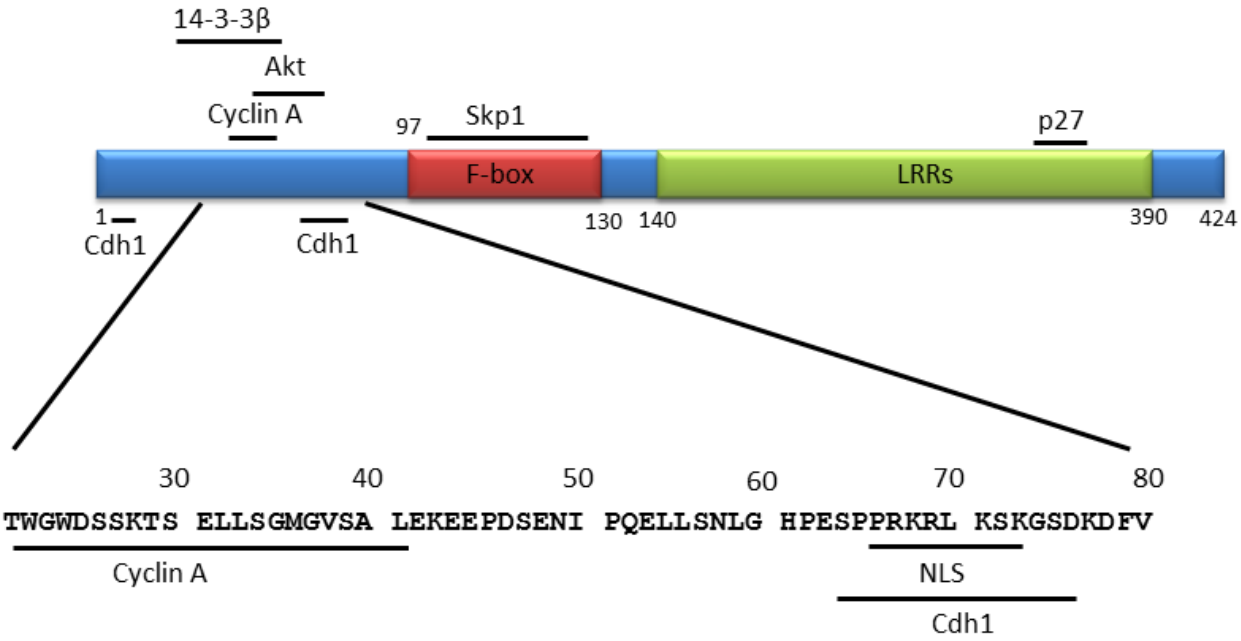

Figure 6.1: Schematic representation of Skp2. The F-box and LRRs are required for the ubiquitin ligase function of Skp2. Skp2 is regulated through its N-terminal domain which contains many sites subject to post-translational modification or involved in interactions with other regulatory proteins of which a subset are indicated. Adapted from Ecker and Hengst (2009).

The question of the role of Ser72 phosphorylation in the regulation of SCF^{Skp2} activity is discussed by Ecker and Hengst (2009) and they proposed that Ser72 phosphorylation might induce a structural rearrangement which permits SCF assembly. On the other hand, Rodier and colleagues have shown that mutation of Ser64 and Ser72 to alanines did not affect SCF complex assembly or activity. They showed that unphosphorylated Skp2 was able to bind to cyclin A with a K_d in the range of a few hundreds of nM. If Ser72 phosphorylation were required for complex

assembly, it would therefore not be expected to act by mediating the binding of cyclin A. This prediction could be confirmed through the use of a phosphomimetic Skp2 mutant (for example, the S72D mutation), in order to determine whether cyclin A binding is altered or whether p27 ubiquitination is affected.

There are additional suboptimal Akt consensus phosphorylation sites in Skp2, including Thr21 (Gao et al., 2009, Lin et al., 2009), the phosphorylation of which could affect SCF^{Skp2} complex formation through effects on cyclin A binding (Figure 6.1). In the study by Lin and colleagues, Akt was overexpressed and the effect on SCF formation were determined through pull-down experiments (Lin et al., 2009). Therefore, in this study, Thr21 could have been phosphorylated as well as Ser72. Lin and co-workers then investigated whether Thr21 is phosphorylated by Akt, and determined that a Skp2 T21A mutation lead to reduced phosphorylation of Skp2 upon incubation with Akt. The Skp2 T21A mutant is somewhat deficient in its formation of a complex with SCF in an *in vitro* assay. The tryptophan residues of Skp2 at positions 22 and 24 were identified in this investigation as important for its interaction with cyclin A, and therefore phosphorylation of Thr21 by Akt could conceivably affect cyclin A binding.

6.4 The Skp2/Cdh1 interaction

As well as investigating how the phosphorylation status of Skp2 affects its stability and ability to bind Cdh1, Gao and co-workers found that the Skp2 4A mutant is unable to pull down Cdh1 suggesting that Skp2 is presented to the APC^{Cdh1} complex in association with cyclin A (Gao et al., 2009). In contrast, this investigation has found that Skp2 mutants, that are unable to bind cyclin A, can bind Cdh1 and the ability of Skp2 to bind Cdh1 was not compromised by mutations in either Skp2 or cyclin A (Figure 5.11). WT and Skp2-binding deficient cyclin A were also pulled down by Cdh1 indicating that cyclin A binds to both Cdh1 and Skp2, and that cyclin A might compete with Skp2 for binding to Cdh1. It is unclear whether phosphorylation of Skp2 directly or indirectly protects Skp2 from binding to Cdh1. Further investigation is warranted to determine whether Skp2 is required to be unphosphorylated or part of a specific complex in order to be ubiquitinated by the APC^{Cdh1} complex. Test expressions of recombinant human Cdh1 in *E. coli* generated very low to negligible levels of proteins (Appendix B). Yeast Cdh1 is routinely expressed by other labs, using an insect cell

expression system (He et al., 2013, da Fonseca et al., 2011). Therefore, human Cdh1 might also be amenable to recombinant expression in insect cells for future experiments.

6.5 The role of Spy1 in the ubiquitination of p27

Spy1 is a cell cycle regulator involved in activating CDKs (Porter et al., 2002). It associates with p27 and inhibits p27-induced cell cycle arrest (Porter et al., 2003). Spy1 has been found to be involved in tumourigenesis of breast cancer (Al Sorkhy et al., 2012), it is a critical factor in the stem-like properties of neuroblastoma (Lubanska and Porter, 2014) and has a role in the development of hepatocellular carcinoma (HCC, (Ke et al., 2009)). It was found that Spy1 can phosphorylate p27 on Thr187 when in complex with CDK2 and it can also promote p27 ubiquitination and increased degradation (McAndrew et al., 2007). Spy1 is not closely related to the cyclins, however it is most similar to cyclin A2. This together with its role in degradation of p27 opens up the possibility that Spy1 might be able to bind Skp2 and perhaps aid the ubiquitination of p27 in a non-catalytic fashion as observed with CDK2/cyclin A (Zhu et al., 2004). One way of testing this hypothesis would be to phosphorylate p27 or use a phosphomimetic mutant and then assess whether a kinase dead CDK2/Spy1 complex might be able to enhance the ubiquitination of p27.

6.6 Structural studies of Skp2

The structure of all but the N-terminal 97 residues of Skp2 has been characterised. The flexibility of the Skp2 N-terminus means it is not amenable to crystallisation, at least in the absence of other proteins that might order the sequence. Identifying the region of Skp2 which is involved in the interaction with cyclin A has led to attempts to crystallise a Skp2 N-terminal peptide with CDK2/cyclin A. The finding that the first 20 residues of Skp2 are not required for binding to cyclin A also prompted attempts to crystallise a truncated Skp2 (20-140) with CDK2/cyclin A. Despite more detailed knowledge of the cyclin A binding site, the Skp2 N-terminus has hitherto remained refractory to crystallisation. Alternative CDK2/cyclin A crystallisation conditions have been identified but did not yield a ternary CDK2/cyclin A/Skp2 peptide structure. Deletion of the residues between the cyclin A binding site and the F-box of Skp2 might help to generate a less flexible structure. SAXS data was collected for the

CDK2/cyclin A/Skp1/Skp2-N complex, but further analysis is required to reconcile it with the crystal structures of its constituent sub-complexes.

With the increased interest in the N-terminal regulatory region of Skp2 and its interaction with Cdh1 shown by literature publications (see Appendix B), it would also be of interest to crystallise a peptide of Skp2 with Cdh1. Recently, yeast Cdh1 has been co-crystallised with an Acm1 peptide which inhibits Cdh1 activity (He et al., 2013). The structure revealed the mechanism of binding between Cdh1 and a D-box motif. Only the WD40 domain of yeast Cdh1 was used and this should be sufficient for binding to Skp2.

6.7 Final conclusions

This investigation has set out to characterise protein-protein interactions of Skp2 which could be targeted for drug design. The Skp2/cyclin A interaction was interrogated using mutagenesis and *in vitro* biophysical assays. The binding sites on either protein were identified in an *in vitro* system and futher tested *in cellulo*. The Skp2 and cyclin A mutants created are useful reagents to probe this interaction further. Investigating the phenotypic effect of the mutations to Skp2 and cyclin A *in cellulo* will provide insights into functional mechanisms of Skp2 and what effect would be achieved by inhibition of the Skp2/cyclin A interaction. The cyclin A-binding site on Skp2 has guided crystallisation experiments, and despite the lack of success in crystallisation of CDK2/cyclin A with Skp2 to date, knowledge has been gained as to what might be successful in future crystallisation trials.

Appendix A

Table A1.1: Recipes for common lab reagents

Modified HEPES-buffered saline (mHBS)	40 mL 1 M HEPES stock 20 mL 5 M NaCl stock Make solution up to just less than 1 L and adjust pH with 5 M NaOH to pH 7.0 1 mL of 1 M DTT stock
10 x Tris-glycine running buffer (for Biorad gels used for Western blotting) Buffer was made up to 1 x with dH_2O	144 g Glycine 30 g Tris base 10 g SDS Make solution up to 1 L
Tris-Glycine transfer buffer	40 mL Novex transfer buffer solution (Life Technologies) 40 ml methanol Make up to 1 L ddH_2O
Tris-buffered saline with Tween 20 (TBST)	6.06 g Tris base 30 mL 5 M NaCl stock 500 µL Tween 20 Make up to just less than 1 L and adjust pH with concentrated HCl to pH 7.6
1% (w/v) agarose gels	0.5 g agarose (Ultrapure from Invitrogen) Make up to 50 mL in 1 x TAE (Invitrogen) Microwave for 1 ¾ minutes Add 5 µL of SYBR safe (Life Technologies) once cooled and pour gel

SDS running buffer (TEO-Tricine-SDS) for running Expedeon gels was purchased from Expedeon.

Table A1.2: Oligonucleotide primer sequences for mutagenesis of cyclin A, Skp2 and CDK2, respectively

Primer name	strand	template plasmid	Primer sequence 5' to 3'	%GC content	length (N)	% mismatch	Tm (°C)
Mut9	forward	WT cyclin A	ACC AAG AAA CAA GTT CTG ACA ATG GAG CAT CTA GTT TTG	38	39	2.6	77.2
Mut 9	reverse	WT cyclin A	CAA AAC TAG ATG CTC CAT TGT CAG AAC TTG TTT CTT GGT	38	39	2.6	77.2
Mut10	forward	WT cyclin A	GAG CAT CTA GTT TTG AAA GTC CTT AAG TTT AGG TTA GCT GCT CCA ACA GTA AAT CAG	39	57	8.8	76.8
Mut10	reverse	WT cyclin A	CTG ATT TAC TGT TGG AGC AGC TAA CCT AAA CTT AAG GAC TTT CAA AAC TAG ATG CTC	39	57	8.8	76.8
Mut5	forward	WT cyclin A	GAT AGG TTC CTG TCT TCC CAG GAA AAT GTG CTG AGA GGA AAA CTT CAG	46	45	8.9	76.5
Mut5	reverse	WT cyclin A	CTG AAG TTT TCC TCT CAG CAC ATT TTC CTG GGA AGA CAG GAA CCT ATC	46	45	8.9	76.5
Mut 101	forward	WT cyclin A	CAGATGATACCTACA GCGGGGACCAAGTT CTGAGAATGG	51	39	12.8	68.7
Mut 101	reverse	WT cyclin A	CCATTCTCAGAACTT GGTCCCCGCTGTAG GTATCATCTG	51	39	12.8	68.7
Mut102	forward	Mut 101	GTACATTACAGATGG TGCCTGCAGCGGGG ACCAAGTTCTGAG	55	42	7.1	71.3
Mut102	reverse	Mut 101	CTCAGAACTTGGTCC CCGCTGCAGGCACC ATCTGTAATGTAC	55	42	7.1	71.3
Mut103	forward	Mut 104	GTTCTGACAATGGAG CTTATGATTATGAAA GTCCTTACTTTTGAC	36	45	11.1	64.5
Mut103	reverse	Mut 104	GTCAAAAGTAAGGAC TTTCATAATCATAAG CTCCATTGTCAGAAC	36	45	11.1	64.5
Mut104	forward	Mut 9	GATACCTACACCAAG AAAGAAATTCTGACA ATGGAGCTTATG	38	42	4.8	64.5

Appendix A

Primer name	strand	template plasmid	Primer sequence 5' to 3'	%GC content	length (N)	% mismatch	Tm (°C)
Mut104	reverse	Mut 9	CATAAGCTCCATTGTCAGAATTTCTTTCTTGGTGTAGGTATC	38	42	4.8	64.5
Mut105	forward	Mut 10	GAATGGAGCATCTAGTTATGAAAGCCCTTAAGTTTAGGTTAGCTG	40	45	4.4	66.4
Mut105	reverse	Mut 10	CAGCTAACCTAAACTTAAGGGCTTTCATAACTAGATGCTCCATTC	40	45	4.4	66.4
Mut106	forward	Mut 105	CTAGTTATGAAAGCCCTTAAGTGGAGGTTAGCTGCTCCAAC	46	41	9.8	67.5
Mut106	reverse	Mut 105	GTTGGAGCAGCTAACCTCCACTTAAGGGCTTTCATAACTAG	46	41	9.8	67.5
Mut107	forward	Mut 5	CATTGATAGGTTCCTGGCTACCCAGGAAAATGTGCTGAGG	50	40	5	68.6
Mut107	reverse	Mut 5	CCTCAGCACATTTTCCTGGGTAGCCAGGAACCTATCAATG	50	40	5	68.6

Primer name	strand	template plasmid	Primer sequence 5' to 3'	%GC content	length (N)	% mismatch	Tm (°C)
Skp2 AA1	forward	Skp2 WT	TCC AGC AAG ACT TCT GAA GCG GCG TCA GGC ATG GGC GTC TCC	62.0	42	9.5	81
Skp2 AA1	reverse	Skp2 WT	GGA GAC GCC CAT GCC TGA CGC CGC TTC AGA AGT CTT GCT GGA	62.0	42	9.5	81
Skp2 AA2	forward	Skp2AA1	GTC AGG CAT GGG CGT CGC CGC CGC GGA GAA AGA GGA GCC	72	39	10.3	83
Skp2 AA2	reverse	Skp2AA1	GGC TCC TCT TTC TCC GCG GCG GCG ACG CCC ATG CCT GAC	72	39	10.3	83
Skp2 F20	forward	Skp2 WT	GGAGTTCTGTTCCAGGGCCCCTTCACGTGGGGATGGGATTCCAG	61	44	N/A	90.4

Appendix A

Primer name	strand	template plasmid	Primer sequence 5' to 3'	%GC content	length (N)	% mismatch	Tm (°C)
Skp2 F20	reverse	Skp2 WT	CTGGAATCCCATCCCCACGTGAAGGGCCCCTGGAACAGAACTCC	61	44	N/A	90.4
Skp2 S30	forward	Skp2 WT	GGAGTTCTGTTCCAGGGGCCCTCTGAACTGCTGTCAGGCATGGG	61	44		90.4
Skp2 S30	reverse	Skp2 WT	CCCATGCCTGACAGCAGTTCAGAGGGCCCCTGGAACAGAACTCC	61	44		90.4
Skp2 W22AW24A	forward	Skp2 WT and Skp2AA2	CACCAGCTTCACGGCGGGAGCGGATTCCAGCAAG	65	34	11.7	76.6
Skp2 W22AW24A	reverse	Skp2 WT and Skp2AA2	CTTGCTGGAATCCGCTCCCGCCGTGAAGCTGGTG	65	34	11.7	76.6
Skp2 D25A K28A	forward	Skp2 WT and Skp2AA2	GTGGGGATGGGCTTCCAGCGCGACTTCTGAACTGC	63	35	8.5	79.5
Skp2 D25A K28A	reverse	Skp2 WT and Skp2AA2	GCAGTTCAGAAGTCGCGCTGGAAGCCCATCCCCAC	63	35	8.5	79.5
Skp2 K68L K71L	forward	Skp2 WT	GAGCCCGCCACGGCTACGGCTGCTGAGCAAAGGGAGTGAC	68	40	20	72.5
Skp2 K68L K71L	reverse	Skp2 WT	GTCACTCCCTTTGCTCAGCAGCCGTAGCCGTGGCGGGCTC	68	40	20	72.5
Skp2 S72E	forward	Skp2 WT	CACGGAAACGGCTGAAGGAGAAAGGGAGTGACAAAGAC	53	38	7.9	77.4
Skp2 S75E	forward	Skp2 WT	CGGCTGAAGAGCAAAGGCGAAGACAAAGACTTTGTGATTGTCC	49	43	9.3	76.6
Skp2 S72E	reverse	Skp2 WT	GTCTTTGTCACTCCCTTTCTCCTTCAGCCGTTTCCGTG	53	38	7.9	77.4
Skp2 S72A S75A	forward	Skp2 WT	GAAACGGCTGAAGGCCAAAGGGGCTGACAAAGACTTTGTG	53	40	10	76.3
Skp2 S72A S75A	reverse	Skp2 WT	CACAAAGTCTTTGTCAGCCCCTTTGGCCTTCAGCCGTTTC	53	40	10	76.3
Skp2 S64A	forward	Skp2 S72A S75A	CTGGGACACCCGGAGGCACCACCACGGAAACGG	70	33	11	78.7

Appendix A

Primer name	strand	template plasmid	Primer sequence 5' to 3'	%GC content	length (N)	% mismatch	Tm (°C)
(phospho-null)							
Skp2 S64A (phospho-null)	reverse	Skp2 S72A S75A	CCGTTTCCGTGGTGGTGCCTCCGGGTGTCCCAG	70	33	11	78.7

Primer name	strand	template plasmid	Primer sequence 5' to 3'	%GC content	length (N)	% mismatch	Tm (°C)
CDK2 L25D	forward	CDK2 WT	GAGTTGTGTACAAAGCCAGAAACAAGGACACGGGAGAGGTG	51	41	7.3	78.6
CDK2 L25D	reverse	CDK2 WT	CACCTCTCCCGTGTCCTTGTTTCTGGCTTTGTACACAACTC	51	41	7.3	78.6

Table A1.3: Oligonucleotide primer sequences for InFusion sub-cloning of Skp2, cyclin A and Cdh1

primer name	strand	cloning site	15 bp overhangs	insert-specific sequence	%GC content	length (N)	Tm (°C)
Cyclin A AE mut	forward	*Bam*HI	AGCAAAT GGGTCGC G	GAGTCCCAGA CTATCACGAA GATATCCACA CC	50	32	62
Cyclin A AE mut	reverse	*Eco*RI	TGTCGAC GGAGCTC G	AATCACAGGT TCAGGGTTTC CGGCGGGTTC AG	56	32	68
Cdh1 FL POPIN	forward	*Kpn*I	AAGTTCTG TTTCAGG	GCCCGCGGAA ACCCACCCGC AAGATCTC	68	28	70
Cdh1 FL POPIN	reverse	*Hind*III	ATGGTCTA GAAAGCT	TTACGAACGG GTTTTGCTAAA GACGTTCCAG	45	31	62
Cdh1 WD40 POPIN	forward	*Kpn*I	AAGTTCTG TTTCAGG	CCCGCGGAAA CCCACCCGCA AGATCTC	67	27	68
Cdh1 WD40 POPIN	reverse	*Hind*III	ATGGTCTA GAAAGCT	TTACGAACGG GTTTTGCTAAA GACGTTCCAG	45	31	62
pcDNA3 myc-Skp2	forward	*Eco*RI	GGAAGAT CTGGAATT	CCCGGGGATC CCCATGGAC	74	19	63
pcDNA3 myc-Skp2	reverse	*Hind*III	CATGCTC GAGAAGC T	TACATTTTATG TTAGCTGGTG GACTGACGC	43	30	60
pcDNA5 flag-cyclin A	forward	*Hind*III	GTTTAAAC TTAAGCT	TGAGGAGATA GAACCATGG	47	19	51
pcDNA5 flag-cyclin A	reverse	*Bam*HI	CTGGACT AGTGGAT C	CTTACTTGTCA TCGTC	44	16	43

Gene sequences were synthesised by IDT, subcloned into IDTsmart vectors, PCR amplified using the above primers, and then inserted into pET21d for cyclin A global mutant, POPIN J/M for Cdh1 constructs, pcDNA3 for Skp2, or pcDNA5 for cyclin A after restriction digestion using the indicated restriction enzymes.

Table A1.4: Summary of constructs used for *in vitro* experiments

Protein	Residue numbers	Vector backbone	Tag
Skp1	1-163 with 'loops out'*	pGEX-6P-1	none
Skp2-N	1-140	pGEX-6P-1	N-terminal GST
Skp2-C	89-424	Not determined	GST
CDK2	1-298	pGEX-6P-1	N-terminal GST
Cyclin A	174-432	pET21d	C-terminal His
Cdh1	1-496 (FL)	POPIN J/ POPIN M	N-terminal GST/ MBP
Cdh1	165-478	POPIN J/ POPIN M	N-terminal GST/ MBP
RbCT	792-928	pGEX-2T	GST

*Skp1 'loops out' is lacking residues 38-43; and 67-81 is replaced with DGGSG (single letter amino acid code) as these loops are susceptible to protease-sensitive (Schulman et al., 2000).

A2: Replicate ITC experiments

The following ITC data are replicates of ITC data not shown in the main body of this thesis.

CDK2/cyclin A (WT) interaction with Skp1/Skp2-N (WT)

The interaction between CDK2/cyclin A and Skp1/Skp2-N has been tested with multiple protein preparations. The replicate experiment shown here between CDK2/cyclin A global mut and mut 7 with Skp1/Skp2-N was carried out using a different protein preparation to that shown in the main body of the thesis. The replicate experiments shown here of CDK2/cyclin A mut 5 with Skp1/Skp2-N and CDK2/cyclin A with Skp1/Skp2-N 6A were carried out with the same protein preparation as that shown in the main body of the thesis.

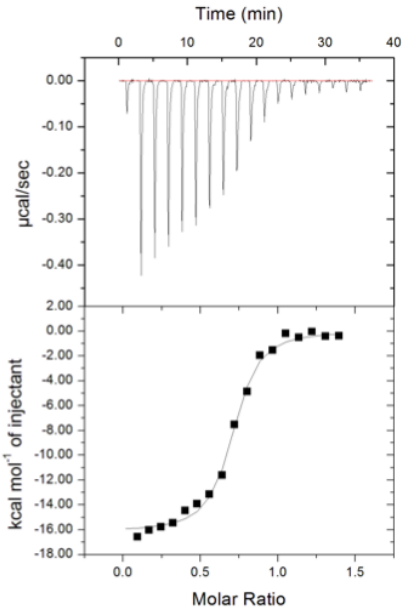

K_d	0.2 ± 1.31 µM
N	0.69
ΔH	-16140 cal/mol
ΔS	-23.5 cal/mol/deg

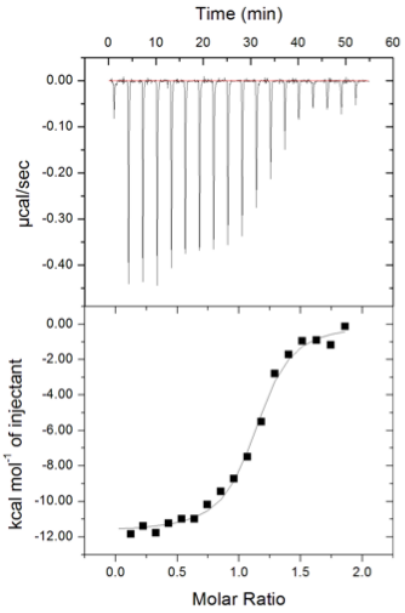

K_d	0.36 ± 2.34 µM
N	1.1
ΔH	-1173 cal/mol
ΔS	-9.84 cal/mol/deg

Appendix A

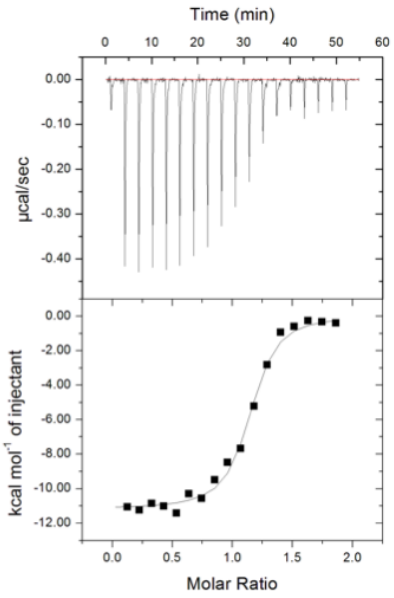

K_d	200 ± 830 nM
N	1.09
ΔH	-11440 cal/mol
ΔS	-7.72 cal/mol/deg

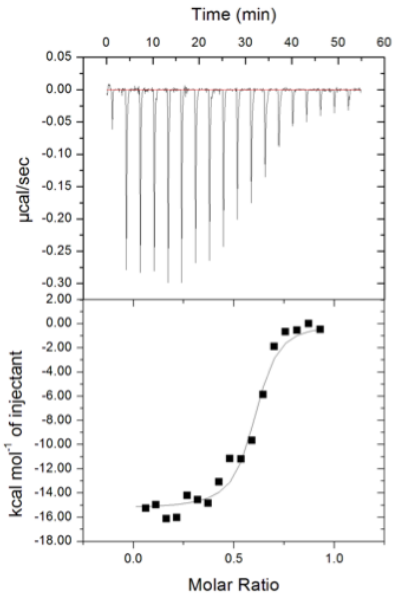

K_d	110 ± 333 nM
N	0.59
ΔH	-15260 cal/mol
ΔS	-19.3 cal/mol/deg

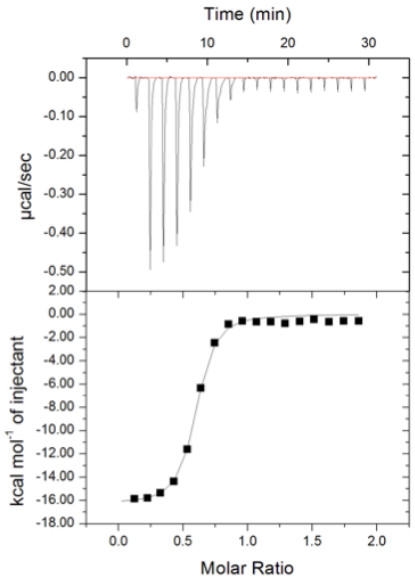

K_d	0.17 ± 1.04 µM
N	0.56
ΔH	-16290 cal/mol
ΔS	-23.7 cal/mol/deg

Appendix A

CDK2/cyclin A global mut interaction with Skp1/Skp2-N

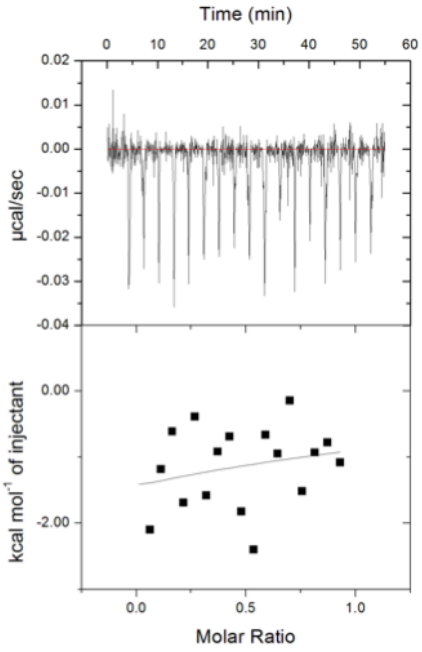

CDK2/cyclin A mut 7 interaction with Skp1/Skp2-N

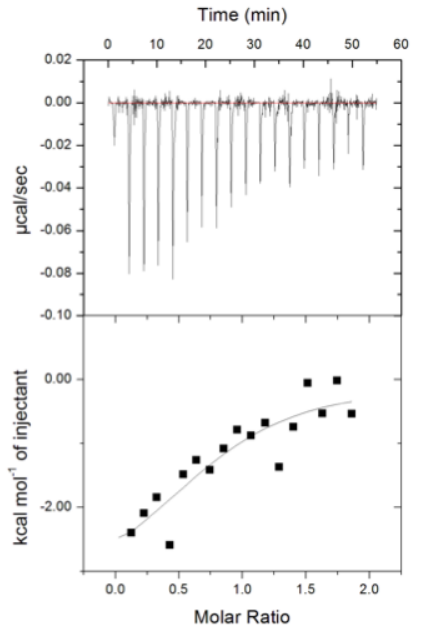

K_d	42.7 ± 35 µM
N	0.15
ΔH	-55610 cal/mol
ΔS	-167 cal/mol/deg

CDK2/cyclin A mut 5 interaction with Skp1/Skp2-N

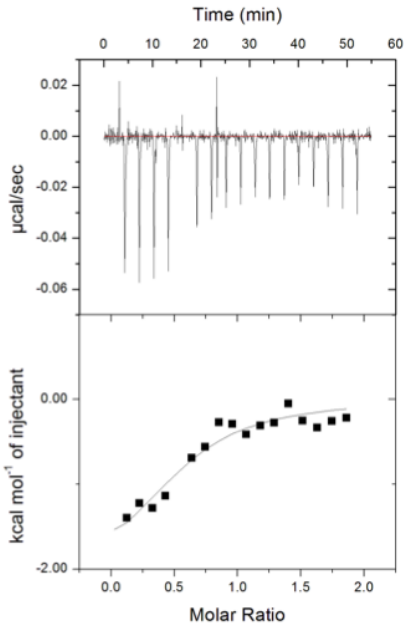

K_d	4.9 ± 9.3 µM
N	0.57
ΔH	-2198 cal/mol
ΔS	16.9 cal/mol/deg

CDK2/cyclin A interaction with Skp1/Skp2-N 6A

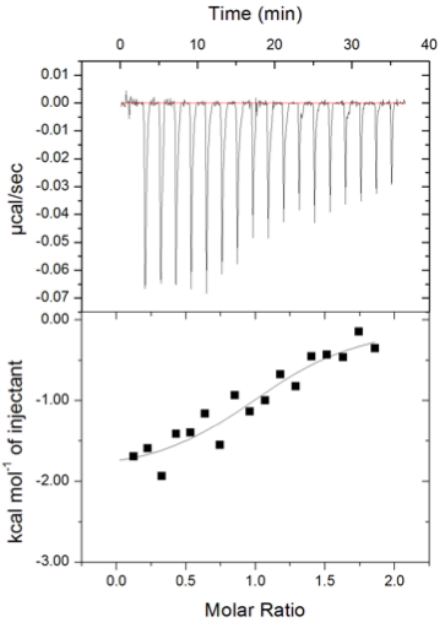

K_d	2.9 ± 5.5 µM
N	1.13
ΔH	-1963 cal/mol
ΔS	18.8 cal/mol/deg

Appendix B

This appendix describes experiments designed to investigate the binding of Skp2 to Cdh1. These experiments are related to those in the main body of the thesis and due to time restraints, were not able to be completed.

B1 Regulation of Skp2 by Cdh1 binding, and post-translational modification of the N-terminus of Skp2

Skp2 is degraded by the APC^{Cdh1} complex in mitosis and early G1. Cdh1 is itself degraded by the $SCF^{\beta TrCP1}$ complex in S and G2 phases of the cell cycle. It was found that CDK2/cyclin A phosphorylates Cdh1, and this promotes its degradation. CDK2/cyclin A is required to phosphorylate Cdh1 to prime it for subsequent phosphorylation by Plk1 (Fukushima et al., 2013). Plk1 plays important roles in mitotic entry and exit, and in cytokinesis (Bahassi, 2011). Cyclin A binds to a conserved RXL motif at the C-terminus of Cdh1. Sorensen et al. (2000) observed that mutation of the RVL motif of Cdh1 stabilises its interaction with the APC/C complex. Interestingly, the Cdh1 RXL to AAA mutant lost its capability to promote ubiquitination of cyclin A suggesting that this motif is required for cyclin A ubiquitination, as well as CDK2/cyclin A-mediated phosphorylation of Cdh1 (Sorensen et al., 2000). Cdh1 can be inactivated by binding of the inhibitory proteins Acm1 (APC^{Cdh1} modulator 1) and Emi1 (early mitotic inhibitor 1), which act as pseudosubstrates binding to Cdh1 through D-box and KEN motifs to block Cdh1 interaction with substrates (Ostapenko et al., 2008, Machida and Dutta, 2007). The structure of Cdh1 in complex with Acm1 was published in 2013 by the Barford group (Chan et al., 2013), and the structure revealed the mechanism of binding of D-box and KEN motifs. Substrates interact with the WD40 β-propeller domain of Cdh1 (Chan et al., 2013). The D-box binds to an inter-blade groove of this domain. Skp2 contains a D-box at the extreme N-terminus, however, a KEN box motif has not been identified within Skp2.

Acetylation of Skp2 by p300 at Lys68 and Lys71 has been shown to promote its nuclear export (Inuzuka et al., 2012). Lys68 and Lys71 are adjacent to the Akt phosphorylation site at Ser72. p300 is an adenoviral E1A-binding protein with a role in histone acetylation and transcriptional co-activation. It is involved in the p53 and

Rb pathways, and may be a factor in the ability of Skp2 to further drive cancer progression of Rb- and p53-deficient tumours (Iyer et al., 2004). Elevated levels of p300 have been reported to be correlated with proliferation, and predict poor outcome in prostate cancer (Debes et al., 2003). p300 was also found to be subject to androgen regulation. Androgen deprivation results in up-regulation of p300. Truncating mutations of p300 (Gayther et al., 2000) and loss of heterozygosity (Iyer et al., 2004) have also been reported in human cancers.

Cdh1 is unable to bind to Skp2 when Skp2 is acetylated at Lys68 and Lys71, further confirming that Cdh1 binds to the Skp2 N-terminus. Mimicking the acetylation through mutagenesis leads to increased oncogenicity through increased cytoplasmic localisation of Skp2 and increased ubiquitination of E-cadherin by Skp2, leading to its degradation. The degraded E-cadherin results in increased migration as determined by *in vitro* wound healing assays (Inuzuka et al., 2012). SIRT3 was identified as a deacetylase capable of removing the acetylation from Skp2 and hence, restores the nuclear localisation of Skp2 (Inuzuka et al., 2012).

Acetylation of Skp2 at Lys68 and Lys71 was reported to cause Skp2 dimerisation. The potential of Skp2 to dimerise upon acetylation was investigated because p300-mediated acetylation has been reported to induce dimerization of other substrates (Tang et al., 2007, Yuan et al., 2005, Inuzuka et al., 2012). Inuzuka and co-workers showed that an acetylation-mimetic mutant of Skp2 was able to pull down other Skp2 molecules and, when chemically crosslinked, a proportion of the acetylated Skp2 runs at twice the expected molecular weight on an immunoblot.

Increased Akt- and p300-mediated modification of Skp2 leads to increased stability of Skp2 and increased oncogenicity. Skp2 could therefore act as a receptor for Akt and p300 activity and through Skp2, Akt and p300 could orchestrate their oncogenic roles. The role of Skp2, and its oncogenic potential appears to be dependent on acetyl- and phosphorylation status, cellular localisation and regulator-bound status.

B1.1 Establishing a method of human Cdh1 purification

In order to investigate the binding of Skp2 to Cdh1 in *in vitro* experiments, a method of expressing and purifying large quantities of Cdh1 must be established. There is an established protocol for recombinant production of yeast Cdh1, however, there are no reports in the literature for human Cdh1. Cdh1 is about 55 kDa, and is predicted to

have an unstructured N-terminal sequence of about 180 residues preceding a 7-bladed β-propeller fold known as a WD40 domain.

A codon optimised human Cdh1 gene sequence was synthesised by IDT. It was sub-cloned into POPIN J and POPIN M vectors from the Oxford Protein Production Facility (OPPF). The advantage of these vectors is that they are compatible with expression in *E. coli*, insect cells and HEK293 cells. POPIN J encodes an N-terminal His tag and GST tag upstream of the protein of interest, and POPIN M encodes an N-terminal His tag and MBP tag.

Cdh1 in both POPIN M and J vectors were transformed into a three *E. coli* strains for test expression. The test expression was done with an undergraduate student, Robert Bloxham. The *E. coli* cells were grown to an OD_{600} of 0.5 and then the temperature was reduced to 18°C and expression was initiated with addition of 100 μM IPTG. Expressing proteins at low temperatures can be favourable for protein folding and stability as it decreases the rate of protein synthesis. Cdh1 was expressed overnight at 18°C as robust expression can often lead to formation of inclusion bodies composed of insoluble aggregates of the expressed protein. The cells were harvested and lysed using BugBuster reagent (Merck Millipore). GST and MBP beads were used to capture any tagged protein which had been expressed. Samples were taken at every stage to track which band corresponded to Cdh1. Unfortunately, it appeared that no Cdh1 was expressed (data not shown).

With the additional GST or MBP tags, the Cdh1 fusion protein is about 80 and 98 kDa in size, respectively. *E. coli* generally does not express large proteins very well, and therefore expression levels might be improved by truncating the protein. Residues 1-164 of Cdh1 were removed in order to obtain a construct similar to the yeast Cdh1 sequence, which has been expressed in insect cells and subsequently crystallised (Figure B1) (Chan et al., 2013).

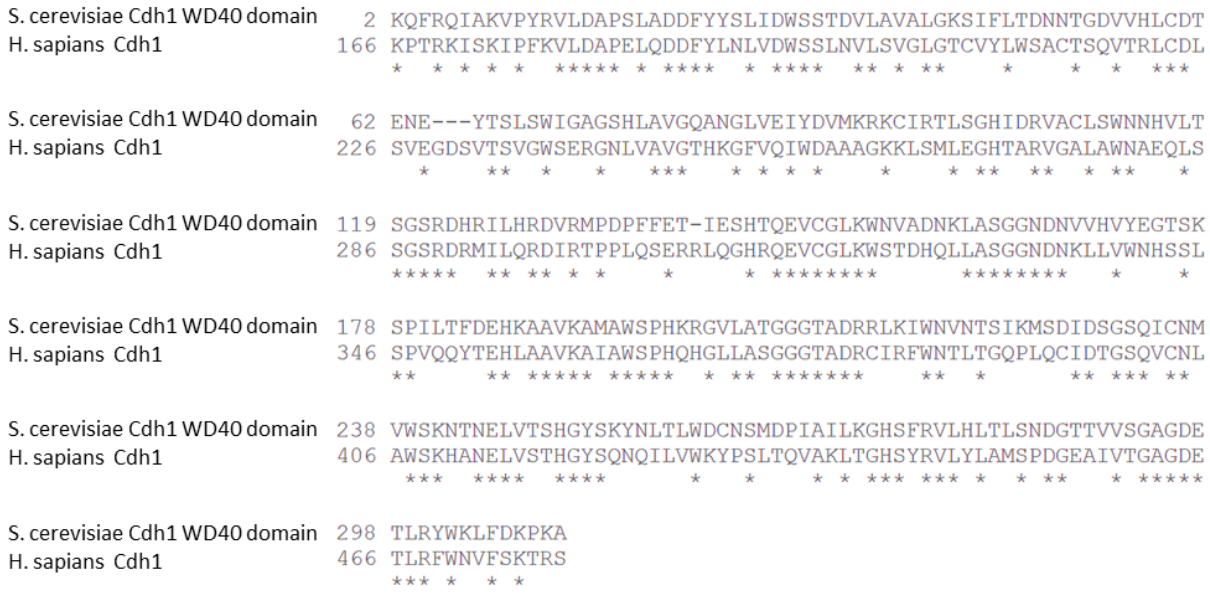

Figure B1: Sequence alignment of the structurally characterised yeast Cdh1 WD40 domain with full-length human Cdh1. The structurally characterised *S. cerevisiae* Cdh1 sequence is from da Fonseca et al. (2011). Uniprot codes P53197 (*S. cerevisiae* Cdh1), Q9UM11 (human Cdh1).

The truncated Cdh1 sequences in the POPIN J vector was transformed into *E. coli* Arctic Express (Agilent) and *E. coli* BL21 Star (DE3) (Life Technologies) strains in order to test expression. *E. coli* Arctic Express cells are optimised for expression of proteins at low temperatures, and co-express cold-adapted chaperonins. *E. coli* BL21 Star (DE3) cells are optimised for high-level expression of proteins. The cells were grown, induced and purified as described for the full-length Cdh1. Results are shown in Figure B2.

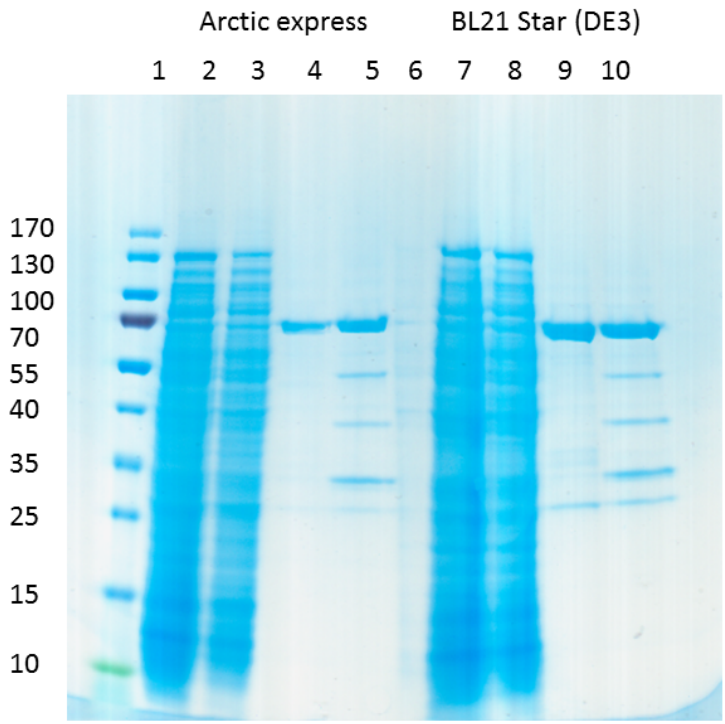

Figure B2: Cdh1 WD40 domain test expression in Arctic Express and BL21 Star (DE3) *E. coli* strains. Lanes 1 and 7 are the WCLs, lanes 2 and 8 are the unbound proteins which have passed through the column, lanes 3 and 9 are the eluates and lanes 4 and 10 are the eluates with 3C protease added. 3C protease is about 46 kDa but runs at about 52 kDa.

The *E. coli* chaperone protein, GroEL, which is involved in helping protein folding is about 60 kDa. GroEL could be the upper band of lanes 4, 5, 9 and 10. GroEL forms an oligomeric complex around proteins, and if a protein is associated with GroEL, there is a 14 to 1 molar ratio of GroEL to protein (Braig et al., 1994). As the GroEL binds to the glutathione-Sepharose beads, this might suggest that there is some Cdh1 being expressed. Extra bands appear after 3C protease is added. The band around 55 kDa is likely to be GST-3C protease. The middle band could be the Cdh1 WD40 domain, which is about 37 kDa in size, or the extra bands could be contaminants from the 3C protease stock solution.

Human Cdh1 might not be amenable to expression in *E. coli*. Insect cells offer the advantage of increasing the likelihood of correct folding and they support post-translational modifications. Test expressions in *E. coli* were not continued with the

aim of continuing work in Sf9 insect cells. However, due to time constraints, this work was not further pursued.

B2 Analysis of the Skp2 N-terminal post-translational modification sites

In order to test the effect of N-terminal post-translational modifications of Skp2 on Cdh1-binding in *in vitro* experiments, a set of mutants were created with residue changes designed to mimic these modifications. The mutagenesis reactions were performed by two summer students, Robert Bloxham and Hannah Fuller. These mutants are shown in Table B1 and primers used in the mutagenesis reactions are shown in Appendix A, Table A1.2.

Skp2 mutants:
S64A S72A S75A
S72E
S75E
K68L K71L

Table B1: Mutants of Skp2 created to test effects of phosphorylation and acetylation on binding of Skp2 to Cdh1.

As recombinant Cdh1 was not available, it was decided to test the hypothesis that acetylation of Skp2 residues 68 and 71 leads to dimerization. On SEC columns, the Skp1/Skp2-N complex runs at an unusually high apparent molecular weight, and at a similar elution volume to the CDK2/cyclin A complex and the GST dimer which are 65 kDa and 52 kDa in size, respectively. As the Skp1/Skp2-N complex is about 33 kDa in size, it is possible that Skp1/Skp2-N exists as a dimer. An acetylation-induced dimerization event might lead to formation of an alternate dimer forming or a dimer of dimers. Analytical gel filtration was initially carried out in order to see if the Skp2 K68L K71L mutant elutes at a different volume than the WT protein.

Skp2 K68L K71L was purified according to the standard Skp2 expression protocol, and the mutations did not seem to affect the stability of the protein. The results of the subsequent SEC experiment were not definitive as Skp1/Skp2 WT and the acetylation mimetic mutant run at similar elution volumes. The small shift to a higher molecular weight observed would not warrant the conclusion that the Skp1/Skp2-N K68L K71L complex dimerises (Figure B3). One cannot exclude, however, the possibility that rather than forming a dimer of dimers, an alternate dimer has been formed. This result

was inconclusive and therefore size-exclusion chromatography-multi-angle laser light scattering (SEC-MALLS) was utilised in order to further determine the oligomeric state, and whether dimerization occurs upon acetylation.

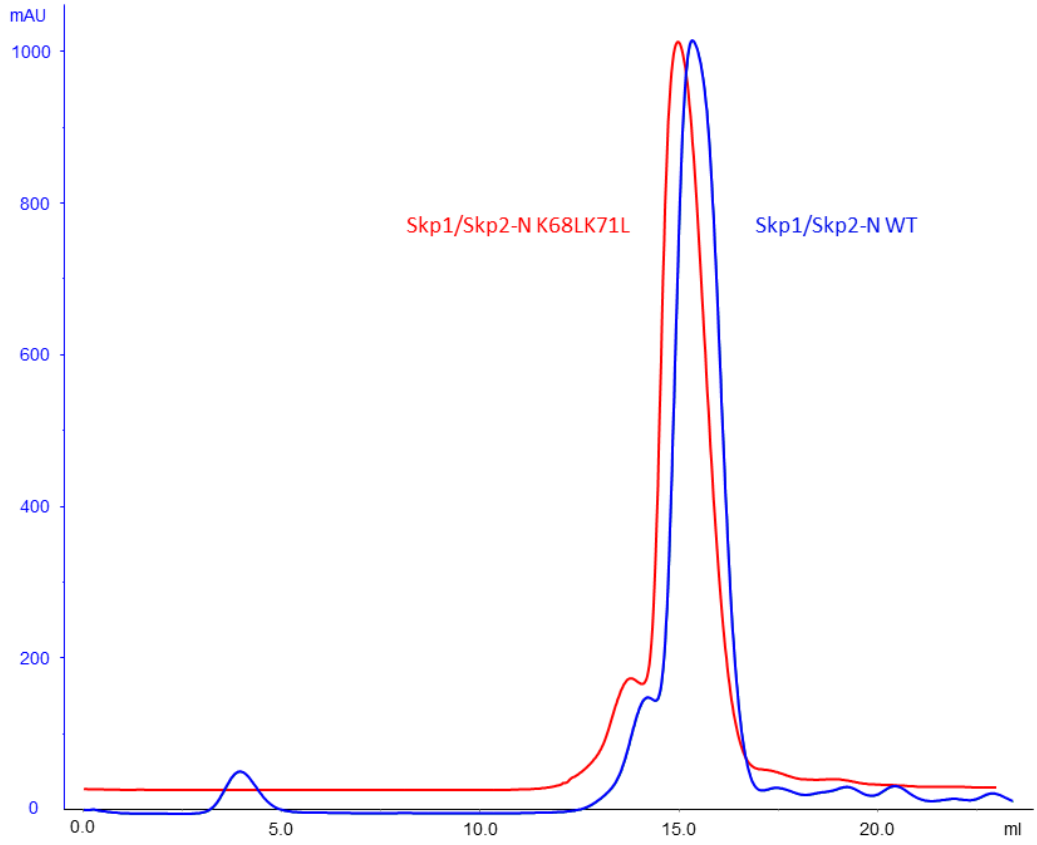

Figure B3: Analytical SEC chromatograms for Skp1/Skp2 WT and Skp1/Skp2-N K68L K71L using a Superdex 200 10/30 column. Protein complexes were fully purified prior to this experiment. The Skp1/Skp2-N WT trace is normalised to the Skp1/Skp2-N K68L K71L trace to account for differences in concentration.

B3 Analysis of the oligomeric state of Skp1/Skp2-N K68L K71L by SEC-MALLS

It was decided to analyse the absolute molecular weights of Skp2 WT and K68L K71L so as to establish whether acetylation does induce dimerisation. SEC-MALLS is a gel filtration-based method of obtaining robust data on the oligomeric states of proteins. This technique is described in Chapter 2 Section 9.

The SEC-MALLS instrument was calibrated with BSA immediately prior to this experiment. The instrument was run at 0.5 mL/minute in mHBS pH 7.0 (Figure B4).

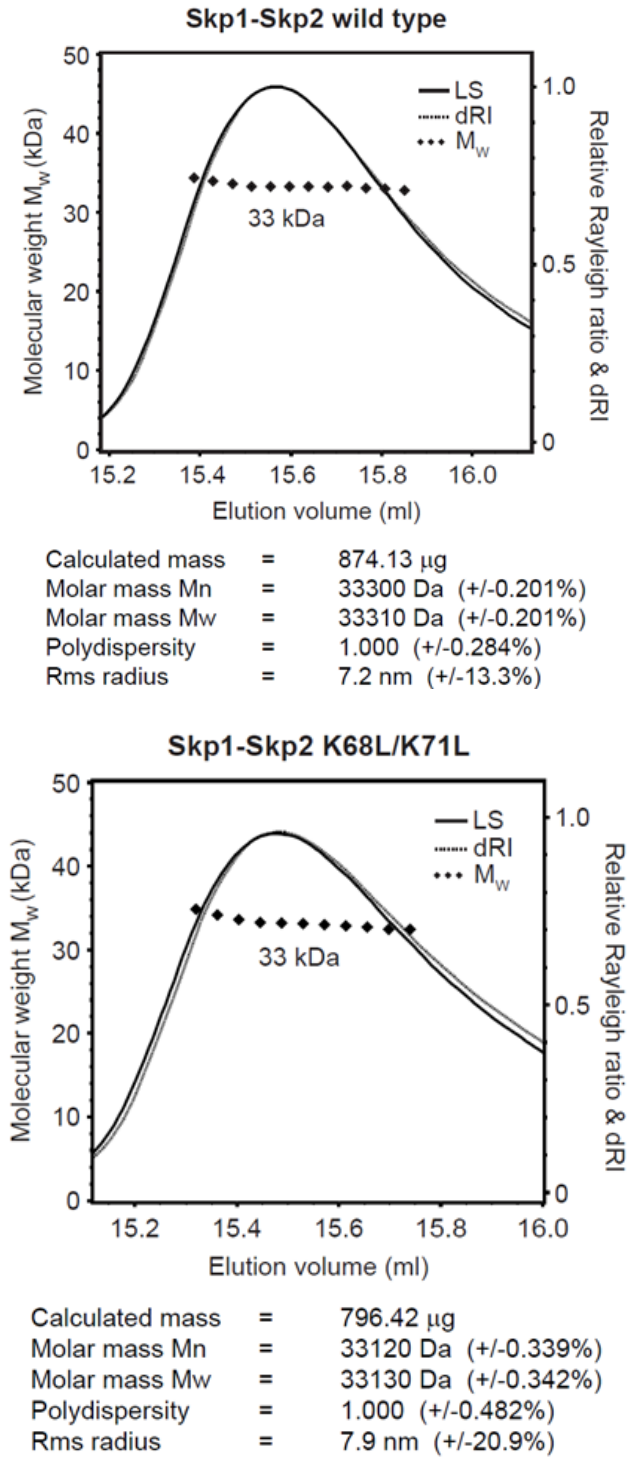

Figure B4: SEC-MALLS data for Skp1/Skp2-N WT and Skp1/Skp2-N K68L K71L. The calculated molecular weight of Skp1/Skp2-N WT is about 32 700 kDa. Experiment was run at room temperature. 1 mL fractions of the eluate were collected.

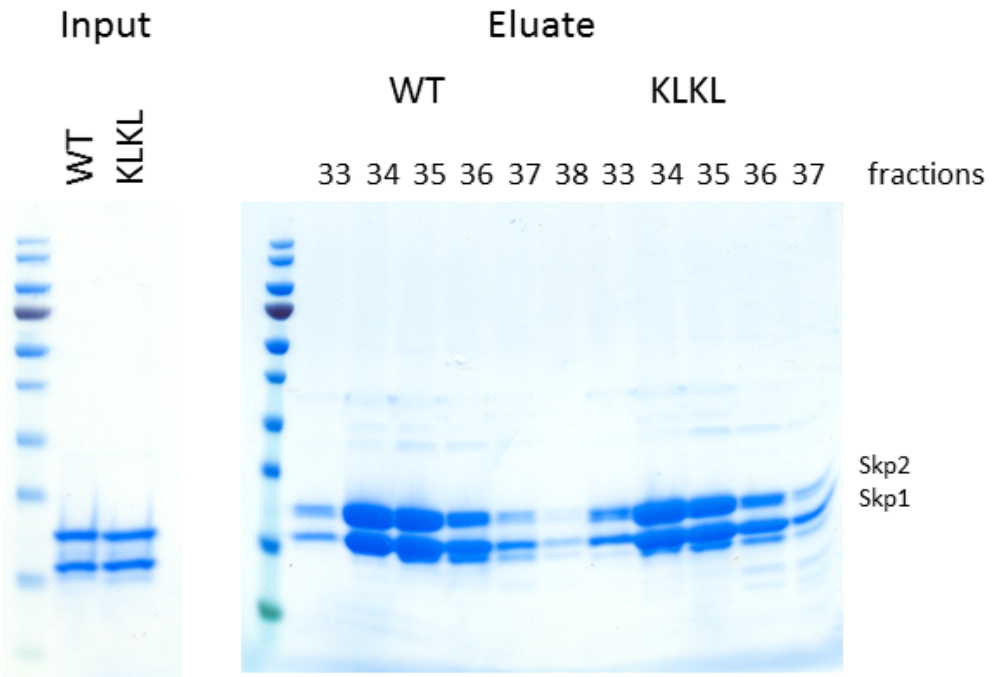

Figure B5: SDS-PAGE analysis of Skp1/Skp2-N input and eluate fractions from the SEC-MALLS experiment. Fractions shown cover the eluted peak.

The SEC-MALLS data show that both the Skp1/Skp2 WT and acetylation mimetic mutant are heterodimers in solution with no tendency to form oligomeric states. The elution profile shown in Figure B3 indicates a small shift to a lower elution volume in the elution profile of the Skp1/Skp2-N K68L K71L complex compared to the WT Skp2 complex. This might result from a change in conformation of N-terminus, with a more elongated protein running at a higher molecular weight than expected. SEC elution profiles are dependent on the shape as well as the size of a protein, suggesting that there might be a structural rearrangement of the Skp2 N-terminal region upon acetylation. SEC-MALLS is not affected by the shape of a protein, and therefore provides an absolute value for the size of a protein, or complex.

The Skp1/Skp2-N complexes showed some degradation during the SEC-MALLS experiment as shown by the tail on both peaks in Figure B4, and the emergence of the lower molecular weight bands in Figure B5. The reason for the degradation is not clear, as Skp1/Skp2-N is usually stable at room temperature for a few hours.

B4 Discussion

This chapter has detailed the Cdh1 constructs and Skp2 mutants created in order to test the effect of post-translational modification of Skp2 on Cdh1 binding in *in vitro* assays. This investigation has shown that mimicking Skp2 acetylation using K to L mutations did not induce dimerization. This investigation does not rule out, however, that the dimerization observed in cells may occur 'end-to-end' with the C-terminus of one Skp2 monomer binding to the acetylated residues of a second. The Skp2 construct used in this work is truncated and starts at residue 140. As the K to L mutation was used in the paper by Inuzuka and co-workers who reported dimerization, it is reasonable to assume that this mutation would have a similar effect *in vitro* as *in vivo* (Inuzuka et al., 2012). However, there could be an additional post-translational modification which follows the acetylation *in vivo* which induces the dimerization, and this would only be observed in cell-based assays.

Bibliography

1994. The CCP4 suite: programs for protein crystallography. *Acta Crystallogr D Biol Crystallogr,* 50**,** 760-3.

ACHENBACH, T. V., MULLER, R. & SLATER, E. P. 2000. Synergistic antitumor effect of chemotherapy and antisense-mediated ablation of the cell cycle inhibitor p27KIP-1. *Clin Cancer Res,* 6**,** 3006-14.

ADAMS, P. D., LI, X., SELLERS, W. R., BAKER, K. B., LENG, X., HARPER, J. W., TAYA, Y. & KAELIN, W. G. 1999. Retinoblastoma Protein Contains a C-terminal Motif That Targets It for Phosphorylation by Cyclin-cdk Complexes. *Molecular and Cellular Biology,* 19**,** 1068-1080.

ADAMS, P. D., SELLERS, W. R., SHARMA, S. K., WU, A. D., NALIN, C. M. & KAELIN, W. G., JR. 1996. Identification of a cyclin-cdk2 recognition motif present in substrates and p21-like cyclin-dependent kinase inhibitors. *Mol Cell Biol,* 16**,** 6623-33.

AGARWAL, A., BUMM, T. G., CORBIN, A. S., O'HARE, T., LORIAUX, M., VANDYKE, J., WILLIS, S. G., DEININGER, J., NAKAYAMA, K. I., DRUKER, B. J. & DEININGER, M. W. 2008. Absence of SKP2 expression attenuates BCR-ABL-induced myeloproliferative disease. *Blood,* 112**,** 1960-70.

AL SORKHY, M., FERRAIUOLO, R. M., JALILI, E., MALYSA, A., FRATILOIU, A. R., SLOANE, B. F. & PORTER, L. A. 2012. The cyclin-like protein Spy1/RINGO promotes mammary transformation and is elevated in human breast cancer. *BMC Cancer,* 12**,** 45.

ALIGUE, R., WU, L. & RUSSELL, P. 1997. Regulation of Schizosaccharomyces pombe Wee1 tyrosine kinase. *J Biol Chem,* 272**,** 13320-5.

ARGYRIOU, A. A., ICONOMOU, G. & KALOFONOS, H. P. 2008. Bortezomib-induced peripheral neuropathy in multiple myeloma: a comprehensive review of the literature. *Blood,* 112**,** 1593-9.

ARVAI, A. S., BOURNE, Y., HICKEY, M. J. & TAINER, J. A. 1995. Crystal Structure of the Human Cell Cycle Protein CksHs1: Single Domain Fold with Similarity to Kinase N-lobe Domain. *Journal of Molecular Biology,* 249**,** 835-842.

ASGHAR, U., WITKIEWICZ, A. K., TURNER, N. C. & KNUDSEN, E. S. 2015. The history and future of targeting cyclin-dependent kinases in cancer therapy. *Nat Rev Drug Discov,* 14**,** 130-46.

ATTARD, G., SARKER, D., REID, A., MOLIFE, R., PARKER, C. & DE BONO, J. S. 2006. Improving the outcome of patients with castration-resistant prostate cancer through rational drug development. *British Journal of Cancer,* 95**,** 767-774.

BAHASSI, E. M. 2011. Polo-like kinases and DNA damage checkpoint: beyond the traditional mitotic functions. *Experimental Biology and Medicine,* 236**,** 648-657.

BAI, C., SEN, P., HOFMANN, K., MA, L., GOEBL, M., HARPER, J. W. & ELLEDGE, S. J. 1996. SKP1 Connects Cell Cycle Regulators to the Ubiquitin Proteolysis Machinery through a Novel Motif, the F-Box. *Cell,* 86**,** 263-274.

BALDASSARRE, G., BELLETTI, B., BRUNI, P., BOCCIA, A., TRAPASSO, F., PENTIMALLI, F., BARONE, M. V., CHIAPPETTA, G., VENTO, M. T., SPIEZIA, S., FUSCO, A. & VIGLIETTO, G. 1999. Overexpressed cyclin D3 contributes to retaining the growth inhibitor p27 in the cytoplasm of thyroid tumor cells. *J Clin Invest,* 104**,** 865-74.

BARBORIC, M., YIK, J. H. N., CZUDNOCHOWSKI, N., YANG, Z., CHEN, R., CONTRERAS, X., GEYER, M., PETERLIN, B. M. & ZHOU, Q. 2007. Tat competes with HEXIM1 to increase the active pool of P-TEFb for HIV-1 transcription. *Nucleic acids research,* 35**,** 2003-2012.

BARTEK, J. & LUKAS, J. 2001. Mammalian G1- and S-phase checkpoints in response to DNA damage. *Curr Opin Cell Biol,* 13**,** 738-47.

BARTEK, J. & LUKAS, J. 2007. DNA damage checkpoints: from initiation to recovery or adaptation. *Curr Opin Cell Biol,* 19**,** 238-45.

BASHIR, T., DORRELLO, N. V., AMADOR, V., GUARDAVACCARO, D. & PAGANO, M. 2004. Control of the SCFSkp2-Cks1 ubiquitin ligase by the APC/C-Cdh1 ubiquitin ligase. *Nature,* 428**,** 190-193.

BASHIR, T., PAGAN, J. K., BUSINO, L. & PAGANO, M. 2010. Phosphorylation of Ser72 is dispensable for Skp2 assembly into an active SCF ubiquitin ligase and its subcellular localization. *Cell cycle,* 9**,** 971-974.

BATES, S., BONETTA, L., MACALLAN, D., PARRY, D., HOLDER, A., DICKSON, C. & PETERS, G. 1994. CDK6 (PLSTIRE) and CDK4 (PSK-J3) are a distinct subset of the cyclin-dependent kinases that associate with cyclin D1. *Oncogene,* 9**,** 71-9.

BAUMLI, S., LOLLI, G., LOWE, E. D., TROIANI, S., RUSCONI, L., BULLOCK, A. N., DEBRECZENI, J. E., KNAPP, S. & JOHNSON, L. N. 2008. The structure of P-TEFb (CDK9/cyclin T1), its complex with flavopiridol and regulation by phosphorylation. *Embo j,* 27**,** 1907-18.

BELL, E., LUNEC, J. & TWEDDLE, D. 2007. Cell cycle regulation targets of MYCN identified by gene expression microarrays. *Cell Cycle,* 6**,** 1249-1256.

BELLA, J., HINDLE, K. L., MCEWAN, P. A. & LOVELL, S. C. 2008. The leucine-rich repeat structure. *Cell Mol Life Sci,* 65**,** 2307-33.

BELLIZZI, A., MANGIA, A., CHIRIATTI, A., PETRONI, S., QUARANTA, M., SCHITTULLI, F., MALFETTONE, A., CARDONE, R. A., PARADISO, A. & RESHKIN, S. J. 2008. RhoA protein expression in primary breast cancers and matched lymphocytes is associated with progression of the disease. *International journal of molecular medicine,* 22**,** 25-31.

BERNARD, S. & HERZEL, H. 2006. Why do cells cycle with a 24 hour period? *Genome Inform,* 17**,** 72-9.

BERNDSEN, C. E. & WOLBERGER, C. 2014. New insights into ubiquitin E3 ligase mechanism. *Nat Struct Mol Biol,* 21**,** 301-7.

BERTHET, C., ALEEM, E., COPPOLA, V., TESSAROLLO, L. & KALDIS, P. 2003. Cdk2 knockout mice are viable. *Curr Biol,* 13**,** 1775-85.

BESSON, A., GURIAN-WEST, M., CHEN, X., KELLY-SPRATT, K. S., KEMP, C. J. & ROBERTS, J. M. 2006. A pathway in quiescent cells that controls p27Kip1 stability, subcellular localization, and tumor suppression. *Genes & development,* 20**,** 47-64.

BHATTACHARJEE, R. N., BANKS, G. C., TROTTER, K. W., LEE, H.-L. & ARCHER, T. K. 2001. Histone H1 phosphorylation by Cdk2 selectively modulates mouse mammary tumor virus transcription through chromatin remodeling. *Molecular and cellular biology,* 21**,** 5417-5425.

BHATTACHARYA, S., GARRIGA, J., CALBO, J., YONG, T., HAINES, D. S. & GRANA, X. 2003. SKP2 associates with p130 and accelerates p130 ubiquitylation and degradation in human cells. *Oncogene,* 22**,** 2443-51.

BIGALKE, J. M., DAMES, S. A., BLANKENFELDT, W., GRZESIEK, S. & GEYER, M. 2011. Structure and dynamics of a stabilized coiled-coil domain in the P-TEFb regulator Hexim1. *J Mol Biol,* 414**,** 639-53.

BLAGOSKLONNY, M. V. & PARDEE, A. B. 2002. The restriction point of the cell cycle. *Cell Cycle,* 1**,** 103-10.

BLAIN, S. W., MONTALVO, E. & MASSAGUE, J. 1997. Differential interaction of the cyclin-dependent kinase (Cdk) inhibitor p27Kip1 with cyclin A-Cdk2 and cyclin D2-Cdk4. *J Biol Chem,* 272**,** 25863-72.

BLANC, E., ROVERSI, P., VONRHEIN, C., FLENSBURG, C., LEA, S. M. & BRICOGNE, G. 2004. Refinement of severely incomplete structures with maximum likelihood in BUSTER–TNT. *Acta Crystallographica Section D: Biological Crystallography,* 60**,** 2210-2221.

BORNSTEIN, G., BLOOM, J., SITRY-SHEVAH, D., NAKAYAMA, K., PAGANO, M. & HERSHKO, A. 2003. Role of the SCFSkp2 ubiquitin ligase in the degradation of p21Cip1 in S phase. *J Biol Chem,* 278**,** 25752-7.

BOURNE, Y., WATSON, M. H., HICKEY, M. J., HOLMES, W., ROCQUE, W., REED, S. I. & TAINER, J. A. 1996. Crystal structure and mutational analysis of the human CDK2 kinase complex with cell cycle-regulatory protein CksHs1. *Cell,* 84**,** 863-74.

BOYERINAS, B., PARK, S. M., HAU, A., MURMANN, A. E. & PETER, M. E. 2010. The role of let-7 in cell differentiation and cancer. *Endocr Relat Cancer,* 17**,** F19-36.

BRAIG, K., OTWINOWSKI, Z., HEGDE, R., BOISVERT, D. C., JOACHIMIAK, A., HORWICH, A. L. & SIGLER, P. B. 1994. The crystal structure of the bacterial chaperonin GroEL at 2.8 A. *Nature,* 371**,** 578-86.

BRANDEIS, M., ROSEWELL, I., CARRINGTON, M., CROMPTON, T., JACOBS, M. A., KIRK, J., GANNON, J. & HUNT, T. 1998. Cyclin B2-null mice develop normally and are fertile whereas cyclin B1-null mice die in utero. *Proc Natl Acad Sci U S A,* 95**,** 4344-9.

BRETONES, G., ACOSTA, J. C., CARABALLO, J. M., FERRANDIZ, N., GOMEZ-CASARES, M. T., ALBAJAR, M., BLANCO, R., RUIZ, P., HUNG, W. C., ALBERO, M. P., PEREZ-ROGER, I. & LEON, J. 2011. SKP2 oncogene is a direct MYC target gene and MYC down-regulates p27(KIP1) through SKP2 in human leukemia cells. *J Biol Chem,* 286**,** 9815-25.

BROSS, P. F., KANE, R., FARRELL, A. T., ABRAHAM, S., BENSON, K., BROWER, M. E., BRADLEY, S., GOBBURU, J. V., GOHEER, A., LEE, S. L., LEIGHTON, J., LIANG, C. Y., LOSTRITTO, R. T., MCGUINN, W. D., MORSE, D. E., RAHMAN, A., ROSARIO, L. A., VERBOIS, S. L., WILLIAMS, G., WANG, Y. C. & PAZDUR, R. 2004. Approval summary for bortezomib for injection in the treatment of multiple myeloma. *Clin Cancer Res,* 10**,** 3954-64.

BROWN, N. R., KOROLCHUK, S., MARTIN, M. P., STANLEY, W. A., MOUKHAMETZIANOV, R., NOBLE, M. E. M. & ENDICOTT, J. A. 2015. CDK1 structures reveal conserved and unique features of the essential cell cycle CDK. *Nature communications,* 6.

BROWN, N. R., LOWE, E. D., PETRI, E., SKAMNAKI, V., ANTROBUS, R. & JOHNSON, L. N. 2007. Cyclin B and cyclin A confer different substrate recognition properties on CDK2. *Cell Cycle,* 6**,** 1350-9.

BROWN, N. R., NOBLE, M. E., ENDICOTT, J. A., GARMAN, E. F., WAKATSUKI, S., MITCHELL, E., RASMUSSEN, B., HUNT, T. & JOHNSON, L. N. 1995. The crystal structure of cyclin A. *Structure,* 3**,** 1235-47.

BROWN, N. R., NOBLE, M. E., ENDICOTT, J. A. & JOHNSON, L. N. 1999. The structural basis for specificity of substrate and recruitment peptides for cyclin-dependent kinases. *Nat Cell Biol,* 1**,** 438-43.

BRUNET, A., KANAI, F., STEHN, J., XU, J., SARBASSOVA, D., FRANGIONI, J. V., DALAL, S. N., DECAPRIO, J. A., GREENBERG, M. E. & YAFFE, M. B. 2002. 14-3-3 transits to the nucleus and participates in dynamic nucleocytoplasmic transport. *The Journal of Cell Biology,* 156**,** 817-828.

BUCHAN, D. W., MINNECI, F., NUGENT, T. C., BRYSON, K. & JONES, D. T. 2013. Scalable web services for the PSIPRED Protein Analysis Workbench. *Nucleic Acids Res,* 41**,** W349-57.

CAO, L., CHEN, F., YANG, X., XU, W., XIE, J. & YU, L. 2014. Phylogenetic analysis of CDK and cyclin proteins in premetazoan lineages. *BMC Evol Biol,* 14**,** 10.

CASTRO, A., VIGNERON, S., BERNIS, C., LABBÉ, J.-C. & LORCA, T. 2003. Xkid is degraded in a D-box, KEN-box, and A-box-independent pathway. *Molecular and cellular biology,* 23**,** 4126-4138.

CATZAVELOS, C., BHATTACHARYA, N., UNG, Y. C., WILSON, J. A., RONCARI, L., SANDHU, C., SHAW, P., YEGER, H., MORAVA-PROTZNER, I., KAPUSTA, L., FRANSSEN, E., PRITCHARD, K. I. & SLINGERLAND, J. M. 1997. Decreased levels of the cell-cycle inhibitor p27Kip1 protein: prognostic implications in primary breast cancer. *Nat Med,* 3**,** 227-30.

CECCARELLI, D. F., TANG, X., PELLETIER, B., ORLICKY, S., XIE, W., PLANTEVIN, V., NECULAI, D., CHOU, Y. C., OGUNJIMI, A., AL-HAKIM, A., VARELAS, X., KOSZELA, J., WASNEY, G. A., VEDADI, M., DHE-PAGANON, S., COX, S., XU, S., LOPEZ-GIRONA, A., MERCURIO, F., WRANA, J., DUROCHER, D., MELOCHE, S., WEBB, D. R., TYERS, M. & SICHERI, F. 2011. An allosteric inhibitor of the human Cdc34 ubiquitin-conjugating enzyme. *Cell,* 145**,** 1075-87.

CEN, B., MAHAJAN, S., ZEMSKOVA, M., BEHARRY, Z., LIN, Y.-W., CRAMER, S. D., LILLY, M. B. & KRAFT, A. S. 2010. Regulation of Skp2 levels by the Pim-1 protein kinase. *Journal of Biological Chemistry,* 285**,** 29128-29137.

CERQUEIRA, A., MARTIN, A., SYMONDS, C. E., ODAJIMA, J., DUBUS, P., BARBACID, M. & SANTAMARIA, D. 2014. Genetic characterization of the role of the Cip/Kip family of proteins as cyclin-dependent kinase inhibitors and assembly factors. *Mol Cell Biol,* 34**,** 1452-9.

CHAN, C.-H., LEE, S.-W., LI, C.-F., WANG, J., YANG, W.-L., WU, C.-Y., WU, J., NAKAYAMA, K. I., KANG, H.-Y., HUANG, H.-Y., HUNG, M.-C., PANDOLFI, P. P. & LIN, H.-K. 2010. Deciphering the transcription complex critical for RhoA gene expression and cancer metastasis. *Nature cell biology,* 12**,** 10.1038/ncb2047.

CHAN, C.-H., LI, C.-F., YANG, W.-L., GAO, Y., LEE, S.-W., FENG, Z., HUANG, H.-Y., TSAI, K. K. C., FLORES, L. G. & SHAO, Y. 2012. The Skp2-SCF E3 ligase regulates Akt ubiquitination, glycolysis, herceptin sensitivity, and tumorigenesis. *Cell,* 149**,** 1098-1111.

CHAN, C.-H., MORROW, JOHN K., LI, C.-F., GAO, Y., JIN, G., MOTEN, A., STAGG, LOREN J., LADBURY, JOHN E., CAI, Z., XU, D., LOGOTHETIS, CHRISTOPHER J., HUNG, M.-C., ZHANG, S. & LIN, H.-K. 2013. Pharmacological Inactivation of Skp2 SCF Ubiquitin Ligase Restricts Cancer Stem Cell Traits and Cancer Progression. *Cell,* 154**,** 556-568.

CHANG, L., ZHANG, Z., YANG, J., MCLAUGHLIN, S. H. & BARFORD, D. 2014. Molecular architecture and mechanism of the anaphase-promoting complex. *Nature,* 513**,** 388-93.

CHAU, V., TOBIAS, J. W., BACHMAIR, A., MARRIOTT, D., ECKER, D. J., GONDA, D. K. & VARSHAVSKY, A. 1989. A multiubiquitin chain is confined to specific lysine in a targeted short-lived protein. *Science,* 243**,** 1576-83.

CHEN, J. Y., WANG, M. C. & HUNG, W. C. 2011. Bcr-Abl-induced tyrosine phosphorylation of Emi1 to stabilize Skp2 protein via inhibition of ubiquitination in chronic myeloid leukemia cells. *Journal of cellular physiology,* 226**,** 407-413.

CHEN, Q., XIE, W., KUHN, D. J., VOORHEES, P. M., LOPEZ-GIRONA, A., MENDY, D., CORRAL, L. G., KRENITSKY, V. P., XU, W., MOUTOUH-DE PARSEVAL, L., WEBB, D. R., MERCURIO, F., NAKAYAMA, K. I., NAKAYAMA, K. & ORLOWSKI, R. Z. 2008. Targeting the p27 E3 ligase SCF(Skp2) results in p27- and Skp2-mediated cell-cycle arrest and activation of autophagy. *Blood,* 111**,** 4690-4699.

CHENG, A., GERRY, S., KALDIS, P. & SOLOMON, M. J. 2005. Biochemical characterization of Cdk2-Speedy/Ringo A2. *BMC Biochem,* 6**,** 19.

CHO, S., KIM, J. H., BACK, S. H. & JANG, S. K. 2005. Polypyrimidine tract-binding protein enhances the internal ribosomal entry site-dependent translation of p27Kip1 mRNA and modulates transition from G1 to S phase. *Mol Cell Biol,* 25**,** 1283-97.

CHU, I., SUN, J., ARNAOUT, A., KAHN, H., HANNA, W., NAROD, S., SUN, P., TAN, C. K., HENGST, L. & SLINGERLAND, J. 2007. p27 phosphorylation by Src regulates inhibition of cyclin E-Cdk2. *Cell,* 128**,** 281-94.

CHU, I. M., HENGST, L. & SLINGERLAND, J. M. 2008. The Cdk inhibitor p27 in human cancer: prognostic potential and relevance to anticancer therapy. *Nature Reviews Cancer,* 8**,** 253-267.

CLURMAN, B. E., SHEAFF, R. J., THRESS, K., GROUDINE, M. & ROBERTS, J. M. 1996. Turnover of cyclin E by the ubiquitin-proteasome pathway is regulated by cdk2 binding and cyclin phosphorylation. *Genes Dev,* 10**,** 1979-90.

COLEMAN, J. & MISKIMINS, W. K. 2009. Structure and activity of the internal ribosome entry site within the human p27 Kip1 5'-untranslated region. *RNA Biol,* 6**,** 84-9.

CONTRERAS, A., HALE, T. K., STENOIEN, D. L., ROSEN, J. M., MANCINI, M. A. & HERRERA, R. E. 2003. The dynamic mobility of histone H1 is regulated by cyclin/CDK phosphorylation. *Molecular and cellular biology,* 23**,** 8626-8636.

COOPER, M. A. 2003. Label-free screening of bio-molecular interactions. *Analytical and bioanalytical chemistry,* 377**,** 834-842.

CROSS, F. R., YUSTE-ROJAS, M., GRAY, S. & JACOBSON, M. D. 1999. Specialization and Targeting of B-Type Cyclins. *Molecular Cell,* 4**,** 11-19.

DA FONSECA, P. C., KONG, E. H., ZHANG, Z., SCHREIBER, A., WILLIAMS, M. A., MORRIS, E. P. & BARFORD, D. 2011. Structures of APC/C(Cdh1) with substrates identify Cdh1 and Apc10 as the D-box co-receptor. *Nature,* 470**,** 274-8.

DANSEN, T. B. & BURGERING, B. M. 2008. Unravelling the tumor-suppressive functions of FOXO proteins. *Trends Cell Biol,* 18**,** 421-9.

DAY, P. J., CLEASBY, A., TICKLE, I. J., O'REILLY, M., COYLE, J. E., HOLDING, F. P., MCMENAMIN, R. L., YON, J., CHOPRA, R. & LENGAUER, C. 2009. Crystal structure of human CDK4 in complex with a D-type cyclin. *Proceedings of the National Academy of Sciences,* 106**,** 4166-4170.

DE BONDT, H. L., ROSENBLATT, J., JANCARIK, J., JONES, H. D., MORGAN, D. O. & KIM, S. H. 1993. Crystal structure of cyclin-dependent kinase 2. *Nature,* 363**,** 595-602.

DEBES, J. D., SEBO, T. J., LOHSE, C. M., MURPHY, L. M., DE ANNA, L. H. & TINDALL, D. J. 2003. p300 in prostate cancer proliferation and progression. *Cancer research,* 63**,** 7638-7640.

DEPHOURE, N., ZHOU, C., VILLEN, J., BEAUSOLEIL, S. A., BAKALARSKI, C. E., ELLEDGE, S. J. & GYGI, S. P. 2008. A quantitative atlas of mitotic phosphorylation. *Proc Natl Acad Sci U S A,* 105**,** 10762-7.

DESAI, D., GU, Y. & MORGAN, D. O. 1992. Activation of human cyclin-dependent kinases in vitro. *Molecular biology of the cell,* 3**,** 571-582.

DESHAIES, R. J. & JOAZEIRO, C. A. 2009. RING domain E3 ubiquitin ligases. *Annu Rev Biochem,* 78**,** 399-434.

DEVOTO, S. H., MUDRYJ, M., PINES, J., HUNTER, T. & NEVINS, J. R. 1992. A cyclin A-protein kinase complex possesses sequence-specific DNA binding activity: p33cdk2 is a component of the E2F-cyclin A complex. *Cell,* 68**,** 167-76.

DI BARI, M. G., CIUFFINI, L., MINGARDI, M., TESTI, R., SODDU, S. & BARILA, D. 2006. c-Abl acetylation by histone acetyltransferases regulates its nuclear-cytoplasmic localization. *EMBO Rep,* 7**,** 727-33.

DIETSCHY, T., SHEVELEV, I., PENA-DIAZ, J., HUHN, D., KUENZLE, S., MAK, R., MIAH, M. F., HESS, D., FEY, M., HOTTIGER, M. O., JANSCAK, P. & STAGLJAR, I. 2009. p300-mediated acetylation of the Rothmund-Thomson-syndrome gene product RECQL4 regulates its subcellular localization. *J Cell Sci,* 122**,** 1258-67.

DIKIC, I., WAKATSUKI, S. & WALTERS, K. J. 2009. Ubiquitin-binding domains—from structures to functions. *Nature reviews Molecular cell biology,* 10**,** 659-671.

DOU, Y. & GOROVSKY, M. A. 2000. Phosphorylation of Linker Histone H1 Regulates Gene Expression In Vivo by Creating a Charge Patch. *Molecular Cell,* 6**,** 225-231.

DOWEN, S. E., SCOTT, A., MUKHERJEE, G. & STANLEY, M. A. 2003. Overexpression of Skp2 in carcinoma of the cervix does not correlate inversely with p27 expression. *Int J Cancer,* 105**,** 326-30.

DRAETTA, G., BRIZUELA, L., POTASHKIN, J. & BEACH, D. 1987. Identification of p34 and p13, human homologs of the cell cycle regulators of fission yeast encoded by cdc2+ and suc1+. *Cell,* 50**,** 319-25.

DROBNJAK, M., MELAMED, J., TANEJA, S., MELZER, K., WIECZOREK, R., LEVINSON, B., ZELENIUCH-JACQUOTTE, A., POLSKY, D., FERRARA, J., PEREZ-SOLER, R., CORDON-CARDO, C., PAGANO, M. & OSMAN, I. 2003. Altered expression of p27 and Skp2 proteins in prostate cancer of African-American patients. *Clin Cancer Res,* 9**,** 2613-9.

DUNCAN, T. J., AL-ATTAR, A., ROLLAND, P., HARPER, S., SPENDLOVE, I. & DURRANT, L. G. 2010. Cytoplasmic p27 expression is an independent prognostic factor in ovarian cancer. *Int J Gynecol Pathol,* 29**,** 8-18.

DYSON, H. J. & WRIGHT, P. E. 2005. Intrinsically unstructured proteins and their functions. *Nat Rev Mol Cell Biol,* 6**,** 197-208.

DYSON, N. 1998. The regulation of E2F by pRB-family proteins. *Genes & development,* 12**,** 2245-2262.

ECKER, K. & HENGST, L. 2009. Skp2: caught in the Akt. *Nature cell biology,* 11**,** 377-379.

ELLEDGE, S. J. & SPOTTSWOOD, M. R. 1991. A new human p34 protein kinase, CDK2, identified by complementation of a cdc28 mutation in Saccharomyces cerevisiae, is a homolog of Xenopus Eg1. *Embo j,* 10**,** 2653-9.

ELSTROM, R. L., BAUER, D. E., BUZZAI, M., KARNAUSKAS, R., HARRIS, M. H., PLAS, D. R., ZHUANG, H., CINALLI, R. M., ALAVI, A., RUDIN, C. M. & THOMPSON, C. B. 2004. Akt stimulates aerobic glycolysis in cancer cells. *Cancer Res,* 64**,** 3892-9.

EMSLEY, P., LOHKAMP, B., SCOTT, W. G. & COWTAN, K. 2010. Features and development of Coot. *Acta Crystallogr D Biol Crystallogr,* 66**,** 486-501.

EVAN, G. & LITTLEWOOD, T. 1998. A matter of life and cell death. *Science,* 281**,** 1317-22.

EVANS, L., CHEN, L., MILAZZO, G., GHERARDI, S., PERINI, G., WILLMORE, E., NEWELL, D. R. & TWEDDLE, D. A. 2015. SKP2 is a direct transcriptional target of MYCN and a potential therapeutic target in neuroblastoma. *Cancer Letters,* 363**,** 37-45.

EVANS, T., ROSENTHAL, E. T., YOUNGBLOM, J., DISTEL, D. & HUNT, T. 1983. Cyclin: A protein specified by maternal mRNA in sea urchin eggs that is destroyed at each cleavage division. *Cell,* 33**,** 389-396.

FACKENTHAL, J. D. & OLOPADE, O. I. 2007. Breast cancer risk associated with BRCA1 and BRCA2 in diverse populations. *Nat Rev Cancer,* 7**,** 937-48.

FERO, M. L., RANDEL, E., GURLEY, K. E., ROBERTS, J. M. & KEMP, C. J. 1998. The murine gene p27Kip1 is haplo-insufficient for tumour suppression. *Nature,* 396**,** 177-180.

FERO, M. L., RIVKIN, M., TASCH, M., PORTER, P., CAROW, C. E., FIRPO, E., POLYAK, K., TSAI, L.-H., BROUDY, V., PERLMUTTER, R. M., KAUSHANSKY, K. & ROBERTS, J. M. 1996. A Syndrome of Multiorgan Hyperplasia with Features of Gigantism, Tumorigenesis, and Female Sterility in p27Kip1-Deficient Mice. *Cell,* 85**,** 733-744.

FINLEY, D. 2009. Recognition and Processing of Ubiquitin-Protein Conjugates by the Proteasome. *Annual review of biochemistry,* 78**,** 477-513.

FOSTER, D. A., YELLEN, P., XU, L. & SAQCENA, M. 2010. Regulation of g1 cell cycle progression distinguishing the restriction point from a nutrient-sensing cell growth checkpoint (s). *Genes & cancer,* 1**,** 1124-1131.

FRESCAS, D. & PAGANO, M. 2008. Deregulated proteolysis by the F-box proteins SKP2 and beta-TrCP: tipping the scales of cancer. *Nat Rev Cancer,* 8**,** 438-49.

FUJITA, N., SATO, S. & TSURUO, T. 2003. Phosphorylation of p27Kip1 at threonine 198 by p90 ribosomal protein S6 kinases promotes its binding to 14-3-3 and cytoplasmic localization. *J Biol Chem,* 278**,** 49254-60.

FUKUSHIMA, H., OGURA, K., WAN, L., LU, Y., LI, V., GAO, D., LIU, P., LAU, A. W., WU, T. & KIRSCHNER, M. W. 2013. SCF-mediated Cdh1 degradation defines a negative feedback system that coordinates cell-cycle progression. *Cell reports,* 4**,** 803-816.

GANIATSAS, S., DOW, R., THOMPSON, A., SCHULMAN, B. & GERMAIN, D. 2001. A splice variant of Skp2 is retained in the cytoplasm and fails to direct cyclin D1 ubiquitination in the uterine cancer cell line SK-UT. *Oncogene,* 20**,** 3641-50.

GANOTH, D., BORNSTEIN, G., KO, T. K., LARSEN, B., TYERS, M., PAGANO, M. & HERSHKO, A. 2001. The cell-cycle regulatory protein Cks1 is required for SCF(Skp2)-mediated ubiquitinylation of p27. *Nat Cell Biol,* 3**,** 321-4.

GAO, D., INUZUKA, H., TSENG, A., CHIN, R. Y., TOKER, A. & WEI, W. 2009. Phosphorylation by Akt1 promotes cytoplasmic localization of Skp2 and impairs APC-Cdh1-mediated Skp2 destruction. *Nature Cell Biology,* 11**,** 397-U92.

GARCÍA-HIGUERA, I., MANCHADO, E., DUBUS, P., CAÑAMERO, M., MÉNDEZ, J., MORENO, S. & MALUMBRES, M. 2008. Genomic stability and tumour suppression by the APC/C cofactor Cdh1. *Nature cell biology,* 10**,** 802-811.

GAYTHER, S. A., BATLEY, S. J., LINGER, L., BANNISTER, A., THORPE, K., CHIN, S.-F., DAIGO, Y., RUSSELL, P., WILSON, A. & SOWTER, H. M. 2000. Mutations truncating the EP300 acetylase in human cancers. *Nature genetics,* 24**,** 300-303.

GELEY, S., KRAMER, E., GIEFFERS, C., GANNON, J., PETERS, J. M. & HUNT, T. 2001. Anaphase-promoting complex/cyclosome-dependent proteolysis of human cyclin A starts at the beginning of mitosis and is not subject to the spindle assembly checkpoint. *J Cell Biol,* 153**,** 137-48.

GIBSON, T. J., THOMPSON, J. D., BLOCKER, A. & KOUZARIDES, T. 1994. Evidence for a protein domain superfamily shared by the cyclins, TFIIB and RB/p107. *Nucleic Acids Res,* 22**,** 946-52.

GIRARD, F., STRAUSFELD, U., FERNANDEZ, A. & LAMB, N. J. 1991. Cyclin A is required for the onset of DNA replication in mammalian fibroblasts. *Cell,* 67**,** 1169-79.

GLOTZER, M., MURRAY, A. W. & KIRSCHNER, M. W. 1991. Cyclin is degraded by the ubiquitin pathway. *Nature,* 349**,** 132-8.

GRAVINA, G. L., SENAPEDIS, W., MCCAULEY, D., BALOGLU, E., SHACHAM, S. & FESTUCCIA, C. 2014. Nucleo-cytoplasmic transport as a therapeutic target of cancer. *Journal of hematology & oncology,* 7**,** 85.

GREENFIELD, N. J. 2006. Using circular dichroism collected as a function of temperature to determine the thermodynamics of protein unfolding and binding interactions. *Nature protocols,* 1**,** 2527-2535.

GRIMMLER, M., WANG, Y., MUND, T., CILENSEK, Z., KEIDEL, E. M., WADDELL, M. B., JAKEL, H., KULLMANN, M., KRIWACKI, R. W. & HENGST, L. 2007. Cdk-inhibitory activity and stability of p27Kip1 are directly regulated by oncogenic tyrosine kinases. *Cell,* 128**,** 269-80.

GU, J., BABAYEVA, N. D., SUWA, Y., BARANOVSKIY, A. G., PRICE, D. H. & TAHIROV, T. H. 2014. Crystal structure of HIV-1 Tat complexed with human P-TEFb and AFF4. *Cell Cycle,* 13**,** 1788-1797.

GU, Y., ROSENBLATT, J. & MORGAN, D. O. 1992. Cell cycle regulation of CDK2 activity by phosphorylation of Thr160 and Tyr15. *EMBO J,* 11**,** 3995-4005.

HADWIGER, J. A., WITTENBERG, C., MENDENHALL, M. D. & REED, S. I. 1989. The Saccharomyces cerevisiae CKS1 gene, a homolog of the Schizosaccharomyces pombe suc1+ gene, encodes a subunit of the Cdc28 protein kinase complex. *Mol Cell Biol,* 9**,** 2034-41.

HANAHAN, D. & WEINBERG, R. A. 2011. Hallmarks of cancer: the next generation. *Cell,* 144**,** 646-74.

HAO, B., OEHLMANN, S., SOWA, M. E., HARPER, J. W. & PAVLETICH, N. P. 2007. Structure of a Fbw7-Skp1-cyclin E complex: multisite-phosphorylated substrate recognition by SCF ubiquitin ligases. *Mol Cell,* 26**,** 131-43.

HAO, B., ZHENG, N., SCHULMAN, B. A., WU, G., MILLER, J. J., PAGANO, M. & PAVLETICH, N. P. 2005. Structural basis of the Cks1-dependent recognition of p27(Kip1) by the SCFSkp2 ubipuitin ligase. *Molecular Cell,* 20**,** 9-19.

HARBOUR, J. W., LUO, R. X., DEI SANTI, A., POSTIGO, A. A. & DEAN, D. C. 1999. Cdk phosphorylation triggers sequential intramolecular interactions that progressively block Rb functions as cells move through G1. *Cell,* 98**,** 859-69.

HARPER, J. W., BURTON, J. L. & SOLOMON, M. J. 2002. The anaphase-promoting complex: it's not just for mitosis any more. *Genes & development,* 16**,** 2179-2206.

HAYLES, J., BEACH, D., DURKACZ, B. & NURSE, P. 1986. The fission yeast cell cycle control gene cdc2: isolation of a sequence suc1 that suppresses cdc2 mutant function. *Mol Gen Genet,* 202**,** 291-3.

HE, J., CHAO, W. C., ZHANG, Z., YANG, J., CRONIN, N. & BARFORD, D. 2013. Insights into degron recognition by APC/C coactivators from the structure of an Acm1-Cdh1 complex. *Mol Cell,* 50**,** 649-60.

HELIN, K., LEES, J. A., VIDAL, M., DYSON, N., HARLOW, E. & FATTAEY, A. 1992. A cDNA encoding a pRB-binding protein with properties of the transcription factor E2F. *Cell,* 70**,** 337-350.

HENGST, L. & REED, S. I. 1996. Translational Control of p27Kip1 Accumulation During the Cell Cycle. *Science,* 271**,** 1861-1864.

HERSHKO, A. 1983. Ubiquitin: roles in protein modification and breakdown. *Cell,* 34**,** 11-2.

HERSHKO, A. 2005. The ubiquitin system for protein degradation and some of its roles in the control of the cell division cycle*. *Cell Death & Differentiation,* 12**,** 1191-1197.

HERSHKO, D. D. 2008. Oncogenic properties and prognostic implications of the ubiquitin ligase Skp2 in cancer. *Cancer,* 112**,** 1415-1424.

HERSHKO, D. D. 2010. Cyclin-dependent kinase inhibitor p27 as a prognostic biomarker and potential cancer therapeutic target. *Future Oncology,* 6**,** 1837-1847.

HOCHSTRASSER, M. 1995. Ubiquitin, proteasomes, and the regulation of intracellular protein degradation. *Curr Opin Cell Biol,* 7**,** 215-23.

HONDA, R., LOWE, E. D., DUBININA, E., SKAMNAKI, V., COOK, A., BROWN, N. R. & JOHNSON, L. N. 2005. The structure of cyclin E1/CDK2: implications for CDK2 activation and CDK2-independent roles. *EMBO J,* 24**,** 452-63.

HORIUCHI, A., IMAI, T., WANG, C., OHIRA, S., FENG, Y., NIKAIDO, T. & KONISHI, I. 2003. Up-regulation of small GTPases, RhoA and RhoC, is associated with tumor progression in ovarian carcinoma. *Laboratory investigation,* 83**,** 861-870.

HSU, Y. H., CHANG, C. C., YANG, N. J., LEE, Y. H. & JUAN, S. H. 2014. RhoA-mediated inhibition of vascular endothelial cell mobility: positive feedback through reduced cytosolic p21 and p27. *J Cell Physiol,* 229**,** 1455-65.

HU, D., LIU, W., WU, G. & WAN, Y. 2011. Nuclear translocation of Skp2 facilitates its destruction in response to TGFβ signaling. *Cell Cycle,* 10**,** 285-292.

HUANG, J., ZHOU, N., WATABE, K., LU, Z., WU, F., XU, M. & MO, Y. Y. 2014. Long non-coding RNA UCA1 promotes breast tumor growth by suppression of p27 (Kip1). *Cell Death Dis,* 5**,** e1008.

HUET, X., RECH, J., PLET, A., VIE, A. & BLANCHARD, J. M. 1996. Cyclin A expression is under negative transcriptional control during the cell cycle. *Mol Cell Biol,* 16**,** 3789-98.

HUGGINS, C. & HODGES, C. V. 1941. Studies on prostatic cancer. *Cancer research,* 1**,** 297.

HUGHES, B. T., SIDOROVA, J., SWANGER, J., MONNAT, R. J., JR. & CLURMAN, B. E. 2013. Essential role for Cdk2 inhibitory phosphorylation during replication stress revealed by a human Cdk2 knockin mutation. *Proc Natl Acad Sci U S A,* 110**,** 8954-9.

HUSSAIN, S., ZHANG, Y. & GALARDY, P. 2009. DUBs and cancer: the role of deubiquitinating enzymes as oncogenes, non-oncogenes and tumor suppressors. *Cell cycle,* 8**,** 1688-1697.

IKEDA, F. & DIKIC, I. 2008. Atypical ubiquitin chains: new molecular signals. *EMBO reports,* 9**,** 536-542.

INUZUKA, H., GAO, D., FINLEY, L. W. S., YANG, W., WAN, L., FUKUSHIMA, H., CHIN, Y. R., ZHAI, B., SHAIK, S. & LAU, A. W. 2012. Acetylation-dependent regulation of Skp2 function. *Cell,* 150**,** 179-193.

IYER, N. G., ÖZDAG, H. & CALDAS, C. 2004. p300/CBP and cancer. *Oncogene,* 23**,** 4225-4231.

JACKSON, S. P. & BARTEK, J. 2009. The DNA-damage response in human biology and disease. *Nature,* 461**,** 1071-8.

JEFFREY, P. D., RUSSO, A. A., POLYAK, K., GIBBS, E., HURWITZ, J., MASSAGUE, J. & PAVLETICH, N. P. 1995. Mechanism of CDK activation revealed by the structure of a cyclinA-CDK2 complex. *Nature,* 376**,** 313-20.

JI, P., GOLDIN, L., REN, H., SUN, D., GUARDAVACCARO, D., PAGANO, M. & ZHU, L. 2006. Skp2 contains a novel cyclin a binding domain that directly protects cyclin a from inhibition by p27(Kip1). *Journal of Biological Chemistry,* 281**,** 24058-24069.

JI, P., SUN, D., WANG, H., BAUZON, F. & ZHU, L. 2007. Disrupting Skp2-cyclin A interaction with a blocking peptide induces selective cancer cell killing. *Mol Cancer Ther,* 6**,** 684-91.

JIA, L. & SUN, Y. 2011. SCF E3 Ubiquitin Ligases as Anticancer Targets. *Current Cancer Drug Targets,* 11**,** 347-356.

JIN, J., CARDOZO, T., LOVERING, R. C., ELLEDGE, S. J., PAGANO, M. & HARPER, J. W. 2004. Systematic analysis and nomenclature of mammalian F-box proteins. *Genes Dev,* 18**,** 2573-80.

JOAZEIRO, C. A. P. & WEISSMAN, A. M. 2000. RING Finger Proteins: Mediators of Ubiquitin Ligase Activity. *Cell,* 102**,** 549-552.

JOHNSON, A. & SKOTHEIM, J. M. 2013. Start and the Restriction Point. *Current opinion in cell biology,* 25**,** 10.1016/j.ceb.2013.07.010.

KALDIS, P., SUTTON, A. & SOLOMON, M. J. 1996. The Cdk-Activating Kinase (CAK) from Budding Yeast. *Cell,* 86**,** 553-564.

KAMURA, T., HARA, T., KOTOSHIBA, S., YADA, M., ISHIDA, N., IMAKI, H., HATAKEYAMA, S., NAKAYAMA, K. & NAKAYAMA, K. I. 2003. Degradation of p57Kip2 mediated by SCFSkp2-dependent ubiquitylation. *Proc Natl Acad Sci U S A,* 100**,** 10231-6.

KANE, R. C., DAGHER, R., FARRELL, A., KO, C. W., SRIDHARA, R., JUSTICE, R. & PAZDUR, R. 2007. Bortezomib for the treatment of mantle cell lymphoma. *Clin Cancer Res,* 13**,** 5291-4.

KARDINAL, C., DANGERS, M., KARDINAL, A., KOCH, A., BRANDT, D. T., TAMURA, T. & WELTE, K. 2006. Tyrosine phosphorylation modulates binding preference to cyclin-dependent kinases and subcellular localization of p27Kip1 in the acute promyelocytic leukemia cell line NB4. *Blood,* 107**,** 1133-1140.

KASTAN, M. B., ONYEKWERE, O., SIDRANSKY, D., VOGELSTEIN, B. & CRAIG, R. W. 1991. Participation of p53 protein in the cellular response to DNA damage. *Cancer Res,* 51**,** 6304-11.

KATSOGIANNOU, M., ZIOUZIOU, H., KARAKI, S., ANDRIEU, C., HENRY DE VILLENEUVE, M. & ROCCHI, P. 2015. The hallmarks of castration-resistant prostate cancers. *Cancer Treatment Reviews,* 41**,** 588-597.

KE, Q., JI, J., CHENG, C., ZHANG, Y., LU, M., WANG, Y., ZHANG, L., LI, P., CUI, X., CHEN, L., HE, S. & SHEN, A. 2009. Expression and prognostic role of Spy1 as a novel cell cycle protein in hepatocellular carcinoma. *Experimental and Molecular Pathology,* 87**,** 167-172.

KIM, H. S., PATEL, K., MULDOON-JACOBS, K., BISHT, K. S., AYKIN-BURNS, N., PENNINGTON, J. D., VAN DER MEER, R., NGUYEN, P., SAVAGE, J., OWENS, K. M., VASSILOPOULOS, A., OZDEN, O., PARK, S. H., SINGH, K. K., ABDULKADIR, S. A., SPITZ, D. R., DENG, C. X. & GIUS, D. 2010. SIRT3 is a mitochondria-localized tumor suppressor required for maintenance of mitochondrial integrity and metabolism during stress. *Cancer Cell,* 17**,** 41-52.

KIM, J., JONASCH, E., ALEXANDER, A., SHORT, J. D., CAI, S., WEN, S., TSAVACHIDOU, D., TAMBOLI, P., CZERNIAK, B. A. & DO, K. A. 2009. Cytoplasmic sequestration of p27 via AKT phosphorylation in renal cell carcinoma. *Clinical Cancer Research,* 15**,** 81-90.

KIM, K. K., CHAMBERLIN, H. M., MORGAN, D. O. & KIM, S.-H. 1996. Three-dimensional structure of human cyclin H, a positive regulator of the CDK-activating kinase. *Nature Structural & Molecular Biology,* 3**,** 849-855.

KOBE, B. & KAJAVA, A. V. 2001. The leucine-rich repeat as a protein recognition motif. *Curr Opin Struct Biol,* 11**,** 725-32.

KOKONTIS, J. M., LIN, H. P., JIANG, S. S., LIN, C. Y., FUKUCHI, J., HIIPAKKA, R. A., CHUNG, C. J., CHAN, T. M., LIAO, S., CHANG, C. H. & CHUU, C. P. 2014. Androgen suppresses the proliferation of androgen receptor-positive castration-resistant prostate cancer cells via inhibition of Cdk2, CyclinA, and Skp2. *PLoS One,* 9**,** e109170.

KOMANDER, D., CLAGUE, M. J. & URBE, S. 2009. Breaking the chains: structure and function of the deubiquitinases. *Nat Rev Mol Cell Biol,* 10**,** 550-563.

KOMANDER, D. & RAPE, M. 2012. The ubiquitin code. *Annu Rev Biochem,* 81**,** 203-29.

KORKOLOPOULOU, P., VASSILOPOULOS, I., KONSTANTINIDOU, A. E., ZORZOS, H., PATSOURIS, E., AGAPITOS, E. & DAVARIS, P. 2002. The combined evaluation of p27 Kip1 and Ki-67 expression provides independent information on overall survival of ovarian carcinoma patients. *Gynecologic oncology,* 85**,** 404-414.

KRATZAT, S., NIKOLOVA, V., MIETHING, C., HOELLEIN, A., SCHOEFFMANN, S., GORKA, O., PIETSCHMANN, E., ILLERT, A. L., RULAND, J., PESCHEL, C., NILSSON, J., DUYSTER, J. & KELLER, U. 2012. Cks1 is required for tumor cell proliferation but not sufficient to induce hematopoietic malignancies. *PLoS One,* 7**,** e37433.

KREK, W., XU, G. & LIVINGSTON, D. M. 1995. Cyclin A-kinase regulation of E2F-1 DNA binding function underlies suppression of an S phase checkpoint. *Cell,* 83**,** 1149-58.

KUERBITZ, S. J., PLUNKETT, B. S., WALSH, W. V. & KASTAN, M. B. 1992. Wild-type p53 is a cell cycle checkpoint determinant following irradiation. *Proc Natl Acad Sci U S A,* 89**,** 7491-5.

KULLMANN, M., GOPFERT, U., SIEWE, B. & HENGST, L. 2002. ELAV/Hu proteins inhibit p27 translation via an IRES element in the p27 5'UTR. *Genes Dev,* 16**,** 3087-99.

KUMAR, S., TSAI, C.-J. & NUSSINOV, R. 2000. Factors enhancing protein thermostability. *Protein Engineering,* 13**,** 179-191.

LABAER, J., GARRETT, M. D., STEVENSON, L. F., SLINGERLAND, J. M., SANDHU, C., CHOU, H. S., FATTAEY, A. & HARLOW, E. 1997. New functional activities for the p21 family of CDK inhibitors. *Genes Dev,* 11**,** 847-62.

LACY, E. R., FILIPPOV, I., LEWIS, W. S., OTIENO, S., XIAO, L., WEISS, S., HENGST, L. & KRIWACKI, R. W. 2004. p27 binds cyclin-CDK complexes through a sequential mechanism involving binding-induced protein folding. *Nat Struct Mol Biol,* 11**,** 358-64.

LACY, E. R., WANG, Y., POST, J., NOURSE, A., WEBB, W., MAPELLI, M., MUSACCHIO, A., SIUZDAK, G. & KRIWACKI, R. W. 2005. Molecular Basis for the Specificity of p27 Toward Cyclin-dependent Kinases that Regulate Cell Division. *Journal of Molecular Biology,* 349**,** 764-773.

LADBURY, J. E. 2004. Application of isothermal titration calorimetry in the biological sciences: things are heating up! *Biotechniques,* 37**,** 885-7.

LADBURY, J. E. & CHOWDHRY, B. Z. 1996. Sensing the heat: the application of isothermal titration calorimetry to thermodynamic studies of biomolecular interactions. *Chem Biol,* 3**,** 791-801.

LAM, Y. A., LAWSON, T. G., VELAYUTHAM, M., ZWEIER, J. L. & PICKART, C. M. 2002. A proteasomal ATPase subunit recognizes the polyubiquitin degradation signal. *Nature,* 416**,** 763-767.

LAMBER, E. P., BEURON, F., MORRIS, E. P., SVERGUN, D. I. & MITTNACHT, S. 2013. Structural insights into the mechanism of phosphoregulation of the retinoblastoma protein. *PLoS One,* 8**,** e58463.

LANE, H. A., BEUVINK, I., MOTOYAMA, A. B., DALY, J. M., NEVE, R. M. & HYNES, N. E. 2000. ErbB2 potentiates breast tumor proliferation through modulation of p27(Kip1)-Cdk2 complex formation: receptor overexpression does not determine growth dependency. *Mol Cell Biol,* 20**,** 3210-23.

LARKIN, M. A., BLACKSHIELDS, G., BROWN, N. P., CHENNA, R., MCGETTIGAN, P. A., MCWILLIAM, H., VALENTIN, F., WALLACE, I. M., WILM, A., LOPEZ, R., THOMPSON, J. D., GIBSON, T. J. & HIGGINS, D. G. 2007. Clustal W and Clustal X version 2.0. *Bioinformatics,* 23**,** 2947-8.

LEE, J. G. & KAY, E. P. 2007. Two populations of p27 use differential kinetics to phosphorylate Ser-10 and Thr-187 via phosphatidylinositol 3-Kinase in response to fibroblast growth factor-2 stimulation. *J Biol Chem,* 282**,** 6444-54.

LEE, J. H. & PAULL, T. T. 2005. ATM activation by DNA double-strand breaks through the Mre11-Rad50-Nbs1 complex. *Science,* 308**,** 551-4.

LEE, M. G. & NURSE, P. 1987. Complementation used to clone a human homologue of the fission yeast cell cycle control gene cdc2. *Nature,* 327**,** 31-5.

LEVINE, A. J. 1997. p53, the cellular gatekeeper for growth and division. *Cell,* 88**,** 323-31.

LI, M. & ZHANG, P. 2009. The function of APC/CCdh1 in cell cycle and beyond. *Cell Div,* 4**,** 2.

LI, T., PAVLETICH, N. P., SCHULMAN, B. A. & ZHENG, N. 2005. High-Level Expression and Purification of Recombinant SCF Ubiquitin Ligases. *In:* RAYMOND, J. D. (ed.) *Methods in Enzymology.* Academic Press.

LIANG, J., SHAO, S. H., XU, Z.-X., HENNESSY, B., DING, Z., LARREA, M., KONDO, S., DUMONT, D. J., GUTTERMAN, J. U., WALKER, C. L., SLINGERLAND, J. M. & MILLS, G. B. 2007. The energy sensing LKB1-AMPK pathway regulates p27kip1 phosphorylation mediating the decision to enter autophagy or apoptosis. *Nat Cell Biol,* 9**,** 218-224.

LIANG, J., ZUBOVITZ, J., PETROCELLI, T., KOTCHETKOV, R., CONNOR, M. K., HAN, K., LEE, J. H., CIARALLO, S., CATZAVELOS, C., BENISTON, R., FRANSSEN, E. & SLINGERLAND, J. M. 2002. PKB/Akt phosphorylates p27, impairs nuclear import of p27 and opposes p27-mediated G1 arrest. *Nat Med,* 8**,** 1153-60.

LIBERAL, V., MARTINSSON-AHLZEN, H. S., LIBERAL, J., SPRUCK, C. H., WIDSCHWENDTER, M., MCGOWAN, C. H. & REED, S. I. 2012. Cyclin-dependent kinase subunit (Cks) 1 or Cks2 overexpression overrides the DNA damage response barrier triggered by activated oncoproteins. *Proc Natl Acad Sci U S A,* 109**,** 2754-9.

LIN, D. I. & DIEHL, J. A. 2004. Mechanism of cell-cycle control: ligating the ligase. *Trends in biochemical sciences,* 29**,** 453-455.

LIN, H.-K., CHEN, Z., WANG, G., NARDELLA, C., LEE, S.-W., CHAN, C.-H., YANG, W.-L., WANG, J., EGIA, A., NAKAYAMA, K. I., CORDON-CARDO, C., TERUYA-FELDSTEIN, J. & PANDOLFI, P. P. 2010a. Skp2 targeting suppresses tumorigenesis by Arf-p53-independent cellular senescence. *Nature,* 464**,** 374-379.

LIN, H.-K., WANG, G., CHEN, Z., TERUYA-FELDSTEIN, J., LIU, Y., CHAN, C.-H., YANG, W.-L., ERDJUMENT-BROMAGE, H., NAKAYAMA, K. I., NIMER, S., TEMPST, P. & PANDOLFI, P. P. 2009. Phosphorylation-dependent regulation of cytosolic localization and oncogenic function of Skp2 by Akt/PKB. *Nature Cell Biology,* 11**,** 420-U144.

LIN, J. J., MILHOLLEN, M. A., SMITH, P. G., NARAYANAN, U. & DUTTA, A. 2010b. NEDD8-targeting drug MLN4924 elicits DNA rereplication by stabilizing Cdt1 in S phase, triggering checkpoint activation, apoptosis, and senescence in cancer cells. *Cancer Res,* 70**,** 10310-20.

LITTLEPAGE, L. E. & RUDERMAN, J. V. 2002. Identification of a new APC/C recognition domain, the A box, which is required for the Cdh1-dependent destruction of the kinase Aurora-A during mitotic exit. *Genes & development,* 16**,** 2274-2285.

LIU, B., LIU, M., WANG, J., ZHANG, X., WANG, X., WANG, P., WANG, H., LI, W. & WANG, Y. 2015. DICER-dependent biogenesis of let-7 miRNAs affects human cell response to DNA damage via targeting p21/p27. *Nucleic acids research,* 43**,** 1626-1636.

LIU, D., MATZUK, M. M., SUNG, W. K., GUO, Q., WANG, P. & WOLGEMUTH, D. J. 1998. Cyclin A1 is required for meiosis in the male mouse. *Nat Genet,* 20**,** 377-80.

LIU, P., BEGLEY, M., MICHOWSKI, W., INUZUKA, H., GINZBERG, M., GAO, D., TSOU, P., GAN, W., PAPA, A., KIM, B. M., WAN, L., SINGH, A., ZHAI, B., YUAN, M., WANG, Z., GYGI, S. P., LEE, T. H., LU, K. P., TOKER, A., PANDOLFI, P. P., ASARA, J. M., KIRSCHNER, M. W., SICINSKI, P., CANTLEY, L. & WEI, W. 2014. Cell-cycle-regulated activation of Akt kinase by phosphorylation at its carboxyl terminus. *Nature,* 508**,** 541-5.

LOLLI, G. 2010. Structural dissection of cyclin dependent kinases regulation and protein recognition properties. *Cell Cycle,* 9**,** 1551-61.

LOOG, M. & MORGAN, D. O. 2005. Cyclin specificity in the phosphorylation of cyclin-dependent kinase substrates. *Nature,* 434**,** 104-108.

LOWE, E. D., TEWS, I., CHENG, K. Y., BROWN, N. R., GUL, S., NOBLE, M. E., GAMBLIN, S. J. & JOHNSON, L. N. 2002. Specificity determinants of recruitment peptides bound to phospho-CDK2/cyclin A. *Biochemistry,* 41**,** 15625-34.

LOYER, P., TREMBLEY, J. H., KATONA, R., KIDD, V. J. & LAHTI, J. M. 2005. Role of CDK/cyclin complexes in transcription and RNA splicing. *Cellular Signalling,* 17**,** 1033-1051.

LU, L., SCHULZ, H. & WOLF, D. A. 2002. The F-box protein SKP2 mediates androgen control of p27 stability in LNCaP human prostate cancer cells. *BMC Cell Biol,* 3**,** 22.

LU, Z., BAUZON, F., FU, H., CUI, J., ZHAO, H., NAKAYAMA, K., NAKAYAMA, K. I. & ZHU, L. 2014. Skp2 suppresses apoptosis in Rb1-deficient tumours by limiting E2F1 activity. *Nat Commun,* 5**,** 3463.

LUBANSKA, D. & PORTER, L. A. 2014. The atypical cell cycle regulator Spy1 suppresses differentiation of the neuroblastoma stem cell population. *Oncoscience,* 1**,** 336.

LUKAS, C., SORENSEN, C. S., KRAMER, E., SANTONI-RUGIU, E., LINDENEG, C., PETERS, J.-M., BARTEK, J. & LUKAS, J. 1999. Accumulation of cyclin B1 requires E2F and cyclin-A-dependent rearrangement of the anaphase-promoting complex. *Nature,* 401**,** 815-818.

MACHIDA, Y. J. & DUTTA, A. 2007. The APC/C inhibitor, Emi1, is essential for prevention of rereplication. *Genes & development,* 21**,** 184-194.

MALLER, J., GAUTIER, J., LANGAN, T. A., LOHKA, M. J., SHENOY, S., SHALLOWAY, D. & NURSE, P. 1989. Maturation-promoting factor and the regulation of the cell cycle. *J Cell Sci Suppl,* 12**,** 53-63.

MALUMBRES, M. & BARBACID, M. 2005. Mammalian cyclin-dependent kinases. *Trends in Biochemical Sciences,* 30**,** 630-641.

MALUMBRES, M. & BARBACID, M. 2009. Cell cycle, CDKs and cancer: a changing paradigm. *Nat Rev Cancer,* 9**,** 153-166.

MARTI, A., WIRBELAUER, C., SCHEFFNER, M. & KREK, W. 1999. Interaction between ubiquitin-protein ligase SCFSKP2 and E2F-1 underlies the regulation of E2F-1 degradation. *Nat Cell Biol,* 1**,** 14-19.

MARTINSSON, H. S., STARBORG, M., ERLANDSSON, F. & ZETTERBERG, A. 2005. Single cell analysis of G1 check points-the relationship between the restriction point and phosphorylation of pRb. *Exp Cell Res,* 305**,** 383-91.

MARTINSSON-AHLZEN, H. S., LIBERAL, V., GRUNENFELDER, B., CHAVES, S. R., SPRUCK, C. H. & REED, S. I. 2008. Cyclin-dependent kinase-associated proteins Cks1 and Cks2 are essential during early embryogenesis and for cell cycle progression in somatic cells. *Mol Cell Biol,* 28**,** 5698-709.

MASCIULLO, V., FERRANDINA, G., PUCCI, B., FANFANI, F., LOVERGINE, S., PALAZZO, J., ZANNONI, G., MANCUSO, S., SCAMBIA, G. & GIORDANO, A. 2000. p27Kip1 expression is associated with clinical outcome in advanced epithelial ovarian cancer: multivariate analysis. *Clinical cancer research,* 6**,** 4816-4822.

MATSUOKA, S., BALLIF, B. A., SMOGORZEWSKA, A., MCDONALD, E. R., 3RD, HUROV, K. E., LUO, J., BAKALARSKI, C. E., ZHAO, Z., SOLIMINI, N., LERENTHAL, Y., SHILOH, Y., GYGI, S. P. & ELLEDGE,

S. J. 2007. ATM and ATR substrate analysis reveals extensive protein networks responsive to DNA damage. *Science,* 316**,** 1160-6.

MATSUSHIME, H., EWEN, M. E., STROM, D. K., KATO, J. Y., HANKS, S. K., ROUSSEL, M. F. & SHERR, C. J. 1992. Identification and properties of an atypical catalytic subunit (p34PSK-J3/cdk4) for mammalian D type G1 cyclins. *Cell,* 71**,** 323-34.

MCANDREW, C. W., GASTWIRT, R. F., MEYER, A. N., PORTER, L. A. & DONOGHUE, D. J. 2007. Spy1 enhances phosphorylation and degradation of the cell cycle inhibitor p27. *Cell Cycle,* 6**,** 1937-1945.

MEIJER, L., ARION, D., GOLSTEYN, R., PINES, J., BRIZUELA, L., HUNT, T. & BEACH, D. 1989. Cyclin is a component of the sea urchin egg M-phase specific histone H1 kinase. *The EMBO Journal,* 8**,** 2275-2282.

MEYERSON, M., ENDERS, G. H., WU, C. L., SU, L. K., GORKA, C., NELSON, C., HARLOW, E. & TSAI, L. H. 1992. A family of human cdc2-related protein kinases. *Embo j,* 11**,** 2909-17.

MILHOLLEN, M. A., THOMAS, M. P., NARAYANAN, U., TRAORE, T., RICEBERG, J., AMIDON, B. S., BENCE, N. F., BOLEN, J. B., BROWNELL, J. & DICK, L. R. 2012. Treatment-emergent mutations in NAEβ confer resistance to the NEDD8-activating enzyme inhibitor MLN4924. *Cancer cell,* 21**,** 388-401.

MILLARD, S. S., VIDAL, A., MARKUS, M. & KOFF, A. 2000. A U-rich element in the 5' untranslated region is necessary for the translation of p27 mRNA. *Mol Cell Biol,* 20**,** 5947-59.

MILLER, J. J., SUMMERS, M. K., HANSEN, D. V., NACHURY, M. V., LEHMAN, N. L., LOKTEV, A. & JACKSON, P. K. 2006. Emi1 stably binds and inhibits the anaphase-promoting complex/cyclosome as a pseudosubstrate inhibitor. *Genes & development,* 20**,** 2410-2420.

MITRA, J., ENDERS, G. H., AZIZKHAN-CLIFFORD, J. & LENGEL, K. L. 2006. Dual regulation of the anaphase promoting complex in human cells by cyclin A-Cdk2 and cyclin A-Cdk1 complexes. *Cell Cycle,* 5**,** 662-667.

MITTNACHT, S., LEES, J. A., DESAI, D., HARLOW, E., MORGAN, D. O. & WEINBERG, R. A. 1994. Distinct sub-populations of the retinoblastoma protein show a distinct pattern of phosphorylation. *EMBO J,* 13**,** 118-27.

MONTAGNOLI, A., FIORE, F., EYTAN, E., CARRANO, A. C., DRAETTA, G. F., HERSHKO, A. & PAGANO, M. 1999. Ubiquitination of p27 is regulated by Cdk-dependent phosphorylation and trimeric complex formation. *Genes Dev,* 13**,** 1181-9.

MORGAN, D. O. 1997. Cyclin-dependent kinases: engines, clocks, and microprocessors. *Annu Rev Cell Dev Biol,* 13**,** 261-91.

MORGAN, D. O. 2007. *The Cell Cycle: Principles of Control*, OUP/New Science Press.

MOYNAHAN, M. E. & JASIN, M. 2010. Mitotic homologous recombination maintains genomic stability and suppresses tumorigenesis. *Nat Rev Mol Cell Biol,* 11**,** 196-207.

MULLIGAN, G. & JACKS, T. 1998. The retinoblastoma gene family: cousins with overlapping interests. *Trends Genet,* 14**,** 223-9.

MURPHY, M., STINNAKRE, M. G., SENAMAUD-BEAUFORT, C., WINSTON, N. J., SWEENEY, C., KUBELKA, M., CARRINGTON, M., BRECHOT, C. & SOBCZAK-THEPOT, J. 1997. Delayed early embryonic lethality following disruption of the murine cyclin A2 gene. *Nat Genet,* 15**,** 83-6.

MURRAY, A. W. 2004. Recycling the Cell Cycle: Cyclins Revisited. *Cell,* 116**,** 221-234.

MURSHUDOV, G. N., VAGIN, A. A. & DODSON, E. J. 1997. Refinement of macromolecular structures by the maximum-likelihood method. *Acta Crystallographica Section D: Biological Crystallography,* 53**,** 240-255.

NAKAYAMA, K., ISHIDA, N., SHIRANE, M., INOMATA, A., INOUE, T., SHISHIDO, N., HORII, I., LOH, D. Y. & NAKAYAMA, K.-I. 1996. Mice Lacking p27Kip1 Display Increased Body Size, Multiple Organ Hyperplasia, Retinal Dysplasia, and Pituitary Tumors. *Cell,* 85**,** 707-720.

NAKAYAMA, K., NAGAHAMA, H., MINAMISHIMA, Y. A., MATSUMOTO, M., NAKAMICHI, I., KITAGAWA, K., SHIRANE, M., TSUNEMATSU, R., TSUKIYAMA, T., ISHIDA, N., KITAGAWA, M., NAKAYAMA, K. & HATAKEYAMA, S. 2000. Targeted disruption of Skp2 results in accumulation of cyclin E and p27(Kip1), polyploidy and centrosome overduplication. *EMBO J,* 19**,** 2069-81.

NAKAYAMA, K., NAGAHAMA, H., MINAMISHIMA, Y. A., MIYAKE, S., ISHIDA, N., HATAKEYAMA, S., KITAGAWA, M., IEMURA, S., NATSUME, T. & NAKAYAMA, K. I. 2004. Skp2-mediated degradation of p27 regulates progression into mitosis. *Dev Cell,* 6**,** 661-72.

NAKAYAMA, K. I. & NAKAYAMA, K. 2006. Ubiquitin ligases: cell-cycle control and cancer. *Nat Rev Cancer,* 6**,** 369-381.

NARASIMHA, A. M., KAULICH, M., SHAPIRO, G. S., CHOI, Y. J., SICINSKI, P. & DOWDY, S. F. 2014. Cyclin D activates the Rb tumor suppressor by mono-phosphorylation. *Elife,* 3**,** e02872.

NASH, P., TANG, X., ORLICKY, S., CHEN, Q., GERTLER, F. B., MENDENHALL, M. D., SICHERI, F., PAWSON, T. & TYERS, M. 2001. Multisite phosphorylation of a CDK inhibitor sets a threshold for the onset of DNA replication. *Nature,* 414**,** 514-21.

NAWAZ, Z. & O'MALLEY, B. W. 2004. Urban renewal in the nucleus: is protein turnover by proteasomes absolutely required for nuclear receptor-regulated transcription? *Mol Endocrinol,* 18**,** 493-9.

NIGRO, J. M., BAKER, S. J., PREISINGER, A. C., JESSUP, J. M., HOSTELLER, R., CLEARY, K., SIGNER, S. H., DAVIDSON, N., BAYLIN, S., DEVILEE, P., GLOVER, T., COLLINS, F. S., WESLON, A., MODALI, R., HARRIS, C. C. & VOGELSTEIN, B. 1989. Mutations in the p53 gene occur in diverse human tumour types. *Nature,* 342**,** 705-708.

NOBLE, M. E., ENDICOTT, J. A., BROWN, N. R. & JOHNSON, L. N. 1997. The cyclin box fold: protein recognition in cell-cycle and transcription control. *Trends Biochem Sci,* 22**,** 482-7.

OKAMOTO, Y., OZAKI, T., MIYAZAKI, K., AOYAMA, M., MIYAZAKI, M. & NAKAGAWARA, A. 2003. UbcH10 is the cancer-related E2 ubiquitin-conjugating enzyme. *Cancer research,* 63**,** 4167-4173.

OOI, L.-C., WATANABE, N., FUTAMURA, Y., SULAIMAN, S. F., DARAH, I. & OSADA, H. 2013. Identification of small molecule inhibitors of p27Kip1 ubiquitination by high-throughput screening. *Cancer Science,* 104**,** 1461-1467.

ORLICKY, S., TANG, X., WILLEMS, A., TYERS, M. & SICHERI, F. 2003. Structural Basis for Phosphodependent Substrate Selection and Orientation by the SCFCdc4 Ubiquitin Ligase. *Cell,* 112**,** 243-256.

ORLOWSKI, R. Z. & KUHN, D. J. 2008. Proteasome inhibitors in cancer therapy: lessons from the first decade. *Clin Cancer Res,* 14**,** 1649-57.

ORTEGA, S., MALUMBRES, M. & BARBACID, M. 2002. Cyclin D-dependent kinases, INK4 inhibitors and cancer. *Biochim Biophys Acta,* 1602**,** 73-87.

ORTEGA, S., PRIETO, I., ODAJIMA, J., MARTIN, A., DUBUS, P., SOTILLO, R., BARBERO, J. L., MALUMBRES, M. & BARBACID, M. 2003. Cyclin-dependent kinase 2 is essential for meiosis but not for mitotic cell division in mice. *Nat Genet,* 35**,** 25-31.

OSHITA, F., KAMEDA, Y., NISHIO, K., TANAKA, G., YAMADA, K., NOMURA, I., NAKAYAMA, H. & NODA, K. 2000. Increased expression levels of cyclin-dependent kinase inhibitor p27 correlate with good responses to platinum-based chemotherapy in non-small cell lung cancer. *Oncology reports,* 7**,** 491-496.

OSTAPENKO, D., BURTON, J. L., WANG, R. & SOLOMON, M. J. 2008. Pseudosubstrate inhibition of the anaphase-promoting complex by Acm1: regulation by proteolysis and Cdc28 phosphorylation. *Molecular and cellular biology,* 28**,** 4653-4664.

OU, L., FERREIRA, A. M., OTIENO, S., XIAO, L., BASHFORD, D. & KRIWACKI, R. W. 2011. Incomplete folding upon binding mediates Cdk4/cyclin D complex activation by tyrosine phosphorylation of inhibitor p27 protein. *J Biol Chem,* 286**,** 30142-51.

PAGANO, M., PEPPERKOK, R., VERDE, F., ANSORGE, W. & DRAETTA, G. 1992. Cyclin A is required at two points in the human cell cycle. *Embo j,* 11**,** 961-71.

PAGANO, M., TAM, S. W., THEODORAS, A. M., BEER-ROMERO, P., DEL SAL, G., CHAU, V., YEW, P. R., DRAETTA, G. F. & ROLFE, M. 1995. Role of the ubiquitin-proteasome pathway in regulating abundance of the cyclin-dependent kinase inhibitor p27. *Science,* 269**,** 682-5.

PARDEE, A. B. 1989. G1 events and regulation of cell proliferation. *Science,* 246**,** 603-8.

PARGE, H. E., ARVAI, A. S., MURTARI, D. J., REED, S. I. & TAINER, J. A. 1993. Human CksHs2 atomic structure: a role for its hexameric assembly in cell cycle control. *Science,* 262**,** 387-95.

PAVLIDES, S. C., HUANG, K.-T., REID, D. A., WU, L., BLANK, S. V., MITTAL, K., GUO, L., ROTHENBERG, E., RUEDA, B. & CARDOZO, T. 2013. Inhibitors of SCF-Skp2/Cks1 E3 ligase block estrogen-induced growth stimulation and degradation of nuclear p27kip1: therapeutic potential for endometrial cancer. *Endocrinology,* 154**,** 4030-4045.

PFLEGER, C. M. & KIRSCHNER, M. W. 2000. The KEN box: an APC recognition signal distinct from the D box targeted by Cdh1. *Genes & Development,* 14**,** 655-665.

PINES, J. 1993. Cyclins and their associated cyclin-dependent kinases in the human cell cycle. *Biochem Soc Trans,* 21**,** 921-5.

PINES, J. 1995. Cyclins and cyclin-dependent kinases: a biochemical view. *Biochem J,* 308 (Pt 3)**,** 697-711.

PINES, J. 1996. Cyclin from sea urchins to HeLas: making the human cell cycle. *Biochem Soc Trans,* 24**,** 15-33.

PINES, J. 2006. Mitosis: a matter of getting rid of the right protein at the right time. *Trends Cell Biol,* 16**,** 55-63.

PINES, J. 2011. Cubism and the cell cycle: the many faces of the APC/C. *Nat Rev Mol Cell Biol,* 12**,** 427-38.

PLAS, D. R. & THOMPSON, C. B. 2005. Akt-dependent transformation: there is more to growth than just surviving. *Oncogene,* 24**,** 7435-42.

POLYAK, K., KATO, J. Y., SOLOMON, M. J., SHERR, C. J., MASSAGUE, J., ROBERTS, J. M. & KOFF, A. 1994a. p27Kip1, a cyclin-Cdk inhibitor, links transforming growth factor-beta and contact inhibition to cell cycle arrest. *Genes Dev,* 8**,** 9-22.

POLYAK, K., LEE, M. H., ERDJUMENT-BROMAGE, H., KOFF, A., ROBERTS, J. M., TEMPST, P. & MASSAGUE, J. 1994b. Cloning of p27Kip1, a cyclin-dependent kinase inhibitor and a potential mediator of extracellular antimitogenic signals. *Cell,* 78**,** 59-66.

PORTER, L. A., DELLINGER, R. W., TYNAN, J. A., BARNES, E. A., KONG, M., LENORMAND, J. L. & DONOGHUE, D. J. 2002. Human Speedy: a novel cell cycle regulator that enhances proliferation through activation of Cdk2. *J Cell Biol,* 157**,** 357-66.

PORTER, L. A., KONG-BELTRAN, M. & DONOGHUE, D. J. 2003. Spy1 interacts with p27Kip1 to allow G1/S progression. *Mol Biol Cell,* 14**,** 3664-74.

RADKE, S., PIRKMAIER, A. & GERMAIN, D. 2005. Differential expression of the F-box proteins Skp2 and Skp2B in breast cancer. *Oncogene,* 24**,** 3448-58.

RATH, A., GLIBOWICKA, M., NADEAU, V. G., CHEN, G. & DEBER, C. M. 2009. Detergent binding explains anomalous SDS-PAGE migration of membrane proteins. *Proc Natl Acad Sci U S A,* 106**,** 1760-5.

REED, S. I. 2003. Ratchets and clocks: the cell cycle, ubiquitylation and protein turnover. *Nat Rev Mol Cell Biol,* 4**,** 855-64.

REED, S. I. 2005. Skp'n with Cks1: Revelations from the Skp1-Skp2-Cks1-p27 Structure. *Molecular Cell,* 20**,** 1-2.

REYNISDOTTIR, I., POLYAK, K., IAVARONE, A. & MASSAGUE, J. 1995. Kip/Cip and Ink4 Cdk inhibitors cooperate to induce cell cycle arrest in response to TGF-beta. *Genes Dev,* 9**,** 1831-45.

RILEY, T., SONTAG, E., CHEN, P. & LEVINE, A. 2008. Transcriptional control of human p53-regulated genes. *Nat Rev Mol Cell Biol,* 9**,** 402-12.

ROBERTS, J. M. 1999. Evolving Ideas about Cyclins. *Cell,* 98**,** 129-132.

RODIER, G., COULOMBE, P., TANGUAY, P. L., BOUTONNET, C. & MELOCHE, S. 2008. Phosphorylation of Skp2 regulated by CDK2 and Cdc14B protects it from degradation by APCCdh1 in G1 phase. *The EMBO journal,* 27**,** 679-691.

RODIER, G., MONTAGNOLI, A., DI MARCOTULLIO, L., COULOMBE, P., DRAETTA, G. F., PAGANO, M. & MELOCHE, S. 2001. p27 cytoplasmic localization is regulated by phosphorylation on Ser10 and is not a prerequisite for its proteolysis. *EMBO J,* 20**,** 6672-82.

ROY, A., LAHIRY, L., BANERJEE, D., GHOSH, M. & BANERJEE, S. 2013. Increased cytoplasmic localization of p27(kip1) and its modulation of RhoA activity during progression of chronic myeloid leukemia. *PLoS One,* 8**,** e76527.

RUDDICK, H. 2010. *In vitro characterisation of Skp2 binding to CyclinA using CyclinA mutants.* MSc, Oxford University.

RUFFNER, H., JIANG, W., CRAIG, A. G., HUNTER, T. & VERMA, I. M. 1999. BRCA1 is phosphorylated at serine 1497 in vivo at a cyclin-dependent kinase 2 phosphorylation site. *Mol Cell Biol,* 19**,** 4843-54.

RUSSELL, P., MORENO, S. & REED, S. I. 1989. Conservation of mitotic controls in fission and budding yeasts. *Cell,* 57**,** 295-303.

RUSSO, A. A., JEFFREY, P. D., PATTEN, A. K., MASSAGUÉ, J. & PAVLETICH, N. P. 1996a. Crystal structure of the p27Kip1 cyclin-dependent-kinase inhibitor bound to the cyclin A-Cdk2 complex. *Nature,* 382**,** 325-331.

RUSSO, A. A., JEFFREY, P. D. & PAVLETICH, N. P. 1996b. Structural basis of cyclin-dependent kinase activation by phosphorylation. *Nat Struct Biol,* 3**,** 696-700.

SAKAGUCHI, K., HERRERA, J. E., SAITO, S., MIKI, T., BUSTIN, M., VASSILEV, A., ANDERSON, C. W. & APPELLA, E. 1998. DNA damage activates p53 through a phosphorylation-acetylation cascade. *Genes Dev,* 12**,** 2831-41.

SANTAMARIA, D., BARRIERE, C., CERQUEIRA, A., HUNT, S., TARDY, C., NEWTON, K., CACERES, J. F., DUBUS, P., MALUMBRES, M. & BARBACID, M. 2007. Cdk1 is sufficient to drive the mammalian cell cycle. *Nature,* 448**,** 811-5.

SARCEVIC, B., LILISCHKIS, R. & SUTHERLAND, R. L. 1997. Differential phosphorylation of T-47D human breast cancer cell substrates by D1-, D3-, E-, and A-type cyclin-CDK complexes. *J Biol Chem,* 272**,** 33327-37.

SATYANARAYANA, A. & KALDIS, P. 2009. Mammalian cell-cycle regulation: several Cdks, numerous cyclins and diverse compensatory mechanisms. *Oncogene,* 28**,** 2925-39.

SCHNEIDER, G., SAUR, D., SIVEKE, J. T., FRITSCH, R., GRETEN, F. R. & SCHMID, R. M. 2006. IKKalpha controls p52/RelB at the skp2 gene promoter to regulate G1- to S-phase progression. *EMBO J,* 25**,** 3801-12.

SCHREIBER, A., STENGEL, F., ZHANG, Z., ENCHEV, R. I., KONG, E. H., MORRIS, E. P., ROBINSON, C. V., DA FONSECA, P. C. & BARFORD, D. 2011. Structural basis for the subunit assembly of the anaphase-promoting complex. *Nature,* 470**,** 227-32.

SCHUELLER, N. 2001. *Structural characterisation of Skp1 and Skp2: Assembly into complexes with CDK2/cyclin A and as components of human SCF^{Skp2}.* MSc, Oxford University.

SCHULMAN, B. A., CARRANO, A. C., JEFFREY, P. D., BOWEN, Z., KINNUCAN, E. R., FINNIN, M. S., ELLEDGE, S. J., HARPER, J. W., PAGANO, M. & PAVLETICH, N. P. 2000. Insights into SCF ubiquitin ligases from the structure of the Skp1-Skp2 complex. *Nature,* 408**,** 381-6.

SCHULZE, A., ZERFASS, K., SPITKOVSKY, D., MIDDENDORP, S., BERGES, J., HELIN, K., JANSEN-DURR, P. & HENGLEIN, B. 1995. Cell cycle regulation of the cyclin A gene promoter is mediated by a variant E2F site. *Proc Natl Acad Sci U S A,* 92**,** 11264-8.

SCHULZE-GAHMEN, U., UPTON, H., BIRNBERG, A., BAO, K., CHOU, S., KROGAN, N. J., ZHOU, Q. & ALBER, T. 2013. The AFF4 scaffold binds human P-TEFb adjacent to HIV Tat. *Elife,* 2**,** e00327.

SEELIGER, M. A., BREWARD, S. E., FRIEDLER, A., SCHON, O. & ITZHAKI, L. S. 2003. Cooperative organization in a macromolecular complex. *Nat Struct Biol,* 10**,** 718-24.

SEKIMOTO, T., FUKUMOTO, M. & YONEDA, Y. 2004. 14-3-3 suppresses the nuclear localization of threonine 157-phosphorylated p27Kip1. *The EMBO journal,* 23**,** 1934-1942.

SHAPIRA, M. A., KAKIASHVILI, E., ROSENBERG, T. & HERSHKO, D. D. 2006. The mTOR inhibitor rapamycin down-regulates the expression of the ubiquitin ligase subunit Skp2 in breast cancer cells. *Breast Cancer Research,* 8**,** R46.

SHERR, C. J. 1993. Mammalian G 1 cyclins. *Cell,* 73**,** 1059-1065.

SHERR, C. J. 1995. D-type cyclins. *Trends in Biochemical Sciences,* 20**,** 187-190.

SHERR, C. J. 2000. Cell cycle control and cancer. *Harvey Lect,* 96**,** 73-92.

SHERR, C. J. 2012. Ink4-Arf locus in cancer and aging. *Wiley Interdiscip Rev Dev Biol,* 1**,** 731-41.

SHERR, C. J. & ROBERTS, J. M. 1999. CDK inhibitors: positive and negative regulators of G1-phase progression. *Genes Dev,* 13**,** 1501-12.

SHERR, C. J. & ROBERTS, J. M. 2004. Living with or without cyclins and cyclin-dependent kinases. *Genes & development,* 18**,** 2699-2711.

SHI, L., WANG, S., ZANGARI, M., XU, H., CAO, T. M., XU, C., WU, Y., XIAO, F., LIU, Y. & YANG, Y. 2010. Over-expression of CKS1B activates both MEK/ERK and JAK/STAT3 signaling pathways and promotes myeloma cell drug-resistance. *Oncotarget,* 1**,** 22.

SHICHIRI, M., HANSON, K. D. & SEDIVY, J. M. 1993. Effects of c-myc expression on proliferation, quiescence, and the G0 to G1 transition in nontransformed cells. *Cell Growth Differ,* 4**,** 93-104.

SHORT, J. D., DERE, R., HOUSTON, K. D., CAI, S.-L., KIM, J., BERGERON, J. M., SHEN, J., LIANG, J., BEDFORD, M. T., MILLS, G. B. & WALKER, C. L. 2010. AMPK-Mediated Phosphorylation of Murine p27 at T197 Promotes Binding of 14-3-3 Proteins and Increases p27 Stability. *Molecular carcinogenesis,* 49**,** 10.1002/mc.20613.

SIEVERS, F., WILM, A., DINEEN, D., GIBSON, T. J., KARPLUS, K., LI, W., LOPEZ, R., MCWILLIAM, H., REMMERT, M. & SÖDING, J. 2011. Fast, scalable generation of high-quality protein multiple sequence alignments using Clustal Omega. *Molecular systems biology,* 7**,** 539.

SIGNORETTI, S., DI MARCOTULLIO, L., RICHARDSON, A., RAMASWAMY, S., ISAAC, B., RUE, M., MONTI, F., LODA, M. & PAGANO, M. 2002. Oncogenic role of the ubiquitin ligase subunit Skp2 in human breast cancer. *J Clin Invest,* 110**,** 633-41.

SINGH, S. P., LIPMAN, J., GOLDMAN, H., ELLIS, F. H., JR., AIZENMAN, L., CANGI, M. G., SIGNORETTI, S., CHIAUR, D. S., PAGANO, M. & LODA, M. 1998. Loss or altered subcellular localization of p27 in Barrett's associated adenocarcinoma. *Cancer Res,* 58**,** 1730-5.

SITRY, D., SEELIGER, M. A., KO, T. K., GANOTH, D., BREWARD, S. E., ITZHAKI, L. S., PAGANO, M. & HERSHKO, A. 2002. Three different binding sites of Cks1 are required for p27-ubiquitin ligation. *J Biol Chem,* 277**,** 42233-40.

SKAAR, J. R. & PAGANO, M. 2009. Control of cell growth by the SCF and APC/C ubiquitin ligases. *Current Opinion in Cell Biology,* 21**,** 816-824.

SONG, G., OUYANG, G. & BAO, S. 2005. The activation of Akt/PKB signaling pathway and cell survival. *Journal of cellular and molecular medicine,* 9**,** 59.

SONODA, H., INOUE, H., OGAWA, K., UTSUNOMIYA, T., MASUDA, T. A. & MORI, M. 2006. Significance of skp2 expression in primary breast cancer. *Clin Cancer Res,* 12**,** 1215-20.

SOOS, T. J., KIYOKAWA, H., YAN, J. S., RUBIN, M. S., GIORDANO, A., DEBLASIO, A., BOTTEGA, S., WONG, B., MENDELSOHN, J. & KOFF, A. 1996. Formation of p27-CDK complexes during the human mitotic cell cycle. *Cell Growth Differ,* 7**,** 135-46.

SØRENSEN, C. S., LUKAS, C., KRAMER, E. R., PETERS, J.-M., BARTEK, J. & LUKAS, J. 2001. A conserved cyclin-binding domain determines functional interplay between anaphase-promoting complex–Cdh1 and cyclin A-Cdk2 during cell cycle progression. *Molecular and cellular biology,* 21**,** 3692-3703.

SORENSEN, C. S., LUKAS, C., KRAMER, E. R., PETERS, J. M., BARTEK, J. & LUKAS, J. 2000. Nonperiodic activity of the human anaphase-promoting complex-Cdh1 ubiquitin ligase results in continuous DNA synthesis uncoupled from mitosis. *Mol Cell Biol,* 20**,** 7613-23.

SOUCY, T. A., SMITH, P. G., MILHOLLEN, M. A., BERGER, A. J., GAVIN, J. M., ADHIKARI, S., BROWNELL, J. E., BURKE, K. E., CARDIN, D. P., CRITCHLEY, S., CULLIS, C. A., DOUCETTE, A., GARNSEY, J. J., GAULIN, J. L., GERSHMAN, R. E., LUBLINSKY, A. R., MCDONALD, A., MIZUTANI, H., NARAYANAN, U., OLHAVA, E. J., PELUSO, S., REZAEI, M., SINTCHAK, M. D., TALREJA, T., THOMAS, M. P., TRAORE, T., VYSKOCIL, S., WEATHERHEAD, G. S., YU, J., ZHANG, J., DICK, L. R., CLAIBORNE, C. F., ROLFE, M., BOLEN, J. B. & LANGSTON, S. P. 2009. An inhibitor of NEDD8-activating enzyme as a new approach to treat cancer. *Nature,* 458**,** 732-736.

SPRUCK, C., STROHMAIER, H., WATSON, M., SMITH, A. P., RYAN, A., KREK, T. W. & REED, S. I. 2001. A CDK-independent function of mammalian Cks1: targeting of SCF(Skp2) to the CDK inhibitor p27Kip1. *Mol Cell,* 7**,** 639-50.

SPRUCK, C. H., DE MIGUEL, M. P., SMITH, A. P., RYAN, A., STEIN, P., SCHULTZ, R. M., LINCOLN, A. J., DONOVAN, P. J. & REED, S. I. 2003. Requirement of Cks2 for the first metaphase/anaphase transition of mammalian meiosis. *Science,* 300**,** 647-50.

SREERAMA, N. & WOODY, R. W. 1994. Protein secondary structure from circular dichroism spectroscopy: Combining variable selection principle and cluster analysis with neural network, ridge regression and self-consistent methods. *Journal of molecular biology,* 242**,** 497-507.

ST CROIX, B., FLORENES, V. A., RAK, J. W., FLANAGAN, M., BHATTACHARYA, N., SLINGERLAND, J. M. & KERBEL, R. S. 1996. Impact of the cyclin-dependent kinase inhibitor p27Kip1 on resistance of tumor cells to anticancer agents. *Nat Med,* 2**,** 1204-10.

STEVENSON, L. M., DEAL, M. S., HAGOPIAN, J. C. & LEW, J. 2002. Activation mechanism of CDK2: role of cyclin binding versus phosphorylation. *Biochemistry,* 41**,** 8528-34.

SUDAKIN, V., GANOTH, D., DAHAN, A., HELLER, H., HERSHKO, J., LUCA, F. C., RUDERMAN, J. V. & HERSHKO, A. 1995. The cyclosome, a large complex containing cyclin-selective ubiquitin ligase activity, targets cyclins for destruction at the end of mitosis. *Mol Biol Cell,* 6**,** 185-97.

SUN, L., CAI, L., YU, Y., MENG, Q., CHENG, X., ZHAO, Y., SUI, G. & ZHANG, F. 2007. Knockdown of S-phase kinase-associated protein-2 expression in MCF-7 inhibits cell growth and enhances the cytotoxic effects of epirubicin. *Acta Biochim Biophys Sin (Shanghai),* 39**,** 999-1007.

SUTTERLUTY, H., CHATELAIN, E., MARTI, A., WIRBELAUER, C., SENFTEN, M., MULLER, U. & KREK, W. 1999. p45SKP2 promotes p27Kip1 degradation and induces S phase in quiescent cells. *Nat Cell Biol,* 1**,** 207-14.

SWORDS, R. T., ERBA, H. P., DEANGELO, D. J., BIXBY, D. L., ALTMAN, J. K., MARIS, M., HUA, Z., BLAKEMORE, S. J., FAESSEL, H., SEDARATI, F., DEZUBE, B. J., GILES, F. J. & MEDEIROS, B. C. 2015. Pevonedistat (MLN4924), a First-in-Class NEDD8-activating enzyme inhibitor, in patients with acute myeloid leukaemia and myelodysplastic syndromes: a phase 1 study. *British Journal of Haematology,* 169**,** 534-543.

TAHIROV, T. H., BABAYEVA, N. D., VARZAVAND, K., COOPER, J. J., SEDORE, S. C. & PRICE, D. H. 2010. Crystal structure of HIV-1 Tat complexed with human P-TEFb. *Nature,* 465**,** 747-51.

TAKAKI, T., ECHALIER, A., BROWN, N. R., HUNT, T., ENDICOTT, J. A. & NOBLE, M. E. 2009. The structure of CDK4/cyclin D3 has implications for models of CDK activation. *Proc Natl Acad Sci U S A,* 106**,** 4171-6.

TALASZ, H., HELLIGER, W., PUSCHENDORF, B. & LINDNER, H. 1996. In vivo phosphorylation of histone H1 variants during the cell cycle. *Biochemistry,* 35**,** 1761-7.

TANG, X., GAO, J. S., GUAN, Y. J., MCLANE, K. E., YUAN, Z. L., RAMRATNAM, B. & CHIN, Y. E. 2007. Acetylation-dependent signal transduction for type I interferon receptor. *Cell,* 131**,** 93-105.

TEDESCO, D., LUKAS, J. & REED, S. I. 2002. The pRb-related protein p130 is regulated by phosphorylation-dependent proteolysis via the protein-ubiquitin ligase SCF(Skp2). *Genes Dev,* 16**,** 2946-57.

TEIXEIRA, L. K. & REED, S. I. 2013. Ubiquitin ligases and cell cycle control. *Annual review of biochemistry,* 82**,** 387-414.

TENNO, T., FUJIWARA, K., TOCHIO, H., IWAI, K., MORITA, E. H., HAYASHI, H., MURATA, S., HIROAKI, H., SATO, M., TANAKA, K. & SHIRAKAWA, M. 2004. Structural basis for distinct roles of Lys63- and Lys48-linked polyubiquitin chains. *Genes Cells,* 9**,** 865-75.

TOTH, J. I., YANG, L., DAHL, R. & PETROSKI, M. D. 2012. A gatekeeper residue for NEDD8-activating enzyme inhibition by MLN4924. *Cell reports,* 1**,** 309-316.

TOYOSHIMA, H. & HUNTER, T. 1994. p27, a novel inhibitor of G1 cyclin-Cdk protein kinase activity, is related to p21. *Cell,* 78**,** 67-74.

TSIHLIAS, J., KAPUSTA, L. R., DEBOER, G., MORAVA-PROTZNER, I., ZBIERANOWSKI, I., BHATTACHARYA, N., CATZAVELOS, G. C., KLOTZ, L. H. & SLINGERLAND, J. M. 1998. Loss of cyclin-dependent kinase inhibitor p27Kip1 is a novel prognostic factor in localized human prostate adenocarcinoma. *Cancer Res,* 58**,** 542-8.

TSVETKOV, L. M., YEH, K. H., LEE, S. J., SUN, H. & ZHANG, H. 1999. p27(Kip1) ubiquitination and degradation is regulated by the SCF(Skp2) complex through phosphorylated Thr187 in p27. *Curr Biol,* 9**,** 661-4.

UNGERMANNOVA, D., GAO, Y. & LIU, X. 2005. Ubiquitination of p27Kip1 requires physical interaction with cyclin E and probable phosphate recognition by SKP2. *J Biol Chem,* 280**,** 30301-9.

UNGERMANNOVA, D., LEE, J., ZHANG, G., DALLMANN, H. G., MCHENRY, C. S. & LIU, X. 2013. High-throughput screening AlphaScreen assay for identification of small-molecule inhibitors of ubiquitin E3 ligase SCFSkp2-Cks1. *J Biomol Screen,* 18**,** 910-20.

VAGIN, A. & TEPLYAKOV, A. 1997. MOLREP: an automated program for molecular replacement. *Journal of applied crystallography,* 30**,** 1022-1025.

VAN DER LEE, R., BULJAN, M., LANG, B., WEATHERITT, R. J., DAUGHDRILL, G. W., DUNKER, A. K., FUXREITER, M., GOUGH, J., GSPONER, J. & JONES, D. T. 2014. Classification of intrinsically disordered regions and proteins. *Chemical reviews,* 114**,** 6589-6631.

VANDER HEIDEN, M. G., CANTLEY, L. C. & THOMPSON, C. B. 2009. Understanding the Warburg Effect: The Metabolic Requirements of Cell Proliferation. *Science (New York, N.Y.),* 324**,** 1029-1033.

VARADAN, R., ASSFALG, M., HARIRINIA, A., RAASI, S., PICKART, C. & FUSHMAN, D. 2004. Solution conformation of Lys63-linked di-ubiquitin chain provides clues to functional diversity of polyubiquitin signaling. *J Biol Chem,* 279**,** 7055-63.

VERMEULEN, K., VAN BOCKSTAELE, D. R. & BERNEMAN, Z. N. 2003. The cell cycle: a review of regulation, deregulation and therapeutic targets in cancer. *Cell proliferation,* 36**,** 131-149.

VIGLIETTO, G., MOTTI, M. L., BRUNI, P., MELILLO, R. M., D'ALESSIO, A., CALIFANO, D., VINCI, F., CHIAPPETTA, G., TSICHLIS, P. & BELLACOSA, A. 2002. Cytoplasmic relocalization and inhibition of the cyclin-dependent kinase inhibitor p27Kip1 by PKB/Akt-mediated phosphorylation in breast cancer. *Nature medicine,* 8**,** 1136-1144.

VON DER LEHR, N., JOHANSSON, S., WU, S., BAHRAM, F., CASTELL, A., CETINKAYA, C., HYDBRING, P., WEIDUNG, I., NAKAYAMA, K., NAKAYAMA, K. I., SÖDERBERG, O., KERPPOLA, T. K. & LARSSON, L.-G. 2003. The F-Box Protein Skp2 Participates in c-Myc Proteosomal Degradation and Acts as a Cofactor for c-Myc-Regulated Transcription. *Molecular Cell,* 11**,** 1189-1200.

WALKER, D. H. & MALLER, J. L. 1991. Role for cyclin A in the dependence of mitosis on completion of DNA replication. *Nature,* 354**,** 314-7.

WALTREGNY, D., LEAV, I., SIGNORETTI, S., SOUNG, P., LIN, D., MERK, F., ADAMS, J. Y., BHATTACHARYA, N., CIRENEI, N. & LODA, M. 2001. Androgen-driven prostate epithelial cell proliferation and differentiation in vivo involve the regulation of p27. *Mol Endocrinol,* 15**,** 765-82.

WANG, H., BAUZON, F., JI, P., XU, X., SUN, D., LOCKER, J., SELLERS, R. S., NAKAYAMA, K., NAKAYAMA, K. I., COBRINIK, D. & ZHU, L. 2010. Skp2 is required for survival of aberrantly proliferating Rb1-deficient cells and for tumorigenesis in Rb1+/- mice. *Nat Genet,* 42**,** 83-88.

WANG, W., CALDWELL, M. C., LIN, S., FURNEAUX, H. & GOROSPE, M. 2000. HuR regulates cyclin A and cyclin B1 mRNA stability during cell proliferation. *The EMBO Journal,* 19**,** 2340-2350.

WANG, Y., FISHER, J. C., MATHEW, R., OU, L., OTIENO, S., SUBLETT, J., XIAO, L., CHEN, J., ROUSSEL, M. F. & KRIWACKI, R. W. 2011. Intrinsic disorder mediates the diverse regulatory functions of the Cdk inhibitor p21. *Nature chemical biology,* 7**,** 214-221.

WANG, Y. & PRIVES, C. 1995. Increased and altered DNA binding of human p53 by S and G2/M but not G1 cyclin-dependent kinases. *Nature,* 376**,** 88-91.

WANG, Y., WANG, Y., XIANG, J., JI, F., DENG, Y., TANG, C., YANG, S., XI, Q., LIU, R. & DI, W. 2014. Knockdown of CRM1 inhibits the nuclear export of p27Kip1 phosphorylated at serine 10 and plays a role in the pathogenesis of epithelial ovarian cancer. *Cancer Letters,* 343**,** 6-13.

WEI, W., AYAD, N. G., WAN, Y., ZHANG, G.-J., KIRSCHNER, M. W. & KAELIN, W. G. 2004. Degradation of the SCF component Skp2 in cell-cycle phase G1 by the anaphase-promoting complex. *Nature,* 428**,** 194-198.

WEINBERG, R. A. 1995. The retinoblastoma protein and cell cycle control. *Cell,* 81**,** 323-30.

WELCKER, M., LARIMORE, E. A., SWANGER, J., BENGOECHEA-ALONSO, M. T., GRIM, J. E., ERICSSON, J., ZHENG, N. & CLURMAN, B. E. 2013. Fbw7 dimerization determines the specificity and robustness of substrate degradation. *Genes Dev,* 27**,** 2531-6.

WESTERMANN, F., HENRICH, K.-O., WEI, J. S., LUTZ, W., FISCHER, M., KÖNIG, R., WIEDEMEYER, R., EHEMANN, V., BRORS, B. & ERNESTUS, K. 2007. High Skp2 expression characterizes high-risk neuroblastomas independent of MYCN status. *Clinical Cancer Research,* 13**,** 4695-4703.

WINN, M. D., BALLARD, C. C., COWTAN, K. D., DODSON, E. J., EMSLEY, P., EVANS, P. R., KEEGAN, R. M., KRISSINEL, E. B., LESLIE, A. G. W., MCCOY, A., MCNICHOLAS, S. J., MURSHUDOV, G. N.,

PANNU, N. S., POTTERTON, E. A., POWELL, H. R., READ, R. J., VAGIN, A. & WILSON, K. S. 2011. Overview of the CCP4 suite and current developments. *Acta Crystallographica Section D: Biological Crystallography,* 67**,** 235-242.

WINTER, G. 2009. xia2: an expert system for macromolecular crystallography data reduction. *Journal of applied crystallography,* 43**,** 186-190.

WISEMAN, T., WILLISTON, S., BRANDTS, J. F. & LIN, L. N. 1989. Rapid measurement of binding constants and heats of binding using a new titration calorimeter. *Anal Biochem,* 179**,** 131-7.

WU, G., XU, G., SCHULMAN, B. A., JEFFREY, P. D., HARPER, J. W. & PAVLETICH, N. P. 2003. Structure of a beta-TrCP1-Skp1-beta-catenin complex: destruction motif binding and lysine specificity of the SCF(beta-TrCP1) ubiquitin ligase. *Mol Cell,* 11**,** 1445-56.

WU, J., LEE, S. W., ZHANG, X., HAN, F., KWAN, S. Y., YUAN, X., YANG, W. L., JEONG, Y. S., REZAEIAN, A. H., GAO, Y., ZENG, Y. X. & LIN, H. K. 2013. Foxo3a transcription factor is a negative regulator of Skp2 and Skp2 SCF complex. *Oncogene,* 32**,** 78-85.

WU, L., GRIGORYAN, ARSEN V., LI, Y., HAO, B., PAGANO, M. & CARDOZO, TIMOTHY J. 2012. Specific Small Molecule Inhibitors of Skp2-Mediated p27 Degradation. *Chemistry & Biology,* 19**,** 1515-1524.

XIONG, Y., HANNON, G. J., ZHANG, H., CASSO, D., KOBAYASHI, R. & BEACH, D. 1993a. p21 is a universal inhibitor of cyclin kinases. *Nature,* 366**,** 701-4.

XIONG, Y., ZHANG, H. & BEACH, D. 1993b. Subunit rearrangement of the cyclin-dependent kinases is associated with cellular transformation. *Genes & development,* 7**,** 1572-1583.

XU, M., SHEPPARD, K. A., PENG, C. Y., YEE, A. S. & PIWNICA-WORMS, H. 1994. Cyclin A/CDK2 binds directly to E2F-1 and inhibits the DNA-binding activity of E2F-1/DP-1 by phosphorylation. *Mol Cell Biol,* 14**,** 8420-31.

YAKES, F. M., CHINRATANALAB, W., RITTER, C. A., KING, W., SEELIG, S. & ARTEAGA, C. L. 2002. Herceptin-induced inhibition of phosphatidylinositol-3 kinase and Akt Is required for antibody-mediated effects on p27, cyclin D1, and antitumor action. *Cancer research,* 62**,** 4132-4141.

YAM, C. H., FUNG, T. K. & POON, R. Y. 2002. Cyclin A in cell cycle control and cancer. *Cell Mol Life Sci,* 59**,** 1317-26.

YAM, C. H., NG, R. W. M., SIU, W. Y., LAU, A. W. S. & POON, R. Y. C. 1999. Regulation of cyclin A-Cdk2 by SCF component Skp1 and F-box protein Skp2. *Molecular and cellular biology,* 19**,** 635-645.

YANG, J. Y. & HUNG, M. C. 2009. A new fork for clinical application: targeting forkhead transcription factors in cancer. *Clin Cancer Res,* 15**,** 752-7.

YANG, R., MOROSETTI, R. & KOEFFLER, H. P. 1997. Characterization of a second human cyclin A that is highly expressed in testis and in several leukemic cell lines. *Cancer Research,* 57**,** 913-920.

YE, Y. & RAPE, M. 2009. Building ubiquitin chains: E2 enzymes at work. *Nat Rev Mol Cell Biol,* 10**,** 755-764.

YEH, K. H., KONDO, T., ZHENG, J., TSVETKOV, L. M., BLAIR, J. & ZHANG, H. 2001. The F-box protein SKP2 binds to the phosphorylated threonine 380 in cyclin E and regulates ubiquitin-dependent degradation of cyclin E. *Biochem Biophys Res Commun,* 281**,** 884-90.

YOKOI, S., YASUI, K., IIZASA, T., TAKAHASHI, T., FUJISAWA, T. & INAZAWA, J. 2003. Down-regulation of SKP2 induces apoptosis in lung-cancer cells. *Cancer Sci,* 94**,** 344-9.

YOON, M. K., MITREA, D. M., OU, L. & KRIWACKI, R. W. 2012. Cell cycle regulation by the intrinsically disordered proteins p21 and p27. *Biochem Soc Trans,* 40**,** 981-8.

YUAN, X., SRIVIDHYA, J., DE LUCA, T., LEE, J. H. & POMERENING, J. R. 2014. Uncovering the role of APC-Cdh1 in generating the dynamics of S-phase onset. *Mol Biol Cell,* 25**,** 441-56.

YUAN, Z.-L., GUAN, Y.-J., CHATTERJEE, D. & CHIN, Y. E. 2005. Stat3 dimerization regulated by reversible acetylation of a single lysine residue. *Science,* 307**,** 269-273.

YUNG, Y., WALKER, J. L., ROBERTS, J. M. & ASSOIAN, R. K. 2007. A Skp2 autoinduction loop and restriction point control. *J Cell Biol,* 178**,** 741-7.

ZARKOWSKA, T. & MITTNACHT, S. 1997. Differential phosphorylation of the retinoblastoma protein by G1/S cyclin-dependent kinases. *Journal of Biological Chemistry,* 272**,** 12738-12746.

ZERFASS-THOME, K., SCHULZE, A., ZWERSCHKE, W., VOGT, B., HELIN, K., BARTEK, J., HENGLEIN, B. & JANSEN-DURR, P. 1997. p27KIP1 blocks cyclin E-dependent transactivation of cyclin A gene expression. *Mol Cell Biol,* 17**,** 407-15.

ZETTERBERG, A., LARSSON, O. & WIMAN, K. G. 1995. What is the restriction point? *Curr Opin Cell Biol,* 7**,** 835-42.

ZHANG, H., KOBAYASHI, R., GALAKTIONOV, K. & BEACH, D. 1995. p19 (Skp1) and p45 (Skp2) are essential elements of the cyclin A-Cdk2 S-phase kinase. *Cell,* 82**,** 915-925.

ZHANG, L. & WANG, C. 2006. F-box protein Skp2: a novel transcriptional target of E2F. *Oncogene,* 25**,** 2615-27.

ZHANG, Q., TIAN, L., MANSOURI, A., KORAPATI, A. L., JOHNSON, T. J. & CLARET, F. X. 2005. Inducible expression of a degradation-resistant form of p27 Kip1 causes growth arrest and apoptosis in breast cancer cells. *FEBS letters,* 579**,** 3932-3940.

ZHAO, H., BAUZON, F., FU, H., LU, Z., CUI, J., NAKAYAMA, K., NAKAYAMA, K. I., LOCKER, J. & ZHU, L. 2013. Skp2 deletion unmasks a p27 safeguard that blocks tumorigenesis in the absence of pRb and p53 tumor suppressors. *Cancer Cell,* 24**,** 645-59.

ZHENG, N., SCHULMAN, B. A., SONG, L., MILLER, J. J., JEFFREY, P. D., WANG, P., CHU, C., KOEPP, D. M., ELLEDGE, S. J., PAGANO, M., CONAWAY, R. C., CONAWAY, J. W., HARPER, J. W. & PAVLETICH, N. P. 2002. Structure of the Cul1-Rbx1-Skp1-F boxSkp2 SCF ubiquitin ligase complex. *Nature,* 416**,** 703-709.

ZHENG, Y. & MISKIMINS, W. K. 2011. Far Upstream Element Binding Protein 1 Activates Translation of p27(Kip1) mRNA Through Its Internal Ribosomal Entry Site. *The international journal of biochemistry & cell biology,* 43**,** 1641-1648.

ZHOU, N. E., KAY, C. M. & HODGES, R. S. 1992. Synthetic model proteins. Positional effects of interchain hydrophobic interactions on stability of two-stranded alpha-helical coiled-coils. *Journal of Biological Chemistry,* 267**,** 2664-2670.

ZHOU, W., SRINIVASAN, S., NAWAZ, Z. & SLINGERLAND, J. M. 2014. ERalpha, SKP2 and E2F-1 form a feed forward loop driving late ERalpha targets and G1 cell cycle progression. *Oncogene,* 33**,** 2341-53.

ZHU, X. H., NGUYEN, H., HALICKA, H. D., TRAGANOS, F. & KOFF, A. 2004. Noncatalytic requirement for cyclin A-cdk2 in p27 turnover. *Mol Cell Biol,* 24**,** 6058-66.

ZHU, Y., PE'ERY, T., PENG, J., RAMANATHAN, Y., MARSHALL, N., MARSHALL, T., AMENDT, B., MATHEWS, M. B. & PRICE, D. H. 1997. Transcription elongation factor P-TEFb is required for HIV-1 tat transactivation in vitro. *Genes & development,* 11**,** 2622-2632.

ZHU, Y., YAN, Y., PRINCIPE, D. R., ZOU, X., VASSILOPOULOS, A. & GIUS, D. 2014. SIRT3 and SIRT4 are mitochondrial tumor suppressor proteins that connect mitochondrial metabolism and carcinogenesis. *Cancer Metab,* 2**,** 15.

ZOU, L. & ELLEDGE, S. J. 2003. Sensing DNA damage through ATRIP recognition of RPA-ssDNA complexes. *Science,* 300**,** 1542-8.